Sponsors

BOOK OF ABSTRACTS

22 - 24 JUNE 2022 AT KHAO YAI CONVENTION CENTER (KYCC), NAKHON RATCHASIMA, THAILAND

“Carbon Neutrality”

Siam Physics Congress 2022

"Carbon Neutrality"

22 - 24 June 2022

Khao Yai Convention Center (KYCC)
Nakhon Ratchasima, Thailand

Sponsors

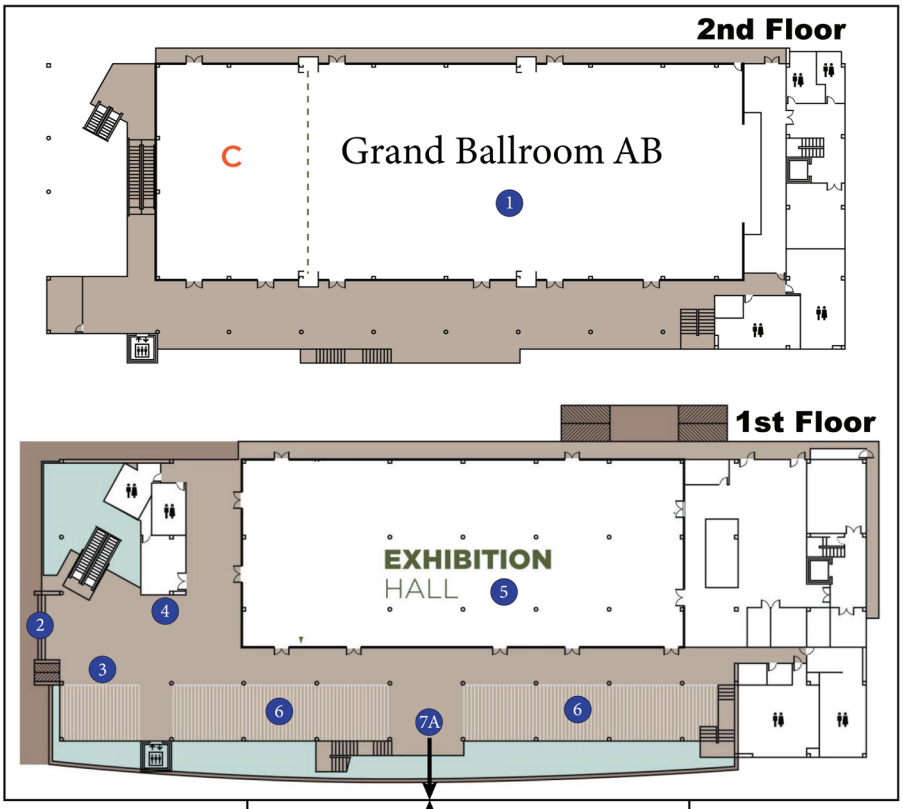

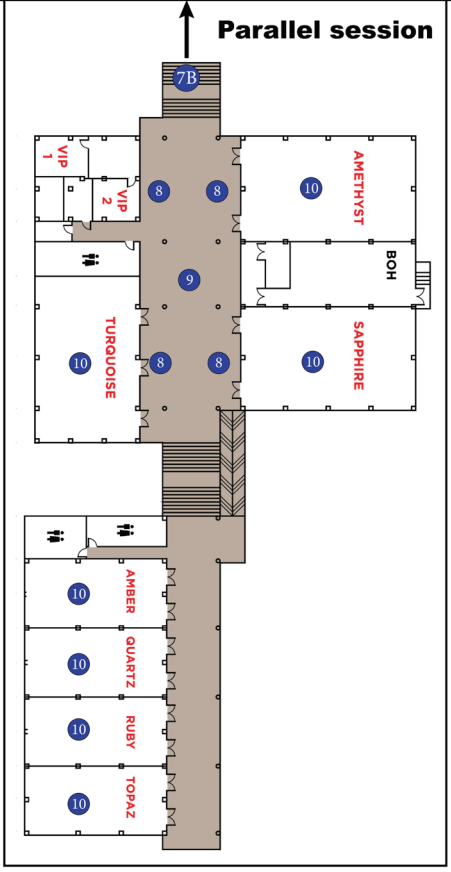

1 Grand Ballroom AB
- Opening ceremony
- Plenary session
- Dinner

2 Main entrance

3 Backdrop

4 Registration desk

5 Exhibition Hall
- Lunch

6 Poster session

7A To meeting rooms (parallel session)

7B To Grand Ballroom AB

8 Booth zone

9 Coffee break zone

10 Meeting rooms (parallel session)
- Amethyst room
- Sapphire room
- Turquoise room
- Amber room
- Quartz room
- Ruby room
- Topaz room

Overall Program of SPC 2022

June 22, 2022								
Time	**Grand Ballroom**							
15.00-17.00	Registration / Exhibition and poster presentation set up							
June 23, 2022								
Time	**Grand Ballroom**							
9.00-9.30	Welcome speech by Rector of Suranaree University of Technology							
	Reported by Dean of Institute of Science, Suranaree University of Technology							
	Opening speech by President of Thai Physics Society							
	Opening remark by President of AAPPS							
9.30-10.30	Plenary talk (Prof. Hiroshi Segawa)							
10.30-10.45	Preparation and coffee break							
	AMETHYST	**SAPPHIRE**	**TURQUOISE**	**AMBER**	**QUARTZ**	**RUBY**	**TOPAZ**	**Poster Hall**
10.45-11.00	INV-S1-1	INV-S1-2	INV-S2-1	INV-S3-1	INV-S4-1	INV-S5-1	O-S4-43	
11.00-11.15							O-S4-44	
11.15-11.30	O-S1-1	O-S1-7	O-S2-1	O-S3-1	O-S4-1	O-S5-1	O-S4-45	
11.30-11.45	O-S1-2	O-S1-8	O-S2-2	O-S3-2	O-S4-2	O-S5-2	O-S4-46	
11.45-12.00	O-S1-3	O-S1-9	O-S2-3	O-S3-3	O-S4-3	O-S5-3	O-S4-23	
12.00-13.00	Lunch							
13.00-14.00	Plenary talk (Prof. Vinich Promarak) at Grand Ballroom						Senior Project Competition	
14.00-15.00	Plenary talk (Prof. Manabu Ihara) at Grand Ballroom							
15.00-15.15	Coffee break							
15.15-15.30	O-S1-4	O-S1-10	O-S2-4	O-S3-4	O-S4-4	QT		
15.30-15.45	O-S1-5	O-S1-11	O-S2-5	O-S3-5	O-S4-5	QT		
15.45-16.00	O-S1-6	O-S1-12	O-S2-6	O-S3-6	O-S4-6	QT		
16.00-16.15	TheP	TNAM	O-S2-7		O-S4-7	QT		Poster Session
16.15-16.30	TheP	TNAM	O-S2-8		O-S4-8	O-S5-4		
16.30-16.45	TheP	TNAM	O-S2-25			O-S5-5		
16.45-17.00	TheP	TNAM	O-S2-26			O-S5-6		
17.00-17.15	TheP	TNAM				O-S5-7		
17.15-17.30	TheP	TNAM				O-S5-8		
17.30-18.30	TPS Annual Meeting							
18.30	Dinner							
June 24, 2022								
Time	**AMETHYST**	**SAPPHIRE**	**TURQUOISE**	**AMBER**	**QUARTZ**	**RUBY**	**TOPAZ**	**Poster Hall**
9.00-9.15	INV-S1-3	O-S1-30	INV-S2-2	INV-S3-2	INV-S4-2	INV-S5-2	O-S4-24	
9.15-9.30		O-S1-31					O-S4-25	
9.30-9.45	O-S1-13	O-S1-32	O-S2-9	O-S3-7	O-S4-9	O-S5-9	O-S4-26	
9.45-10.00	O-S1-14	O-S1-33	O-S2-10	O-S3-8	O-S4-10	O-S5-10	O-S4-27	
10.00-10.15	O-S1-15	O-S1-34	O-S2-11	O-S3-9	O-S4-11	O-S5-11	O-S4-28	
10.15-10.30	Coffee break							
10.30-11.30	Plenary talk (Prof. Jianzhong Zhang) broadcast to all meeting rooms							
11.30-11.45	O-S1-16	O-S1-35	O-S2-12	O-S3-10	O-S4-12	O-S5-12	O-S4-29	
11.45-12.00	O-S1-17	O-S1-36	O-S2-13	O-S3-11	O-S4-13	O-S5-13	O-S4-30	
12.00-13.00	Lunch							
13.00-13.15	O-S1-18	O-S1-37	INV-S2-3	INV-S3-3	INV-S4-3	INV-S5-3	O-S4-31	
13.15-13.30	O-S1-19	O-S1-38					O-S4-32	
13.30-13.45	O-S1-20	O-S1-39	O-S2-14	INV-S3-4	O-S4-14	O-S5-14	O-S4-33	
13.45-14.00	O-S1-21	O-S1-40	O-S2-15		O-S4-15	O-S5-15	O-S4-34	
14.00-14.15	O-S1-22	O-S1-41	O-S2-16	O-S3-12	O-S4-16	O-S5-16	O-S4-35	
14.15-14.30	O-S1-23	O-S1-42	O-S2-17	O-S3-13	O-S4-17	O-S5-17	O-S4-36	
14.30-14.45	O-S1-24	O-S1-43	O-S2-18	O-S3-14	O-S4-18	O-S5-18	O-S4-37	
14.45-15.00	O-S1-25	O-S1-44	O-S2-19		O-S4-19		O-S4-38	
15.00-15.15	Coffee break							
15.15-15.30	O-S1-26	O-S1-45	O-S2-20		O-S4-20	O-S4-39	O-S4-41	
15.30-15.45	O-S1-27	O-S1-29	O-S2-21		O-S4-21	O-S4-40	O-S4-42	
15.45-16.00	O-S1-28	O-S1-46	O-S2-22		O-S4-22		O-S4-43	
16.00-16.15	O-S1-47	O-S1-48	O-S2-23					
16.15-16.30	O-S1-50	O-S1-49	O-S2-24					
16.30-16.45	Closing Ceremony							

Poster Presentation

Code	Abstract ID	Title	Author
P001	365	Carbon Neutralization of Sugarcane by Super Farm Model	Kanittha Pamonpol
P002	270	STUDY OF PLASMA ACTIVATED WATER AND SECONDARY EFFECTS ON WATER USING GAMMA RADIATION WITH FTIR IN SEEDS GERMINATION	Aonkaet Somjaimak
P003	345	Isotropic and Anisotropic Materials Characterization Technique by Polarization Sensitive Optical Coherence Tomography	Kunakorn Palawong
P004	341	Development of a low budget and compact Optical Coherence Tomography at 840 nm wavelength region for 3D imaging of biological tissues	Jadsada Saetiew
P005	337	Development of Low-Cost Automatic Groundwater Level Measurement System Based on The Internet of Things	Chalermpong Polee
P006	336	Experiment and simulation of heat treatment for disinfection in the chicken farm using IR and UV irradiation	Wuttipan Satienpaisan
P007	335	Development of food packaging materials from rice straw waste and sugarcane residue by hot pressing	Pakpoom Buabthong
P008	331	Analysis of temperature oscillations due to low current in a circuit of a resistor and a thermostat's bimetallic plate	Tanapat Chansaeng
P009	330	Spectrophotometer based on light-emitting diode(LED) for DOBI measurement for crude palm oil quality control	Suttirak Kaewpawong
P010	326	Development of magnetically well-type plasma torch for high-temperature process	Ridhvee Taleh
P011	324	Characteristics of plasma activated water (PAW) produced by moderated pressure RF discharges	Karaket Wattanasit
P012	209	STRAIGHTNESS MEASUREMENT BY REVERSAL METHOD	Watcharin Samit
P013	184	Exploring Spratly Islands using VIIRS Boat Detection Satellite Image Analytics	Ryan manuel Guido
P014	90	A simple pendulum study using a smartphone video camera	Pranee Disrattakit
P015	281	Estimation of solar radiation and optimum tilt angles for south-facing surface in Nakhon Pathom and Chiang Mai stations	Rungrat Wattan
P016	277	The development of smart farm systems by controlling via the internet	Piriya Praneekit
P017	276	Effect of Drying Temperature on Color Change of Green Banana Flour under Infrared Radiation Heating	Suminya Teeta
P018	275	Efficacy of vermicompost on growth and yield of organic rice with the participation of farmer groups to create a model community network in Roi Et and Maha Sarakham provinces	Mali Sarobol
P019	273	Moina macrocopa culture using plasma activated water (PAW)	Nichanun Neamtad
P020	269	Bio-based Content Measurement by Radiocarbon Analysis in Thailand	Nichtima Uapoonphol
P021	266	The Smartphone and Low-Cost Microcontroller as an AC Circuit Study Kit for high-school students	Kridsada Luangthongkham
P022	253	Development of optical tomography at 840 nm wavelength for sex classification of newborn Korat chickens.	Jadsada Saetiew
P023	250	A cost-effective apparatus for colloidal assembly by convective deposition	Jeerasak Phooarphit
P024	247	Application of Ultrasonic Sensor and Arduino in Analyzing Motion of Damped Pendulum	Surasak Methet
P025	241	Surveying physics laboratory skill in measurement and uncertainty: A case study of pre-service teachers and in-service teachers	Trai Unyapoti
P026	234	The varying permanent magnetic field by angle and distance for spin Seebeck effect measurement	Punthawat WONGDAENG
P027	233	Monitoring of Local Monsoon in Thailand using Stable Isotope Technique	Chakrit Saengkorakot
P028	230	Thai Voice Command System for Mobile Robot	Wisit Mangthas
P029	227	INCREASING THE HEIGHT OF BOUNCING BALL BY SPIN	Ratchaphon Noiaek
P030	214	Design and implementation of a low-cost real-time photovoltaic panel monitoring and recording system using LabVIEW for rural areas	Natawee Chaijum
P031	210	Comparison of carbon dioxide emissions produced between paper-based and computer-based for demonstration indirect light concepts	Tiantada Hiranyachattada
P032	208	Design, Fabrication and Performance Evaluation of Solar Dryer for Thai Glutinous Rice, Khao Tan Rice Cracker Herbal	Mali Sarobol
P033	207	Demonstration kits for locating an image formed by a concave mirror	Pakanat Srijaroen
P034	201	Fabrication and Evaluation of Soil Pressure Sensor for Stress State Transducer	Chompoonud Kulketwong
P035	192	Study of the impact force of falling chains using force sensor	Nitat Sripongpun
P036	174	Topological Analysis of the Transfer Entropy Network of Cryptocurrencies During the Uptrend and Downtrend Periods.	Gingkamon Jaroenkobun
P037	97	Traffic flow simulation of bi- lane systems through the two positions of traffic light signal	Puwarin Narkjanthuk
P038	122	Question-Answer Teaching Method to Develop Student Understanding of Buoyant Force	Kwan Arayathanitkul
P039	125	Online physics experiment creation on resonance in the LC circuit with simple metal detector circuit	Niyom Hongsith

Poster Presentation

Code	Abstract ID	Title	Author
P040	126	Measurement and analysis of sound frequencies in beehive with smart electronic sensor systems for health status monitoring and specific behavioral study from native bees (Apis ceran	Suphansa Chansuriya
P041	127	The study of solvent ratio of diphenyl oxalate on chemiluminescence	Kachain Dangudom
P042	60	Optical properties of freeze-dried partial delignified balsa wood	Piyawath Tapsanit
P043	56	Estimation of rainfall from the amount of water vapor in the atmosphere	Sayan Phokate
P044	52	The effects of mechanically gated ion channels of the inner ear on thermal sensitivity of spontaneous otoacoustic emissions	Kittisak Sawangwareesakul
P045	243	Development of intelligent nanogels by gamma radiation as theranostic agents for diagnosis and therapy of cancer	Thitirat Rattanawongwiboon
P046	16	Optical properties of carbon dots derived from table sugar via gamma irradiation	Kanokorn Wechakorn
P047	20	DEVELOPMENT OF AN EDUCATIONAL PC BASED SIMULATOR FOR TRR-1/M1	Kanokrat Tiyapun
P048	8	Elemental analysis in rice samples by wavelength dispersive X-ray fluorescence spectrometry	Supalak Kongsri
P049	9	Specific activities and gamma radiation hazard evaluation in rice cultivated soils in Nakhon Si Thammarat province	Chunyapuk Kukusamude
P050	352	Fabrication and Thermoelectric Properties of MWCNTs/Recycled Pulp	Suthat Ladkham
P051	348	The content calculation of hexagonal phase inclusions in hexagonal GaN films on GaAs (001) substrates grown by metalorganic vapor phase epitaxy	Wiraphat Thanyaphirak
P052	339	Synthesis and characteristic of reduced graphene oxide from the Siam weed, (Cromulent Odorata)	Piyachat Keeraj
P053	338	3D printing of carbon-based composite resin and mechanical properties	Chanwit Pa-art
P054	318	Paste-Injection Molding of Low-Density Barium Hexaferrite Magnets	Chitnarong Sirisathitkul
P055	315	Effect of Ni-Co transition metal ratios on structure-function of Lithium Aluminum Borate Glasses by synchrotron-based XAS and XPS	Jidapa Lomon
P056	310	Coalescence of nematic liquid crystal droplets on freely suspended liquid crystal films	Jutarat Kaewthong
P057	304	Fabrication of single-walled carbon nanotube photodetectors using the dielectrophoretic assembly	NIramai Chirapraphusak
P058	286	High-performance supercapacitor electrode using microwave reflux-assisted modification of the activated carbon derived from Kapok shell	Mavin Punon
P059	274	EFFECT OF SINTERING TIME ON PHASE, PHYSICAL PROPERTIES, MICROSTRUCTURE AND THERMAL CONDUCTIVITY OF Y(Ba1-xLax)2Cu3O7-δ CERAMI	Sireetone Yawirach
P060	72	Gamma Irradiation Assisted Nickel Impregnation on Activated Carbon Derived from Water Hyacinth for Electrocatalyst Application	Piyapat Tonkaew
P061	284	Synthesis and characterization of manganese dioxide for high electrochemical performance supercapacitor electrode	Pawinee Klangtakai
P062	255	EFFECT OF ANNEALING TEMPERATURE ON THERMOELECTRIC PROPERTIES OF YBa2Cu3O7-x CERAMICS	Anucha Watcharapasorn
P063	249	Characterization of biofuel pellets production from woody biomass blends	Wassachol Wattana
P064	171	Photocatalytic Activity of Copper Doped on Bismuth Oxychloride Based for Degradation Rhodamine B under UV-light Irradiation	Thirawit Phonkhokkong
P065	166	Giant Dielectric Properties of Ca[$Cu {3-x}Ti x]Ti 4O {12}$ Ceramics	Narong Chanlek , Prasit Thongbai , Piyanud Wongtongdee
P066	168	Effect of Sulfur Doping in Bismuth Oxychloride on Degradation and Photocatalytic of Rhodamine B Under UV irradiation	Warut Koonnasoot
P067	176	Fabrication, characterization and magnetic properties of La0.5Sr0.5TiO3 nanofibers	Wichaid Ponhan
P068	175	Influence of glycerin addition on formation and magnetic properties of MnBi prepared by vacuum sintering technique	Satienrapong Ngamsomrit
P069	206	Multifunction Acoustic Board Production from Corncob-Derived Activated Carbon and Corn Husk Waste Composite as Sound and Smell Absorbers with Natural Latex Adhesive	Samroeng Narakaew
P070	205	Development of Latent Fingerprints on Non-Porous Surfaces by Small Particle Reagent with Zinc oxide nanoparticles	Penpicha Mode-on
P071	158	A NOVEL MUTTILAYER PARTICLEBOARDS PREPARED FROM MILK PACKAGE (U.H.T.) WASTES AND COCONUT FIBERS	Pongsathorn Kongkaew
P072	223	The spin Hall thermopile of Si/YIG/Co,Fe	wimutti Kumpor
P073	226	Observation of spin Seebeck effect in YIG/Co100-xNbx alloys	Nithiporn Photimas
P074	229	The multilayer of Si/YIG/W for spin Seebeck effect by sputtering technique	Chananyapat Wongsakilkhamkhota
P075	279	CVD Synthesis of Intermediate State-Free, Large-Area and Continuous MoS2 via Single-Step Vapor-Phase Sulfurization of MoO2 Precursor	Ratchanok Somphonsane
P076	150	Microscopic studies of magnetic MnBi powder particles	Jongrak Borsup
P077	149	Effects of volume and compression on magnetic properties and homogeneity of MnBi prepared by liquid-phase sintering	Puttamawan Juntree
P078	141	Effect of Mn grinding time on structural, chemical and magnetic properties of the Manganese Bismuth prepared by sintering in vacuum	Satienrapong Ngamsomrit
P079	139	Effect of Self-Assembled Iron-Tannic Nanoparticles on Fastness and Antibacterial Properties of Natural Indigo (Strobilanthes Cusia) Dyed Cotton Fabrics	Yanee Keereeta

Poster Presentation

Code	Abstract ID	Title	Author
P080	123	Enhancement of Perovskite Solar Cells Performance using Electrochemically Grown TiO2 Quantum Dots	Thanakrit Sintiam
P081	114	Microwave-assistant preparation of ZnO nanostructures optical and morphological properties for photocatalytic activity	Rattanaporn Somrit
P082	110	Preparation of superhydrophobic paper using PDMS modified SiO2 nanoparticles	Wola Jiraprapa
P083	109	Surface modification of filter paper by TiO2-PDMS-KH550 nanocomposite with superhydrophobic, self-cleaning and oil/water separation properties	Kupalang Suwanna
P084	100	Systematical investigation and correction of measured magnetic hysteresis obtained by vibrating sample magnetometry	Sasithon Santikulthani
P085	93	Investigation of Cu-atomic ratio in the second step of the 3-stage deposition process of Cu(In,Ga)Se2 thin film solar cells	Boonyaluk Namnuan
P086	88	The Natural Fibers ratio are Affected to Mechanical Properties of Kaolin/Fly-ash at Low Temperature Ceramics	Watee Panthuwat
P087	87	Effect of Fly-ash Doped Kaolin on Mechanical Properties and Heat-insulating of Ceramics	Narit Funsueb
P088	86	Surface treatment of PTAA hole transport layer for inverted perovskite solar cells	Kwanruthai Butsriruk
P089	82	Theoretical study of electrical transport across 1D ferromagnet-insulator-ferromagnet junction	Adithep butburee
P090	73	Structural, mechanical properties and corrosion performance of multilayer Ti/Ti doped-DLC films deposited on low-carbon steel	Ukit Rittihong
P091	67	Electronic and magnetic properties of $MoTe {2}$ monolayer doped with single and double transition metal configuration: spin density functional theory	Waritsara Thajitr
P092	47	Synthesis and Application of Nickel Compound Quantum Dots by Electrochemical Process	Prapasiri Phimsarn
P093	46	Nickel Oxide Thin Films Prepared by Using Nickel Nitrate/Acetate for Hole Transporting Layer in Perovskite Solar Cells	Kritsada Hongsith
P094	26	Ohmic heating as an effective path to rapidly cure and strengthen alkali activated material	Nattapong Chuewangkam
P095	45	Microstructure and Electrical Properties of Green Electrospun PVDF-HFP nanofibers	JAKKAPAT KHAO-IAM
P096	24	Thermoelectric properties of Cu2Se and densified by cold sintering process	Piyawat Piyasin
P097	25	Synthesis of Fe3O4 Ceramic Magnet Via Cold sintering Process	Nuchjaree Salidkul
P098	28	INTEGRATION OF METAL-ORGANIC FRAMEWORK AND AMORPHOUS CARBON FROM BACTERIAL CELLULOSE FOR LI-ION BATTERIES	Dejwikom Theprattanakorn
P099	33	Effect of hydrochloric acid modification on physical and optical properties of PEDOT:PSS thin films	Sasimonton Moungsrijun
P100	31	Mechanical Properties of Fly Ash Geopolymers Reinforced with Graphene Oxide	Jariya Lasiw
P101	39	Effects of Temperature on Persistence Probabilities in Molecular Beam Epitaxy Model	Pipitton Sanseeha
P102	40	Fractional Little-Park effect in hybrid superconductor-ferromagnet proximity cylinders	Boonlit Krunavakarn
P103	30	The Effect of Graphene Oxide Addition in Copper Selenide Compound on Thermoelectric Efficiency	Wanida Duangsimma
P104	325	Diagnostics of electron temperature and plasma density by OES and Langmuir probe in linear helicon plasma device	Suttirak Kaewpawong
P105	306	Proton-induced luminescence of scintillating Ce3+-barium-gadolinium-fluoroborate glass	Phongnared Boontueng
P106	316	Optimization of Current Transformers for Linear Accelerator System at PBP-CMU electron Linac Laboratory	Watchara Jaikla
P107	317	Design, Construction and Measurement of Electromagnetic Steering Magnet for 25-MeV Electron Accelerator System	Pitchayapak Kitisri
P108	320	Construction and Tests of Phosphor View Screen Station for Monitoring Transverse Profile of Electron Beam at PCELL	Noppadon Khangrang
P109	118	Assessment of Radon Concentration of Vegetables and Fruits in local markets in Muang Nakhon Phanom Municipality, Thailand	Yodprem Pookamnerd
P110	128	Conceptual design of a compact THz radiation source	Siriwan Jummunt
P111	129	A study design of faraday cup for a 50 MeV electron beam current	Siriwan Jummunt
P112	130	Design of the prototype quadrupole magnet for a compact THz radiation source	Siriwan Jummunt
P113	135	Optical Design of BL7.3 beamline Synchrotron Light Research Institute	Prayoon Songsiriritthigul
P114	200	The radiation response of Cholangiocarcinoma cell growth in two-dimension cultures	Yuwadee Malad
P115	74	Development of a 6 MeV Electron Beam Energy Linac for Fruit Sterilization	Somjai Chunjarean
P116	69	Synchrotron Radiation Fourier Transform Infrared (SR-FTIR) Spectroscopy in Exploring Crosslinked Chitosan-Rice Husk Bio-composite by Gamma Irradiation	Pawitra Aim-O
P117	18	Sensitivity of GEB function of MCNP pulse height spectra on CLYC7 scintillator detector	Sawarin Buakham
P118	7	Optimization for Fuel Loading and Thermal Hydraulic Analysis for TRR-1/M1 Research Reactor	KANOKRAT TIYAPUN
P119	374	Electromagnetic form factors of Δ-N transition	Moh Moh Aung

Poster Presentation

Code	Abstract ID	Title	Author
P120	342	Study of imaging system in Proton computed tomography with data acquisition from ALPIDE sensor	Nakarin Ratsuntia
P121	289	Optical Transient Counterpart to GW Event with TAROT Telescopes	Kanthanakorn Noysena
P122	217	A demonstration of absolute polarization angle calibration at 6 GHz using ATCA	Kitiyanee Asanok
P123	213	Holographic RG flows from four-dimensional N=6 and N=2 gauged supergravities	ณัฐภัทร ลุนราศรี
P124	220	Exploring the extinction in the line of sight of the Galactic bulge through the VVV data	Ponlawat Yoifoi
P125	225	Internal and external effects on Ganymede's footprint location	Tatphicha Promfu
P126	267	The Engineering Design of the Ultra-High Vacuum Chamber for Astrochemistry Experimental Station	Watchara jaikla
P127	282	Reveal chemical compositions in the exoplanetary atmospheres using the transmission spectroscopy technique	Thammasorn Padjaroen
P128	161	Thermodynamics of AdS Black String from Renyi entropy in de Rham-Gabadaze-Tolley Massive Gravity Theory	พีรวัชร ศรีหลิ่ง
P129	153	The period variation of an eclipsing binary system BQ Ari.	Supachai Awiphan
P130	119	Development of Data Archive for the Spectroscopic Data from Thai National Observatory (TNO)	Onjira Krataithong
P131	120	Collective expansion of K-mesons in heavy-ion collisions on the effect of in-medium Kaon potential and the nuclear equation of state	Phacharatouch Chaimongkon
P132	142	Maser polarization simulation in the circumstellar envelope of an evolving star	Montree Phetra
P133	84	The Transit Timing Variation and Atmosphere of WASP-43 b	Rattiyakorn Rattanasai
P134	68	Transmission spectroscopy analysis of water vapor for the exoplanets atmospheres using HST database.	Thansuda Chulikorn
P135	58	Monte Carlo analysis for enhancing radiation safety of Thai neutron imaging system	Weerawat Pornroongruengchok
P136	70	Gamma Irradiation Induced the Conversion of 5-Hydroxymethylfurfuraldehyde under Aqueous and Dimethyl Sulfoxide Solution	Nurulsafeelanaria Benwannamas
P137	5	Metallicity Analysis of Proxima Centauri at $0.004 < Z < 0.01$	Bea Marie Cajandig
P138	132	Influence of temperature on laser diode inside external cavity diode laser	Sitti Buathong
P139	124	Simulation of Three-Nodes Quantum Network with Entangled Photon Pair Source (EPPS) Protocol via International Space Station (ISS)	Poramat Chianvichai
P140	77	Qubit decoherence and phase correction in Gaussian white-noise environment	Atirat Meunson
P141	76	Estimating unknown qubit phase under telegraph noises using Recurrent Neural Network	Suttavee Rojanasirivanit
P142	75	Size Separation of FAPbBr3 Nanocrystals through Differential Centrifugation	Kunlasatree Kunsaeng
P143	64	Random-telegraph noise mitigation and qubit decoherence in solid-state experiments	Nattawut Kamjam
P144	63	Quantum Diamond Spectrometer for Magnetic Field Sensing	Napoom Thooppanom
P145	43	Performance comparison of Amplitude-decorrelation and Speckle Variance algorithms for OCT Angiography	Wuttikorn Kampong
P146	21	Optically Detected Electron Spin Resonance in Diamond for Vector Magnetometry	Rapeephat Yodsungnoen
P147	10	Time-domain measurements with superconducting flux qubits for diabatic quantum annealing experiments	Nuttamas Tubsrinuan
P148	292	High Speed Video Analysis of Magnetic Rollers	Kanokporn Intakaew
P149	295	Sugarcane leaf lamp	Yaowapa Saengpayab
P150	297	Optical Coherence Tomography Retina Scanner	Thanapol Tuntrakool
P151	298	3D printing of barium hexaferrite magnets with complex shapes	Yaowarat Sirisathitkul
P152	300	Electrolyte Drink Analysis by Electronic Tongue Using Carbon Nanotube Paste Electrodes	Tanakorn Osotchan
P153	311	Rotation Stage for Phantom in the Prototype for Proton Computed Tomography	Atirat Pitaktrakul
P154	314	Efficient fabrication of smart pH-responsive gold nanohybrids for targeted anticancer drug delivery systems	Sakchai Laksee
P155	204	Development of dual wavelength light sources for transmission and backscattering Raman spectroscopy	Tachawit Pao-In Charoenrit
P156	131	Laboratory implementation of Fourier Transform Infrared (FTIR) spectrograph using a super-continuum laser	Nirawit Kunanta
P157	285	Design and build of time domain optical coherence tomography for high resolution by using broadband supercontinuum pulse laser	Yutana Lenaphet
P158	3	Coalescence of nematic liquid crystal droplets on freely suspended liquid crystal films	Jutarat Kaewthong
P159	191	Optimization of adiabatic optical coupling between Silicon nitride and Germanium-based nanostructures for energy-efficient photonic integrated circuits	Natdanai Khongpetch
P160	252	The study of pigment color mixing by microfluidic systems and smartphone technology	Puenisara Limnonthakul

Oral Presentation

June 23, 2022
Symposium 1 (Room : AMETHYST)
Chair: Asst. Prof. Dr. Phichet Kittara
Co-chair: Dr. Monchai Jitvisate

Time	Code	Abstract ID	Title	Speaker
10.45-11.00 11.00-11.15	INV-S1-1	372	Development of chemical sensors from lab research to tech startup business	Asst. Prof. Dr. Teerakiat Kerdcharoen
11.15-11.30	O-S1-1	263	Colorimetric Sensor for Formaldehyde Detection Using Thiol-Functionalized Polydiacetylene and Zinc Oxide Nanocomposites	Papaorn Siribunbandal
11.30-11.45	O-S1-2	186	Analysis and prediction of vegetation, croplands, and urbanization change in The Philippines using data sattelite images between 2001-2018	Earon Cabasal
11.45-12.00	O-S1-3	189	UV germicidal rays working with timer and motion sensors	Chatpong Kobkam
12.00-13.00			Lunch	
			Chair: Asst. Prof. Dr. Phichet Kittara **Co-chair: Dr. Monchai Jitvisate**	
15.15-15.30	O-S1-4	94	Simulation Sensitivities Study to the Wind Characteristics over Uttaradit Rajabhat University at Lamrang Thungkalo campus with WRF model	Chainarong Raktham
15.30-15.45	O-S1-5	190	Night-time Human Mobility during Pandemic in the Philippines as Observed by VIIRS Satellite	Ryan Manuel Guido
15.45-16.00	O-S1-6	333	Flow dependence of handheld breath analyzer for body fuel utilization monitoring	Chan Sricharoen

June 23, 2022
Symposium 1 (Room : SAPPHIRE)
Chair: Assoc. Prof. Dr. Pornrat Wattanakasiwich
Co-chair: Dr. Narasak Pandech

Time	Code	Abstract ID	Title	Speaker
10.45-11.00 11.00-11.15	INV-S1-2	375	How to make important ideas in science learnable? A design case study of an educational robotics toolkit	Dr. Arnan (Roger) Sipitakiat
11.15-11.30	O-S1-7	85	A baby mobile as a STEM activity for promoting students' learning and interest in a simple harmonic motion	Panupon Samaimongkol
11.30-11.45	O-S1-8	231	Using a pre-instruction math test to predict first-year physics exam results	Meta Popanao
11.45-12.00	O-S1-9	167	How does student skill on interpreting circular motion situation change in an online physics classroom?	Arunee Eambaipreuk
12.00-13.00			Lunch	
			Chair: Dr. Arnan (Roger) Sipitakiat **Co-chair: TBA**	
15.15-15.30	O-S1-10	185	Attitudes and motivation of internship students towards physics, astronomy, and space science sattellite technology virtual internship program	Ryan Manuel Guido
15.30-15.45	O-S1-11	103	Compact and easy-to-use smartphone based experimental set for studying simple and damped harmonic motion patterns.	Somporn Buaprathoom
15.45-16.00	O-S1-12	218	Development of circular motion experiment set with the reduction of friction for high school physics students	Anucha Pratumma

Oral Presentation

June 23, 2022
Symposium 2 (Room : TURQUOISE)
Chair: Assoc. Prof. Dr. Jiraroj T-Thienprasert
Co-chair: Assoc. Prof. Dr. Adisak Boonchum

Time	Code	Abstract ID	Title	Speaker
10.45-11.00 11.00-11.15	INV-S2-1	357	Alkali titanates as a bride for solid state chemistry and soft matter	Tosapol Maluangnont
11.15-11.30	O-S2-1	308	External pressure effects on superfluid density of isotropic s-wave superconductors	Grittichon Chanilkul
11.30-11.45	O-S2-2	198	Surface critical magnetic field (Hc3) of K0.73Fe1.68Se2 superconductors by two band Ginzburg-Landau approach	Suppanyou Meakniti
11.45-12.00	O-S2-3	280	Effect of annealing temperature on the structure and hardness of DC reactive magnetron sputtered CrAlN thin films	Adisorn Buranawong / Nirun Witit-anun
12.00-13.00	Lunch			
	Chair: Assoc. Prof. Dr. Supree Pinitsoontorn **Co-chair: Assoc. Prof. Dr. Prasit Thongbai**			
15.15-15.30	O-S2-4	41	1-over-f noise characterization of random-network single-walled carbon nanotube photodetectors	Yodchay Jompol
15.30-15.45	O-S2-5	35	Investigation of the high-field transport, Joule-heating-driven conductivity improvement and low-field resistivity behaviour in lightly-reduced free-standing graphene oxide papers	Harihara Ramamoorthy
15.45-16.00	O-S2-6	34	Remote Mesoscopic Signatures of Induced Magnetic Texture in Graphene	Ratchanok Somphonsane
16.00-16.15	O-S2-7	343	Electrospun carbon nanofibers decorated by TiO2 hollow nanospheres for high-performance flexible supercapacitor electrode	Suchunya Wongprasod
16.15-16.30	O-S2-8	312	Improving quality of graphene grown on copper foil by physical polishing, wet-chemical polishing and thermal annealing pretreatment processes	Methawut Sirisom
16.30-16.45	O-S2-25	50	Dielectric and non-ohmic properties of Ca2Cu2-xGexTi4O12 ceramic composites	Jirata Prachamon
16.45-17.00	O-S2-26	78	Metal-Insulator Transition effect on Graphene/VO2 via temperature dependent Raman Spectroscopy	Kittitat Lerttraikul

Oral Presentation

June 23, 2022
Symposium 3 (Room : AMBER)
Chair : Prof. Dr. Dheerawan Boonyawan
Co-chair: Dr. Prapong Klysubun

Time	Code	Abstract ID	Title	Speaker
10.45-11.00 11.00-11.15	INV-S3-1	197	Can Fusion Energy Contribute in Achieving Carbon Neutrality in Thailand?	Assoc Prof. Dr. Somsak Dangtip
11.15-11.30	O-S3-1	112	Three-Dimensional Simulation of the Supersonic Molecular Beam Injection in Thailand Tokamak 1	Kitti Rongpuit
11.30-11.45	O-S3-2	80	On the analysis of the fast-ion motion in Thailand Tokamak-1 using NUBEAM and LORBIT codes	Worathat Paenthong
11.45-12.00	O-S3-3	116	3D Range-Modulators: Near field simulations with FLUKA and comparison with film measurements	Warisara Charuchinda
12.00-13.00			Lunch	
Chair : Assoc. Prof. Dr. Mudtorlep Nisoa **Co-chair: Dr. Narongrit Ritjhoho**				
15.15-15.30	O-S3-4	91	The Effect of Magnetic Topology of Polywell Fusion Devices on The Electron Confinement Time	Rattacha Boonchoo
15.30-15.45	O-S3-5	92	Investigation of an edge transport barrier formation in fusion tokamak using the BOUT++ framework	Thiti Aungcharoen
15.45-16.00	O-S3-6	104	The study of fusion neutrons captured in Tritium breeding blanket of Tokamak wall using GEANT4	Paphatchaya Kheawyoi

Oral Presentation

June 23, 2022
Symposium 4 (Room : QUARTZ)
Chair: Asst. Prof. Dr. Siramas Komonjibda
Co-chair: Asst. Prof. Tirawut Worrakitpoonpon

Time	Code	Abstract ID	Title	Speaker
10.45-11.00 11.00-11.15	INV-S4-1	358	Implications of the Interacting Quark EoS in the Quark Stars with 4D Einstein-Gauss-Bonnet gravity	Daris Samart
11.15-11.30	O-S4-1	6	SUSY Breaking and R-symmetry Breaking in Gauged Wess-Zumino Model	Sirapat Lookrak
11.30-11.45	O-S4-2	27	Memorization and Prediction Capability of Interacting Phase Oscillators	Chanin Kumpeerakij
11.45-12.00	O-S4-3	165	Auroral Initial Brightening and Maximum Poleward Expansion Locations based on POLAR/VIS and POLAR/UVI Observations	Suwicha Wannawichian
12.00-13.00			Lunch	
			Chair: Asst. Prof. Dr. Siramas Komonjibda **Co-chair: Asst. Prof. Tirawut Worrakitpoonpon**	
15.15-15.30	O-S4-4	57	Charmed baryon pair production in effective Lagrangian and Regge approaches	Thanat Sangkhakrit
15.30-15.45	O-S4-5	66	Parameters of a potential model for tetraquarks from S- and P-wave charmonium mesons	Nattapat Tagsinsit
15.45-16.00	O-S4-6	81	Review of Fluid-Gravity Correspondence	Thepprasith Svetatula
16.00-16.15	O-S4-7	107	Search for BSM Higgs bosons using Machine Learning techniques	Jinna Waiwattan
16.15-16.30	O-S4-8	113	Proton Track reconstruction in a Telescope for Proton Computed Tomography	Arnon Songmoolnak

June 23, 2022
Symposium 4 (Room : TOPAZ)
Chair: Asst. Prof. Dr. Norraphat Srimanobhas
Co-chair: Dr. Apimook Watcharangkool

Time	Code	Abstract ID	Title	Speaker
10.45-11.00	O-S4-43	83	Phased-resolved energy distribution of pulsar PSRJ1825-0935	Nawamin Intrarat
11.00-11.15	O-S4-44	89	The Origin of Maser Flares	Malcolm Gray
11.15-11.30	O-S4-45	96	Machine learning application for dark matter - background classification in JUNO experiment	Jaruchit Siripak
11.30-11.45	O-S4-46	98	Orion's Magnetic Gems	Evgenii Semenko
11.45-12.00	O-S4-23	145	Solar gamma-ray analysis during the latest solar cycle using FERMI-LAT data	Daiki Hazama
12.00-13.00			Lunch	

Oral Presentation

June 23, 2022
Symposium 5 (Room : RUBY)
Chair: Dr.Piyaphat Phoonthong
Co-Chair: Dr.Pimonpan Sompet

Time	Code	Abstract ID	Title	Speaker
10.45-11.00	INV-S5-1	368	Quantum-inspired Computation for Optimization and Supervised Machine Learning	Thiparat Chotibut
11.00-11.15				
11.15-11.30	O-S5-1	64	Random-telegraph noise mitigation and qubit decoherence in solid-state experiments	Nattawut Kamjam
11.30-11.45	O-S5-2	76	Estimating unknown qubit phase under telegraph noises using Recurrent Neural Network	Suttavee Rojanasirivanit
11.45-12.00	O-S5-3	77	Qubit decoherence and phase correction in Gaussian white-noise environment	Atirat Meunson
12.00-13.00	Lunch			
	Chair: Dr.Sojiphong Chatraphorn **Co-Chair: Dr.Rachsak Sakdanuphab**			
16.15-16.30	O-S5-4	10	Time-domain measurements with superconducting flux qubits for diabatic quantum annealing experiments	Nuttamas Tubsrinuan
16.30-16.45	O-S5-5	261	Simulation of diatomic ground state energy in IBM quantum	Nuttha Utsaha
16.45-17.00	O-S5-6	222	The Dirac impenetrable barrier in the limit point of the Klein energy zone	Salvatore De Vincenzo
17.00-17.15	O-S5-7	232	Identifying Electronic Transition for 2 eV Hexagonal Boron Nitride Quantum Emitters	Cheewawut Na Talang
17.15-17.30	O-S5-8	177	Determination of the concentration of glucose-ethanol-water mixtures using spectroscopic surface plasmon resonance on smartphone	Prasert Chimplikanon

Oral Presentation

June 24, 2022
Symposium 1 (Room : AMETHYST)
Chair: Asst. Prof. Dr. Teerakiat Kerdcharoen
Co-chair: Dr. Monchai Jitvisate

Time	Code	Abstract ID	Title	Speaker
9.00-9.15	INV-S1-3	370	Green energy applications under ANSEE project in Khao Yai National Park	Assoc. Prof. Dr. Worawat Meevasana
9.15-9.30				
9.30-9.45	O-S1-13	235	An estimation of net radiation from global solar radiation in the main regions of Thailand	Korntip Tohsing
9.45-10.00	O-S1-14	193	Carbon electrode for perovskite solar cell	Supavidh Burimart
10.00-10.15	O-S1-15	187	The relationship of solar activity to Western Worth Pacific tropical cyclone frequency	Eliezer Caccam
10.15-10.30			Coffee break	
10.30-11.30			Plenary talk (Prof. Jianzhong Zhang) broadcast to all meeting rooms	
11.30-11.45	O-S1-16	211	A model for estimating solar ultraviolet radiation for vitamin D photosynthesis	Pradthana Laiwarin
11.45-12.00	O-S1-17	44	A mathematical study on the effects of fluid density on the impact cavity formation	Sarith Chopara
12.00-13.00			Lunch	
			Co-chair: Dr. Monchai Jitvisate **Co-chair: Assoc. Prof. Dr. Worawat Meevasana**	
13.00-13.15	O-S1-18	51	A Modification of Newton's Cooling Law with Correlation to Fractional Derivative	Kumkup Keeratisiwakul
13.15-13.30	O-S1-19	99	Monte Carlo study of uncertainty propagation in Euler rotational kinematic equation	Chanasorn Nutsathaporn
13.30-13.45	O-S1-20	101	Coordinates transformation method for pointer gauge reading by machine vision	Noparit Jinuntuya
13.45-14.00	O-S1-21	146	The moment of inertia of a Mahogany seed	Bodin Worrasookwanich
14.00-14.15	O-S1-22	117	Assessment of annual effective dose due to inhalation and ingestion of radon from groundwater at Kantharawichai District, Maha Sarakham Province	Vitsanusat Atyotha
14.15-14.30	O-S1-23	251	Experimental study of tap water activated by commercial fruit and vegetable purifier	Wasin Nupangtha
14.30-14.45	O-S1-24	257	The study of ring surface water wave generated by impacting droplets of using Free Surface Synthetic Schlieren (FS-SS) technique	Pakorn srirathat
14.45-15.00	O-S1-25	148	A study on optics: Invisibility properties of a lenticular lens	Bangon Prasutham
15.00-15.15			Coffee break	
			Chair: Dr. Arnan (Roger) Sipitakiat **Co-chair: TBA**	
15.15-15.30	O-S1-26	62	The effects of hair-cell polarity on the dynamics of two coupled hair-cell bundles of the inner ear	Tanawat Ngampattrapan
15.30-15.45	O-S1-27	258	Modeling the navigation of a weaver ant in a simple, unfamiliar environment	Lattawat Charoonratana
15.45-16.00	O-S1-28	239	Networks structure and entropy of stocks in the Stock Exchange of Thailand (SET)	Nawee Jaroonchokanan
16.00-16.15	O-S1-47	53	Fabrication of Radiative Cooling Matrix through Low-Cost Scalable Method and High Adaptability	Pongporn Wintakorn
16.15-16.30	O-S1-50	221	The Dynamics of Pill Millipedes' Flipping	Nutchaya Preechanukul

June 24, 2022
Symposium 1 (Room : SAPPHIRE)
Chair: Assoc. Prof. Dr. Pornrat Wattanakasiwich
Co-chair: Dr. Arnan (Roger) Sipitakiat

Time	Code	Abstract ID	Title	Speaker
9.00-9.15	O-S1-30	265	Competition of SARS-CoV-2 Delta and Omicron variants: A modeling study	Chatchapat Chaiaiad
9.15-9.30	O-S1-31	152	Mathematical modeling of vaccination strategies for COVID-19 in Thailand	Nattawadee Arbsuwan
9.30-9.45	O-S1-32	173	Association of COVID-19 pandemic with meteorological and PM 10 in Thailand using LSTM models	Chanidapa Winalai
9.45-10.00	O-S1-33	242	The determination of the effectiveness of mouth covering method while coughing using Background-oriented schlieren technique	Phongthep Chansamphan
10.00-10.15	O-S1-34	262	Air convection demonstration via background-oriented schlieren technique	Phongthep Chansamphan
10.15-10.30			Coffee break	
10.30-11.30			Plenary talk (Prof. Jianzhong Zhang) broadcast to all meeting rooms	
11.30-11.45	O-S1-35	55	Development of nanobubbles carrier in drug delivery system of melatonin encapsulated particle	Likit Temprom
11.45-12.00	O-S1-36	133	Experimental and theoretical studies of spread factor of swine blood- and deionized water-drop on glass surface.	Suparat Raweenroj
12.00-13.00			Lunch	
			Chair: Assoc. Prof. Dr. Worawat Meevasana **Co-chair: Dr. Monchai Jitvisate**	
13.00-13.15	O-S1-37	196	The Python programming code on cloud computing service for the stellar photometry astrophysics teaching	Watcharawuth Krittinatham
13.15-13.30	O-S1-38	65	The application of machine learning based on OpenCV for automatic digital dial gauge calibration	Sirichanya Thamphet
13.30-13.45	O-S1-39	144	An approach to the development of Raman spectroscopy system for field usage	Thiti Saeyee
13.45-14.00	O-S1-40	288	Design and development of the trigger system for proton computed tomography applications	Passakorn Phumara

Oral Presentation

June 24, 2022
Symposium 2 (Room : TURQUOISE)
Chair: Assoc. Prof. Dr. Tosapol Maluangnont
Co-chair: Assoc. Prof. Dr. Jiraroj T-Thienprasert

Time	Code	Abstract ID	Title	Speaker
9.00-9.15	INV-S2-2	356	Magnetic Bacterial Cellulose and Carbon Fiber Nanocomposites	Supree Pinitsoontorn
9.15-9.30				
9.30-9.45	O-S2-9	248	Characterization of TiN thin film deposited by reactive DC unbalanced magnetron sputtering at different N2 flow rates	Siriwat Alaksanasuwan
9.45-10.00	O-S2-10	237	Improvement in Reproducibility of Large-scale Perovskite Solar Cells Using Automatic Liquid Injection in Antisolvent Method	Watcharakiart Insri
10.00-10.15	O-S2-11	260	Synthesis of (Zn + Nb) co-doped TiO2 rutile nanoparticles and dielectric properties	Theeranuch Nachaithong
10.15-10.30	Coffee break			
10.30-11.30	Plenary talk (Prof. Jianzhong Zhang) broadcast to all meeting rooms			
11.30-11.45	O-S2-12	38	Giant Dielectric Response and Maxwell–Wagner Relaxation in Isovalent and Pentavalent Co–doped Rutile–TiO_{2}	Yasumin Mingmuang
11.45-12.00	O-S2-13	17	Versatile, Low-Cost, and Portable 2D Material Transfer Setup with a Facile and Highly Efficient DIY Inert-Atmosphere Glove Compartment Option	Harihara Ramamoorthy
12.00-13.00	Lunch			
	Chair: Assoc. Prof. Dr. Adisak Boonchum **Co-chair: Dr. Ittipon Fongkeaw**			
13.00-13.15	INV-S2-3	**355**	Electron-pinned defect-dipole and internal/surface barrier layer capacitor effects for high-performance giant dielectric oxides	Prasit Thongbai
13.15-13.30				
13.30-13.45	O-S2-14	290	Improving Heterointerface Abruptness of InGaAs/InP Superlattice by Optimizing a Purging Period of Group-V Gas	Warakorn Yanwachirakul
13.45-14.00	O-S2-15	154	EFFECT OF ANNEALING CONDITIONS ON VO2 THIN FILMS PREPARED BY SOL-GEL METHOD	Pongsatorn Panburana
14.00-14.15	O-S2-16	29	PREPARATION OF UiO-66-MOFs FROM PLASTIC BOTTLE WASTE FOR GAS ADSORPTION MATERIAL APPLICATION	Chawisa Visanupornprasit
14.15-14.30	O-S2-17	37	Ab-initio study and Atomistic spin model simulations of α-Cr2O3 thin films	Boonthum Kunyangyuen
14.30-14.45	O-S2-18	32	Classification of metal polyhydride critical temperature using support vector machine	Vichayut Imchitr
14.45-15.00	O-S2-19	309	On the origin of high performance V2O5 cathodes of aqueous Mg-ion batteries: A computational study	Panupol Untarabut
15.00-15.15	Coffee break			
	Chair: Assoc. Prof. Dr. Prasit Thongbai **Co-chair: Dr. Narasak Pandech**			
15.15-15.30	O-S2-20	157	First principles study on thermal conductivity of nitrogen substituted diamane	Sakarn Khamkaeo
15.30-15.45	O-S2-21	49	First-principles prediction of configurational order-disorder phase transition in ((Ti$_{1-x}$V$_{x})$_{1/3}Mo_{2/3})$_3C$_2$ MXene alloys	Chayanon Atthapak
15.45-16.00	O-S2-22	140	Fabrication and characterization of the Si p-n junction prepared by thermal diffusion	Nanthawat Toarun
16.00-16.15	O-S2-23	22	Synthesis of antibacterial nanofibers composite from poly butylene succinate and copper nanoparticle as a filter layer in a surgical mask	Jaggawut Suwannachot
16.15-16.30	O-S2-24	111	High−Performance Giant Dielectric Properties of (Tb+Nb) Co−Doped TiO2 Ceramics	Noppakorn Thanamoon

Oral Presentation

14.00-14.15	O-S1-41	319	An Application of Autocollimator for Surface Profile Measurement	Surasak Kaewpho
14.15-14.30	O-S1-42	323	A design of laser triangulation system with combined diffuse and specular reflection modes for dull and shiny surface measurements	Chaturaporn Kerdkaew
14.30-14.45	O-S1-43	347	Online monitoring and control of 3D printer with open source software and embedded systems	Piyachon Ketsuwan
14.45-15.00	O-S1-44	332	parison of an auto-regressive with exogenous variable (ARX) model to that of the artificial neural network (ANN) in simulating a solar vapour compression refrigeration Sy	Sattra Sirikaew
15.00-15.15	Coffee break			
	Chair: Dr. Monchai Jitvisate **Co-chair: TBA**			
15.15-15.30	O-S1-45	271	Investigation of plasma activated water in the growth of green microalgae (Chlorella spp.)	Prangnapat Silapasert
15.30-15.45	O-S1-29	272	Utilization of DBD plasma in shelf-life extension for climacteric fruits	Konkanok Udtachee
15.45-16.00	O-S1-46	371	The study of spin effects on the bouncing trajectory of a ball	Ai Tungsatitchai, Ratchaphon Noiaek
16.00-16.15	O-S1-48	291	A model for estimating global spectral solar radiation under all-sky conditions for Nakhon Pathom station Thailand	Sunisa Khakhu
16.15-16.30	O-S1-49	138	Hydrogen sulfide (H2S) detection system in risky areas with real-time display via smartphone	Wiphu Kitsamret

Oral Presentation

24-Jun-22
Symposium 3 (Room : AMBER)
Chair : Assoc Prof. Dr. Somsak Dangtip
Co-chair: Dr. Dhanaj Saengchantr

Time	Code	Abstract ID	Title	Speaker
9.00-9.15	INV-S3-2	334	Intense Helicon Plasma in the Thailand Linear Device	Assoc. Prof. Dr. Mudtorlep Nisoa
9.15-9.30				
9.30-9.45	O-S3-7	302	Design of Dipole Magnets for Siam Photon Source II	Prapaiwan Sunwong
9.45-10.00	O-S3-8	54	DESIGNING AND SIMULATION OF A LOW-ENERGY SINGLE ION IRRADIATION SYSTEM FOR BIOLOGICAL SAMPLE BOMBARDMENT	Prutchayawoot Thopan
10.00-10.15	O-S3-9	354	Specific activities of natural and anthropogenic radionuclides in organic Sungyod rice samples collected from Don Pradu sub-district in Pak Phayun district in Phatthalung province, Thailand	Prasong Kessaratikoon
10.15-10.30	Coffee break			
10.30-11.30	Plenary talk (Prof. Jianzhong Zhang) broadcast to all meeting rooms			
11.30-11.45	O-S3-10	301	G4beamline simulation for rotating telescope at SLRI BTF	Jetnipit Kaewjai
11.45-12.00	O-S3-11	327	Fabrication and development of neutron shielding materials based on natural rubber and boron carbide	Jittinun Saenpoowa
12.00-13.00	Lunch			

Chair : Assoc. Prof. Dr. Worawat Meevasana
Co-chair: Prof. Dr. Dheerawan Boonyawan

13.00-13.15	INV-S3-3	366	SPS-II: A 4th Generation Synchrotron Light Source in Southeast Asia	Dr. Prapong Klysubun
13.15-13.30				
13.30-13.45	INV-S3-4	364	Radioisotope Application for Plant and Process Inspection in Petroleum and Petrochemical	Dr. Dhanaj Saengchantr
13.45-14.00				
14.00-14.15	O-S3-12	121	Experimental study of radiolytic oxygen removal in irradiated water	Pharewa Karoon
14.15-14.30	O-S3-13	105	ELMs Dynamics Simulations Based on Bifurcation Approach	Danis Klanurak
14.30-14.45	O-S3-14	344	A feasibility study of using BNCT to treat Cholangiocarcinoma (CCA)	Yuwadee Malad

Oral Presentation

June 24, 2022
Symposium 4 (Room : QUARTZ)
Chair: Asst. Prof. Tirawut Worrakitpoonpon
Co-chair: Dr. Apimook Watcharangkool

Time	Code	Abstract ID	Title	Speaker
9.00-9.15 9.15-9.30	INV-S4-2	360	Highlights of LHC Run-2 and Preparation for Run-3 and High Luminosity LHC	Norraphat Srimanobhas
9.30-9.45	O-S4-9	115	Modification of hadron multiplicity ratios at the chiral phase transition	Thiranat Bumnedpan
9.45-10.00	O-S4-10	134	Non-minimal scalar field coupling to gravity with holographic effect in non flat universe	Amornthep Tita
10.00-10.15	O-S4-11	143	production of charged particles and the kaonic nuclei K-p, K+anti-p in pp collisions at √(s) = 7 TeV and K-pp, K+anti-pp in Au + Au collisions at beam energy 130	Natthaphat Thongyoo
10.15-10.30	Coffee break			
10.30-11.30	Plenary talk (Prof. Jianzhong Zhang) broadcast to all meeting rooms			
11.30-11.45	O-S4-12	159	Anisotropic flow in Au + Au collision at 1 A GeV by using Quantum Molecular Dynamics Model	Jiraphat Phusamlee
11.45-12.00	O-S4-13	162	Soliton Solution to Schamel-Korteweg-de Vries Equation with Shooting Method	Chainarong Taepanich
12.00-13.00	Lunch			

Chair: Asst. Prof. Dr. Norraphat Srimanobhas
Co-chair: Dr. Apimook Watcharangkool

13.00-13.15 13.15-13.30	INV-S4-3	359	High Energy Astroparticles from Antarctica	Waraporn Nuntiyakul
13.30-13.45	O-S4-14	170	he effectiveness of relativistic electron Acceleration at geosynchronous orbit during high-intensity, long-duration, continuous AE activity (HILDCAA) during 2015 -	Thana Yeeram
13.45-14.00	O-S4-15	240	sine-Gordon expansion method for the kink solion to Oskolkov equation	Songvudhi Chimchinda
14.00-14.15	O-S4-16	278	Bianchi Cosmological Model with Quadratic Equation of State	Bjorn Jasper Raquel
14.15-14.30	O-S4-17	293	Generalised Uncertainty Relations and the Problem of Dark Energy	Matthew J. Lake
14.30-14.45	O-S4-18	363	Geometrical representation of the multi-dimensional consistency : 1-form case	Thanadon Kongkoom
14.45-15.00	O-S4-19	12	Tension in rope coiling on a rotating plane	Sitichoke Amnuanpol
15.00-15.15	Coffee break			

Chair: Asst. Prof. Dr. Norraphat Srimanobhas
Co-chair: Dr. Apimook Watcharangkool

15.15-15.30	O-S4-20	14	Investigation of perturbation effects on the periastron shifts of stellar orbits around super-massive black hole	Bhattaradon Sukon
15.30-15.45	O-S4-21	23	The effect of AGN feedback on shape of dark matter haloes	Netipon Naree
15.45-16.00	O-S4-22	108	The potential scientific capabilities of the Evanescent Wave Coronagraph EvWaCo	Matthew Ridsdill-Smith
16.00-16.15				
16.15-16.30				
16.30-16.45				

June 24, 2022
Symposium 4 (Room : TOPAZ)
Chair: Asst. Prof. Dr. Siramas Komonjibda
Co-chair: TBA

Time	Code	Abstract ID	Title	Speaker
9.00-9.15	O-S4-24	179	\emph{Gaia} Early Data Release 3 peculiar velocity distribution of Galactic high-mass x-ray binaries	Pornisara Nuchvanichakul
9.15-9.30	O-S4-25	181	Analysis of the gamma-ray halo candidate 3HWC J1928+178 with Fermi-LAT data.	Supphakit Wiweko
9.30-9.45	O-S4-26	183	Investigation of Open Cluster NGC 7789 Using GAIA EDR3 Data	Princess Tucio
9.45-10.00	O-S4-27	195	Unveiling Circumstellar Structure of High-mass Protostars via Multiple Species of MASERs in KaVA-LP with EAVN	Koichiro Sugiyama
10.00-10.15	O-S4-28	147	Searching for dark matter with the Cherenkov Telescope Array.	Armelle Jardin-Blicq
10.15-10.30	Coffee break			
10.30-11.30	Plenary talk (Prof. Jianzhong Zhang) broadcast to all meeting rooms			
11.30-11.45	O-S4-29	151	Selection efficiency of galactic-scale outflow at z ~0.1: Imaging vs Spectroscopy	Kantapon Jensangjun
11.45-12.00	O-S4-30	238	Simulating AGN feedback and its evolution in galaxy mergers: case study for NGC 5252	Manus Boonmalai
12.00-13.00	Lunch			

Chair: Asst. Prof. Tirawut Worrakitpoonpon
Co-chair: TBA

13.00-13.15	O-S4-31	245	Earth microlensing zone: how safe is the Earth from long-range detection by other civilisations?	Supachai Awiphan
13.15-13.30	O-S4-32	246	The Development of the Astrophysical Laboratory for the Study of Interstellar Surface Chemistry	Chutipong Suwannajak
13.30-13.45	O-S4-33	259	A Computational Study of the Gas-Phase Formose-Like Reactions under the Interstellar-medium-like conditions	Pitch Wongkummoon
13.45-14.00	O-S4-34	299	Thai National Telescope pointing and tracking: An analysis using secondary data product from science observation	Puji Irawati
14.00-14.15	O-S4-35	303	Discovery of tsunami-like pulsation waves in the very fast rotating A-type stars	David Mkrtichian
14.15-14.30	O-S4-36	349	Mock HI-galaxy catalogs and HI Mass Functions for future large-scale surveys	Narenrit Thananusak
14.30-14.45	O-S4-37	36	The Hubble tension problem with variation of the speed of light from Pantheon supernova dataset	Teeraparb Chantavat
14.45-15.00	O-S4-38	79	Improving Constraint on Evolution of Galaxies with Large-scale Outflow at z<1.5 with Subaru/Hyper Suprime-Cam Survey	Suraphong Yuma
15.00-15.15	Coffee break			

Chair: Asst. Prof. Tirawut Worrakitpoonpon
Co-chair: TBA

Time	Code	Abstract ID	Title	Speaker
15.15-15.30	O-S4-41	256	Study on halo structure of Helium-6 nuclei	Chanatip Yensoung
15.30-15.45	O-S4-42	172	Multi-frequency variabilities: blazar classification and statistical properties	Rattanapong Yoyponsan
15.45-16.00	O-S4-43	169	Photometric Variability of High Amplitude Delta Scuti Stars from AAVSO International Database	Nareemas Chehlaeh
16.00-16.15				

June 24, 2022
Symposium 4 (Room : RUBY)
Chair: Dr. Sorawis Sangtawesin
Co-chair: TBA

Time	Code	Abstract ID	Title	Speaker
15.15-15.30	O-S4-39	160	A Study of Unidirectional Gradient of Galactic Cosmic Ray Intensity at Different Cut-off Rigidities and Solar Magnetic Polarities	Cherdchai Wuttiya
15.30-15.45	O-S4-40	164	Spectrum of H-atom in Gravitational Waves from Black Hole Binary	Nontapat Wanwieng

Oral Presentation

June 24, 2022
Symposium 5 (Room : RUBY)
Chair: Dr.Sojiphong Chatraphorn
Co-Chair: Dr.Thiparat Chotibut

Time	Code	Abstract ID	Title	Speaker
9.00-9.15 9.15-9.30	INV-S5-2	361	Quantum Simulation via Quantum Gas Microscope	Pimonpan Sompet
9.30-9.45	O-S5-9	254	Active vibration isolator using piezoelectric actuator	Nuttanan Tanasanchai
9.45-10.00	O-S5-10	307	Atomic Vapor Glass Cell Fabrication for Quantum Experiment	Apiwit Kaewko
10.00-10.15	O-S5-11	283	OBSERVATION OF ZEEMAN SPLITTING IN RUBIDIUM ATOMS USING DOPPLER-FREE SATURATED ABSORPTION SPECTROSCOPY	Prin Insang
10.15-10.30	Coffee break			
10.30-11.30	Plenary talk (Prof. Jianzhong Zhang) broadcast to all meeting rooms			
11.30-11.45	O-S5-12	106	Design and implementation of a laboratory prototype of a fiber-fed Fourier transform spectrograph for the Thai National Telescope	Pornapa Artsang
11.45-12.00	O-S5-13	264	Design and analysis of Hollow-core fiber with anti-resonant structure for Ethylene Detection	Kwanjira Joonmasa
12.00-13.00	Lunch			

Chair: Dr.Sojiphong Chatraphorn
Co-Chair: Dr.Rachsak Sakdanuphab

13.00-13.15 13.15-13.30	INV-S5-3	367	Towards the Optical Second: The next generation of Thailand Standard Time	Piyaphat Phoonthong
13.30-13.45	O-S5-14	63	Quantum Diamond Spectrometer for Magnetic Field Sensing	Napoom Thooppanom
13.45-14.00	O-S5-15	21	Optically Detected Electron Spin Resonance in Diamond for Vector Magnetometry	Rapeephat Yodsungnoen
14.00-14.15	O-S5-16	43	Performance comparison of Amplitude-decorrelation and Speckle Variance algorithms for OCT Angiography	Wuttikorn Kampong
14.15-14.30	O-S5-17	294	Quantum diffusion map for nonlinear dimensionality reduction	Apimuk Sornsaeng
14.30-14.45	O-S5-18	137	Determination of phase change correction on gauge block measurement in two different interferometric measurement system	Angkoonna Pringkasemchai

Contents

(Click on the title to see the details of abstract)

Plenary talk - Board: PL−1 / **373**

Material Engineering toward High Performance Perovskite Solar Cells and Modules

Author: Hiroshi Hasegawa[1]

[1] *Institute of Space and Astronautical Science, JAXA*

Corresponding Author: hase@stp.isas.jaxa.jp

Organometal halide perovskites have captured wide interest as a promising material for lightweight and high-efficiency solar cells. Through recent studies of the organometal halide perovskite solar cells (PSCs), the composition of organometal halide perovskites is recognised as one of the key factors in the improvement of the PCE. In this study, we investigated mixed cation perovskite absorber. The results revealed that incorporating a small amount of K^+ into the double organic cation perovskite absorber ($FA_{0.85}MA_{0.15}Pb(I_{0.85}Br_{0.15})_3$) improved the photovoltaic performance of PSCs significantly, and K^+ incorporation diminished I-V hysteresis. Consequently, the 0.187 cm^2 PSC of 22% power conversion efficiency (PCE) without I-V hysteresis were constructed. The crystal lattice of the organometal halide perovskite was expanded with increasing of the K^+ ratio, where both absorption and photoluminescence spectra shifted to the longer wavelength, suggesting that the optical band gap decreased. It is concluded that stagnation-less carrier transportation could minimise the I-V hysteresis of PSCs. Additionally, we successfully constructed 2.76 cm^2 monolithic PSC mini-module of 20.5% PCE without I-V hysteresis. In the case of MA-free PSCs, the 24.9% PCE (0.187 cm^2) and 21.6% PCE (2.76 cm^2 monolithic PSC mini-module) were obtained, respectively.
On the other hand, the micro-structural aspects within the organometal halide perovskite are still unknown, even though it belongs to a crystal system. In this study, direct observation of the microstructure of the thin film organometal halide perovskite using transmission electron microscopy was investigated. Unlike previous reports, it is identified that the tetragonal and cubic phases coexist at room temperature, and it is confirmed that superlattices composed of a mixture of tetragonal and cubic phases are selforganized without a compositional change. The organometal halide perovskite self-adjusts the configuration of phases and automatically organizes a buffer layer at boundaries by introducing a superlattice. These results shows the fundamental crystallographic information for the organometal halide perovskite and demonstrates new possibilities toward high performance perovskite solar cells.

Keywords: organometal halide perovskite, perovskite solar cell, tetragonal, cubic, superlattice

Plenary talk - Board: PL-2 / **369**

Advanced Organic Luminescent Materials for Efficient Organic Light-Emitting Diodes

Author: Vinich Promarak[1]

[1] *Vidyasirimedhi Institute of Science and Technology (VISTEC)*

Corresponding Author: vinich.p@vistec.ac.th

In the past decades, organic light-emitting diodes (OLEDs) have been well commercialized due to the maturity of fluorescent (1^{st} generation) and phosphorescent (2^{nd} generation) emissive materials. However, both materials still are not perfect emitters for OLEDs. Recently, the 3^{rd} generation of organic light-emitting materials has been developed by combining the key advantages of the 1^{st} generation materials: simple structure and low cost and the 2^{nd} generation materials: capable of up to 100% intrinsic quantum efficiency (IQE) due to its emission from both singlet and triplet excitons. The 3^{rd} generation emissive materials still retain the basic structure of the 1^{st} generation organic molecule, but they are structurally modified at the molecular level to harvest additional light emissions from triplet excitons, giving rise to high IQE, simple molecular structure, and low-cost emissive material. In this talk, I will focus on our recent developments in 3^{rd} generation of organic luminescent materials capable of producing high IQE *via* several mechanisms, including thermally activated delayed fluorescence (TADF), hybridized local and charge-transfer excited state (HLCT), triplet-triplet annihilation (TTA), excited-state intramolecular proton transfer (ESIPT) and aggregation-induced emission (AIE) for high-performance organic light-emitting diodes (OLEDs). Our latest achievement in developing and utilizing fluorescence metal-organic framework (MOF) as advanced luminescent materials for OLEDs will be discussed. Finally, the study and development of novel solution-processable luminescent materials in which the essential elemental functions of an OLED, namely an intense solid-state light emission, electron/hole injection and transport capabilities, and solution-processability, would be incorporated by design into a single molecular architecture, will be illustrated. Some examples of solution-processable emissive materials will be discussed in terms of the structure-property relationships, with particular attention to the molecular design that affects the OLED device performance.

Keywords: organic luminescent materials, organic light-emitting diodes (OLED), thermally-activated delayed fluorescence (TADF), hybridized local and charge-transfer excited state (HLCT), triplet–triplet annihilation (TTA), solution-processable luminescent materials, fluorescence metal-organic framework (MOF)

Plenary talk - Board: PL–3 / **378**

A carbon-neutral intelligent energy system using hydrogen technologies and big data

Author: Manabu Ihara[1]

[1] *Dept. of Chemical Science and Technology, Tokyo Institute of Technology, Tokyo Tech "InfoSyEnergy consortium", Tokyo Tech Academy of Energy and Informatics*

Corresponding Author: mihara@chemeng.titech.ac.jp

Controlling global warming is an essential social issue that humankind must solve in the future. With the Paris Agreement at COP21 (21st Conference of the Parties to the United Nations Framework Convention on Climate Change), Many countries try to limit future temperature rises to 1.5-2 ° C or less compared to pre- industrial levels. Furthermore, we are aiming to "pursue the 1.5 ° C effort target" agreed in November 2021 at COP26 in Glasgow, UK. In order to achieve such extremely high reduction targets, it is necessary to accelerate research and development in the energy field.
Tokyo Tech "InfoSy**Energy** consortium" and "Academy of Energy and Informatics" were established as global research / education organization for industry-academia collaboration toward carbon-neutral society to develop the energy technologies by utilizing energy science and informatics. Twenty-five companies and 16 overseas universities are the members including over 70 Tokyo Tech professors and associate professors.
In the presentation, I will firstly explain the importance of nine priority research fields in InfoSy**Energy** toward carbon neutrality, which are (1) Distribution energy systems controlled by using energy big data, (2) Technology for Renewable energy base-load, (3) Solar energy conversion, (4) Fuel cells, electrolysis, hydrogen energy, battery„,energy storage, (5) Energy economy, Electricity free market, (6) Energy carriers, low carbon process by catalysts, (7) Hydrogen combustion, heat utilization, (8) Future energy technologies and (9)Tech trends, future scenarios, services in energy sector. I also introduce the present developmental status of the grid cooperated/distributed energy system named as "*Ene-Swallow*" using big data and required hydrogen technologies like solid oxide fuel cell/electrolysis cell, and finally introduce "carbon air battery system" developed as an original energy storage system.

Keywords: energy system, big data, renewable energy, carbon neutrality, hydrogen energy, energy device

Plenary talk - Board: PL-4 / **362**

Specialty optical fibers and Its manufacture technology

Author: Jianzhong Zhang[1]

[1] *College of Physics and Optoelectronic Engineering, Harbin Engineering University, Harbin, 150001, China*

Corresponding Author: zhangjianzhong@hrbeu.edu.cn

Optical silica fiber demonstrated its priority in communications, which make a global village become a reality. It was predicted as a long term and irreplaceable communication technology. However, Internet of anything and big data are requiring the huge bandwidth and challenging the development speed of optical fiber communications. New All-wave fiber makes the O-L band transmission with low loss possible. Broadband optical fiber devices become the bottleneck. New designed active optical fiber with the O-L broadband emission and their 3D printing based manufacture technology are developed to supply the broadband demand and given in this talk.

Poster: S1 Physics innovation - Board: P-040 / **126**

Measurement and analysis of sound frequencies in beehive with smart electronic sensor systems for health status monitoring and specific behavioral study from native bees (Apis cerana Fabricius, 1758) for non-migratory beekeeping in the safe agricultural area

Authors: KHEMIKA INTARASUWAN[1]; NIYOM HONGSITH[1]; SOMRIT UNI[1]; SUKANYA KUMNIMIT[1]; SUPHANSA CHANSURIYA[1]; WUTTIKORN WONGTHONGTHIW[1]

[1] *Department of Physics, University of Phayao*

Corresponding Author: suphansa.ch@up.ac.th

Bees are well known as social insects with divisions of labor. In a dark beehive, it was long thought that communication within the hive was based on chemical signals. However, specific sound signals have been identified, and science is beginning to decode what the bees are signaling in the beehive. This work has developed a sound frequency monitoring system from native bees (*Apis cerana Fabricius, 1758*) based on the Arduino board and NB-IoT module. Sound samples have been acquired using mini microphones and placed inside the beehive with some environmental parameters acquisition, such as temperature and humidity at the same time. The signal voltage in the time domain was received and converted to the frequency domain using a fast Fourier transform (FFT) and sent data to cloud storage every minute for a week. The range frequencies of the acoustic signals produced by a honey bee colony are in the range of 10 to 1 kHz. The first (1^{st}), second (2^{nd}), and third (3^{rd}) frequencies of sound have been studied. However, most of the sound frequencies may change with time, temperature, and humidity, probably owing to specific behavior. Finally, the sound produced by ventilating workers as a function of the period time, temperature, and moisture has been identified. As a result, this intelligent electronic sensor system could be potentially applied for health status monitoring for non-migratory beekeeping on farms.

Poster: S1 Physics innovation - Board: P001 / **365**

Carbon Neutralization of Sugarcane by Super Farm Model

Authors: Kanittha Pamonpol[1]; Natsima Tokhun[None]; Nopparat Wairojjana[None]; Weerasak Srirarat[None]; Weerawat Ounsaneha[None]

[1] *Faculty of Science and Technology, Valaya Alongkorn Rajabhat University under the Royal Patronage, Pathum Thani*

Corresponding Author: kanittha@365.vru.ac.th

Climate change and global warming are main global problems. Greenhouse gases are released from various human activities, including agricultural practices from open burning in the field. Sugarcane leaves combustion generated air pollution problem during dry season every year. This research aims at balancing carbon in sugarcane field to consider carbon released from sugarcane leaves burning and propose Super Farm Model to reduce global warming effect. Carbon neutralization was considered by considering input and output biomass in the sugarcane field. The field survey and interview were conducted to obtain agricultural practices. Fraction of burned biomass was analyzed from burned sugarcane production reported by Office of the Cane and Sugar Board. Carbon emission was analyzed by specific emission factor to the sugarcane leaves burning to consider global warming potential from sugarcane field. The alternative solution of global warming emission from open burning of sugarcane residues was proposed by Super Farm Model.

Poster: S1 Physics innovation - Board: P002 / **270**

STUDY OF PLASMA ACTIVATED WATER AND SECONDARY EFFECTS ON WATER USING GAMMA RADIATION WITH FTIR IN SEEDS GERMINATION

Authors: Aonkaet Somjaimak[1]; Keratiya Janpong[1]; Sakhorn Rimjaem[2]; Kittikhun Prakrajang[1]; Sureeporn Sarapirom[3]

[1] *Maejo University*

[2] *Chiang Mai University*

[3] *Maejo University*

Corresponding Author: aonkate.9305@gmail.com

Plasma activated water (PAW) and gamma radiation has intensively been used in many agricultural applications which includes increasing the germination rate, promoting plant growth. However it is important to pay attention to the both effect of PAW and gamma radiation to study the detailed characteristics of chemical composition of tap water and distilled water stimulated by plasma and gamma radiation on seed germination by Fourier transform infrared spectroscopy (FTIR) technique and optical emission spectroscopy (OES). In this work, plasma and gamma radiation were utilized to prepare water for seed germination. Plasma activation and gamma radiation are treated on both tap water (TW) and distilled water (DW) with 2.5, 5.0,7.5 and 10.0 sec. The experiment shows the chemical compound of oxygen and nitrogen species diffused through the water such as O_3, NO_2, NO, NO_3, HNO_3, HNO_2 and H_2O_2. Plasma activation and Gamma radiation were utilized to modify both tap water and distilled water in this work. The plasma activation and gamma radiation may cause reactive oxygen and nitrogen species (RONS) which could be favorable for the germination of seeds.

Keywords: Plasma Activated Water, Air plasma, Gemination rate, Gamma radiation

Poster: S1 Physics innovation - Board: P003 / **345**

Isotropic and Anisotropic Materials Characterization Technique by Polarization Sensitive Optical Coherence Tomography

Authors: KUNAKORN PALAWONG[None]; Panomsak Meemon[1]

[1] *Suranaree University of Technology*

Corresponding Author: k.palawong@gmail.com

Isotropic and anisotropic are type of materials, which is considered from the structural nature of the material with a symmetry and asymmetry structure, respectively. The structure can affect the optical properties of different materials. Due to the symmetrical structure of the material, there will be no effect on the incident polarized light, different from asymmetrical materials. It affects polarized light by causing a change in polarized light. Therefore, the type of material can be determined by the polarized light changed from the material. In this paper, we would like to present a material characterization technique by polarization sensitive optical coherence tomography technique. This technique is cross-sectional imaging by measuring the change in polarized light reflected from a sample material. The example as cover slide glass, plastic tape and double-sided adhesive are presented. The experimental results verified that PS-OCT can analyze the symmetry and asymmetry structure of the materials.

Keyword: polarization sensitive optical coherence tomography, PS-OCT, isotropic, anisotropic

Poster: S1 Physics innovation - Board: P004 / **341**

Development of a low budget and compact Optical Coherence Tomography at 840 nm wavelength region for 3D imaging of biological tissues

Authors: Jadsada Saetiew[None]; Jiraporn Saenjae[None]; Panomsak Meemon[1]

[1] *Suranaree University of Technology*

Corresponding Authors: saetiew@g.sut.ac.th, aomjae.domon@gmail.com

Optical coherence tomography or OCT is an optical imaging technology that is capable of high-speed three-dimensional cross-sectional imaging of samples, such as biological samples as well as other transparent media, at high resolution. Most importantly, OCT can be operated at a light wavelength in near-infrared region with a low illumination power of a few milliwatts. Therefore, OCT is a non-destructive and non-invasive imaging technique that has potential for large area of applications in biology, biomedical science, agriculture, as well as in material science. In this work, we present a custom design and implementation of a portable OCT prototype that aims for low budget, compact size for field operation. For this purpose, the system has been designed at an operating wavelength of around 840 nm. The prototype was designed in the form of microscope setup. The implementation was based on all commercially available optical components. To the current progression, the developed prototype can perform depth cross-sectional imaging of up to 2 mm from the sample's surface. The maximum imaging speed is about 20 frames per second for the image size of 1000 depth scans per frame as limited by the speed of the detection unit. The depth resolution and lateral resolution of the developed system were measured to be about 10 microns and 10 microns, respectively. The prototype has been used for 3D imaging of several biological samples. Some imaging results will be presented and discussed.

Poster: S1 Physics innovation - Board: P005 / **337**

Development of Low-Cost Automatic Groundwater Level Measurement System Based on The Internet of Things

Author: Chalermpong Polee[1]

Co-authors: Chakrit Saengkorakot ; Kiattipong Kamdee ; Manit Jitpukdee [2]; Monthon Yongprawat ; Nichtima UAPOONPHOL ; Patchareeya Chanrueng ; Sasiphan Khaweerat

[1] *Thailand Institute of Nuclear Technology*

[2] *Kasetsart University*

Corresponding Author: chalermpong@tint.or.th

Monitoring of groundwater fluctuations is mandatory in order to evaluate the groundwater resources and develop groundwater management solutions. In particular, the area has intensively groundwater demand such as the upper Chao Phraya River basin. We have developed an automated groundwater level measurement system that integrates the real-time measurement system, automatic data transfer, data recorder and data processing. A pressure sensor probe was used to measure the groundwater pressure. Its real-time signal was transferred along a cable to a microcontroller box, which was installed at the base station module beside the borehole. The microcontroller box processed the data to be ground water level. Then the processing data will be sent wirelessly to the management central system through a telephone network, the IOT (Internet of Things). In general, a borehole is located in rural area with limited access to electricity. Therefore, the developed system was designed to use a small amount of electricity which is sufficiently generated by the solar cell system. The developed system cost approximately 20,000 baht (600 dollars) in total. By comparing the data of groundwater level from the developed system to the manual measurement system, it was found that the developed system provided an error of 1 %. Finally, we can conclude that the low-cost developed system provided real-time data with accuracy measurement. However, the groundwater level data from this developed system will be compared to the amount of precipitation in order to prepare a more accurate groundwater database.

Poster: S1 Physics innovation - Board: P007 / **335**

Development of food packaging materials from rice straw waste and sugarcane residue by hot pressing

Authors: Pongsak Jittabut[1]; Pakpoom Buabthong[1]

Co-authors: Julara Pornmanee [1]; Benyapa Chueakamchan [1]

[1] *Nakhon Ratchasima Rajabhat University*

Corresponding Author: pakpoom.b@nrru.ac.th

The increase in demand for renewable materials and strict regulations on organic waste are pushing the food packaging industry toward more sustainable alternatives. Agricultural waste, namely, rice straw and sugarcane residue, is one of the promising replacements for the traditional synthetic polymer in food packaging applications because of its biodegradability, low cost, and low carbon emissions. Herein, we present the procedure to develop food packaging materials from rice straw and sugarcane residue using the hot-pressing technique. The resulting materials were then characterized by water absorption, material density, tensile strength, and the outgassing of CO2. Rice straw and sugarcane residues produce the highest-density materials when pressed at 200℃ for 200 s and 230℃ for 230 s, respectively. The outgassing of CO2 in both rice straw and sugarcane waste was substantially lower than that of the traditional synthetic polymer-based food packaging.

Poster: S1 Physics innovation - Board: P008 / **331**

Analysis of temperature oscillations due to low current in a circuit of a resistor and a thermostat's bimetallic plate

Authors: Tanapat CHANSAENG[None]; Supphanat Anantachaisophon[1]; Witchukorn PHUTHONG[None]

[1] *Kamnoetvidya Science Academy*

Corresponding Author: tanapat.chans@ku.th

Oscillations have been well-studied in many branches of physics due to their periodic behavior and the solution compactness of the solutions, which allows a variety of applications. In addition to electromagnetic or mechanical oscillation experiments usually available in the university or high school physics laboratories, the setup that undergraduate students can explore the oscillation of other parameters, especially those that involve direct observation, would engage their learning. The safer (e.g., from electrical hazards) the apparatus is, the more widely it would be adopted. Here, we present a simple circuit of a resistor exchanging heat with a thermostat, creating a temperature oscillation with an ultra-low frequency. We propose an analysis that considers the dynamics of carefully chosen bimetallic plates of the thermostat and the heat transfer between the two components. The model during oscillations comprises two phases: (i) temperature rising in the closed circuit and (ii) temperature dropping in the open-circuit configuration. Our setup achieves the ultra-low frequency of 5-50 mHz at the working current of < 1A. Furthermore, we also found a relatively good agreement between the observed and predicted frequencies. This work highlights the importance of equipment selection that eases the demonstration of a niche oscillation phenomenon that student can comprehend and apply the physical concepts.

Poster: S1 Physics innovation - Board: P009 / **330**

Spectrophotometer based on light-emitting diode(LED) for DOBI measurement for crude palm oil quality control

Authors: Karaket Wattanasit[None]; Suttirak Kaewpawong[1]; Mudtorlep Nisoa[None]

[1] *Plasmas and electromagnetic waves research laboratory, Walailak University*

Corresponding Author: nmudtorl@mail.wu.ac.th

Modern analysis for absorbed of organic chemistry is very popular both in industrial laboratories. In general use a UV-VIS spectrophotometer, which a light source for gas. Each wavelength can be measured with high precision but UV-VIS spectrophotometer dispersing Devices system complex light. To import from abroad the country and most expensive because of advances in the development of a LED light source. The wavelength of light depends on the optical semiconductor material wavelength from UV (ultraviolet) to IR (infrared). A research study will compare the ratio absorption of light at a wavelength at 269 nm of palm oil. When using Full Width value light at Half Maximum (FWHM) is different from a UV-VIS spectrophotometer has a value of 2 nm FWHM and light from LED at 40 nm FWHM values. A difference in absorption is associated with functions of palm oil for Interactions between light and function.

Poster: S1 Physics innovation - Board: P010 / **326**

Development of magnetically well-type plasma torch for high-temperature process

Author: Ridhvee Taleh[None]

Co-author: Mudtorleb Nisoa

Corresponding Author: ridhvee@gmail.com

The 30 kW DC plasma torch system with the well-type cathode (WTC) has been developed to generate thermal plasma above 1200 0C, which is adding the external magnetic coil on the cathodic part of the torch. The well-type torch is hollow cylindrical copper's 5 mm thickness, whose cathode electrode and anode electrode was 150 mm in each length, the diameter is 22 mm through the center, The gap between both electrodes is 1.5 mm isolated with a swirl gas ring. Under the experimental conditions at 0.5 - 0.8 MPa compressed air is applied to both sides of the torch, the airflow rate is 60 L/min and 120 L/min from the sides, and above, as followed. the thermal plasma has been generated, their maximum current is 200 A and 160 V, the length is about 30 cm, its diameter about 3 to 5 cm wide, recognized UV emission has been present. In this work, the 500 G of the magnetic field produced by an external solenoid has been developed, to drive the arc root and reduce the cathode erosion damage. The result shows the necessity of a magnetic field, a rotational arc root inside the cathode surface, and electrode life hours are compared with the case of un magnetic field-driven has been present. Finally, the knowledge of this work to extend electrode life and applied to the system to be suitable for the disposal of infectious wastes.

Poster: S1 Physics innovation - Board: P011 / **324**

Characteristics of plasma activated water (PAW) produced by moderated pressure RF discharges

Authors: Karaket Wattanasit[1]; Mudtorlep Nisoa[1]; Suttirak Kaewpawong[1]

[1] *Plasmas and electromagnetic waves research laboratory, Walailak University*

Recently, plasma activated waters (PAW) have been investigated intensively for sustainable agriculture and post-harvest technology. The waters can be used effectively as green fertilizers, decontamination agent and green pesticides, while no harmful by products left over[1-2]. The acidic characteristics of the PAW, resulted from nitrate and hydrogen peroxide, can produce high germination rate of various seeds[1,3]. In this work, PAW produced by RF cold atmospheric plasma in moderated pressure will be presented. The plasma is generated in closed chamber, whereas part of the chamber volume was filled with water. The floating electrode, made of tungsten rod and inserted in the Pyrex glass tube, is powered by RF power supply of 7 – 9 kV and 50 – 800 kHz. The plasmas, generated above the water surface, for production of PAW. Various characteristics of large volume PAW for the setup will be discussed.

Poster: S1 Physics innovation - Board: P012 / **209**

STRAIGHTNESS MEASUREMENT BY REVERSAL METHOD

Author: Watcharin Samit[1]

Co-author: Ketsaya Vacharanukul [1]

[1] *National Institute of Metrology (Thailand)*

Corresponding Author: watcharin@nimt.or.th

Straightness measurement is an important parameter of dimension metrology. It is widely used in various instruments and machines especially in the industrial segment such as rulers, CNC machines, theodolites and infrastructures. At the moment, there are not have high performance straightness measuring system in Thailand because there is no approved calibration system. This leads to a questionable performance of the straightness in the instruments and machines. We have developed the self-calibration straightness method to solve this problem. It consists of straightedge and straightness measuring machine. The measurement principle of a self-calibration is based on the Reversal Method. The system provides the uncertainty of measurement of 0.6 micrometer per meter. The system can be used to validate and to evaluate straightness instruments.

Poster: S1 Physics innovation - Board: P013 / **184**

Exploring Spratly Islands using VIIRS Boat Detection Satellite Image Analytics

Authors: Gian Paulo Santos[1]; Ryan Manuel Guido[None]

[1] *Rizal Technological University*

Corresponding Author: rmdguido@rtu.edu.ph

We provide a method for evaluating the feasibility of monitoring or estimating island activities carried out by dredgers and support boats in the Spratly Islands region using VIIRS Boat Detection data, salient to other countries having their claims, especially the Philippines. From 2012 to 2020, an annual summary grid for VIIRS Boat Detection was utilized to compare the number of VBD detections and their average radiance with remote sensing satellite photos in Spratly. This article described the temporal history of detected light from boats between 2015 and 2020, demonstrating an increase in brightness and a rise in the number of boats identified. Satellite photographs collected by the GeoEye-1 satellite revealed an increase in the number of dredging vessels on several islands, including Mischief Reef, Fiery Cross Reef, and Subi Reef. The increase in light reported from boats in the Spratlys and the developed reclaimed islands occurs at the same time. Indicating a forced dominance of the maritime sovereignty and non-obedience to the United Nations Convention on the Law of the Sea (UNCLOS). This study could also be used for policy-making on the borders of the Philippines.

Poster: S1 Physics innovation - Board: P014 / **90**

A simple pendulum study using a smartphone video camera

Authors: Jarupat Disrattakit[1]; Pranee Disrattakit[None]

[1] *Srinakharinwirot University*

Corresponding Authors: jarupat@g.swu.ac.th, pranee.dis@mwit.ac.th

In general, a simple harmonic motion is studied by measuring and recording the time required for the bob to complete a cycle. In addition, many experiments use smartphone or motion sensor to measure the motion. This method requires the installation of additional equipment into the system, and thus the moment of inertia of the system involves in those devices. In this study, we present the new method for measuring the angular frequency and maximum angular position. In the method, the motion of a simple pendulum is recorded by a smartphone video camera. The video is analyzed by the software (Tracker). From the video, the relationship between angular position and time is represented the sinusoidal pattern. Therefore, the maximum angular position and angular frequency are received by fitting the sinusoidal pattern. Furthermore, the frequency, period, and acceleration due to the gravity are calculated from the angular frequency. The result shows that the new method is as good as the general methods. Furthermore, the new method can also be applied to the complicated systems as well.

Poster: S1 Physics innovation - Board: P015 / **281**

Estimation of solar radiation and optimum tilt angles for south-facing surface in Nakhon Pathom and Chiang Mai stations

Author: Rungrat Wattan[1]

Co-authors: Baramee Klinkhajohnsak [1]; Titisuda Tungsub [1]; Sumaman Buntoung [1]; Somjet Pattarapanitchai [1]

[1] *Department of Physics, Faculty of Science, Silpakorn University*

Corresponding Author: rungrat.wattan@gmail.com

In this research, optimum tilt angles for south-facing surface obtaining the highest solar energy in Nakhon Pathom (13.82 N, 100.04 E) and Chiang Mai (18.78 N, 98.98 E) stations were estimated for monthly, seasonal and annual basis. The solar radiation incident the inclined surface consists of beam radiation, sky diffuse radiation and reflected radiation. Liu & Jordan (1962) model and Iqbal (1983) model were selected to calculate sky diffuse radiation on tilted surfaces using diffuse radiation on horizontal surface and reflected radiation on tilted surface. Beam radiation on tilted surface was calculated from beam radiation on horizontal surface and beam conversion factor. The solar radiation on horizontal surface measured at the two stations were used for over a period of 5 years (2014-2018). The daily total solar radiation (in MJ/m^2-day) for an inclined surface is calculated every 0.2 degrees from 0-90 degrees. The total solar radiation on tilted surface based on monthly, seasonal and annual optimum tilt angles at Chiang Mai and Nakhon Pathom stations were performed. For the analysis results, annual optimum tilt angle for Chiang Mai and Nakhon Pathom stations was found as 18.9 and 14.5 degrees, respectively. Estimated gains in annual average solar radiation based on monthly, seasonal and annual optimum tilt angles in comparison to a horizontal surface were 11.95%, 10.53% and 6.11% for Chiang Mai, and 6.20%, 5.42% and 1.98% for Nakhon Pathom, respectively. The solar energy losses of 1.27% and 5.22% (for Chiang Mai) and 0.74% and 3.98% (for Nakhon Pathom) were occurred when compared the solar energy on the seasonal and annual optimum tilt angle surfaces, respectively, with that on the monthly optimum tilt angle surface. Therefore, from the result, the inclined surface should be tilted on monthly or seasonal optimum tilt angle for better utilization of solar energy.

Poster: S1 Physics innovation - Board: P016 / **277**

The development of smart farm systems by controlling via the internet

Authors: Piriya Praneekit[None]; Pongsathorn Kongkaew[1]

Co-author: Thanin Rudchapo [2]

[1] *Program of Physics, Faculty of Science and Technology, Rajabhat Maha Sarakham University.*

[2] *rajabhat maha sarakham*

Corresponding Author: piriya.pr@rmu.ac.th

The aim of this research was developed for agriculture by using internet technology to control plant growth factors with automation. Plants are planted in greenhouses to facilitate control of various factors affecting plant growth. A greenhouses dimension of 2 meters width, 3 meters length, 2 meters high, and the volume is 10.5 cubic meters. The greenhouses are covered with plastic to prevent insects. However, this will result in an increase in the temperature inside the greenhouse. Therefore, an exhaust fan and spray unit are installed in the house to help reduce the temperature. In addition, a temperature sensor is installed to determine the operation of the fan and spray unit. There was also a soil moisture sensor be used to compare the optimum moisture to the actual humidity to control the soil moisture according to plant growth.

The temperature sensor was calibrated by comparing the temperature measured by the sensor with the temperature measured by a thermometer. The statistical results showed that there was no significant difference between the temperature measured by the sensor and the thermometer. The temperature control capability was then tested by measuring the temperature both outside and inside the house. The result was no difference, indicating that the temperature was well controlled. Kale growth was compared between kale grown in greenhouses and kale grown outdoors. The results showed that the overall growth in the first period was not different and the later period of kale grown in the greenhouse showed better growth.

Poster: S1 Physics innovation - Board: P017 / **276**

Effect of Drying Temperature on Color Change of Green Banana Flour under Infrared Radiation Heating

Author: Suminya Teeta[1]

Co-authors: Mali Sarobol [1]; Ploypailin Promdonkloy [1]

[1] *Rajabhat Mahasarakham University*

Corresponding Author: suminya99@gmail.com

The objective of this study was to investigate the effects of three drying temperatures (55, 60, and 65 ℃) on the quality attributes of green banana flour (color change) and process variables (drying time, rate of drying). The banana was used in ripeness stage 2 (green with a trace of yellow). Experiments were conducted using far-infrared power of 3000 watts. The drying process reduced the moisture content down to between 10 and 12 % d.b. The lightness (L*) and yellowness/blueness (b*) decreased with the increase in temperature from 83.40±0.39 to 82.44±0.76 and 17.70±0.52 to 10.24±0.85, respectively. However, the redness/greenness (a*) value increased from 0.32±0.15 to 0.50±0.53. The lowest total color change (ΔE) was obtained at a drying air temperature of 65 ℃, then 60 ℃, and finally 55 ℃ with a drying time of 210, 300, and 330 minutes, respectively. Thus, drying temperature and dying time had a great effect on the total color change of dried banana flour. Drying at the temperature of 65℃ provided a browner product color than the other drying temperatures, as manifested by the lowest lightness and hue values. The changes in hue angle values were not significant ($P<0.05$) compared to drying temperatures.

Poster: S1 Physics innovation - Board: P018 / **275**

Efficacy of vermicompost on growth and yield of organic rice with the participation of farmer groups to create a model community network in Roi Et and Maha Sarakham provinces

Author: Pongsathorn Kongkaew[1]

Co-author: Mali Sarobol [2]

[1] *Program of Physics, Faculty of Science and Technology, Rajabhat Maha Sarakham University.*

[2] *Rajabhat Mahasarakham University*

Corresponding Authors: sanawong_14@hotmail.com, tockatod@hotmail.com

The objective of this study aimed to investigate the effect of vermicompost on organic rice production. The experiment was conducted at Posai subdistrict, Sri-somdet district in Roi-Et province and Maung district in Maha Sarakham province. The experimental design was Randomized Complete Design (RCD) with 3 replications. The experiment consisted of 6 treatments as followed: 1) Rice berry without fertilizer 2) Red jasmine rice without fertilizer 3) Rice berry with vermicompost 4) Red jasmine rice with vermicompost 5) Rice berry with chemical fertilizer and 6) Red jasmine rice with chemical fertilizer. The results showed that there was no significant difference (P 0.05) in plant height, leaf length, leaf width, fresh weight, dry weight and yield weight among treatment. The results of the study found that Plant height, leaf length, number of shoots per clump, and seed weight of rice berry and red jasmine rice applied with earthworm manure there were statistically significant differences (P 0.05) and higher values for all experimental conditions. And from the research results, farmers in the community realized the importance of using vermicompost and can create a model community for other interested communities to study and learn extensive exchange of experiences.

Poster: S1 Physics innovation - Board: P019 / **273**

Moina macrocopa culture using plasma activated water (PAW)

Authors: Nichanun Neamtad[1]; Chokchai Yatongchai[2]; Sureeporn Sarapirom[1]

[1] *Maejo University*

[2] *Maejo University*

Corresponding Author: n.earth13081@gmail.com

***Moina macrocopa* culture using plasma activated water (PAW)**

Nichanan Neamtad[a], Chokchai Yatongchai[b] and Sureeporn Sarapirom[a]*

[a]Applied Physics, Faculty of Science, Maejo University, Chiang Mai, Thailand, 50290
[b]Program of Materials Science, Maejo University, Chiang Mai, Thailand, 50290;
*Corresponding author Email Address: ssarapirom@gmail.com

Water flea (*Moina macrocopa*) is high protein food for nursing of cultured freshwater fish. Production of Moina and their food is practical in commercial fish culture. In good environmental conditions, females are parthenogenetic. In this case, water fleas are able to multiply rapidly if the water conditions are suitable. However, when conditions deteriorate, some of the offsprings become males and these males mate with other females to produce fertilised eggs. To meet the optimal conditions, oxygen level and feeding should be well controlled. This research utilized plasma activated water (PAW) to increase reactive oxygen nitrogen species (RONS) in the water. This work investigated the use of PAW in culturing water flea in tap water and water treated with activated plasma for different activation times. Samples of water flea were cultured in PAW for 7 days. Sex determination was then carried out. It was found that concentration of the reactive oxygen nitrogen species increased with the treatment time. Flea water in this work appeared lighter red than commonly observed because of high oxygen dissolved in water, leading to lack of oxygen in hemoglobin. Sex determination revealed that female population in plasma treated water was observed to be more than that in tap water but less than that in the one commonly used in water flea culture. This might be due to the lack of Chlorella, essential food for water flea.

Keywords: plasma activated water (PAW), plasma arc discharge, Moina, oxygen levels,

Poster: S1 Physics innovation - Board: P020 / **269**

Bio-based Content Measurement by Radiocarbon Analysis in Thailand

Author: Nichtima Uapoonphol[1]

Co-authors: Chalermpong Polee ; Kiattipong Kamdee

[1] *Thailand Institute of Nuclear Technology*

Corresponding Author: nichtima@tint.or.th

Using of bio-based plastic products is one of popular solution for reducing environmental problems. Bio-based plastics is combination of bio-based carbon (have radioactive carbon isotope) and fossil carbon (no longer have radiocarbon remaining), accordingly, radiocarbon or carbon-14 in plastic product comes from bio-based carbon. Identification of bio-based content in plastic products is measurement of carbon-14 which is based on ASTM D6866; Standard Test Methods for Determining the Biobased Content of Solid, Liquid, and Gaseous Samples Using Radiocarbon Analysis. Benzene synthesis under vacuum condition was used as conventional sample preparing process. Benzene from bio-based plastic sample is mixed with scintillator and measured carbon-14 activity contained in plastic sample by liquids scintillation counter (LSC). For accuracy and reliability of result, carbon-14 activity in bio-based plastic samples are compared with activity of reference materials (as background and standard activity).

Poster: S1 Physics innovation - Board: P021 / **266**

The Smartphone and Low-Cost Microcontroller as an AC Circuit Study Kit for high-school students

Author: Kridsada Luangthongkham[1]

Co-authors: Watcharawuth Krittinatham [2]; Somrit Unai [3]

[1] *University of Phapao*

[2] *University of Phayao*

[3] *Division of Physics, School of Science, University of Phayao, Phayao 56000, Thailand*

Corresponding Author: kridsada.lu@up.ac.th

This article presents a smartphone and Arduino microcontroller-based AC circuit educational module focusing on the measurements of an alternating voltage, frequency, phase difference, and a phasor diagram. A smartphone provides a signal generator as a signal source, the Arduino UNO R3 working for signal acquisition, and the beadboard RC series circuit as a test circuit. In-house developed software, based on Microsoft Visual Basic (VB), was used for monitoring the input signal like an oscilloscope. The measured frequency and phase difference agree with the results obtained from the commercial oscilloscope benchtop. This developed module is an apparatus that may be useful in online learning situations with the home experiment during the COVID-19 pandemic and used in high school that lacks the instruments, i.e., function generator and oscilloscope.
Keywords: Arduino, Oscilloscope, RC series circuit, Smartphone

Poster: S1 Physics innovation - Board: P022 / **253**

Development of optical tomography at 840 nm wavelength for sex classification of newborn Korat chickens.

Authors: Jadsada Saetiew[None]; Aom Saenjae[None]; Papawit Nongkhunsan[None]; Ittipon Fongkaew[1]; Panomsak Meemon[1]

[1] *Suranaree University of Technology*

Corresponding Authors: saetiew@g.sut.ac.th, aomjae.domon@hotmail.com

The classification of sex of a newborn chicken is crucial for optimizing the cost of chicken meet production. The current classification technique relies on visual inspection by human naked eyes, which required years of training to expertise. There is no commercially available gender-classification tool for newborn chicks. Recently, a new optical imaging technology for cross-sectional imaging of biological tissues at high speed, high resolution, and high sensitivity has been developed, called Optical Coherence Tomography (OCT). OCT uses near-infrared light for imaging, which is non-destructive and non-invasive for biological tissues. Here, we presents the development of an OCT prototype that has an operating wavelength of around 840 nm for subcutaneous cross-sectional imaging of the bottom of newborn chicks. The depth penetration of the developed OCT prototype was up to 2 mm from the sample's surface. An imaging speed of the developed prototype was about 20 frames per second. The depth resolution was measured to be about 15 microns in air. The capability of the prototype for deep tissue imaging of newborn chickens was verified. The analysis and identification of the sex of newborn chickens by using OCT cross-section images together with machine learning algorithm has been investigated. Some preliminary experimental results will be presented and discussed. The results show that OCT imaging system equip with machine learning technique has potential for determination of newborn chicks at high accuracy. Furthermore, a design and implementation of the field prototype to be installed in the hatchery area of Korat chick to verify the capability of the developed technology for on-site sex determination of the newborn Korat chickens will be presented.

Poster: S1 Physics innovation - Board: P023 / **250**

A cost-effective apparatus for colloidal assembly by convective deposition

Authors: Ekkarat Pongophas[1]; Jeerasak Phooarphit[None]; Kittidhaj Dhanasiwawong[2]; Mati Horprathum[2]; Tossaporn Lertvanithphol[2]

[1] *Division of Physics, Faculty of Science and Technology*

[2] *National Electronics and Computer Technology Center*

Corresponding Author: jeerasak.phu@dome.tu.ac.th

Jeerasak Phooarphit[1], Ekkarat Pongophas[1], *Tossaporn Lertvanithphol[2], Kittidhaj Dhanasiwawong[2], and Mati Horprathum[2]*
[1]Division of Physics, Faculty of Science and Technology, Thammasat University, Pathum Thani 12120, Thailand
*[2] National Electronics and Computer Technology Center, Pathum Thani 12120, Thailand*Corresponding author: e_pong@tu.ac.th
The apparatus is based on the blade coating technique which is simple and economical compared to the other. The blade is attached to the substrate at an angle of 10-90 degrees and the polystyrene-beads solution is dropped in between. The whole system is then in the humidity-control box. The blade is moved by a stepping motor with the resolution of 3 μm/s and is also vibrated using a piezo-electric actuator. This vibration helps the polystyrene beads align hexagonal-close-packed. By microscopic examination, the hexagonal-close-packed monolayer of the polystyrene bead is found in extensive areas of order 10 mm^2.

Poster: S1 Physics innovation - Board: P024 / **247**

Application of Ultrasonic Sensor and Arduino in Analyzing Motion of Damped Pendulum

Authors: Narupon Chattrapiban[None]; Pornrat Wattanakasiwich[None]; Surasak Methet[1]

[1] *Department of Physics and Materials Science, Faculty of Science, Chiang Mai University*

Corresponding Author: surasak_mi@cmu.ac.th

An easy-to-setup experiment designed to measure period and air drag coefficients of damped pendulums is reported. The setup is made up of a solid metal ball and cylindrical shells with various sizes to create air drag. The ultrasonic position sensor (HC-SR04) and an Arduino Uno board was located at the lowest point of motion. The pendulum was released from the same height with small angles. The period of oscillations of different cylindrical shells were obtained from the time series plots of the pendulum position as its motion moving back and forth above the sensor. The periods of damped pendulum were measured with five different values of string length. The drag coefficient was proportional to the size of the cylindrical shell and in agreement with the drag equation for a small Reynolds number.

Poster: S1 Physics innovation - Board: P025 / **241**

Surveying physics laboratory skill in measurement and uncertainty: A case study of pre-service teachers and in-service teachers

Author: Trai Unyapoti[1]

Co-authors: Arunee EAMBAIPREUK [2]; Thanida Sujarittham [3]

[1] *Department of Curriculum and Instruction, Faculty of Education, Srinakharinwirot University*

[2] *Division of Science Education, Department of Education, Faculty of Education, Kasetsart University*

[3] *Department of General Science, Faculty of Education, Bansomdejchaopraya Rajabhat University*

Corresponding Author: trai@g.swu.ac.th

In physics laboratory, an experimental result along with its uncertainty is meaningful to allows other people making judgment about the quality of the experiment. This is the important skill for high-school physics teachers. This study aimed to investigate physics laboratory skill; in particular, measurement and uncertainty. Data were obtained from pre-service science teachers, pre-service physics teachers, and in-service teachers in the academic year 2021. A measurement and uncertainty test was distributed to the participants during the laboratory class. Their responses were analyzed based on reading an estimate value and uncertainty from a measurement, giving the uncertainty from the repeated measurement, making propagation of uncertainty, and writing the final results. It was found from the test that most of the answers still lack of the concept of uncertainty and propagation of uncertainty. They wrote the incorrect answers and could not give their reasonable responses. In this work, the result will be discussed along with the future direction of the research.

Keywords: Physics laboratory skill, measurement, uncertainty, pre-service teacher

Poster: S1 Physics innovation - Board: P026 / **234**

The varying permanent magnetic field by angle and distance for spin Seebeck effect measurement

Authors: Punthawat WONGDAENG[1]; Peerawat Worraradchaipana [2]; Punthawat Wongdaeng[2]; poramed wongjom[None]

[1] *Division of Physics, Fac- ulty of Science and Technology, Thammasat University, Pathum Thani 12120, Thailand*

[2] *Division of Physics, Faculty of Science and Technology, Thammasat University, Pathum Thani 12120, Thailand*

The conversion of heat to spin current is well known as spin Seebeck effect (SSE). In this study, we constructed the cost-effective instrument for measuring SSE by varying permanent magnetic field with angle and distance. The magnetic field strength and temperature gradient were also performed. We measured the spin Seebeck effect, anomalous Nernst effect, spin Hall effect and anisotropic magnetoresistance and then we compared the results with the commercial instrument (PPMS@TMVersaLab). The results show that our instrument can be used to measure these phenomena

Poster: S1 Physics innovation - Board: P027 / **233**

Monitoring of Local Monsoon in Thailand using Stable Isotope Technique

Author: Chakrit Saengkorakot[None]

Co-authors: Monthon Yongprawat ; Kiattipong Kamdee ; Patchareeya Chanrueng ; Chalermpong Polee ; Nichtima Uapoonphol ; Sasiphan Khaweerat ; Teeranai Pliansakul

Corresponding Author: chakrit@tint.or.th

In May and June 2021, Cyclone Yaas and Tropical Storm Koguma caused high rainfall in various parts of Thailand. The precipitation samples during this period were collected on a daily from six rain gauge stations in the southwest, north, and northeast. All samples were analyzed with cavity ring-down spectroscopy, CRDS which is a highly sensitive spectroscopic technique. The stable isotope composition of precipitation illustrated a considerably depleted value, with the $\delta^{18}O$ values ranging from -8 to -3‰ and the $\delta^{2}H$ values ranging from -40 to -15‰. Yaas, which originated from the north of the Bay of Bengal, may have an impact on some areas of the southwest (Prachuap Khiri Khan, Ranong, and Phuket). Ranong province is remarkable among others of the depleted isotopic values (-5.54 to -3.98‰ $\delta^{18}O$ and -29.79 to -21.22‰ $\delta^{2}H$) and a large amount of precipitation (>35.1 mm). Identically, the heavy precipitation and the depleted isotope values of the north (-2.49‰ $\delta^{18}O$ and 11.94‰ $\delta^{2}H$ of Nan) and northeast (-3.36‰ $\delta^{18}O$; 18.21‰ $\delta^{2}H$ of Nong Khai, and -5.01‰ $\delta^{18}O$; -30.02‰ $\delta^{2}H$ of Ubon Ratchathani) were influenced by the Koguma from the Gulf of Tonkin. In recent times, the isotopic composition might be a significant parameter to adjust the simulation of a weather forecast for higher accuracy and precision.

Poster: S1 Physics innovation - Board: P028 / **230**

Thai Voice Command System for Mobile Robot

Author: Wisit Mangthas[None]

Corresponding Author: wisit.ma@up.ac.th

In this research the Turtlebot2 robot is equipped with the ReSpeaker Mic Array sound sensor infacing through the ROS (Robot Operating System) and using Dialogflow. It works from the Google Cloud Platform and helps convert voice messages into variables for data processing with TurtleBot2. The Kinect is replaced by Lidar to improve the quality of map creation and automatic navigation. The experiment simulates coordinates in various locations and testing automatic navigation with Thai voice commands. From the results of the experiment, the robot can move to the specified coordinates with Thai voice commands. The average error is 3.7 cm. And percentage error is 10.5 when compared with the size of the robot.

Poster: S1 Physics innovation - Board: P029 / **227**

INCREASING THE HEIGHT OF BOUNCING BALL BY SPIN

Authors: Ai Tungsatitcha[None]; Ratchaphon Noiaek[None]

Corresponding Authors: ai.tungsatitchai@gmail.com, ratchaphon.noiaek@gmail.com

Basketball is a very technical sport, one of the techniques used among athletes is spinning the ball to further influence the ball's path. This experiment will be studying the height of the ball when throwing with different spin, namely back spin, top spin, and no spin. Heights of the bouncing balls dropped was captured by an iPhone 12 camera and analyzed by an open video analysis software called Tracker. The position of the falling objects was tracked 120 times per second and was evaluated from a series of images. The velocity was averaged from the change in position during each interval. For the experiment, height will be measured before and after release to compare the ratio. Basketball with spin-launching has a higher height ratio than without spin-launching and launching with back spin has a higher height ratio than top spin. Launching the basketball with spin can increase the height ratio of the bouncing ball.

Poster: S1 Physics innovation - Board: P030 / **214**

Design and implementation of a low-cost real-time photovoltaic panel monitoring and recording system using LabVIEW for rural areas

Author: Natawee Chaijum[1]

Co-authors: Panuwat Poothongpeng [1]; Sorawit Ninthuk [2]

[1] *Bansomdejchaopraya Rajabhat University*

[2] *Bansomdejchaopraya Rajabhat University*

Corresponding Author: natawee.ch@bsru.ac.th

Solar power generation from photovoltaic panels is likely to increase in the future, especially in rural areas where the power grid is inaccessible. Over time, such systems are subject to deteriorate due to environmental conditions, as well as the current and voltage systems. If not properly maintained, the photovoltaic panel may deteriorate faster than normal. This research aims to design and operate a low-cost and easy-to-use real-time photovoltaic panel measurement and data recording system for rural areas using labVIEW program on Arduino Nano, ACS712-20A, FZ0430 and DHT11. The sensor system sends data to the Arduino Nano board for processing which then sends the data to the LabVIEW program to display and record the electricity production. The results show that the sensors used are able to measure accurately. The measurement and data recording of the system can be performed completely and continuously without any errors. Therefore, it can be said that this measurement and data acquisition system can accurately and efficiently measure various parameters, is easy to use, suitable for small solar power generation system in rural areas where WIFI signal is not stable and can detect initial malfunctions of photovoltaic panels. It can also be further developed for use in solar power generation measurement and prediction systems or to check the reliability. Failure of the photovoltaic systems in rural areas in the future is possible. In addition, this research can also be developed for future measurement and prediction of solar photovoltaic systems in rural areas, bringing many benefits to improving the quality of life for local people.

Poster: S1 Physics innovation - Board: P031 / **210**

Comparison of carbon dioxide emissions produced between paper-based and computer-based for demonstration indirect light concepts

Authors: Kasem Kamolchaipisit[1]; Tiantada Hiranyachattada[None]

[1] *Bansomdejchaopraya Rajabhat University*

Corresponding Author: tiantada.hi@bsru.ac.th

The quality of education is one of the UN sustainable development goals. Nowadays, greenhouse gas emissions have escalated to record levels and there are concerns in urgently finding sustainable methods to reduce carbon to avoid climate change and to reduce greenhouse gas emissions (GHGe). Studying in SLR lab, indirect lighting demonstration is one of the important topics where paper is required to conduct the demonstration experiment using worksheets and exam paper which will be disposed of every semester. To take the current global warming situation into account, the demonstration of indirect lighting has been changed to entirely use computer-based (paperless) demonstration. In this research, we compare the amount of carbon dioxide emitted from the paper-based demonstration and computer-based demonstration in the form cradle-to-gate. We collect the data from SLR lab from two semesters then report the carbon footprint calculation to compare the results. Also, the assignment is given to the students to assess and compare their understanding. The results indicate that the GHGe of the average paper-based and paperless are 0.76 kg and 0.06 carbon dioxide equivalents (CO2-e) per person respectively which shows that it can be reduced up to 0.70 kg per person. For the assignment results by comparing the students understanding, we found that the average scores from the written part and practical part are not different. In conclusion, we can reduce the use of paper demonstration and fully convert to computer-based demonstration. Moreover, reducing the use of paper can help to reduce global warming situation. Also, these data will enable comparisons between changes in dietary intake and GHGe over time, as well as provide a reference point for developing the quality of education.

Poster: S1 Physics innovation - Board: P032 / **208**

Design, Fabrication and Performance Evaluation of Solar Dryer for Thai Glutinous Rice, Khao Tan Rice Cracker Herbal

Authors: Mali Sarobol[1]; Piriya Praneekit[None]; Pongsathorn Kongkaew[2]; Suminya Teeta[None]

[1] *Rajabhat Mahasarakham University*

[2] *Program of Physics, Faculty of Science and Technology, Rajabhat Maha Sarakham University.*

Corresponding Author: sanawong_14@hotmail.com

Thai glutinous rice, khao tan rice cracker herbal is a popular Thai traditional snack, which is economically important for local entrepreneurs in Mahasarakham province, Thailand. Drying process is an important step in acquiring good quality for final products. The main scope of this research is to assess the feasibility of using the heat demand – temperature function for heat demand forecast. The dryer capacity was about 100 kg. Drying time was about 19 hr to reduce initial moisture content of the khao tan rice cracker herbal from approximately 90% dry basis to below 8% dry basis. The physical properties of dried khao tan rice cracker herbal were found to be acceptable. Based on resultant energy efficiency, the new solar energy dryer. Overall, the proposed solar energy dryer proved to reduce operational energy consumption, operating cost and still provide acceptable products qualities.

Poster: S1 Physics innovation - Board: P033 / **207**

Demonstration kits for locating an image formed by a concave mirror

Authors: Pakanat Srijaroen[1]; Narumon Emarat[1]; Kwan Arayathanitkul[1]

[1] *Department of Physics, Faculty of Science, Mahidol University, Thailand*

Corresponding Author: pakanat.sri@student.mahidol.edu

To improve student understanding about an image formed by a concave mirror, 2 demonstration kits were developed. One kit is used to view images formed, and show how to locate and find the image distances and sizes. The other uses a laser beam to show the incident and reflected light rays and relate to the ray diagram normally used to find the image location. The demonstration kits were applied to 58 year-11 Thai high-school students and the teaching process was designed to be usable for both online (N = 34) and on-site (N = 24) classes. The 4 diagnostic questions were used in the investigation of student understanding both before and after instruction. The questions cover the image visualization, the mirror equation, and the ray diagrams of a concave mirror. The overall mean scores (N = 58) of the pre- and post-test are 1.3 and 5.3 out of 13, respectively, and the normalized gain is 0.34, which is at the medium level. Interestingly, the normalized gains of the two classes are not significantly different indicating that the demonstration kits can be applied to either an online or on-site class. The best improvement was found in the first question (post mean score = 55%) which is about the image visualization. Seeing an image by themselves using the demonstration kit, accompanied with the teaching process, helps students to have a better understanding of visualization. On the other hand, the lowest improvement was shown in the second question (post mean score = 19%) which indicates that the students are still unable to apply the mirror equation. This might be because that the teaching process does not encourage them to do calculations. Apart from these results, the demonstration kits make the physics content enjoyable. The students found it exciting and fun while much is being learned.

Poster: S1 Physics innovation - Board: P034 / **201**

Fabrication and Evaluation of Soil Pressure Sensor for Stress State Transducer

Author: Chompoonud Kulketwong[None]

Co-author: Dithaporn Thungsotanon

Corresponding Author: chompoonud.ku@kmitl.ac.th

The actual stress measurement is important to the studies in soil mechanics. The sensor that measures the stress must be thoroughly designed and assessed with the soil medium since the soil-structure interaction is complex and depends on many factors. This article presented the design and fabrication of the diaphragm type of soil stress sensor with the built-in amplifier and compared the properties and phenomena with the commercial pressure sensor for applying the sensors to be a soil stress state transducer (SST). The prototype soil sensor made of the diaphragm strain gauge was bonded on a 15-mm circular membrane that was analyzed by the linear finite element method with the pressure ranges of 0-500 kPa. The experimental procedures were divided into two steps: the air calibration to evaluate the basic properties of the sensor and the granular materials to determine the effect of particle size and layer thickness. The results found that the prototype sensor showed the high linear with the coefficient of determination (R^2) of 0.99, the hysteresis error of 5.45% and the 3.14% of non-linearity error for the air calibration. As the values of the sensor in the two kinds of the granular media were over the register pressure and the proper applied condition should be performed below 60 mm from the bearing surface.

Poster: S1 Physics innovation - Board: P035 / **192**

Study of the impact force of falling chains using force sensor

Author: Nitat Sripongpun[None]

Co-author: Chakrit Samarnrak [1]

[1] *Mahidol Wittayanusorn School*

Corresponding Author: nitat.sri@mwit.ac.th

The impact force exerted by falling chains was investigated using a plastic cup attached on the top of a force sensor. Two different linear mass densities of the chains with mass of 0.1452 and 0.1956 kg/m was examined by releasing one meter of their lengths from rest with the lower end just touching at the bottom of the plastic cup. The force sensor was connected with LabQuest and the sample rate was set to be 1000 Hz. The motion of the chain was recorded using a video camera with 60 FPS. The total time of the falling chain was analyzed using tracker video analysis and compared with the total time of the impact forces hitting on the cup. The results show that the total time of falling chain, starting from the increase of impact force exerted by the lower end until the upper end touching on the bottom of the cup, evaluated by the data from LabQuest and tracker video analysis program is agreement well with the time of freely falling condition but the experimental results are slightly lower than theoretical prediction due to a small pile of the chain occurring. Furthermore, the instantaneous force or apparent weight increases quadratically in time and equal 3 times the weight of the part of the chain and the maximum force exerted on the cup is also 3 times the total weight of the chain. These results can be explained by two forces exerted by the chain. For the first force, a part of the chain lied at rest, resulting the weight due to gravity whereas the second one comes from the change of momentum per unit time due to the collision between the remaining part of the falling chain and the cup.

Poster: S1 Physics innovation - Board: P036 / **174**

Topological Analysis of the Transfer Entropy Network of Cryptocurrencies During the Uptrend and Downtrend Periods.

Author: Gingkamon Jaroenkobun[1]

Co-authors: Thana Sutthibutpong [1]; Teerasit Termsaithong [2]

[1] *Theoretical and Computational Science Center (TaCS), King Mongkut's University of Technology Thonburi, Bangkok, Thailand*

[2] *Learning Institute, King Mongkut's University of Technology Thonburi, Bangkok, Thailandl*

Corresponding Author: gingkamon.log@gmail.com

Cryptocurrency is a decentralized payment tool that generally does not require any government backing or intermediary. Currently, there are a large number of low-fee exchanges for buying and selling cryptocurrencies with less restrictions. However, the pricing behavior of this highly-dynamic type of market and driving factors for changes of market prices remain unclear. The cryptocurrency market has various nonlinear and overlapping linear drivers, in which the conventional Granger causality analysis was shown to be inefficient. Therefore, the Granger causality analysis was replaced by the Transfer entropy calculations between all pairs of cryptocurrencies. Calculations were performed on two datasets consisting of time series of 40 cryptocurrency prices: (1) the 'upward trend' dataset with a monotonic increase of the Bitcoin price and (2) the 'downward trend' dataset with a monotonic decrease of the Bitcoin price. Then, information flow networks were created from transfer entropy between each pair of cryptocurrencies. Lastly, we analyzed topological parameters to observe the behavior during the upward and downward trends of the market. The results showed that the 'In Degree' and 'Out Degree' values for the transfer entropy network from the 'downward trend' dataset were twice those from the 'upward trend' dataset, indicating the higher level of data transmission during the 'downward trend' period. Similarly, the Transitivity value from the 'downward trend' was almost twice that from the 'upward trend', indicating that changes in cryptocurrency prices in the 'downward trend' were more likely to occur in the same direction.

Poster: S1 Physics innovation - Board: P037 / **97**

Traffic flow simulation of bi- lane systems through the two positions of traffic light signal

Authors: Puwarin Narkjanthuk[1]; Kritsanapat Puangrak[1]; Sirawit Yoosiri[1]; Pranee Disrattakit[2]; Thanyanan Phuphachong[2]

[1] *Mahidol Wittayanusorn School*

[2] *Department of Physics, Mahidol Wittayanusorn School*

Corresponding Authors: puwarin.nar_g30@mwit.ac.th, kritsanapat.pua_g30@mwit.ac.th, sirawit.yoo_g30@mwit.ac.th

In this work, we investigated traffic flow simulation of bi- lane systems through the two traffic light signal positions based on the Nagel–Schreckenberg (NS) model, which is well-known as a Cellular Automata (CA) traffic flow model. In the CA model, time, position, speed and acceleration of vehicle are discrete variables. The speed of vehicle is defined as the discrete lattice (cell) number of movements in each time step. The road is divided into unit cells. The driving behaviors, which are randomly defined in different maximum vehicle speeds without lane-changing were used in our model. The effect of time duration management between two positions of traffic light signal on vehicle density and average speed were explored and discussed. The results show that the consistency of the two positions of traffic light signal affects the traffic flow. We found that turning on the overlap traffic signals cause better traffic conditions than that of two traffic lights simultaneously. In addition, our model can be used to illustrate a traffic situation of the bi- lane systems through the two traffic light signal positions.

Poster: S1 Physics innovation - Board: P038 / **122**

Question-Answer Teaching Method to Develop Student Understanding of Buoyant Force

Author: Kwan Arayathanitkul[1]

Co-authors: Songphon Chirayangyuenyong ; Narumon Emarat [1]

[1] *Mahidol University*

There have been many studies in physics education research showing that students have difficulties with the buoyant force topic. One difficulty is that students do not understand that the buoyant force is the resultant force of the fluid pressure. This work designed a worksheet based on the question-answer teaching method aiming to help students understand the concept. This method asks students to answer a set of designed questions which consist of (i) the concept-guiding questions, (ii) the comprehension-checking questions, and (iii) the concept-applying questions. Students are required to express and discuss their own ideas with other students and instructors. The designed questions encourage and challenge the students to correct their misconceptions and understand the concept by themselves. A conceptual test (multiple-choice questions) was used to measure the improvement of a control group who learned by a traditional lecture (N = 88) and an experimental group who learned by this method (N = 12). According to the results, the pre-test and post-test scores of the experimental group are significantly different (p-value = 0.01). The normalized gains of the control group and the experimental group are 0.08 and 0.63, respectively. These findings show that the question-answer teaching method can be used to improve students' understanding effectively. In addition, after teaching, 7 out of 12 students in the experimental group understood that the buoyant force acting on an object results from the fluid pressure difference and that the force magnitude is equal to the weight of the fluid displaced, consistent with the Archemedes' principle. The method also helps students realize that the buoyant force does not depend on the depth or the type of the object, and sinking or floating depends on the magnitude of the buoyant force and the weight of the object.

Poster: S1 Physics innovation - Board: P039 / **125**

Online physics experiment creation on resonance in the LC circuit with simple metal detector circuit

Author: NIYOM HONGSITH[1]

Co-authors: EKASIDDH WONGRAT [1]; PIYACHON KETSUWAN [1]; CHONTICHA KRITPETCH [1]; PHONGSAPHAT RANGDEE [1]; SUPHAKORN CHUNLEN [1]; TRAITOT LIANGHIRANTHAWORN [1]; THANAKRID TONGMEE [1]; KETMANEE CHANCHAIMONGKOL [1]; NATTHAWUT KRUABOON [1]; RATTIKARN BOONPEAW [1]; SITTIPHON PRASONGCHAROEN [1]; NUR-IMAN TOHKENG [1]

[1] *Department of Physics, University of Phayao*

Corresponding Author: hongsith@gmail.com

Online learning is necessary and challenging to develop effective teaching strategies to support student learning during the COVID-19 period. This course has seven students. Some essential equipment is sent to students by post. We demonstrate a simple experiment on the resonance frequency in the LC circuit with a simple metal detector circuit based on a 2n2222 transistor. In principle, Metal objects within the magnetic field of inductance affect the resonance frequency resulting in oscillator frequency changes. So, we could study the resonance frequency of the LC circuit from frequency changes by changing the inductance of the inductor. The sound frequency has been generated from the metal detector circuit and is altered depending on the coil's inductance. The frequency change is measured by a sound detector application on the smartphone. From the results, we discuss the equation of the resonance frequency and the oscillator frequency changes and calculate the relationship between the frequency of sound and the inductance value of the coil. As a result, it is possible to adapt the simple metal detector to use the study of the resonance formula and calculate the inductance of any coil with accuracy.

Poster: S1 Physics innovation - Board: P041 / **127**

The study of solvent ratio of diphenyl oxalate on chemiluminescence

Authors: Kachain Dangudom[None]; Warunee Khampa[None]; Parvinee Boonyaras[None]

Corresponding Author: kachaind@nu.ac.th

This research aimed at studying the effect of the solvent ratio on chemiluminescence that has been widely applied in glow sticks. Dichloromethane and ethyl acetate were used as solvents. The fluorescent solution was the mixture of diphenyl oxalate solvent and fluorescent dye rhodamine B that was stimulated by 405-nanometers laser for fluorescent spectrum measurement before the chemiluminescence experiment. The fluorescent solution was varied the concentration and solvent ratio. For the chemiluminescence experiment, diphenyl oxalate substance was dissolved in solvents combined with rhodamine B that interacts with the mixture of hydrogen peroxide and acetonitrile, which result in chemiluminescence. Then, it was measured the duration and intensity of light by a photodiode detector. The study revealed that the concentration and solvent ratio of fluorescent solution impact the fluorescent spectrum due to the opacity and solubility. Also, the increasing of ethyl acetate and decreasing of dichloromethane affected a longer duration of light. The intensity of light in some ratios was alternating high and low. It should emit the light as a long time and high intensity that be suitable for applications. The solvent ratio at 3:7 and 5:5 (1:1) is better than the other samples in this research.

Poster: S1 Physics innovation - Board: P042 / **60**

Optical properties of freeze-dried partial delignified balsa wood

Author: Piyawath Tapsanit[1]

Co-author: Jakkrawut Maitip [2]

[1] *King's Mongkut University of Technology North Bangkok*

[2] *King Mongkut's University of Technology*

Corresponding Author: piyawath.t@sciee.kmutnb.ac.th

Radiative cooling (RC) is natural phenomenon in which an object passively cools itself by highly radiating mid-infrared waves to the cold outer space (temperature 3 K). The delignified wood (DW), in which light-absorbing lignin compounds in woods are removed from natural wood, shows promising performance of daytime radiative cooling (DRC). The drying of DW with hot pressing is usually considered as necessary step to return the strength to the DW. However, the hot-pressing results in the reduction of microscopic pores present in the DW. The absence of pores in DW may reduce either the solar reflection or the thermal emission of mid-infrared waves. In this study, we fabricated partial delignified woods (PDWs) from natural balsa wood. The delignification of balsa wood was performed with boiling hydrogen peroxide (H2O2) solution in renewable system. The quantities of lignin compounds in PDWs were varied via the boiling time. The PDWs were dried with freeze-drying process. We've found that the freeze-drying process can keep the shape and size of PDWs as shown in Fig. 1. We discussed the solar reflectance of PDWs by measuring the UV-Vis-NIR spectroscopy. The thermal radiation of mid-infrared waves from PDWs was also discussed by measuring the FTIR spectroscopy. Our findings give the fundamental understanding of freeze-dried partial delignified woods for the invention of novel wood composite materials for construction industry.

Keywords: daytime radiative cooling, hydrogen peroxide, freeze-drying, balsa wood

Poster: S1 Physics innovation - Board: P043 / **56**

Estimation of rainfall from the amount of water vapor in the atmosphere

Author: Sayan Phokate[1]

[1] *Department of Applied Physics, Faculty of Engineering, Rajamangala University of Technology Isan, Khon Kaen Campus*

Corresponding Author: syphokate@hotmail.com

The objective of the study was to estimate the rainfall from the amount of water vapor in the air. The relationship between the upper air data and the surface data from 2007 to 2017 was used to create a mathematical model at the same station to determine the amount of water vapor. The findings indicated that, the relationship has a relatively high level of reliability, the correlation coefficient was 0.891. The amount of water vapor from upper air data nearly was equal to the value from the model. The difference in the root mean square error was 0.528 cm. The results showed that the rainfall is related to the amount of water vapor in the air in mathematical models which are different for each region. When tested against an independent data set, monthly average of daily rainfall from the model agree with that obtained from the measurements showed that both were consistent, which are not significantly different at the level of 0.05. The root mean square error was 38.693 mm. The correlation coefficient was 0.879.

Keywords: water vapor; rainfall; cloud cover; upper air data; mathematical model

Poster: S1 Physics innovation - Board: P044 / **52**

The effects of mechanically gated ion channels of the inner ear on thermal sensitivity of spontaneous otoacoustic emissions

Author: Kittisak Sawangwareesakul[None]

Co-author: Yuttana Roongthumskul

Corresponding Author: kittisakdong@gmail.com

In quiet environments, the inner ear of vertebrates can produce low-intensity sounds that are detectable in the ear canal, termed spontaneous otoacoustic emissions (SOAEs). This production of acoustic energy has been regarded as an epiphenomenon of the active processes performed by hair cells – the sensory receptors of the auditory system. Experimental measurements of SOAEs emitted from the ears of ectothermic species, including frogs and lizards, reveal a linear increase of SOAE frequency with body temperature. Moreover, SOAEs at higher frequencies always display greater thermal sensitivity. In this work, we will elucidate the cellular mechanism underlying the sensitivity of SOAE frequency to temperature by investigating the transduction process of hair cells, mediated by mechanically gated ion channels. We employ the previously proposed gating-spring model which describes an individual ion channel by a two-state system, whose activation energy associated with channel gating depends on the level of temperature. The stability of the two states is further modulated by the tension of a molecular filament. Our results from numerical simulations reveal that the free energy difference between the open and closed states greatly dictates the magnitude of thermal sensitivity. Additionally, our findings suggest that SOAEs with higher frequencies are produced by hair cells whose ion channels are anchored by molecular filaments with greater stiffness.

Poster: S1 Physics innovation - Board: P045 / **243**

Development of intelligent nanogels by gamma radiation as theranostic agents for diagnosis and therapy of cancer

Author: Thitirat Rattanawongwiboon[1]

Co-authors: Sakchai Laksee [2]; Pattra Lertsarawut [2]; Kasinee Hemvichian [2]

[1] *Thailand Institue of Nuclear Technology (Public*

[2] *Thailand Institute of Nuclear Technology (Public Organization)*

Corresponding Author: thitirat@tint.or.th

Nowadays, cancer is well known that it cause the most disease of human death. Chemotherapy or direct uptake of anticancer drugs was generally employed for cancer treatment. To ease the risk of normal cells and side effects of patient, nanocarrier contained anticancer drug and contrast agent is continuously developed to increase the survival rate. Theranostic agent is a multifunctional molecule, which is well-designed for more specificity to disease area or targeting area by combination of diagnostic and therapeutic capabilities into one single molecule. Based on this reason, researchers are interesting to develop a theranostic agent from biocompatible and biodegradable polymers for cancer treatement. In this research, the proton-donating polyacrylic acid (PAA) and the proton-accepting polyethylene oxide (PEO) were used as the starting materials, PAA and PEO were mixed with 1:1 molar stoichiometric ratio in 25% (v/v) acetone/water mixture to form the interpolymer complexe (IPC) through cooperative H-bonding interaction. Subsequently, IPC solution was irradiated to create a strong covalent bond between polymer chains as IPC nanogels. The effects of dose, pH and temperature on size and stability of IPC nanogel were studied, comparing with IPC. After irradiation only at 3 kGy, IPC nanogel exhibited suitable size for drug delivery (87.01 ± 9.04 nm) and stable size over a period of 1 month at ambient temperature. Furthermore, Berberine (BBR) as a model anticancer drug was encapsulated into the IPC nanogel. The particle size, number of particle and surface area as well as surface charge of IPC nanogel before and after encapsulation was observed by dynamic light scattering, zetasizer and transmission electron microscopy. Drug release study revealed that the BBR drug was slowly released from IPC nanogels into PBS buffer (pH 7.4) at 37 ^{o}C over a period of 54 hrs. IPC nanogels not only encapsulate anticancer drug but also chelate metal ion as a contrast agent. The results of this research indicated that IPC nanogel prepared by radiation processing has the potential to be used as theranostic agents.

Poster: S1 Physics innovation - Board: P046 / **16**

Optical properties of carbon dots derived from table sugar via gamma irradiation

Authors: Kanokorn Wechakorn[1]; Tanagorn Kwamman[2]

Co-authors: Teerawat Utapong [2]; Threeraphat Chutimasakul [2]; Natee Sirisit [3]

[1] *Department of Chemistry, Faculty of Science and Technology, Rajamangala University of Technology Thanyaburi, Pathum Thani 12110, Thailand*

[2] *Thailand Institute of Nuclear Technology (Public Organization), Nakhon Nayok 26120, Thailand*

[3] *Department of Chemistry, Faculty of Science and Technology, Thammasat University, Pathum Thani 12120, Thaila*

Corresponding Authors: kanokorn_w@rmutt.ac.th, tanagorn@tint.or.th

Gamma irradiation is the one method of green environmental synthesis without further treatment waste. Carbon dots are optical nanomaterials in the carbon family with excellent properties such as tunable fluorescence emissions, biocompatibility, non-toxicity, water-soluble and photo-stability. Therefore, this research used gamma irradiation for carbon dot synthesis at room temperatures. The table sugar was used as starting materials without toxic chemicals. Carbon dots were successfully synthesized by gamma irradiation at 25 kGy using the sugar concentrations of 4, 20, and 40% w/v. The effect of gamma doses was also studied for the carbon dot preparation. The chemical composition of the as-synthesized carbon dots was characterized by X-ray photoelectron spectroscopy (XPS), and the optical properties were elucidated by UV-Visible absorption and fluorescence spectroscopy. The as-synthesized carbon dots strongly absorbed in the UV region (271 nm) and exhibited tunable fluorescence emission.

Poster: S1 Physics innovation - Board: P047 / **20**

DEVELOPMENT OF AN EDUCATIONAL PC BASED SIMULATOR FOR TRR-1/M1

Authors: KANOKRAT TIYAPUN[None]; Kunthida Waree[None]; SAENSUK WETCHAGARUN[None]

Corresponding Author: ssyamama@gmail.com

The human resource development is very important issue for Thailand Institute of Nuclear Technology (TINT). TINT has established education and training programmes on active learning about nuclear reactor and reactor experiments using the PC-based basic principle simulator. This simulator provides efficient hands-on learning of the reactor operation and reactor experiment related to reactor physics and basic reactor engineering of TRR-1/M1 research reactor. The simulator operates on personal computers and are provided for a broad audience of technical and non-technical professionals, graduated students and instructors as an introductory educational tool. This simulator can be used for developing domestic nuclear engineering courses and international nuclear school for ASEAN region. It can be used as a tool for reactor experiments including criticality, reactivity, reactor period, reactor operation and rod worth calculation. The simulation system was developed using the LabVIEW® (Laboratory Virtual Instruments Engineering Workbench) software, offering a graphical programming approach which is modern concept of virtual instruments (VI's). This visualization makes it simple to integrate with measurement hardware, develop data analysis algorithms, and design custom engineering user interfaces. The main objective of the TRR-1/M1 simulator system is to provides hands-on experiences for the reactor operation and basic reactor engineering of TRR-1/M1 research reactor to interested professionals. The TRR-1/M1 simulator system will provide insight and understanding of the designs parameters as well as a better understanding of the operational characteristics of the TRIGA reactor without the necessity of using the facility.
Keywords: simulator, LabVIEW, TRR-1/M1

Poster: S1 Physics innovation - Board: P048 / **8**

Elemental analysis in rice samples by wavelength dispersive X-ray fluorescence spectrometry

Authors: Supalak Kongsri[1]; Chunyapuk Kukusamude[1]

Co-authors: Sasiwimon Naksuriyawong [2]; Ratchai Fungklin [2]

[1] *Nuclear Technology Research and Development Center (NTRDC), Thailand Institute of Nuclear Technology (Public Organization)*

[2] *Nuclear Technology Service Center, Thailand Institute of Nuclear Technology (Public Organization)*

Corresponding Author: supalak@tint.or.th

Elemental composition including P, Mg, K, S, Cl, Ca, Zn, Mn, and Fe in rice samples cultivated from Phatthalung, Nakhon Si Thammarat, and Songkhla provinces using a simple, rapid and non-destructive wavelength dispersive X-ray fluorescence (WDXRF) spectrometry. A good agreement was achieved between the certified and measured values with the recoveries higher than 94%. The repeatability was found to be satisfactory with the relative standard deviations lower than 12%. The mean concentrations of P, Mg, K, S, Cl, Ca, Zn, Mn, and Fe found in rice samples were 3321.8, 3159.7, 3333.8, 1278.1, 288.9, 124.0, 23.8, 37.3, and 13.3 mg kg-1. Statistical differences in the elements in rice collected from different regions were tested by one-way ANOVA and Duncan's post hoc. There were statistical differences in the mean concentrations of Mg, K, Cl, Mn, and Fe in rice cultivated from different provinces in the south of Thailand.

Poster: S1 Physics innovation - Board: P049 / **9**

Specific activities and gamma radiation hazard evaluation in rice cultivated soils in Nakhon Si Thammarat province

Authors: Chunyapuk Kukusamude[1]; Supalak Kongsri[1]

Co-author: Nopparit Changkit [2]

[1] *Nuclear Technology Research and Development Center (NTRDC), Thailand Institute of Nuclear Technology (Public Organization)*

[2] *Nuclear Safety Section, Thailand Institute of Nuclear Technology (Public Organization)*

Corresponding Author: chunyapuk@tint.or.th

In this study, the specific activities of natural radionuclides in 22 rice cultivated soils collected from 5 districts in Nakhon Si Thammarat province, southern Thailand were measured. The measurements were conducted using a high-purity germanium (HPGe) detector and gamma spectrometer at Thailand Institute of Nuclear Technology (Public Organization). The specific activities of 238U, 232Th, and 40K were in the ranges of 26.60-174.45, 47.71-168.98, and 149.69-701.33 Bq/kg with mean values of 82.49, 121.09, and 435.53 Bq/kg, respectively. The values of radium equivalent activity (Raeq), the external hazard index (Hex), the gamma-absorbed dose rate (D) and the annual effective dose rate (AEDR) were also calculated in order to evaluate radiological hazards in rice cultivated soils in Nakhon Si Thammarat province.

Poster: S1 Physics innovation - Board: P149 / **295**

Sugarcane leaf lamp

Author: Yaowapa Saengpayab[1]

Co-authors: Noppamas Pratummasoot [2]; Wichai Kongsri [1]; Krissadang Sookramoon [3]

[1] *Industrial Metrology and Quality System & Applied Physics Program, Faculty of Science and Technology, Valaya Alongkorn Rajabhat University under the Royal Patronage, Pathum Thani, 13180, Thailand*

[2] *Applied Physics Program, Faculty of Science and Technology, Valaya Alongkorn Rajabhat University under the Royal Patronage, Pathum Thani, 13180, Thailand*

[3] *Faculty of Industrial Technology, Valaya Alongkorn Rajabhat University under the Royal Patronage, Pathum Thani, 13180, Thailand*

Corresponding Author: yaowapa.saeng@vru.ac.th

The main propose of the present study was to study the forming of sugarcane tissue in order to produce a sugarcane leaf lamp. To obtain a soft tissue of the leaf, the leaf residues were mechanical and chemical processed similar to that of making a sheet of mulberry paper. After that, the tissue was formed as a cone shape by a forming machine which was developed specially for this work. The temperature and time conditions of the forming process were studied. It was found that the moisture content in the cone was affected by the temperature and time variation. In addition, the thickness of the tissue affected significantly to the lamp brightness. This research provides economic value added to the sugarcane residue and provide an option for sugarcane farmer to sell their leaf residue instead of burning it which led in PM2.5 air pollution.

Poster: S1 Physics innovation - Board: P150 / **297**

Optical Coherence Tomography Retina Scanner

Author: Thanapol Tuntrakool[None]

Co-author: Panomsak Meemon [1]

[1] *Suranaree University of Technology*

Corresponding Author: thanapol.aof@gmail.com

Nowadays, there are many patients with retina disorders, e.g., diabetes retinopathy. Investigation and treatment of the retina disorder in its earlier stage can reduce permanent vision loss. The robust imaging technology that can help the doctor to diagnose the retina disorder in its earlier stage is the Optical Coherence Tomography (OCT) retina scanner. The OCT retina scanner is capable of non-invasive and non-contact 3D imaging of the retina tissues. In this work, we aim to design and implement the OCT retina scanner for retinal imaging.

Poster: S1 Physics innovation - Board: P151 / **298**

3D printing of barium hexaferrite magnets with complex shapes

Author: Yaowarat Sirisathitkul[1]

Co-authors: Wannisa Thongsamrit [2]; Chesta Rattanapan [3]; Thanida Charoensuk [4]; Chitnarong Sirisathitkul [5]

[1] *School of Engineering and Technology, Walailak University,*

[2] *Thailand Center of Excellence in Physics, Ministry of Higher Education, Science, Research and Innovation, 328 Si Ayutthaya Road, Bangkok 10400, Thailand*

[3] *Center of Excellence in Smart Materials Research and Innovation, King Mongkut's Institute of Technology Ladkrabang, Chalongkrung Road, Ladkrabang, Bangkok 10520, Thailand*

[4] *Thailand Center of Excellence in Physics, Ministry of Higher Education, Science, Research and Innovation, 328 Si Ayutthaya Road, Bangkok 10400, Thailand;*

[5] *School of Science, Walailak University*

Additive manufacturing can produce near-net-shape permanent magnets with varying geometries. Interestingly, the magnetic properties of 3D-printed alloys from selective laser melting were comparable to those of conventional sintered and bonded magnets with the same compositions. The fuse filament fabrication successfully printed strontium hexaferrite were with high magnetic loadings in thermoplastics. In this study, a commercial 3D printer was modified for extrusion free-forming of barium hexaferrites with complex shapes. Ceramic pastes were prepared by mixing BaCo3, Fe2O3, PVA binder, EFKA®FA4620 dispersant, and PEG-400 plasticizer. The printability of ceramic pastes is dependent on the viscosity of the pastes. PEG-400 was adjusted to obtain printed structures with appropriate density after the heat treatment. Similar set-ups could produce other functional ceramics from appropriate paste formulation.

Poster: S1 Physics innovation - Board: P152 / **300**

Electrolyte Drink Analysis by Electronic Tongue Using Carbon Nanotube Paste Electrodes

Author: Tanakorn Osotchan[1]

Co-authors: Suk Hyun Suh ; Arthit Jityen ; Tanant Waritanant ; Nungnit Wattanavichean

[1] *Asst Prof*

Corresponding Author: sctos1@gmail.com

Electrolyte drink becomes very popular nowadays that drinking aid in rehydration which mostly contain water, sugar, and electrolytes (Na, K, Mg, Ca ions). In this work, several electrolyte drinks including M sport, M-plus, Sponsor, Sponsor citrus, Gatorade were analyzed by electronic tongue comparing to mineral and tap water. Non-specified electrode array used in electronic tongue was fabricated by mixing carbon nanotube with copper oxide or several types of metal-phthalocyanine (MPc) including MnPc, FePc, CoPc and ZnPc. The electronic tongue system was developed by using automatic electrochemical measurement setup with rotating eight beaker tray together with electrode holder slider in up and down position. This system was controlled by Arduino with developed python protocol. The cyclic voltammetry measurement indicated an ion current flow between electrodes with peaks in some cases. These cyclic graphs were converted to the specific line graphs for further analysis. Principle component analysis was used to classify the signal into several distingue groups. It was found that with the first two principal components, the mineral water and tap water can be totally separate from the other electrolyte drinks with total variation of about 77%.

Poster: S1 Physics innovation - Board: P153 / **311**

Rotation Stage for Phantom in the Prototype for Proton Computed Tomography

Author: Atirat Pitaktrakul[1]

[1] *Suranaree University of Technology*

Corresponding Author: b6080341@g.sut.ac.th

Proton Computed Tomography (pCT) is an imaging technique used to determine the location of cancer. This equipment simplifies the treatment planning process in proton therapy. The rotation stage is a significant part of our pCT prototype. It can rotate the object 360 degrees for use in the 3D image reconstruction process. The purpose of this work is to design a rotation stage capable of supporting an object, develop an algorithm for controlling the rotation stage, and configure it to operate synchronously with proton beams. For proton computed tomography, only 1 degree of rotation is required to create 360 projection images, which can be combined and converted to 3D images. It can be improved and used to find the position of the cancer inside the patient.

Poster: S1 Physics innovation - Board: P154 / **314**

Efficient fabrication of smart pH-responsive gold nanohybrids for targeted anticancer drug delivery systems

Author: Sakchai Laksee[1]

Co-authors: Amporn Kuntinuguntanon [1]; Pattra Lertsarawut [1]; Thitirat Rattanawongwiboon [1]; Kasinee Hemvichian [1]

[1] *Nuclear Technology Research and Development Center, Thailand Institute of Nuclear Technology (Public Organization), Nakhon Nayok 26120, Thailand*

Corresponding Author: sakchai@tint.or.th

Cancer has become the main leading cause and reason of death worldwide. Chemotherapy is the most common cancer treatment by using anticancer drugs. However, its treatment is limited by its high toxicity to healthy tissues, causing undesirable side effects. Accordingly, research has combined drugs with nanocarriers, especially gold nanohybrids (AuNHs), to achieve better therapeutic effects. Moreover, AuNHs have been extensively studied for their potential applications in anticancer drug delivery systems. This work reported an efficient method to fabricate smart pH-responsive AuNHs stabilized by folate-targeted pullulan derivative (FTPD) for delivery of camptothecin (CPT) to improve the selectivity, efficacy, and safety of these systems. Monodispersed FTPD@AuNHs were successfully synthesized by the green reduction with the addition of FTPD as a reducing/capping/stabilizing/functionalizing agent. After that, the combination of FTPD@AuNHs-CPT was prepared by subsequent loading of CPT into FTPD@AuNHs via intermolecular interactions. These systems were characterized by TEM, EDS, DLS, Zeta-potential, UV-VIS, XRD, and FTIR analyses, offering sphere-shaped particles with an average size of 11.0 nm. The UV-VIS spectrum of FTPD@AuNHs-CPT showed a redshift from 519 to 528 nm, confirming the formation of a protective layer on the AuNHs surface upon binding to CPT to form the larger NHs. pH-responsive FTPD@AuNHs-CPT demonstrated a faster release rate under acidic conditions. At the end of 72 h, the cumulative amount of CPT released from FTPD@AuNHs-CPT at pH 5.0 was 66.2%, whereas the release rate at pH 7.4 was 29.8%. The FTPD@AuNHs-CPT exhibited 2.8-fold higher cytotoxicity against human lung cancer cells (Chago-k1) than CPT. These systems also displayed high intracellular uptake by folate receptor-mediated endocytosis and induced cell death through the apoptosis pathway by arresting the cell cycle at the G0-G1 phase (9.3-11.4%). Consequently, it is suggested that FTPD@AuNHs-CPT should be considered as a new way for targeted anticancer drug delivery systems.

Poster: S1 Physics innovation - Board: P155 / **204**

Backscattering and Transmission Raman Spectroscopy Systems in the Quantitative Analysis of Solution Concentration

Authors: Tachawit Pao-In Charoenrit[1]; Suwan Plaipichit[1]

Co-authors: Chokchai Puttharugsa [2]; Surawut Wicharn [1]; Prathan Buranasiri [3]; Puenisara Limnonthakul [1]; Wasunun Sassuvun [3]

[1] *Srinakharinwirot University*

[2] *Srinakharinwirot university*

[3] *King Mongkut's Institute of Technology Ladkrabang*

Corresponding Author: tachawitpaoin.charoenrit@g.swu.ac.th

Raman spectroscopy is a set of techniques based on Raman scattering properties, widely applied to analyze the composition of various substances. The techniques consist of 1) Backscattering, which collects Raman signals scattered from the surface of a sample; and 2) Transmission, which collects Raman signals transmitted by the surface of a sample in the opposite direction of a light source (which triggers less fluorescence than the Backscattering). This paper combines Transmission Raman with Backscattering Raman to observe optical accessories such as convex lenses, beamspliters, optical filters, and objective lenses. The experiment system is set up on an optical table using a 532 nanometer diode laser with 100 milliwatt power as the light source. A long-pass filter is used to block light (with a wavelength shorter than 532 nanometers) from the excited samples, as the Raman signals are much weaker than the light source. At the same time, an objective lens is used for amplifying the Raman signals from the sample substances. Then, the amplified Raman signals are collected and analyzed by a dispersive spectrometer. For the experimental samples, there are 3 substances being analyzed in this system; Toluene solution, Acetone solution, and n-Hexane solution, each prepared at a few ranges of concentrations, which are 5 mol/L, 10 mol/L, and 15 mol/L. The result reveals that the system is able to distinguish the sample solutions at different concentrations, either liquid or solid state, as the system is set to enable two selectable modes in one configuration. So, this Raman system is more adaptable for a greater variety of objects.

Keywords: Raman spectroscopy, Backscattering Raman spectroscopy, Transmission Raman spectroscopy, Molarity

Poster: S1 Physics innovation - Board: P158 / **3**

Coalescence of nematic liquid crystal droplets on freely suspended liquid crystal films

Author: Jutarat Kaewthong[1]

[1] *Kasetsart University*

Corresponding Author: jutarat.kaew@ku.th

Freely suspended smectic films of a few molecular layers thick is a model system that can be used to study two dimensional phenomena. In our study, smectic C film was drawn across a few millimeter hole and stabilized under strong surface tension that can suspend 5CB nematic liquid crystal droplets sprayed onto it. Thermal fluctuation of liquid crystal molecules is observed across the smectic C film and can cause the droplets to be driven closer and coalesce. The coalescence in this environment has yet to be studied more extensively [1,2]. When two droplets are touching each other, connecting bridge between them forms and rapidly grows while they merge. Coalescence between them was thoroughly studied through high-speed camera observation and different regimes during coalescence process were analyze. Scaling law for different regimes will be discussed and explained. To understand the experimental result further, we also perform the study of droplet coalescence through finite element software which include inertial force, interfacial force and viscous force in the model. Experimental result and simulation result are compared and analyzed.

Poster: S2 Condensed Matter Physics - Board: P050 / **352**

Fabrication and Thermoelectric Properties of MWCNTs/Recycled Pulp

Authors: Suthat Ladkham[1]; Korapin Pinsuk[1]; Dulyawich Palaporn[2]; Supree Pinitsoontorn[2]

Co-author: Wanthana Silpawilawan [1]

[1] *Division of Physics, Faculty of Science and Technology, Nakhon Ratchasima Rajabhat University*

[2] *Department of Physics, Faculty of Science and Institute of Nanomaterials Research and Innovation for Energy (INRIE), NANOTEC-KKU RNN on Nanomaterials Research and Innovation for Energy*

Corresponding Authors: sutant.ladcam2542@gmail.com, korapin1356@gmail.com, wanthana.s@nrru.ac.th

To utilize heat sources around us, which provide low-temperature waste heat. Carbon-based or organic materials are capable thermoelectric applications in low temperature range, non-toxic, lightweight, and so on. Multi-wall carbon nanotubes (MWCNTs) show excellent electrical conductivity that leading to good thermoelectric property. Herein, we fabricated thermoelectric paper by using vacuum filtration technique. Both p and n-type thermoelectric paper were formed by recycled pulp and MWCNTs. P-type paper were changed electrical charge to n-type paper by polyetherimide (PEI) treatment. Seebeck coefficients of 24.909 μV/K and -9.276 μV/K obtained respectively for p-type and n-type at 360 K. The thermal conductivity of p-type and n-type were 1.75 W/m.K and 0.75 W/m.K, respectively. Furthermore, this thermoelectric paper be able to establish thermoelectric module without substrate.

Poster: S2 Condensed Matter Physics - Board: P051 / **348**

The content calculation of hexagonal phase inclusions in hexagonal GaN films on GaAs (001) substrates grown by metalorganic vapor phase epitaxy

Author: Wiraphat Thanyaphirak[1]

Co-authors: Nattamon Suwannaharn [2]; Warakorn Yanwachirakul [1]; Sakuntam Sanorpim [1]

[1] *Department of Physics, Faculty of Science, Chulalongkorn University.*

[2] *Nanoscience and Technology, Graduate School, Chulalongkorn University.*

Corresponding Author: weraphat81@gmail.com

Hexagonal GaN (h-GaN) films were grown on GaAs (001) substrates by metalorganic vapor phase epitaxy (MOVPE). Two GaN samples were grown with different the thickness of each was 2.35 ± 0.08 and 3.07 ± 0.12 μm, respectively. High resolution X-ray diffraction was used to study the secondary crystallographic phases presented in the h-GaN films. The phase composition of the epilayers was determined by X-ray reciprocal space mapping. The intensities of the c-GaN (002) and h-GaN (10-11) planes detected in the mapping were investigated by ⍵-scans. To quantify the amount of hexagonal phase inclusions in the h-GaN films with a large thickness, the effects of GaN X-ray absorption and of the diffraction geometry were considered. In this case, the content of the hexagonal phase inclusions in the h-GaN films was calculated to about 85.8 and 93.2% for the thickness of 2.35 ± 0.08 and 3.07 ± 0.12 μm, respectively. However, without correction of the X-ray absorption and the diffraction geometry, the content of the hexagonal phase inclusions was reduced by 2.3% and 1.75%, respectively. Diffraction geometry factor can eliminate the effects of ⍵ angles on the irradiated surface areas for different scattered planes.

Poster: S2 Condensed Matter Physics - Board: P054 / **318**

Paste-Injection Molding of Low-Density Barium Hexaferrite Magnets

Author: Chitnarong Sirisathitkul[1]

Co-authors: Wannisa Thongsamrit ; Thanida Charoensuk

[1] *Walailak University*

Corresponding Author: chitnarong.siri@gmail.com

Facile paste-injection molding is an alternative to produce barium hexaferrite magnets with comparable magnetic properties of higher-density compact magnets. Aqueous-based pastes were prepared by mixing barium carbonate and iron oxide powders, with poly(vinyl alcohol) as the binder, poly(ethylene glycol) as the plasticizer, and EFKA® FA4620 as the dispersing agent. The homogeneous ceramic-polymer paste was injected into the mold using syringes and allowed to dry for 3 h at room temperature. Dried magnets were sintered at 1150 ℃ for 5 h and subsequently polished to obtain approximate sizes of 0.4x0.5x1.8 cm3. The amount of polymer additives was varied, yielding the density of magnets from 1.95–2.30 g/cm3. The external magnetic field can also be applied during the obtained this paste-injection molding process.

Poster: S2 Condensed Matter Physics - Board: P055 / **315**

Effect of Ni-Co transition metal ratios on structure-function of Lithium Aluminum Borate Glasses by synchrotron-based XAS and XPS

Author: Jidapa Lomon[None]

Co-authors: Jintara Padchasri ; Narong Chanlek [1]; Pinit Kidkhunthod ; Prayoon Songsiriritthigul [2]; Sumeth Siriro ; amorntep montreeupathum

[1] *Suranaree University of Technology (TH)*

[2] *Research Network NANOTEC–SUT on Advanced Nanomaterials and Characterization, School of Physics, Suranaree University of Technology, Nakhon Ratchasima 30000, Thailand, Thailand Center of Excellence in Physics, MHESRI, Bangkok 10400, Thailand, Synchrotron Light Research Institute, Muang, Nakhon Ratchasima 30000, Thailand*

Corresponding Author: dreemda55@gmail.com

X-ray absorption spectroscopy (XAS) were employed for the investigations on the local structure and oxidation state of Lithium Aluminum Borate Glasses(Li_2O-Al_2O_3 -B_2O_3) doped with various concentrations of xNi:Co (where x = 1, 2, 3, and 4).XAS analyses revealed that all glasses comprise the mixed oxidation state of Ni^{+2} and Ni^{+3} corresponding to cyclic voltammetry (CV) results measured. TEM diffraction pattern and XRD patterns were used to confirm phase structure of all samples. Interestingly, electrochemical properties of prepared (Li_2O-Al_2O_3 -B_2O_3) glasses could be enhanced by changing the Ni/Co ratio in glass structure.

Poster: S2 Condensed Matter Physics - Board: P056 / **310**

Coalescence of nematic liquid crystal droplets on freely suspended liquid crystal films

Authors: Jutarat Kaewthong[1]; Wuttipan Satienpaisan[2]; Natthawat Hongkarnjanakul[3]; Padetha Tin[4]; Nattaporn Chattham[1]

[1] *Kasetsart University*

[2] *Department of Physics, Faculty of Sciences, Kasetsart University, Bangkok 10900, Thailand*

[3] *Geo-Infomatics and Space Technology Development Agency (GISTDA)*

[4] *NASA Glenn Research Center*

Corresponding Author: jutarat.kaew@ku.th

Freely suspended smectic films of a few molecular layers thick is a model system that can be used to study two dimensional phenomena. In our study, smectic C film was drawn across a few millimeter hole and stabilized under strong surface tension that can suspend 5CB nematic liquid crystal droplets sprayed onto it. Thermal fluctuation of liquid crystal molecules is observed across the smectic C film and can cause the droplets to be driven closer and coalesce. The coalescence in this environment has yet to be studied more extensively [1,2]. When two droplets are touching each other, connecting bridge between them forms and rapidly grows while they merge. Coalescence between them was thoroughly studied through high-speed camera observation and different regimes during coalescence process were analyze. Scaling law for different regimes will be discussed and explained. To understand the experimental result further, we also perform the study of droplet coalescence through finite element software which include inertial force, interfacial force and viscous force in the model. Experimental result and simulation result are compared and analyzed.

Poster: S2 Condensed Matter Physics - Board: P057 / **304**

Fabrication of single-walled carbon nanotube photodetectors using the dielectrophoretic assembly

Author: NIramai Chirapraphusak[None]

Co-author: Yodchay Jompol

Corresponding Author: niramai.fern23@gmail.com

We present a simple technique based on a bottom-up approach to assembling single-walled carbon nanotubes (SWCNTs) in between two metal electrodes, making the SWCNT photodetectors with the capability of being operated at room temperature. This technique is known as dielectrophoresis (DEP) that exploits an electric field across the microelectrode gap with an application of a high-frequency AC field. As the geometry of the electrodes is different, the resulting imbalance of electric field intensity leads to a net force that pulls the nanotubes suspended in a liquid to attract the metal. In this work, an oscilloscope was used to monitor the change of a voltage drop across a constant resistor (1kΩ), connecting in series with the electrodes, to justify the close-circuit condition during the DEP assembly. By varying the SWCNT concentrations in Toluene from 0.01 μg/ml to 0.42 μg/ml, we were able to deposit the nanotubes in the electrode gaps at different densities, ranging from individuals to densely-packed networks. After the device fabrication, we performed photocurrent measurement by optical excitation using a near-infrared laser (NIR) (λ = 975 nm) and then evaluated the device's photoresponsivity at different laser powers of up to 450 mW. Further work on a temporal measurement will be needed to verify the time response of the devices. Based on our experimental results, the DEP technique can permit various nanomaterials to be deposited into micrometre or nanoscale-gapped electrodes for further development of nanoelectronics on transparent and flexible non-conductive substrates.

Poster: S2 Condensed Matter Physics - Board: P058 / **286**

High-performance supercapacitor electrode using microwave reflux-assisted modification of the activated carbon derived from Kapok shell

Author: Mavin Punon[None]

Co-author: Nattakan Kanjana [1]

[1] *Physic of mahasarakham university*

Corresponding Author: nattakan.kan@msu.ac.th

In this study, the high-performance supercapacitor electrodes were fabricated via an activated carbon derived from Kapok shell. The raw biomass carbonization at 800 ℃ under Ar atmosphere was followed by microwave reflux process using the mixture of HNO3/H2SO4 ratio of 3:1 as a catalytic solution. The activated carbons with and without reflux treatment were characterized by TG, XRD, Raman and SEM techniques. Electrochemical properties of as-prepared materials were investigated within potential ranges from −1 to 0 V in a 6 M KOH solution. The electrochemical measurements were analysis with CV, G/CD and EIS techniques. When applied as a supercapacitor electrode material, it exhibited good electrochemical performance with a specific capacitance of 156.18 F g−1 at 1 A g−1 with current density achieved in the sample with 10 min reflux time. Conversely, the sample without microwave reflux modification exhibited electrochemical performance with a specific capacitance of 83.1 F g−1 at 1 A g−1. The electrochemical performance showed that activated carbon from Kapok shells synthesis with microwave-assisted reflux was an interesting material to create electrode for a supercapacitor.

Poster: S2 Condensed Matter Physics - Board: P058 / **274**

EFFECT OF SINTERING TIME ON PHASE, PHYSICAL PROPERTIES, MICROSTRUCTURE AND THERMAL CONDUCTIVITY OF Y(Ba1-xLax)2Cu3O7-δ CERAMICS

Author: Sireetone Yawirach[None]

Co-authors: Pimpilai Wannasut ; anucha Watcharapasorn

Corresponding Author: anucha@stanfordalumni.org

EFFECT OF SINTERING TIME ON PHASE, PHYSICAL PROPERTIES, MICROSTRUCTURE AND THERMAL CONDUCTIVITY OF $Y(Ba_{1-x}\ La_x)_2Cu_3O_{7-\delta}$ CERAMICS

Sireetone Yawirach [a,b], Pimpilai Wannasut[a], Anucha Watcharapasorn[a,c*]
[a]Department of Physics and Materials Science, Faculty of Science, Chiang Mai University, Chiang Mai 50200, Thailand
[b]Graduate School, Chiang Mai University, Chiang Mai 50200, Thailand
[c]Center of Excellence in Materials Science and Technology, Materials Science Research Center, Faculty of Science, Chiang Mai University, Chiang Mai 50200, Thailand
*Corresponding author, e-mail: anucha@stanfordalumni.org

Abstract: This work investigates the effects of various sintering conditions on phase, physical properties microstructure and thermal conductivity of $Y(Ba_{1-x}\ La_x)_2Cu_3O_{7-\delta}$ where x = 0, 0.05,0.10, 0.15, 0.20 and 0.25 mol fraction. The sintering conditions involved the sintering temperature of 920 ^oC and sintering time of 6, 8, 10 and 12 h. It was found that pure phase could be obtained in the samples sintered for 6 h regardless of composition. However, small amount of $BaCuO_2$ secondary phase was obtained at other sintering time. The relatively low density and significantly reduced grain size was obtained in the samples with high La content (e.g.x = 0.20 and 0.25) regardless of the sintering time. This showed that La addition had apparent effects on sinterability and grain growth. Phase analysis indicated that the structure changed from orthorhombic to tetragonal when the La concentration reached 0.20 and 0.25 mol fraction. SEM images of all ceramics also indicated irregular shaped grains. The effects of variation in density, microstructure and composition on the thermal conductivity of all ceramics were also discussed in details.

Poster: S2 Condensed Matter Physics - Board: P060 / **72**

Gamma Irradiation Assisted Nickel Impregnation on Activated Carbon Derived from Water Hyacinth for Electrocatalyst Application

Authors: Piyapat Tonkaew[1]; Nicharee Deechakawan[1]; Nichawadee Kanjanakosit[1]; Suranan Anantachaisilp[1]; Threeraphat Chutimasakul[2]; Kwamman Tanagorn[2]

[1] *Kamnoetvidya Science Academy*

[2] *Thailand Institute of Nuclear Technology (Public Organization)*

Corresponding Authors: piyapat_t@kvis.ac.th, nicharee_d@kvis.ac.th, nichawadee_k@kvis.ac.th

Water hyacinth (WH) is an invasive floating plant causing water pollution. However, its leaves contain a high cellulose content, which can be utilized as biomass to synthesize activated carbon. Thus, in this study, water hyacinth was subjected to the KOH activation process to obtain water hyacinth-based activated carbon (WH/AC). Moreover, as a novel method for nickel impregnation, gamma irradiation was proposed as an alternative to replacing the traditional method due to its high penetration power and energy. To obtain the best conditions for nickel impregnation, different absorbed doses of gamma-ray (0, 20, 100 kGy) were applied to commercial activated carbon (AC), denoted as 0-AC, 20-AC, and 100-AC, respectively. These samples were thoroughly characterized with BET, SEM-EDS, FT-IR, XRD, XPS, and Raman spectroscopy. The higher I_D/I_G ratio in Raman spectroscopy, implying the greater disorder of the sample and, consequently, the more incredible amount of nickel impregnated on the sample. The SEM images showed that the surface morphology of the activated carbon significantly changed, becoming more spherical in structure, and distributed after gamma irradiation. The BET surface areas of AC, 0-AC, 20-AC, and 100-AC were 717, 718, 789, and 798 m^2/g, respectively. As a result, the optimum absorbed dose for nickel impregnation is 20 kGy. Thus, a 20 kGy absorbed dose of gamma-ray was carried out in WH/AC. The activated carbon electrocatalysts were investigated for applying electrochemical carbon dioxide reduction reaction (CO_2RR) by linear sweep voltammetry (LSV). The 20-WH/AC electrocatalyst exhibited the highest efficiency compared to others. Further studies are needed to improve the efficiency of the electrocatalyst in the CO_2RR process. Finally, the results show that water hyacinth can potentially be used as a raw material in the production of nickel-impregnated activated carbon irradiated with gamma rays.

Keywords: Activated carbon; Water hyacinth; Gamma irradiation; Nickel impregnation; Electrocatalyst

Poster: S2 Condensed Matter Physics - Board: P061 / **284**

Synthesis and characterization of manganese dioxide for high electrochemical performance supercapacitor electrode

Authors: Pawinee Klangtakai[None]; Phatcharinrat Arromsawa[1]

[1] *Khon Kaen University*

Corresponding Author: pawinee@kku.ac.th

In this study, manganese dioxide (MnO2) was synthesized by hydrothermal method using different urea (CO(NH2)2) of No Urea, Urea 0.0686 mL, Urea 0.686 mL, and Urea 6.86 mL. Crystal structure of synthesized MnO2 was evaluated by X-ray diffraction technique to be delta-MnO2 structure (No Urea and Urea 0.0686 mL) and alpha-MnO2 structure (Urea 0.686 mL and Urea 6.86 mL). Morphology of delta-MnO2 and alpha-MnO2 structures show a nanoflower and a nanorod shape, respectively. The specific capacitance of four MnO2 electrodes in a 1 M Na2SO4 electrolyte are 118.40, 108.77, 60.30, and 41.15 F g-1 at a current density of 0.3 A g-1, for No Urea, Urea 0.0686 mL, Urea 0.686 mL and Urea 6.86 mL MnO2 electrodes, respectively. The No Urea MnO2 electrode gives the highest specific capacitance due to its largest pore size of 25.04 nm. The charge/discharge mechanism of electrodes could be explained by energy dispersive spectroscopy. It was found that SO42- ions are attracted to the MnO2 electrode surface at charging state from 0.0 V up to 0.9 V. In contrast, the SO42- ions move away from the MnO2 electrode surface at discharging state from 0.9 V to 0.0 V.

Poster: S2 Condensed Matter Physics - Board: P062 / **255**

EFFECT OF ANNEALING TEMPERATURE ON THERMOELECTRIC PROPERTIES OF YBa2Cu3O7-x CERAMICS

Authors: Anucha Watcharapasorn[1]; Paitoon Boonsong[2]; Pimpilai Wannasut[None]; Sireetone Yawirach[3]

[1] *1Department of Physics and Materials Science, Faculty of Science, Chiang Mai University, Chiang Mai 50200, Thailand 3Center of Excellence in Materials Science and Technology, Materials Science Research Center, Faculty of Science, Chiang Mai University, Chiang Mai 50200, Thailand*

[2] *Department of Physics and Materials Science, Faculty of Science, Chiang Mai University, Chiang Mai 50200, Thailand*

[3] *Graduate School, Chiang Mai University, Chiang Mai 50200, Thailand*

Corresponding Author: pimpilai.mats@gmail.com

Abstract: The research studied the effect of annealing temperature on phase and thermoelectric properties of YBa2Cu3O7-x ceramics synthesized by hot pressing method. The hot-pressing condition involved the applied pressure of 70 MPa at 800 ⁰C for 1 h under Ar atmosphere. The YBCO ceramic samples were annealed in oxygen atmosphere at 700 and 750 ⁰C for 4 h. The XRD patterns of all samples showed single phase of YBCO. The annealing process had the most impact on the electrical conductivity by causing the values to decrease and changed the conduction mechanism from metallic-like to semiconductor-like behavior when the annealing temperature was increased. The trend of ZT therefore followed that of the electrical conductivity which may be attributed to the charged defects present in these samples.

Poster: S2 Condensed Matter Physics - Board: P063 / **249**

Characterization of biofuel pellets production from woody biomass blends

Author: Wassachol Wattana[None]

Co-author: Warunee Bawornkiatkaew

Corresponding Author: wassachol.wa@kmitl.ac.th

In this study biofuel pellet made from Para rubber wood (*Hevea brasiliensis* Muell. Arg.) blended with branches and leaves of She Oak (*Casuarina Equisetifolia*) and Cajuput trees (*Melaleuca Cajuputi*) were characterized. Para rubber wood sawdust was the main raw material as 70% of whole content. The branches and leaves of She Oak and Cajuput were selected for blending materials as the rest ratio for each type of raw materials. The pellet production was produced from a single pellet machine in the laboratory. After that, proximate analysis, heating value, thermogravimetric analysis of pellets was analyzed. Moreover, microstructure of cross section area of pellets was illustrated via SEM picture. This study revealed that the overall quality of rubber sawdust pellet fuel was of medium quality, however it can modify or improved by blending with another materials. The fuel pellet containing the Cajuput branches provided good combustion properties. The SEM picture showed that the pellet made from blending material provided more void fraction than only one material. The suitable raw materials from this study that recommend to adding for improved the quality of biofuel pellet are branches and leaves of the Cajuput tree.

Poster: S2 Condensed Matter Physics - Board: P064 / **171**

Photocatalytic Activity of Copper Doped on Bismuth Oxychloride Based for Degradation Rhodamine B under UV-light Irradiation

Author: Thirawit Phonkhokkong[1]

[1] *faculty of science buriram rajabhat university*

Corresponding Author: teerawitphon@gmail.com

The aim of research was successfully synthesized copper doping on bismuth oxychloride based by microwave assisted radiation method power 300 watt for 15 minutes. Defining conditions of samples preparation copper were doped following 0, 2.5, 5.0 and 7.5 %mol. All samples were examined for their properties and characteristics using X-ray diffraction (XRD), Field Emission scanning Electron Microscope (FE-SEM), UV-Visible Spectrophotometer, Energy Dispersive X-Ray Spectroscopy (EDX). Examination for degradation of Rhodamine B (RhB) under UV light irradiation. Found result, the most effective sample in degradation of RhB by using copper doped on bismuth oxychloride 5.0 %mol the best reaction with highest percentage of photodegradation RhB 64 % for 90 minutes irradiation time.

Poster: S2 Condensed Matter Physics - Board: P065 / **166**

Giant Dielectric Properties of Ca[$Cu_{3-x}Ti_x$]Ti_4O_{12} Ceramics

Authors: Narong Chanlek[1]; Prasit Thongbai[2]; Piyanud Wongtongdee[None]

[1] *Suranaree University of Technology (TH)*

[2] *Khon Kaen University*

Corresponding Author: piyanud.wo@kkumail.com

Ca[$Cu_{3-x}Ti_x$]Ti_4O_{12} (x= 0.00, 0.03, 0.09, 0.15 and 0.30) ceramics were prepared using a solid-state reaction method. The mixed oxides were calcined at 800 ℃ for 5 h and then sintered at 1090 ℃ for 5 h. The effects of Ti doping ions on the microstructure and dielectric properties were studied. The results indicated that the Ca[$Cu_{3-x}Ti_x$]Ti_4O_{12} showed improved dielectric properties, including giant permittivity (ε'~10^4) and low loss tangent (tanδ ~ 0.13-0.01) at room temperature over the frequency range from 40 Hz to 10 MHz. Notably, the Ca[$Cu_{3-x}Ti_x$]Ti_4O_{12} with x=30% showed improved dielectric properties with ε'~ 5.91x10^4 and low tanδ ~ 0.07 at room temperature and 1 kHz. Impedance spectroscopy was used to analyze the electrical properties of the grains and grain boundaries. The giant dielectric properties were explained by an internal boundary layer capacitance (IBLC) effect.

Poster: S2 Condensed Matter Physics - Board: P066 / **168**

Effect of Sulfur Doping in Bismuth Oxychloride on Degradation and Photocatalytic of Rhodamine B Under UV irradiation

Author: Warut Koonnasoot[None]

Corresponding Author: warut.ks@bru.ac.th

This research presents synthesis of sulfur doped bismuth oxychloride (S-doped BiOCl) powder by using microwave radiation with power of 450 Watt for 15 minutes. Different sulfur contents, 0, 2.5, 5 and 7.5 %mol, were purposed. Prepared samples were characterized by using X-ray diffraction (XRD), Fourier transform Infrared Spectroscopy (FT-IR), UV-Visible Spectrophotometer Field Emission scanning Electron Microscopy (FE-SEM) and Energy Dispersive X-Ray Spectroscopy (EDX). The S-doped BiOCl was tested with Rhodamine B under UV irradiation for their degradation and photocatalytic activity studies. Result shows that sulfur doping at 2.5 %mol gave the best reaction with highest degradation rate of 78% at 90 minutes of irradiation time. This study indicates the potential use of S-doped BiOCl for degradation and photocatalytic application.

Poster: S2 Condensed Matter Physics - Board: P067 / **176**

Fabrication, characterization and magnetic properties of La0.5Sr0.5TiO3 nanofibers

Author: Wichaid Ponhan[1]

Co-authors: Tanachai Ponken [1]; Konlayut Deejing [1]

[1] *Program of Physics, Faculty of Science and Technology, Rajabhat Maha Sarakham University, Maha Sarakham, 44000, Thailand*

Corresponding Author: wichaid.po@rmu.ac.th

La0.5Sr0.5TiO3 nanofibers were fabricated by simple electrospinning using a solution that contained poly(vinylpyrrolidone) (PVP), Lanthanum nitrate (La(NO3)3.6H2O), Strontium nitrate (N2O6Sr) and Diisopropoxytitanium bis(acetylacetonate) solution. The La0.5Sr0.5TiO3 nanofibers with average diameters of 109 – 140 nm were successfully obtained from calcination of the as-spun La0.5Sr0.5TiO3/PVP composite nanofibers at 630 – 930 ⁰C in air for 2 h. The as-spun and La0.5Sr0.5TiO3 nanofibers were characterized by SEM, XRD, TEM, and VSM. The results of XRD and TEM with selected electron diffraction (SEAD) analysis indicated that the La0.5Sr0.5TiO3 nanofibers had cubic perovskite structure with high intensity phase. Room temperature magnetization results revealed a diamagnetic behavior for all La0.5Sr0.5TiO3 nanofibers.

Poster: S2 Condensed Matter Physics - Board: P068 / **175**

Influence of glycerin addition on formation and magnetic properties of MnBi prepared by vacuum sintering technique

Author: Satienrapong Ngamsomrit[None]

Co-authors: Tanachat Eknapakul [1]; Supree Pinitsoontorn [2]; Prayoon Songsiriritthigul [3]

[1] *Suranaree University of Technology*

[2] *Khonkaen University*

[3] *Suranaree University of Technology*

Corresponding Author: tanachat88@gmail.com

This work presents an alternative method to reduce the Mn particle size by adding glycerine during the ball-milling process. This glycerin addition is expected to prevent particle agglomeration to achieve the small and non-gathered Mn particles. The Mn and Bi precursors were fixed at an atomic ratio of 1:1 using Mn particles which were ball-milled in glycerin between 1 and 6 hr. It is seen that the average particle size decreases from 35-40 μm to 15-20 μm after 1 and 6 hr grinding time, respectively. The low-temperature phase MnBi (LTP-MnBi) was prepared by vacuum sintering technique using a sintering temperature of 275 ^oC for 12 hours under an ultra-high vacuum (≈10^-8 mbar). The sintered LTP-MnBi samples prepared from 1 (MnG_1Bi), 3 (MnG_3Bi), and 6 hr (MnG_6Bi) glycerine-added Mn grinding time were studied by X-ray diffraction (XRD), scanning electron microscopy (SEM), X-ray photoemission spectroscopy (XPS) and vibrating sample magnetometry. The coercivity values (H_c) are 3.95, 2.35, and 0.95 kOe for MnG_1Bi, MnG_3Bi, and MnG_6Bi samples, respectively. The saturation magnetization (M_s) of MnG_1Bi and MnG_3Bi are relatively similar (~0.18 emu/g), while the M_s of MnG_6Bi is much higher than those. The XRD result shows that there are a few percentages of MnBi concentration in all samples, implying that glycerin addition could hinder the MnBi formation. This could be explained by the interruption of the diffusion mechanism during liquid-phase sintering due to the coverage of hydrocarbon (i.e., NH_2-CH_2-COOH) groups on Mn particles. Moreover, from elemental composition analysis, it was found that the MnO content tends to increase on the Mn surfaces as the grinding time increases.

Poster: S2 Condensed Matter Physics - Board: P069 / **206**

Multifunction Acoustic Board Production from Corncob-Derived Activated Carbon and Corn Husk Waste Composite as Sound and Smell Absorbers with Natural Latex Adhesive

Author: Samroeng Narakaew[1]

Co-author: Phiphop Narakaew [2]

[1] *Lampang Rajabhat University*

[2] *Lampang Rajabhat University*

Corresponding Author: sumreanglpru@gmail.com

This work aims the preparation of corncob-derived activated carbon (CCAC) by using 3M sodium chloride aqueous solution as the activated agent, and was pyrolyzed at 600, 700, and 800 C. Waste composites of CCAC with the activated corn husk fiber (ACH-fiber) and natural rubber latex (NR-latex) adhesive applied for multifunction acoustic board (MCB), and the acoustic board waste composite efficiency for sound and cigarette smell absorption were evaluated and compared with the commercial acoustic foam broad. Brunauer–Emmett–Teller surface area analysis results shows the optimum 2.27 nm CCAC mesopore size with surface area of 525.26 m2/g, and surface morphologies were also confirmed with scanning electron microscope. Densities of MCB samples were observed as similar to commercial acoustic foam broad. The sound absorption coefficient (SAC) of MCB samples in the frequency range of 500-6,400 Hz, increase with increasing the amount of ACH-fiber and CCAC in the range of 2.5-10%w due to the porous sound absorbing-samples have the cubic cells with connecting pore and parallel fiber bundles by the sound incident, transmitted through inside, and converted to heat, and finally absorbed by porous absorbing-materials. The sound absorbing efficient of MCB samples in this work has high as compare to the special commercial acoustic foam broad with confirming from the noise reduction coefficient (NRC). Moreover, the MCB sample in the NR-latex adhesive : ACH-fiber : CCAC w/w ratio of 95.0 : 2.5 : 2 showed 100% cigarette smell absorbing efficient for 6 mins.

Poster: S2 Condensed Matter Physics - Board: P070 / **205**

Development of Latent Fingerprints on Non-Porous Surfaces by Small Particle Reagent with Zinc Oxide Nanoparticles

Authors: Penpicha Mode-on[1]; Supawan Pansiw[2]; Gedsirin Eksinitkun[1]

[1] *Forensic Science program, Department of Chemistry, Faculty of Liberal Arts and Science, Kasetsart University, Kampeang Sean Campus*

[2] *Police Forensic Science Center 1*

Corresponding Author: penpicha.mo@ku.th

Small particle reagent (SPR) is a technique to detect latent fingerprints on wet non-porous surface by suspension of reagent is linked to fatty acid left on fingerprints. SPR can be used to detect latent fingerprints on evidence that has been submerged for a long time. Mostly investigate institution use SPR that import from foreigners, thus it is expensive and wait a long time. Many researchers have tried to develop SPR formulations from chemicals that are easy to come by, cost-effective, and harmless to users from that problem.

In this study, a Small Particle Reagent (SPR) based on nano zinc oxide was developed and mixed with sodium tetradecyl sulfate and diethylene glycol monoethyl ether, a solvent that allows the component to be evenly distributed throughout the reagent and the small particles would be able to bind with fatty acid in the fingerprints. The latent fingerprints were deposited on four different non porous surfaces such as glass slides,stainless spoons,aluminum foil,and plastic slides and immersed in tap water for 1, 3, 7, 14 and 30 days before the examination.

The results of the evidence were clear, and detectable minutiae can be used for visualization and identification of latent prints by using an Automated Fingerprint Identification System (AFIS) more than 20 points of minutiae. In conclusion, this study could help forensic scientists and individuals in the criminalistics field; to be able to develop latent fingerprints with non-hazardous materials in a quicker fashion.

Poster: S2 Condensed Matter Physics - Board: P071 / **158**

A NOVEL MUTTILAYER PARTICLEBOARDS PREPARED FROM MILK PACKAGE (U.H.T.) WASTES AND COCONUT FIBERS

Author: Pongsathorn Kongkaew[1]

[1] *Program of Physics, Faculty of Science and Technology, Rajabhat Maha Sarakham University.*

Corresponding Author: ch_ko29@hotmail.com

The aim of this research was to evaluate the physical, mechanical and thermal properties of multilayer particleboards prepared from milk package (U.H.T.) wastes (TP) and coconut fibers (CO). The particleboards were produced with three layers ; A:(TP/CO/TP), B:(CO/TP/CO), C:(TP/TP+CO/TP), and D:(CO/TP+CO/CO) bonded with and methylene diphenyl diisocyanate (pMDI) 7%. The finding of experiment showed that physical properties of all the sample into requirement of Thai industrial standard 876-2547(TIS 876-2547) for furniture production. The mechanical properties results of B, C and D for Modulus of rupture (MOR) and all sample for Modulus of elastic (MOE) were higher than the value required by TIS 876-2547. The internal bonding (IB) of C and D were higher than the standard value. The thermal properties showed that with in the range 270-500 ° C of D is highest weight lose. However, the use of renewable waste and natural fiber such as milk package (U.H.T.) and coconut fiber respectively, could conduce solution to resource shortage for manufacturing particleboards.

Poster: S2 Condensed Matter Physics - Board: P072 / **223**

The spin Hall thermopile of Si/YIG/Co,Fe

Authors: poramed wongjom[None]; wimutti Kumpor[1]; perawas Kuptapol[2]

[1] *1Department of Physics, Faculty of Science and Technology, Thammasat University, Pathum Thani 12120, Thailand*

[2] *Department of Physics, Faculty of Science and Technology, Thammasat University, Pathum Thani 12120, Thailand*

Corresponding Authors: wimutti.kum@dome.tu.ac.th, perawas.kup@dome.tu.ac.th

The conversion of heat to spin current is well known as spin Seebeck effect. In this study, we observed spin voltage on cobalt (Co) and Iron (Fe) which acing for spin detector whereas the ferrimagnetic (YIG) is used for spin injector. The YIG is coated on Si-wafer by sputtering technique whereas the Co and Fe are prepared by thermal evaporation technique on zigzag pattern. We checked phase diagram, surface structure and magnetic property by XRD, SEM and VSM, respectively. We found that the spin Hall thermopile on Si/YIG/Co,Fe is enhanced by connected the Fe and Co on a series.

Poster: S2 Condensed Matter Physics - Board: P073 / **226**

Observation of spin Seebeck effect in YIG/Co100-xNbx alloys

Authors: Nithiporn Photimas[1]; natthamon Chaikrachang[1]; poramed wongjom[None]

[1] *Department of Physics, Faculty of Science and Technology, Thammasat University, Pathum Thani 12120, Thailand*

Corresponding Authors: nithiporn.pho@dome.tu.ac.th, natthamon.jai@dome.tu.ac.th

The conversion of heat to spin current is well known as spin Seebeck effect (SSE). In this study, we observed spin voltage on Co and Nb which acing for spin detector whereas the ferrimaganetic (YIG) is used for spin injector. We studied phase diagram, surface structure and magnetic property by XRD, SEM and VSM, respectively. For SSE, the magnetic field dependence and temperature dependence are also observed. We found that the voltage of Co and Nb mixing is enhanced which it can be used for spin generator by these methods.

Poster: S2 Condensed Matter Physics - Board: P074 / **229**

The multilayer of Si/YIG/W for spin Seebeck effect by sputtering technique

Authors: Chananyapat Wongsakilkhamkhota[1]; Poowadet Hmontong[1]; poramed wongjom[None]

[1] *Division of Physics, Faculty of Science and Technology, Thammasat University, Pathum Thani 12120, Thailand*

Corresponding Authors: chananyapat.won@dome.tu.ac.th, poowadet.hmo@dome.tu.ac.th

The conversion of heat to spin current is well known as spin Seebeck effect (SSE). In this study, we observed spin voltage on Si/YIG/W by multilayer technique. We studied phase diagram, surface structure and magnetic property by XRD, SEM and VSM, respectively. For SSE, the magnetic field dependence and temperature dependence are also observed. We found that the voltage of Si/YIG/W multilayer is enhanced which it can be used for spin generator by these methods.

Poster: S2 Condensed Matter Physics - Board: P075 / **279**

CVD Synthesis of Intermediate State-Free, Large-Area and Continuous MoS2 via Single-Step Vapor-Phase Sulfurization of MoO2 Precursor

Authors: Tinna Chiawchan[1]; Harihara Ramamoorthy[1]; Kanokwan Buapan[1]; Ratchanok Somphonsane[None]

[1] *King Mongkut's Institute of Technology Ladkrabang*

Corresponding Author: ratchanok.so@kmitl.ac.th

The low evaporation temperature and carcinogen classification of commonly used molybdenum trioxide (MoO3) precursor render it unsuitable for the safe and practical synthesis of molybdenum disulfide (MoS2). Furthermore, as evidenced by several experimental findings, the associated reaction constitutes a multistep process prone to the formation of uncontrolled amounts of intermediate MoS2−yOy phase mixed with the MoS2 crystals. Here, molybdenum dioxide (MoO2), a chemically more stable and safer oxide than MoO3, was utilized to successfully grow cm-scale continuous films of monolayer MoS2. A high-resolution optical image stitching approach and Raman line mapping were used to confirm the composition and homogeneity of the material grown across the substrate. A detailed examination of the surface morphology of the continuous film revealed that, as the gas flow rate increased by an order of magnitude, the grain-boundary separation dramatically reduced, implying a transition from a kinetically to thermodynamically controlled growth. Importantly, the single-step vapor-phase sulfurization (VPS) reaction of MoO2 was shown to suppress intermediate state formations for a wide range of experimental parameters investigated and is completely absent, provided that the global S:Mo loading ratio is set higher than the stoichiometric ratio of 3:1 required by the VPS reaction.

Poster: S2 Condensed Matter Physics - Board: P076 / **150**

Microscopic studies of magnetic MnBi powder particles

Author: Jongrak Borsup[None]

Co-authors: Tanachat Eknapakul [1]; Visittapong Yordsri ; Supree Pinitsoontorn ; Chanchana Thanachayanont ; Prayoon Songsiriritthigul

[1] *Suranaree University of Technology*

Corresponding Author: jongrak.borsup@gmail.com

In this work, the different sizes of LTP-MnBi powder prepared by vacuum sintering at 275°C and time for 12 hr. responds to the magnetic properties, microstructure, and crystal structure. Cross-sectional MnBi powder particles were prepared for investigations by using scanning electron microscopy equipped with energy dispersive X-ray spectroscopy (SEM/EDS). The SEM/EDS results provide information of the formation of MnBi during liquid phase sintering. The formation mechanism will be presented and discussed. Magnetic force microscopy (MFM) was also employed to obtain the magnetic properties of the MnBi. The topography and MFM images of the MnBi samples with and without applied magnetic field were recorded. Before applying the field, MFM image shows the bright and dark regions of the magnetic domain similar to SEM/EDS image that displayed a spider-web feature of the MnBi phase and Mn phase. With aligned magnetic field, the size of the magnetic domain split into the small domain. The small MnBi grain size, the higher coercivity.
Keyword: LTP-MnBi, vacuum sintering, MFM, magnetic domain, domain wall movement

Poster: S2 Condensed Matter Physics - Board: P077 / **149**

Effects of volume and compression on magnetic properties and homogeneity of MnBi prepared by liquid-phase sintering

Author: Puttamawan Juntree[1]

Co-authors: Prayoon Songsiriritthigul [2]; Tanachat Eknapakul [1]

[1] *Suranaree University of Technology*

[2] *Research Network NANOTEC–SUT on Advanced Nanomaterials and Characterization, School of Physics, Suranaree University of Technology, Nakhon Ratchasima 30000, Thailand, Thailand Center of Excellence in Physics, MHESRI, Bangkok 10400, Thailand, Synchrotron Light Research Institute, Muang, Nakhon Ratchasima 30000, Thailand*

Corresponding Author: kaewputtamawan555@gmail.com

The formation of low-temperature phase manganese bismuth (LTP-MnBi) prepared by liquid phase sintering (LPS) can be achieved through the diffusion of liquid Bi into Mn. It is known that the LPS process can produce the solid-liquid separation induced by gravitation which easily results in the non-uniform sintered MnBi particles. In this work, we aim to reduce such inhomogeneity by two processes; reducing the volume and applying compression, in order to reduce the gravitational effect. Here, 1 g of Mn and Bi mixture with 1:1 atomic ratio which is 5 times less than normal operation was used. The mixture was then sintered at 325°C for 24, 48 and 96 hours and cooled down naturally to obtain the MnBi. The XRD results showed that the more sintering time, the MnBi concentration increases which could be described by the diffusion process. A vibrating sample magnetometer was used to measure the magnetic characteristics of the sintered samples. The average energy product ((BH)max) values were 1.81, 2.31, and 3.28 MGOe, respectively, consistent with their phase identifications. The compressed samples with packing density of around 8.61 g/cm3 were sintered at 325°C between 3 - 96 hours. It was found that the MnBi phase is significantly low in the samples prepared at 3 - 36 hours compared to the samples prepared at 48 and 96 hours. This resulted in an average (BH)max of 0.37 MGOe for 24 hours-sintered samples while those of 2.87, and 2.42 MGOe were observed in the samples sintered at 48 and 96 hours, respectively. It is noted that the MnBi purity and magnetic properties of the reduced volume samples are higher and more homogeneous while the compressed samples are worse compared to the regularly sintered MnBi. The homogeneity enhancement could be ascribed by the reduction of gravitational effect during liquid-phase sintering. The reduction of magnetic performance and MnBi concentration in the compressed samples could be caused by the limited spaces and pores that hinder the Bi flow and diffusion during LPS process.

Poster: S2 Condensed Matter Physics - Board: P078 / **141**

Effect of Mn grinding time on structural, chemical and magnetic properties of the Manganese Bismuth prepared by sintering in vacuum

Authors: Satienrapong Ngamsomrit[1]; Tanachat Eknapakul[1]; Supree Pinitsoontorn[2]; Prayoon Songsiriritthigul[3]

[1] *Research Network NANOTEC–SUT on Advanced Nanomaterials and Characterization, School of Physics, Suranaree University of Technology, Nakhon Ratchasima 30000, Thailand, Thailand Center of Excellence in Physics, MHESRI, Bangkok 10400, Thailand*

[2] *Institute of Nanomaterials Research and Innovation for Energy, Khon Kaen University, Khon Kaen 40002, Thailand*

[3] *Research Network NANOTEC–SUT on Advanced Nanomaterials and Characterization, School of Physics, Suranaree University of Technology, Nakhon Ratchasima 30000, Thailand, Thailand Center of Excellence in Physics, MHESRI, Bangkok 10400, Thailand, Synchrotron Light Research Institute, Muang, Nakhon Ratchasima 30000, Thailand*

Corresponding Author: boythailand06@gmail.com

This report presents the changes of structural, chemical and magnetic properties of the low-temperature phase manganese bismuth (LTP-MnBi) magnetic materials as a function of Mn grinding time. The grinding was conducted on the Mn powder with original average size of more than 400 ⊠m using the ball-milling technique. The grinding time was set to be 1-15 hr to obtain different Mn particle sizes prior to the MnBi synthesis. LTP-MnBi powder was successfully prepared by vacuum sintering method which was carried out at 275 oC for 12 hours at pressure below 5 ⊠ 10-7 mbar. Morphology, elemental composition and structure of MnBi powder were investigated by scanning electron microscopy combined with energy dispersive spectroscopy, X-ray photoemission spectroscopy and X-ray diffraction. The magnetic properties were examined using vibrating sample magnetometer. From XRD results, the MnBi content of up to 87.1% was observed with the increment of several oxides from 2.4 wt.% to 3.7wt.% as grinding time increases. This is supported by the XPS results which demonstrate the increment of MnO content on the surface as a function of Mn grinding time. It is seen that the shape of Mn particles is rather similar in all grinding conditions consisting of small and big circular shapes. We found that the average particle size decreases from 30-40 μm to 5-6 μm at 1-15 hr grinding time, respectively. The energy product of 1.59-1.98 MGOe was obtained in the MnBi samples prepared with different Mn grinding time. The saturation magnetization (Ms) decreases from 53.42 to 44.32 emu/g by increasing the Mn grinding time. The unexpected decrease of Ms which strongly results to the decrease of magnetic performance might be explained by the increase of oxides. Oxides on Mn particles could prevent the diffusion of liquid Bi to form the MnBi during sintering.

Poster: S2 Condensed Matter Physics - Board: P079 / **139**

Effect of Self-Assembled Iron-Tannic Nanoparticles on Fastness and Antibacterial Properties of Natural Indigo (Strobilanthes Cusia) Dyed Cotton Fabrics

Author: Yanee Keereeta[None]

Co-authors: Pat Pranamornkith [1]; Siriprapa Srithong [2]; Waranya Tharawatchruk [2]; Ketchamai Boomsom [3]; Sulawan Kaowphong [4]; Arrak Klinbumrung [5]

[1] *Department of Science, Faculty of Science and Agricultural Technology, Rajamangala University of Technology Lanna, Lampang, 52000, Thailand*

[2] *Rajamangala University of Technology Lanna Lampang*

[3] *Rajamangala University of Technology Lanna, Lampang*

[4] *Department of Chemistry, Faculty of Science, Chiang Mai University, Chiang Mai 50200, Thailand*

[5] *Unit of Excellence on Advanced Materials for Sensors Technology and Advance Glass and Ceramics, University of Phayao, Phayao, Thailand*

Corresponding Author: ynkeereeta@gmail.com

In this work, self-assembled iron (III)-tannic nanoparticles (Fe-TA NPs) were exploited as an eco-friendly antibacterial finishing agent for natural indigo (*Strobilanthes Cusia*) dyed cotton fabrics. Fe-TA NPs were synthesized at room temperature using an easy, low-cost, and reproducible method without the use of any toxic agents. The interaction between Fe3+ and TA and particle size of Fe-TA NPs were characterized by UV-Vis spectroscopy and dynamic light scattering (DLS). The modified cotton was fabricated using the exhaustion dyeing process. The Fe-TA NPs with different mole ratios of ferric chloride and tannic acid were one-step deposited onto the surface of natural indigo dyed fabrics. The surface morphology, chemical structure, and thermal stability of the modified cotton were investigated using scanning electron microscopy (SEM), Fourier transform infrared spectroscopy (FTIR), Raman spectroscopy and Thermogravimetric analysis (TGA), respectively. Furthermore, color, color fastness properties and antibacterial properties of modified samples were evaluated.

Poster: S2 Condensed Matter Physics - Board: P080 / **123**

Enhancement of Perovskite Solar Cells Performance using Electrochemically Grown TiO2 Quantum Dots

Author: Thanakrit Sintiam[None]

Co-authors: Sukrit Sucharitakul [1]; Supab Choopun ; Surachet Phadungdhitidhada [1]

[1] *Chiang Mai University*

Corresponding Author: t_p1125@hotmail.com

Abstract

Perovskite solar cells (PSCs) are among the rising technologies for clean energy harvesting. Although the platform is performing better, cheaper and can be more efficiently fabricated than the Si-based solar cells, the device suffers from low stability and durability against the ambient conditions. A general PSCs consists of consist of five layers: including Fluorine doped Tin Oxide glass (FTO), Electron transporting layer (ETL), Perovskite Layer (PSVK), Hole transporting layer (HTL) and Electrode. It has been reviewed that the PSVK/ETL or PSVK/HTL interfaces are most responsible for defects resulting in lowered performance and stability due to higher charge recombination rate through higher number of pinholes. In this work the team aimed to modify the PSVK/ETL layer using TiO2 Quantum Dots (QDs) by varying concentration of TiO2 QDs grown via electrochemical process in KCl-based solution (0%, 2.5%, 5%, 7.5%, 10%) mixed in TTIP. TiO2-based ETL is coated and passivated along with with perovskite layer in conventionally structured PSCs. KCl in base solution of QDs is also used to aid with the passivation while methylammonium formamidinium lead iodide (MAFAPbI3) is used as PSVK layer. The results showed that with optimal percentage of TiO2 QDs can improve efficiency perovskite solar cells. Performance of our reference PSCs shows photoconversion efficiency (PCE) of 14.05 % while with 7.5% of TiO2 QDs passivation on PSCs shows highest performance of 15.72%. This is likely due to the TiO2 QDs formula passivating and reducing the pinholes between PSVK/ETL junction improving electron transport. Additionally, the choice of the electrolyte such as KCl can also aid in TiO2 QDs passivation in the PSC connecting the QDs with the PSVK layer through K+ and Cl- ions. The passivated PSCs with 7.5% condition also lasted for longer than 200 hours proving its improved stability. Sufficient TiO2 QDs in base solution mixed with TTIP has been used to passivate perovskite layer improve efficiency and stability of perovskite solar cells decreasing defect of PSVK/ETL junction.

Keyword: Quantum Dots, TiO2 QDs, TTIP, Perovskite solar cells, Electrochemical Process

Poster: S2 Condensed Matter Physics - Board: P081 / **114**

Microwave-assistant preparation of ZnO nanostructures optical and morphological properties for photocatalytic activity

Author: Rattanaporn Somrit[None]

Corresponding Author: rattanaphorn.sr@bru.ac.th

This research, ZnO nanostructures samples were successfully prepared by 0, 300 and 600 watt microwave-assistant method for 10 min. Characterization properties of ZnO samples were measured by powder using X-ray diffraction , Field emission scanning electron microscope , UV-visible diffuse reflectance spectra and dispersive X-ray spectroscopy . The analysis results found that products were phase and crystallinity structures hexagonal of ZnO growth degree of (101) peaks nanoplate morphology with thickness 13.46 15.17 and 16.23 nm respectively. Elemental composition was showed spectrum have prominent Zn and O confirmed. Elucidate the optical properties of ZnO samples with the UV-Vis absorption spectra can be determined the band gap energy (Eg). Photocatalytic efficiencies has evaluation by degradative solutions of methylene blue (MB) under irradiation UV lamp and visible light lamp. Sample was observed first -order kinetic reation effect of the highest photocatalytic activity degradation methylene blue.

Poster: S2 Condensed Matter Physics - Board: P082 / **110**

Preparation of superhydrophobic paper using PDMS modified SiO2 nanoparticles

Author: Wola Jiraprapa [1]

Co-authors: Kanjana Nattakan [1]; Paveena Laokul [1]

[1] *Mahasarakham University*

Corresponding Author: jiraprapha98@gmail.com

A simple spray coating technique was used to prepare a PDMS-modified SiO2 top layer on the paper substrate. The wettability, microstructure of the coated papers, and durability and adhesion of the coating at different pH settings of the nanosolution (pH2, pH3, pH4 and pH5) were investigated using the water contact angle (WCA) and sliding angle (WSA), Fourier transform infrared spectroscopy (FT-IR), scanning electron microscopy (SEM), energy dispersive X-ray spectroscopy (EDS), and ASTM D4060 Taber abrasion test with wheel type CS-10. The result showed that the paper coated with the nanosolution with pH4 exhibited excellent self-cleaning and superhydrophobicity, with a WCA value of 163.3° and a very low WSA of only 1.65°. The FTIR result showed that the coated paper exhibited absorption peaks related to the asymmetric Si-O and asymmetric Si-O-Si bonding, indicating the adhesion of the SiO2/PDMS to the paper substrate. The abrasion resistance results showed that after 5, 10 and 20 abrasion cycles, the percent weight loss was 0.28%, 0.65% and 1.01%, and the WCA values decreased to 123.69°, 98.62° and 91.74°, respectively. This result shows that the weight loss of the sample after 20 abrasion cycles was only 1.01%. This result was due to the fact that the nanocomposite particles adhered to the paper surface were uniformly distributed on the cellulose fibers, which directly affected the increased surface roughness and resulted in the excellent waterproof and self-cleaning properties of the produced paper. Due to its ease of production and scalability, the produced paper can be used in practice.

Poster: S2 Condensed Matter Physics - Board: P083 / **109**

Surface modification of filter paper by TiO2-PDMS-KH550 nanocomposite with superhydrophobic, self-cleaning and oil/water separation properties

Author: Kupalang Suwanna[1]

Co-authors: Kanjana Nattakan [2]; Paveena Laokul [1]

[1] *Mahasarakham University*

[2] *Mahasarakham Unversity*

Corresponding Author: suwanna2076@gmail.com

In this study, the surface of filter paper was modified with TiO2-PDMS-KH550 nanocomposites using titanium isoproproxide (TTIP) as the starting material by spray coating technique. To obtain the desired active coating, the amount of PPIT in the mixture was changed by 0.39, 0.78, and 1.56 mmol. The wettability, microstructure of the coated papers, and durability and adhesion of the nanocomposite coatings with different TTIP content were determined using water contact angle (WCA) and sliding angle (WSA), Fourier transform infrared spectroscopy (FT-IR), scanning electron microscopy (SEM), energy dispersive X-ray spectroscopy (EDS), and ASTM D4060 Taber abrasion test with wheel type CS-10. The results showed that the sample prepared with a coating solution containing 0.78 mmol TTIP exhibited excellent superhydrophobicity with a WCA of 162.68° and a WSA of 2.45°, as well as excellent self-cleaning property. In addition, the paper exhibited a high abrasion resistance of 0.26% weight loss after 20 abrasion cycles and a water recovery efficiency of > 98% after 10 cycles. This was due to the fact that the nanocomposite particles adhering to the paper surface were uniformly distributed on the cellulose fibers, which directly affected the increased surface roughness and resulted in the excellent waterproof and self-cleaning properties of the produced paper. Due to its environmental friendliness and easy scalability, this paper could have potential for practical applications.

Poster: S2 Condensed Matter Physics - Board: P084 / **100**

Systematical investigation and correction of measured magnetic hysteresis obtained by vibrating sample magnetometry

Author: Sasithon Santikulthani[None]

Co-authors: Tanachat Eknapakul [1]; Supree Pinitsoontorn [2]; Prayoon Songsiriritthigul [3]

[1] *Suranaree University of Technology*

[2] *Khonkaen University*

[3] *Suranaree University of Technology*

Corresponding Author: jjsnibpi@gmail.com

Vibrating sample magnetometry (VSM) is a powerful technique for investigations of magnetic properties of matters. One important drawback of this technique is the 'open-loop' setup which can significantly distort the exact magnetic properties. Thus, appropriate corrections especially in the strong ferromagnet such as permanent magnets is required. In this work, we design the systematic experiments by varying the length/radii ratio between 1-5 and provide the step-by-step corrections of two commercial NdFeB powder magnets with reported energy product ((BH)max) of 6 ± 0.5 and 12.7 ± 0.5 MGOe. It is seen that the raw VSM hysteresis loops contain the paramagnetic-like slope and unsaturated curve which directly pervert their magnetic properties. These effects could be experienced from the equipment calibrations, powder samples and 'open-loop' setup. These hysteresis loops give the calculated (BH)max of 47.3 – 62.6% compared to their reported values with improper values of saturation magnetization (Ms), remnant magnetization (Mr) and Mr/Ms ratio. In order to correct the measured VSM hysteresis loop, firstly, the paramagnetic-like slope of 0.0500 – 0.0735 was subtracted until the flat at high fields was obtained. Secondly, the Ms ratio within ±5% was added to achieve the same Ms for all samples. Finally, the demagnetizing field correction (N) of 0.29287 – 0.43804 depending on their geometry was applied to all samples. The corrected (BH)max after all processes is around 86-95% of the reported values. Moreover, the samples with different packing densities were also examined. The results show that the loose packed sample exhibits hysteresis distortion which could be caused by an unwanted magnetostatic interaction and degree of particle rotation of the powder. This work demonstrates the importance in preparing and interpreting the VSM results and might be a facile way to get credible magnetic performance without performing magnetic alignment of such permanent magnets.

Poster: S2 Condensed Matter Physics - Board: P085 / **93**

Investigation of Cu-atomic ratio in the second step of the 3-stage deposition process of Cu(In,Ga)Se2 thin film solar cells

Author: Boonyaluk Namnuan[1]

Co-author: Sojiphong Chatraphorn [2]

[1] *Department of Physics, Faculty of Science, Silpakorn University*

[2] *Department of Physics, Faculty of Science, Chulalongkorn University*

Corresponding Author: namnuan_b@silpakorn.edu

The high efficiency $CuIn_{1-x}Ga_xSe_2$ (CIGS) solar cells are usually fabricated by the 3-stage deposition process for the CIGS layer. The Cu/[III] atomic ratio (CGI or y) in the 2nd step of the 3-stage process is considered as one of important deposition parameters to achieve high efficiency devices, where [III] refers to group-III elements. In the 3-stage process, the formation of the CIGS layer has to evolve from Cu-poor (Cu/[III] < 1) to Cu-rich (Cu/[III] > 1) in the 2nd stage and finish with slightly Cu-poor in the 3rd stage. In this work, the highest value of Cu/[III] atomic ratio in the 2nd stage was varied from 1.0 to 1.5 while the Ga/[III] atomic ratio (GGI or x) was set at 0.37 as in other works during the 1st and 3rd stages of the deposition process in all devices. The typical thickness of the CIGS layer is approximately 2 microns. The effects of the Cu/[III] atomic ratio were investigated in terms of the elemental depth profiles, cross-sectional images, photovoltaic parameters and quantum efficiency of the CIGS devices. It was discovered that the optimal Cu/[III] atomic ratio of 1.3 yielded the most efficient devices. In addition, the depth profiles also showed the double-grading in the Ga/[III] atomic ratio with high Ga toward the front and back surfaces of the CIGS layer with the minimum Ga/[III] atomic ratio or the notch in the conduction band at approximately one micron below the surface of the CIGS layer. The photovoltaic parameters were obtained under AM1.5 standard test condition with the highest efficiency of 16.8% with V_{OC} of 670 mV, J_{SC} of 33.2 mA/cm^2 and fill factor of 75.5%. The J_{SC} was found to increase in comparison to other Cu/[III] atomic ratio conditions due to the improvement in the spectral response in the short wavelength region.

Poster: S2 Condensed Matter Physics - Board: P086 / **88**

The Natural Fibers ratio are Affected to Mechanical Properties of Kaolin/Fly-ash at Low Temperature Ceramics

Author: Watee Panthuwat[None]

Co-authors: Narit Funsueb [1]; Pat Pranamornkith [1]; Anawin Thipboonraj [2]

[1] *Department of Science, Faculty of Science and Agricultural Technology, Rajamangala University of Technology Lanna, Lampang, 52000, Thailand*

[2] *Department of Industrial Engineering, Faculty of Engineering, Rajamangala University of Technology Lanna, Lampang, 52000, Thailand*

Corresponding Author: ood_turbo@hotmail.com

The study guideline to develop the feasibility of producing low temperature ceramics with the natural fibers. The ceramics prepared by mixed powder of kaolin and fly ash with equal ratio (kaolin/fly-ash: 50/50 wt.%) and milled by ball-milling technique. The natural fibers from local pineapple leaves replaced to ceramics by 5, 10, 15, 20 and 25 wt.%. Green pellets of 30.0 mm diameter were prepared using uniaxial-pressure. Scanning electron microscopy (SEM) was used to determine the sizes of natural fiber and particle size of powder. The mechanical properties of ceramics were investigated by hardness tester. In this study, will be focused on the effect of natural fibers ratio are affected to mechanical properties of ceramics at low temperature.

Poster: S2 Condensed Matter Physics - Board: P087 / **87**

Effect of Fly-ash Doped Kaolin on Mechanical Properties and Heat-insulating of Ceramics

Author: Narit Funsueb[1]

Co-authors: Watee Panthuwat [1]; Anawin Thipboonraj [2]; Pat Pranamornkith [1]

[1] *Department of Science, Faculty of Science and Agricultural Technology, Rajamangala University of Technology Lanna, Lampang, 52000, Thailand*

[2] *Department of Industrial Engineering, Faculty of Engineering, Rajamangala University of Technology Lanna, Lampang, 52000, Thailand*

Corresponding Author: funsueb.n@gmail.com

In this research, ceramics fly-ash doped kaolin 10 to 50 wt.% were fabricated by solid-state reaction. All powders were weighed, mixed and further milled by ball-milling for 4 h. All compositions of powders were uniaxial pressed in pellets and sintered at the temperatures 1100 °C for 4 h. Compositions of the ceramics were investigated by using X-ray diffraction technique. The particle size of powder and microstructure of ceramics were measured by scanning electron microscope. The result shows relationships between ratio of fly-ash doped kaolin with mechanical properties and heat-insulating of ceramics.

Poster: S2 Condensed Matter Physics - Board: P088 / **86**

Surface treatment of PTAA hole transport layer for inverted perovskite solar cells

Authors: Kwanruthai Butsriruk[1]; Passakorn Phiromruk[1]; Sojiphong Chatraphorn[1]

[1] *Department of Physics, Faculty of Science, Chulalongkorn University*

Corresponding Author: kwan_kn_24@hotmail.com

Poly[bis(4-phenyl)(2,4,6-trimethylphenyl)amine] (PTAA) was chosen as a hole transport layer for inverted perovskite layer. It is the first layer deposited on the FTO substrate and thus directly affect the structure and performance of the inverted or p-i-n perovskite solar cells. It was found that untreated PTAA layer yielded large distribution of photovoltaic parameters and low reproducibility. In this work, the PTAA was dissolved in chlorobenzene (CB) and spin-coated on the FTO substrates and baked at 105 deg;C for 10 mins as pristine samples. The surface treatment of PTAA was performed by washing the pristine samples with 200 µl dimenthylformamide (DMF) on a spin coater and followed by dynamic spin of 50 µl and 75 µl of CB or Toluene (TO). It was observed that the surface treatment affected the wettability of PTAA surface by the reduction of contact angle from 46deg; of pristine sample to 25deg; – 35deg; of treated samples that could lead to a better interface and formation of a MAPbI₃ perovskite layer. On the contrary, the optical transmittance, surface morphology and roughness of the treated samples were insignificantly affected. It was demonstrated that the surface treatment of PTAA using DMF and 50 µl of TO could significantly reduce the fluctuation of photovoltaic parameters and also improve the repeatability of the fabrication process. The maximum power conversion efficiency (PCE) of 15.4% was obtained for the optimal condition.

Poster: S2 Condensed Matter Physics - Board: P089 / **82**

Theoretical study of electrical transport across 1D ferromagnet-insulator-ferromagnet junction

Authors: Adithep butburee[1]; Natthagrittha Nakhonthong[None]; Puangratana Pairor[1]

[1] *School of Physics, Institute of Science, Suranaree University of Technology*

Corresponding Author: nakhonthong.n@gmail.com

We theoretically studied the tunneling magnetoresistance of a heterostructure ferromagnetic metal-insulator-ferromagnetic metal junction. By modifying the theoretical model used by Slonczewski with the inclusion of a small external magnetic field, we theoretically consider the impact of the barrier potential, or the band gap and the thickness of the insulating layer. We found that higher insulating barrier potential and thicker barrier can each boost the magnetoresistance. The magnetoresistance is increased with the applied magnetic field and reaches its maximum value at a particular magnetic field strength that depends on the thickness of insulating layer.

Poster: S2 Condensed Matter Physics - Board: P090 / **73**

Structural, mechanical properties and corrosion performance of multilayer Ti/Ti doped-DLC films deposited on low-carbon steel

Author: Ukit Rittihong[1]

Co-authors: Sarayut Tunmee [2]; Ratchadaporn Supruangnet [2]; Artit Chingsungnoen [3]; Phitsanu Poolcharuansin [3]; Thanachai Singhapetcharat [4]; Prapoj Kiattikomol [4]; Tanachat Eknapakul [1]; Hideki Nakajima [2]; Prayoon Songsiriritthigul [5]

[1] *Suranaree University of Technology*

[2] *Synchrotron Light Research Institute (Public Organization)*

[3] *Mahasarakham University*

[4] *PTT Exploration and Production Public Company Limited*

[5] *Suranaree University of Technology*

Corresponding Author: ukitrittihong@gmail.com

In this work, the successful preparation of the multilayer Titanium/Titanium doped diamond-like carbon (Ti/Ti-DLC) films deposited on low-carbon steel (CS) using hybrid magnetron sputtering and plasma enhanced chemical vapor deposition methods (MS-PECVD) has been reported. The chemical and structural properties of the multilayer Ti/Ti-DLC films with varied numbers of Ti/Ti-DLC layers were characterized by Raman spectroscopy, X-ray photoemission spectroscopy (XPS) and near-edge X-ray absorption fine structure spectroscopy (NEXAFS). Their mechanical properties were investigated by using nano-indentation and nano-scratch testers. The electrochemical analysis was used to evaluate the corrosion behavior of the multilayer films which were immersed in the 3.5 wt.% NaCl solution at room temperature. Raman spectroscopic analysis revealed a gradual increase of the I_D/I_G ratio with the addition of the numbers of Ti layer. The XPS and NEXAFS results show that the sp^2 content increases by increasing the numbers of Ti layer which results in the hardness reduction. The adhesive properties were improved by adding the numbers of Ti interlayer between the CS substrate and the multilayer film. Moreover, the thicker multilayer films exhibit progressive homogeneity resulting in better corrosion resistance.

Poster: S2 Condensed Matter Physics - Board: P091 / **67**

Electronic and magnetic properties of $MoTe_2$ monolayer doped with single and double transition metal configuration: spin density functional theory

Author: Waritsara Thajitr[None]

Co-author: Worasak Sukkabot

Corresponding Author: waritsara.th.63@ubu.ac.th

The spin density functional calculations are performed to study the electronic and magnetic properties of $MoTe_2$ monolayer doped with single and double transition metal (V, Cr, Mn, Fe and Co) atoms. The electronic and magnetic properties are sensitive with the types and numbers of the doping transition metals. The semiconductor with narrow band gaps is shown in Cr and Co single-doped $MoTe_2$ monolayer. Mn single-doped $MoTe_2$ monolayer is metal. V and Fe single-doped $MoTe_2$ monolayers demonstrate the half-metallic behaviours with a 100% spin polarization. V and Co provide the first-two lowest formation energies which are used to the co-doping studies. $MoTe_2$ monolayers simultaneously doped with Co and V are characterized as metall. The p-d hybridization of d orbitals of transition-metal dopants and Mo host with Te-p orbitals and d-d hybridization between Mo-d states and d orbital of transition-metal dopants nearby the Fermi level induce the magnetism, called double exchange mechanism.

Poster: S2 Condensed Matter Physics - Board: P092 / **47**

Synthesis and Application of Nickel Compound Quantum Dots by Electrochemical Process

Author: Prapasiri Phimsarn[1]

Co-authors: Kritsada Hongsith [1]; Sukrit Sucharitakul [1]; Surachet Phadungdhitidhada [1]; Supab Choopun

[1] *Chiang Mai University*

Corresponding Author: pinooknam@gmail.com

In this work, nickel compound quantum dots (Ni-QDs) are synthesized by electrochemical process. The electrochemical process known as a facile method is used to prepare Ni-QDs colloid solution. Ni-QDs are synthesized using nickel-metal rods (2 mm in dimension and 5 cm in length) dipped into an electrolyte solution of potassium chloride and citric acid at 0.4M and 0.1M concentrations, respectively, then applied voltages at 1,3 and 6 V for the synthesis process. As the result, Ni-QDs are characterized for size and stability by transmission electron microscopy (TEM), dynamic light scattering (DLS) and Zeta potential technique. The absorption spectra of Ni-QDs are indicated via ultraviolet-visible spectroscopy (UV-vis) at 390, 655, and 731 nm of wavelength which can be assigned to absorption peaks of Ni (OH)2 and NiCl2, respectively. The crystalline structure and photoluminescence properties of Ni-QDs are examined with X-ray diffractometry (XRD), and photoluminescence spectroscopy. It is found that the Ni-QDs growth rate can be controlled by the various voltages applied in the synthesis process. The smallest size and high yield of Ni-QDs are achieved with the low voltage applied (1V), while the higher voltage process produced a strong chemical reaction resulting in the lower yield of Ni-QDs due to the large particles of the obtained products. Thus, the influence of voltage in the synthesis of Ni-QDs is important to optimize the quality of Ni-QDs.

Poster: S2 Condensed Matter Physics - Board: P093 / **46**

Nickel Oxide Thin Films Prepared by Using Nickel Nitrate/Acetate for Hole Transporting Layer in Perovskite Solar Cells

Author: Kritsada Hongsith[1]

Co-authors: Wakul Bumrungsan [1]; Sukrit Sucharitakul [1]; Surachet Phadungdhitidhada [1]; Supab Choopun

[1] *Chiang Mai University*

Corresponding Author: kritsada354@gmail.com

Nickel oxide (NiOx) thin films prepared by using nickel acetate and nitrate as hole transporting layer (HTL) in perovskite solar cells (PSCs) were studied. Herein, the effect of concentrations of nickel acetate (0.1, 0.2, and 0.3 M) mixed with a fixed 0.1 M of nickel nitrate for NiOx thin film preparation was investigated. The crystal structure and optical properties were characterized by X-ray diffractometry (XRD) and ultraviolet-visible spectroscopy (UV-vis). The inverted perovskite solar cell architecture of FTO/NiOx/Perovskite/PC60BM/Ag was carried out and investigated for solar cell characteristics. It is found that the PSC devices fabricated by using nickel nitrate 0.1M mixed with nickel acetate 0.2 M exhibited a maximum power conversion efficiency (PCE) of 14.5 % (compared to 11.0 % of the device fabricated with using only nickel acetate). The PCE enhancement can be elucidated by the significant improvement of the interface between NiOx and perovskite layer as observed in an increase of photocurrent, fill factor, and a decrease of hysteresis. These results suggest that the NiOx thin films prepared by the appropriate mixing of nickel nitrate and acetate can be applied as HTL and can enhance the PCE of perovskite solar cells.

Poster: S2 Condensed Matter Physics - Board: P094 / **26**

Ohmic heating as an effective path to rapidly cure and strengthen alkali activated material

Author: Nattapong Chuewangkam[None]

Co-authors: Supree Pinitsoontorn [1]; Panjasila Payakaniti [2]

[1] *Physics*

[2] *Department of Physics*

Corresponding Author: nattapongchuewongkam@gmail.com

Alkali activated material has been considered as a high potential construction material for replacing or reducing cement usage. However, proper curing at specific temperatures is necessary for optimizing the alkali activated material's strength and durability performance. In this work, a novel technique for curing alkali activated material is proposed based on the ohmic heating principle by passing electrical current through the just casted alkali activated paste. With this method, the alkali activated paste was rapidly cured right from the start. As a result, it set very quickly (~15 min) compared to hours for setting for the controlled sample without ohmic heating. Moreover, the compressive strength (22.9 MPa) and flexural strength (0.42 MPa) of the 80 ℃ ohmic cured samples for 90 min were significantly improved compared to the non-heated sample (compressive strength of 0.68 MPa and unmeasurable for flexural strength). The prolonged mechanical properties (7-day age) were also increased, with the compressive strength (47.0 MPa) nearly double and the flexural strength (1.32 MPa) almost quadruple, compared to the controlled sample. The reasons for the quick setting and enhanced mechanical strengths cannot be related to microstructures from the SEM image analysis. However, the FTIR analysis showed that ohmic heating accelerated early geopolymerization. The Al-O-Si bonding (the absorption band at ~ 948 cm^{−1}), the backbone of the geopolymeric structure, was found to increase almost linearly with the ohmic heating time (R² of 0.93). Rapid formation of the geopolymeric structure was thus responsible for the quick setting and the early and prolonged strength enhancement. Furthermore, this ohmic curing technique does not require the addition of conductive fillers, such as carbon fiber, since ionic conduction from the presence of alkali and hydroxide ions is sufficient to induce ohmic heating. Nevertheless, the carbon fiber addition to alkali activated pastes led to strength enhancement. In addition, this technique is not limited to a lab-scale sample but can be extended to cure alkali activated material in large-scale construction.

Poster: S2 Condensed Matter Physics - Board: P095 / **45**

Microstructure and Electrical Properties of Green Electrospun PVDF-HFP nanofibers

Author: JAKKAPAT KHAO-IAM[None]

Co-authors: CHATCHAI PUTSON [1]; Suphita Chaipo ; Ahamad Salea

[1] *Prince of Songkla University*

Corresponding Author: 6210220069@psu.ac.th

Currently, Most of the research reported on the preparation of Poly (vinylidene fluoride-hexafluoropropylene) (PVDF-HFP) by using N, N- dimethylformamide (DMF) as a solvent which is considered a cancerogenic substance. However, It is important to consider environmental hazards, toxicity and this research will focus on the use of "green" alternative solvents instead of the solvents. we are interested in dimethyl sulfoxide (DMSO) as a low toxicity solvent and not hazardous. In this research, the mixture solvents of acetone/DMSO which was used as a co-solvent and able to excellent solubilize PVDF-HFP. For the preparation of nanofiber membrane with various ratios of A6D4, A7D3, and A8D2. Afterward, the mixture was mixed with 5-gram PVDF-HFP before the electrospinning process with a specific condition. The final nanofiber films were investigated and characterized the morphology, dielectric, and crystallinity. As a result, the dielectric constant increased with the acetone contents. The maximum dielectric constant is devoted to A6D4 at 10 Hz. The copolymers' structure was modified β-phase by a different solvent which affected dielectric properties. This work is shown that the difference in the solution mixture affects the electrical properties and phase orientation, and thus can be developed in terms of energy storage, Harvard energy, sensors, and Electrocaloric.

Poster: S2 Condensed Matter Physics - Board: P096 / **24**

Thermoelectric properties of Cu2Se and densified by cold sintering process

Author: Piyawat Piyasin[1]

Co-author: Supree Pinitsoontorn [2]

[1] *Khonkaen university*

[2] *Khonkaen University*

Corresponding Author: piyawat_piyasin@kkumail.com

The phonon-liquid electron-crystal becomes a fascinating concept for thermoelectric material in recent years. The Cu₂Se is a potential material for this concept. Due to it goods electrical properties of Cu₂Se, this work is successfully synthesized Cu₂Se powder using a high-energy ball milling method. The Cu₂Se disc-shaped pellets were prepared by the cold sintering process (CSP) under 624 MPa pressure at 200 ˚C for varied content of a thiol-amine solution. The sample density was measured with the geometric shape after the post-annealing at 550 ˚C. The bulk densities are greater than 70% of the theoretical density and exhibit excellent thermoelectric properties. The power factor of the CSP-Cu₂Se shows over 1000 181;W/mK² due to the high electrical conductivity and Seebeck coefficient. The highest figure of merit demonstrates about 1.27 at 800 K. In addition, the CSP allows the preparation of the outstanding Cu₂Se at low temperatures.

Poster: S2 Condensed Matter Physics - Board: P097 / **25**

Synthesis of Fe3O4 Ceramic Magnet Via Cold sintering Process

Author: Nuchjaree Salidkul[1]

Co-author: Supree Pinitsoontorn [2]

[1] *Khon kean university*

[2] *Khonkaen University*

Corresponding Author: nuchjarisa@kkumail.com

Iron oxide (Fe3O4) ceramic magnets were prepared by using the cold sintering process. The nitric acid solution and water are liquid mediums. The Fe3O4 1.5g and nitric acid 0wt%, 3%wt%, 5wt%, and 10wt% were used. The phase and morphology were characterized by X-Ray diffraction (XRD) and field emission scanning electron microscope (FESEM), respectively. The XRD analysis showed the peaks corresponding to the cubic phase of magnetite without any secondary phase. The SEM image presented the Fe3O4 nanoparticles are near-spherical/ellipsoidal shape. In addition, the magnetic properties were studied by the vibrating sample magnetometer (VSM). The magnetic properties of all of the samples are soft ferrimagnetic properties

Poster: S2 Condensed Matter Physics - Board: P098 / **28**

INTEGRATION OF METAL-ORGANIC FRAMEWORK AND AMORPHOUS CARBON FROM BACTERIAL CELLULOSE FOR LI-ION BATTERIES

Author: Dejwikom Theprattanakorn[1]

Co-author: Supree Pinitsoontorn [2]

[1] *khon kaen university*

[2] *Khonkaen University*

Corresponding Author: th.dejwikom@kkumail.com

Metal-Organic Frameworks (MOFs) are widely studied as anode materials for lithium-ion batteries (LIBs). They exhibit outstanding properties, such as prominent porosity, and molecular storage capacity, but they have a number of significant limitations, including poor electrical conductivity. In this case, MIL-53(Fe) was successfully prepared using pyrolysis carbon assisted from bacterial cellulose (abbreviated as pBC). To solve the problem, a solvothermal strategy was used to provide a homogenous distribution of particles product, which was not only a result but also a controlled size. After 100 cycles, the electrochemical performance of MIL-53(Fe)@pBC exhibited good specific capacity, however there is an irreversible capacity loss due to the SEI layer. Pyrolysis carbon template synthesis is based on the principle of crystal nucleation kinetics, and it is reasonable for promising electrode materials.

Poster: S2 Condensed Matter Physics - Board: P099 / **33**

Effect of hydrochloric acid modification on physical and optical properties of PEDOT:PSS thin films

Authors: Sasimonton Moungsrijun[1]; Suparat Somsuk[1]; Sawitree Wongrerkdee[2]; Khathawut Lohawet[3]; Supphadate Sujinnapram[1]; Sucheewan Krobthong[1]; Anusit Kaewprajak[3]; Pisist Kumnorkaew[3]; Sutthipoj Wongrerkdee[None]

[1] *Kasetsart University Kamphaeng Saen Campus*

[2] *Rajamangala University of Technology Lanna Tak*

[3] *National Nanotechnology Center*

Corresponding Author: sutthipoj.s@ku.ac.th

In this work, PEDOT:PSS thin films were prepared on F-doped tin oxide SnO2 substrates by the spin coating method. The films were modified with HCl solution for 2 strategies, including doping and post-treatment. Then, some properties were studied. The X-ray diffraction patterns show only SnO2 peaks. However, the FTIR presented functional groups that corresponded to PEDOT and PSS. Contact angle measurement of water on PEDOT:PSS thin films reveal that contact angle values increase for doping and post-treatment, which implies water resistance improvement. The optical transmittance of PEDOT:PSS films for doping and post-treatment conditions presents high transmittance values above 70%. Sheet resistance measured by a four-point probe measurement demonstrates that sheet resistance values decrease to the minimum values of 6.67 and 6.79 ⍰/sq for doping and post-treatment conditions, respectively. It was indicated that the sheet resistance of PEDOT:PSS thin films can be reduced by using HCl for both doping and post-treatment strategies. Thus, this demonstration could be considered as an alternative method for conductive polymer film development.

Poster: S2 Condensed Matter Physics - Board: P100 / **31**

Mechanical Properties of Fly Ash Geopolymers Reinforced with Graphene Oxide

Authors: Jariya Lasiw[1]; Supree Pinitsoontorn[1]

[1] *Khon Kaen University*

Corresponding Author: psupree@kku.ac.th

Geopolymers are a type of binding materials that can be used to replace cement to reduce environmental problems. In this research, the compressive strength, the curing time, was the microstructure and the chemical composition of the graphene oxide-based fly ash geopolymer material were studied, Geopolymer was prepared from high calcium fly ash, sodium silicate (Na2SiO3) sodium hydroxide (NaOH) and graphene oxide powder, reinforcing materials The concentrations of graphene oxide were 0, 0.05, 0.1, 0.2, 0.3 and 0.4 percent by weight. The liquid to fly ash ratio (L/A) was 0.45. The curing temperature was 60℃ and the curing period was 7, 14 and 28 days. From the experiment al results for the flow characteristics, it was found that the viscosity increased as the proportion of graphene oxide increased. When analyzing with of XRD and FTIR techniques, there was a decrease in the crystallinity because the peak is wide. Crystal phase peaks of quartz and hematite derived from fly ash components were found. The spectral bands from the FTIR technique for all samples were similar. An increase in graphene oxide content may result in a change in peak strength. when increasing the amount of graphene oxide more. The addition of graphene oxide did affect the geopolymerization reaction changes. From the Raman spectroscopy technique, it was found that the amount of graphene oxide increased proportion ally with the increased graphene oxide concentration. In addition, the compressive strength tended to increase in proportion with the higher graphene oxide content, and the curing time as well But at the concentration of 0.4% by weight for 28 days, the strength was reduced because the reinforced material had larger particle size or poor adhesion. The SEM results showed that graphene oxide particles were not visible. This could be that graphene oxide is transformed or embedded into the geopolymer body. As a result, graphene oxide particles were not visible.

Poster: S2 Condensed Matter Physics - Board: P101 / **39**

Effects of Temperature on Persistence Probabilities in Molecular Beam Epitaxy Model

Author: Pipitton Sanseeha[None]

Co-authors: Patcha Chatraphorn ; Rangsima Chanphana [1]

[1] *Chulalongkorn University*

Corresponding Author: pipitton@yahoo.co.th

Persistence probability is an interesting quantity used in the study of stochastic processes. According to J. Krug [1], persistence probability of height fluctuation is the probability that the height fluctuation does not return to its initial value throughout a time interval. The persistence probability exhibits power law decay with time with the exponent θ. In this work, we use a numerical simulation approach to investigate the persistence probability in Molecular-Beam Epitaxy (MBE) model which is associated with Molecular-Beam Epitaxy technique [2-4]. In the first half of this work, we study the effects of temperature on the growth exponent (β) and persistence exponent (θ). For the relatively low temperature (associated with nearest neighboring site diffusion length), we obtain $\beta \approx 0.16$ and dynamic exponent (z) ≈ 3.30. When the temperature increases, β decreases while θ increases. In the second half, we study the dependence of persistence probability on initial height fluctuation (h_0), system size (L), and discrete sampling time (δt) and investigate the scaling relation. Our findings show that the steady state persistence probabilities are a function of three parameters: $f(t/L^z, t/L^z, |h_0|/w_{sat})$ which is the same as what was previously found in linear growth models [5]. We also find that the positive persistence probability of negative initial height does not show power law decay unless the initial height is much greater than the saturated interface width (w_{sat}), similar to the Das Sarma–Tamborenea model in [6].

References
[1] Krug, J., et al. "Persistence exponents for fluctuating interfaces." Physical Review E 56.3 (1997): 2702.
[2] Barabási, A-L., and Harry Eugene Stanley. Fractal concepts in surface growth. Cambridge university press, 1995.
[3] Chanyawadee, Soontorn. Modeling of molecular beam epitaxy growth under ehrlich-schwoebel potential barrier effects. Diss. Chulalongkorn University, 2004.
[4] Potepanit, Somjintana. Effects of annealing process on film surfaces grown by molecular beam epitaxy growth model with arrhenius law. Diss. Chulalongkorn University, 2012.
[5] Chanphana, R., P. Chatraphorn, and C. Dasgupta. "Effects of initial height on the steady-state persistence probability of linear growth models." Physical Review E 88.6 (2013): 062402.
[6] Chanphana, R., and P. Chatraphorn. "Persistence probabilities of height fluctuation in thin film growth of the Das Sarma–Tamborenea model." Indian Journal of Physics 95.1 (2021): 187-193.vx

Poster: S2 Condensed Matter Physics - Board: P102 / **40**

Fractional Little-Park effect in hybrid superconductor-ferromagnet proximity cylinders

Author: Boonlit Krunavakarn[None]

Co-authors: N Chamnan ; C Nisaisue

Corresponding Author: boonlit@go.buu.ac.th

We argue that the Little-Parks effect, i.e., the oscillations of the superconducting critical temperature T_c as a function of the magnetic flux threaded the superconducting cylinder, exhibits the feature of the fractional quantized flux when a ferromagnetic metal filled in the thin-walled superconducting shell, which caused by the exchange interaction. Our analysis is based on the transport-like proximity effect theory in the diffusive regime of Takahashi-Tachiki and shows explicitly that the extremum of T_c in the vortex state L corresponds to the fractional values of fluxoid, and in particular the fractional flux quantum occurred at the $L = 1$ vortex state.

Poster: S2 Condensed Matter Physics - Board: P103 / **30**

The Effect of Graphene Oxide Addition in Copper Selenide Compound on Thermoelectric Efficiency

Author: Wanida Duangsimma[1]

Co-author: Supree Pinitsoontorn [2]

[1] *Khon Kaen University*

[2] *Khoa kaen University*

Corresponding Author: psupree@kku.ac.th

In this project, copper selenide compounds (Cu_2Se) were synthesized and used as for use as p-type thermoelectric materials. Graphene oxide (GO) at 0.1, 0.5 and 1 wt% concentrations was added in the Cu_2Se compounds. Cu_2Se was synthesized by a ball mill method, adding GO at various concentrations by crushing and mixing, followed by shaking. It was then hot-pressed to obtain high density bulk pellets. The sample examined by X-ray diffraction (XRD), showed the Cu_2Se phase with a cubic structure, but after hot-pressing, an additional monoclinical Cu2Se phase was formed, due to the phase change at temperatures above 400 K. The analysis from the FE-SEM technique showed that the grain size decreased with increasing GO concentrations, corresponding to the carbon content in EDS, which showed the increased carbon content. From thermoelectric properties measurement, it was found that the Seebeck coefficient was positive and tended to increase slightly with GO concentration. Thermal conductivity was decreased with adding GO. The Cu_2Se+GO showed the increased the ZT up to 0.8 at 500 ℃, at the concentration of 1 wt% GO. However, the ZT was not enhanced significantly compared to the Cu_2Se without GO.

Poster: S2 Condensed Matter Physics - Board: p052 / **339**

Synthesis and characteristic of reduced graphene oxide from the Siam weed, (Cromulent Odorata)

Authors: Piyachat Keeraj[None]; Tanadol Sooktong[1]; Wasan Maiaugree[2]; Yingyot Infahsaeng[2]

[1] *Physics of Thammasat*

[2] *Physics Thammasat*

Corresponding Authors: piyachat.kee@dome.tu.ac.th, tanadol.soo@dome.tu.ac.th

Piyachat Keeraj, Tanadol Sooktong, Wasan Maiaugree, and Yingyot Infahsaeng*
Division of Physics, Faculty of Science and Technology, Thammasat University, Pathum Thani 12120, Thailand

In this work, reduced graphene oxide (rGO) has been synthesized by using Siam weed, (Cromulent Odorata) through carbonization technique and reduced in eco- friendly manner by using Modified Hummer's process. The effects of heating time and temperature on the formation of graphitic carbon were studied. Carbonization of the starting materials was conducted under nitrogen atmosphere at temperatures ranging from 500 to 800 ℃. The morphology and chemical structure of the produced rGO were investigated using FE-SEM, and Raman spectroscopy. Functional groups and crystal structures of carbon from Chromolaena odorata were characterized by Fourier transform infrared spectroscopy (FTIR) and X-ray diffraction (XRD).
Keywords: Reduced Graphene Oxide, Cromulent Odorata, Carbonization, Modified Hummer's process.
E-mail address: yingyot@tu.ac.th

Poster: S2 Condensed Matter Physics - Board: p053 / **338**

3D printing of carbon-based composite resin and mechanical properties

Author: Chanwit Pa-art[1]

Co-author: Wiwat Nuansing [1]

[1] *School of Physics, Institute of Science, Suranaree University of Technology*

Corresponding Author: chanwit.paart@gmail.com

The 3D printing systems based on resin vat photopolymerization such as stereolithography (SLA) and digital light projection (DLP) techniques have become more accessible. These 3D printing technologies have numerous applications in different industries. This research aims to enhance mechanical properties of 3D-printed objects by adding carbon-based material i.e., graphene and carbon nanotubes into liquid polymers. The liquid crystal display (LCD) 3D printing technique, which is adapted from the DLP method, was performed in this work. It uses LCD screen and UV LED backlighting to cure liquid resin in the vat layer-by-layer. The carbon nanotubes and graphene were composited into the liquid resin to enhance the mechanical properties. This carbon material amount compared to initial resin was varied into 0.05, 0.1 and 0.2% w/w. The 3D-printed samples were conducted tensile testing with ASTM D638 type V standard model. The 0.1% w/w graphene mixed resin specimen with 20 seconds exposure time shows the elastic modulus with increasing from 7.31 ± 1.02 MPa to 9.38 ± 0.37 MPa and 3.87 ± 1.13 MPa to 5.28 ± 0.73 MPa for maximum tensile strength.

Poster: S3 Accelerators and Synchrotron Radiations - Board: P104 / **325**

Diagnostics of electron temperature and plasma density by OES and Langmuir probe in linear helicon plasma device

Author: Suttirak Kaewpawong[1]

[1] *1Plasmas and electromagnetic waves research laboratory, Walailak University*

Corresponding Author: suttiran.kea@mail.wu.ac.th

High-density linear plasma devices can generate plasmas, which have similar properties to that of the Tokamaks[1,2]. But, they have a much less complex structure and fewer components. The linear devices are much more cost-effective than the tokamaks for plasma material interaction studies.
In this work, results of plasma diagnostics by optical emission spectroscopy(OES) and Langmuir probe for electron temperatures and plasma densities will be presents. The electron temperatures and plasma densities depend on gas flow rate, gas pressure and rf power. The physics of their dependence will be discussed.
Reference
1. Caughman et al., Plasma source development for fusion-relevant material testing, Journal of Vacuum Science & Technology A: Vacuum, Surfaces, and Films 35, 03E114 (2017)
2. R. H Goulding et al., Progress in the Development of a High Power Helicon Plasma Source for the Materials Plasma Exposure Experiment, Fusion Science and Technology, (2017)

Poster: S3 Accelerators and Synchrotron Radiations - Board: P105 / **306**

Proton-induced luminescence of scintillating Ce3+-barium-gadolinium-fluoroborate glass

Authors: Chinorat Kobdaj[1]; Phongnared Boontueng[None]; Narongrit Ritjoho[2]

[1] *School of Physics, Suranaree University of Technology*

[2] *Suranaree University of Technology*

Corresponding Author: p.boontueng@gmail.com

In this paper, we present the experimental setup for measuring proton-induced luminescence with a fabricated scintillating glass. The glass was synthesized based on barium-gadolinium-fluoroborate glasses using the quenching technique. The luminescence generated by X-ray excitation of the glass demonstrates that an emission band centers around 400 nm owing to the Ce3+ by 5d–4f transition. Furthermore, the proton-induced luminescence experiment was set up to investigate light emission from the glass irradiated by a proton beam at King Chulalongkorn Memorial Hospital (KCMH), Bangkok, Thailand. The beam was operated with an energy of 70 MeV and an absorbed dose of 2,500 MU. A virtual water phantom was put in front of the glass with different thicknesses to observe the position of a Bragg peak. The energy deposition of the proton beam onto the glass scintillator was calculated by using the Gate simulation and compared with light emission from experimental results. We found that the position of the Bragg peak from the experiment and that of the simulation are consistent. According to the measured glass properties, the fabricated scintillating glass is suitable for being applied as a radiation detector or in other applications.

Poster: S3 Accelerators and Synchrotron Radiations - Board: P106 / **316**

Optimization of Current Transformers for Linear Accelerator System at PBP-CMU electron Linac Laboratory

Authors: Watchara Jaikla[1]; Jatuporn Saisut[2]

Co-authors: Panat Nanthanasit [2]; Sakhorn Rimjaem [2]; Noppadon Khangrang [2]

[1] *NARIT*

[2] *Chiang Mai University*

Corresponding Author: jatuporn.saisut@cmu.ac.th

A beam current transformer is one of the most important equipment for electron beam characterization in an accelerator system. The electron beam current can be evaluated from the induced pulse current from the current transformer when the electron beam passes through the transformer. The components of the transformer consist of a ferrite core wound with copper wire for magnetic field coupling and ceramic break with metal housing for image current bypass and magnetic field shielding. This research aims to optimize the number of turns of copper wire which is wound around the commercial ferrite core. For the optimization, a square waveform generator is used as a source of pulse beam. The generator can vary the duty cycle and has a minimum pulse width of 2 μs. The induced voltage pulse of the copper wire is recorded by oscilloscope and is compared with the input signal of the generator. The optimization results suggest that the uniform winding with 30 turns of copper wire provides the best induced pulse shape for these ferrite cores. The optimization results will be presented and discussed.

Poster: S3 Accelerators and Synchrotron Radiations - Board: P107 / **317**

Design, Construction and Measurement of Electromagnetic Steering Magnet for 25-MeV Electron Accelerator System

Author: Pitchayapak Kitisri[None]

Co-authors: Noppadon Khangrang [1]; Theeradon Kitisri [1]; Sakhorn Rimjaem [1]

[1] *Chiang Mai University*

Corresponding Author: pitchayapak_ki@cmu.ac.th

Mid-infrared and terahertz free-electron laser (MIR/THz FEL) facility is under construction at the PBP-CMU Electron Linac Laboratory (PCELL) in Chiang Mai University. For producing MIR-FEL, electron beams with an energy of 25 MeV accelerated by a radio-frequency linear accelerator (RF linac) are required. Transporting the 25-MeV electron beam from the linac to the MIR-FEL station requires magnets for steering the electron beams along the beamline. This work focuses on the design, construction, and measurement of an electromagnetic steering magnet for controlling the electron beam trajectory. A computer software, CST EM STUDIO 2018 is used for the 3D magnetic field simulation of the magnet. The physical length of the magnet and the diameter of copper coils are decided based on the simulation results. After the construction, a hall probe with a measuring system controlled by a computer program is used to measure the magnetic field for comparison with the simulation results. From the simulation results, the steering magnet with a length of 40 mm and the coils with a diameter of 1.06 mm was chosen. At an applied current of 1.8 A, this steering magnet can bend the 25-MeV electron beam with a bending angle of 13.4 mrad. The measurement result showed that the magnetic field was consistent with the simulation results. The advantage of this steering magnet is that it can be assembled on a square frame for steering the beam for both horizontal and vertical direction. It can also be used for the THz-FEL beamline, which requires the electron beam with an energy of 10 - 16 MeV.

Poster: S3 Accelerators and Synchrotron Radiations - Board: P108 / **320**

Construction and Tests of Phosphor View Screen Station for Monitoring Transverse Profile of Electron Beam at PCELL

Authors: Jatuporn Saisut[None]; Noppadon Khangrang[None]; Kittipong Techakaew[1]; Pitchayapak Kitisri[None]; Sakhorn Rimjaem[1]

[1] *Chiang Mai University*

Corresponding Author: nopadon.kh@cmu.ac.th

Development of an accelerator-based light source for generating coherent terahertz (THz) and mid-infrared (MIR) free-electron laser (FEL) is ongoing at the PBP-CMU Electron Linac Laboratory (PCELL). For producing high quality radiation, suitable electron beam property is necessary. In particle accelerator technology, transverse beam distribution and profile can be measured by using several techniques. The beam monitoring using view screen station is one of popular and effective methods. At PCELL, we use stations consisting of phosphor screen equipped with CCD camera to monitor, measure and record the beam image along the accelerator system and beamlines. The phosphor screen was chosen due to its high spatial resolution. The phosphor film is uniformly coated on a thin aluminum plate. Its green emission when electrons hitting the screen is mated well with the respond of the CCD camera. The screen can be moved in and out from the vacuum chamber using the air pressurized linear actuator. This paper presents about design, construction and tests of the screen stations. The resolution of measurements for beam transverse profile and emittance will also be discussed.

Poster: S3 Accelerators and Synchrotron Radiations - Board: P109 / **118**

Assessment of Radon Concentration of Vegetables and Fruits in local markets in Muang Nakhon Phanom Municipality, Thailand

Author: Yodprem Pookamnerd[1]

Co-authors: Vitsanusat Atyotha [2]; Prutchayawoot Thopan [2]; Worawan Poochada [3]

[1] *Nakhon Phanom University*

[2] *Rajamangala University of Technology Isan, Khon Kaen Campus*

[3] *Khon Kaen University*

Corresponding Author: yodprem.p@gmail.com

Aim of this research is a hazards assessment of radon concentration, effective radium content and radon exhalation rate were estimated in 24 vegetables samples and 9 fruits samples that collected randomly from local markets in Muang Nakhon Phanom Municipality, Thailand by active detecting method (RAD 7). The results showed that radon concentrations in vegetables were in the range of 6.27 – 45.11 Bq/m3, the mean was 21.32±2.36 Bq/m3 and radon concentrations in vegetables were in the range of 12.11 – 53.19 Bq/m3, the mean was 27.47±2.81 Bq/m3, respectively. All values of radon concentrations for vegetable and fruits in these study were found to be well below than the international stardard level of radon concentration 190 Bq/m3 recommended by the EPA. These results were also used to calculate the average effective dose equivalent (EDE) of radium from vegetables and fruits, calculation was 0.034 μSv/y, This is lower than the effective dose equivalent for the standard value of 1.3 mSv/y recommended by the EPA. This study show that vegetables and fruits were found to be safe from radon contamination.

Poster: S3 Accelerators and Synchrotron Radiations - Board: P112 / **130**

Design of the prototype quadrupole magnet for a compact THz radiation source

Author: Siriwan Jummunt[1]

Co-authors: Supawich Sinsawat [1]; Prapaiwan Sunwong [2]; Supachai Prawanta [3]; Somjai Chunjarean ; Visitchai Sooksrimuang [1]; Supat Klinkhieo [4]

[1] *Synchrotron Light Research Institute (SLRI)*

[2] *Synchrotron Light Research Institute (Public Organization)*

[3] *Synchrotron Light Research Institute*

[4] *Synchrotron Light Research Institute, SLRI*

Corresponding Author: petecha.ya1649@gmail.com

The terahertz (THz) region of the electromagnetic spectrum covering the frequency range from 0.1 to 10 THz has attracted much attention in terms of new scientific and industrial applications. We are considering producing the THz radiation with an accelerator source based free-electron laser (FEL). The main goal is to achieve intense THz radiation at tunable frequencies of between 0.5 and 5.0 THz, with a high peak power and narrow bandwidth. To generate high-intensity THz radiation, a high-quality electron beam is controlled passing through a periodic field undulator. In order to optimize electron beam properties, the quadrupole magnet is one of the key components. The quadrupole magnet for this system was designed with the magnetic field gradient of 5 T/m2 at operating point. The dimensional tolerances keep within the range of ±5 μm. The prototype quadrupole magnet is in the process of fabrication. The engineering design of prototype quadrupole magnet will be shown in this presentation.

Poster: S3 Accelerators and Synchrotron Radiations - Board: P113 / **135**

Optical Design of BL7.3 beamline Synchrotron Light Research Institute

Author: Prayoon Songsiriritthigul[1]

Co-authors: Jitrin Chaiprapa [2]; Natthapong Saengwises [1]; Thananphat Phonthongchunthuek [1]; Phiraya Suksamran [1]; Puttamawan Juntree [1]; Supagorn Ragmai [2]

[1] *Suranaree University of Technology*

[2] *Synchrotron Light Research Institute*

Corresponding Author: jitrin@slri.or.th

This report presents the design of an optical system to deliver X-rays produced from a 6.5T superconducting wavelength shifter, BL7.3 beamline at the Synchrotron Light Research Institute of Thailand. The beamline is planned for X-ray fluorescence (XRF) and micro-beam XRF measurements. The optical design of this beamline is based on the working principle of a single curved crystal polychromator which acts as both a narrow bandwidth energy transmitter and a focusing X-ray optical element. Detail design considerations will be described. The results from analytical calculations and ray-tracing simulation will be presented and discussed.

Poster: S3 Accelerators and Synchrotron Radiations - Board: P114 / **200**

Dose response curve of Cholangiocarcinoma cell after irradiation with photons and proton beams

Author: Yuwadee Malad[1]

Co-authors: Chinorat Kobdaj [2]; Chutima Talabnin [1]; Dea Aulia Kartini [1]

[1] *Suranaree University of Technology*

[2] *School of Physics, Suranaree University of Technology*

Corresponding Author: tiw.physicsroom@gmail.com

Cholangiocarcinoma (CCA), also known as bile duct cancer, is a silent cancer that is difficult to treat because patients are diagnosed at an advanced stage with incurable disease. Chemotherapy and radiotherapy are additional treatments options for these patients that can help improve their quality of life and survival. Nowadays, radiotherapy utilizing proton beams is gaining interest in the treatment of cancers, including CCA. The purpose of this work is to investigate the radiobiological attributes of CCA cell lines (KKU-213) by observing the response of CCA cells to photons and protons irradiation. KKU-213 cells were cultured in monolayers and cells have been irradiated using 6 MV LINAC and 100 MeV proton beams with dose ranging from 0 – 5 Gy. Measured dose response curves from both photons and protons irradiation were then compared in order to obtain the relative biological effectiveness (RBE) values. By obtaining the RBE value, we could determine whether proton beams would be an alternative approach for CCA treatment.

Poster: S3 Accelerators and Synchrotron Radiations - Board: P116 / **69**

Synchrotron Radiation Fourier Transform Infrared (SR-FTIR) Spectroscopy in Exploring Crosslinked Chitosan-Rice Husk Bio-composite by Gamma Irradiation

Author: Pawitra Aim-O[1]

Co-authors: Siriwan Nawong [2]; Niken Siwi Pamungkas [1]; Nuatawan Thamrongsiripak [3]; Sornwit Thongphanit [4]

[1] *Synchrotron Light Research Institute*

[2] *Synchrotron Light Research Institute, 111 University, Muang, Nakhon Ratchasima, 30000, Thailand.*

[3] *Thailand Institute of Nuclear Technology*

[4] *Thailand Institute of Nuclear Technology*

Corresponding Author: pawitra@slri.or.th

To enhance the physical, chemical, or biological properties of polymer materials, the X-rays beam is used extensively to modify. The heavy metals in wastewater are hardly biodegradable and disposable in human organs because of their toxicity. Thus, an effective removal for the heavy metal ions from wastewater has triggered considerable concerns to environmentalists. Chitosan biomaterials have widely been used to absorb heavy metals from the wastewater and aquatic system due to its low residue generation and the ability to recycle and reuse adsorbents. The chitosan polymer's high abundance of amino groups also allows for numerous chemical changes to improve its adsorbent characteristics and adsorption capacity. This work synthesized the bio-composite from rice husk and coated its by chitosan solutions. The gamma irradiation had been applied to create the crosslinking chitosan to join of two or more intermolecular or intramolecular by a covalent bonding could give a more rigid structure and potentially a better-defined shape of the material. The Chitosan-Rice Husk bio-composite were irradiated using gamma radiation at dose of 50, 100, 200, and 400 kGy. Synchrotron Radiation Fourier Transform Infrared (SR-FTIR) Spectroscopy results revealed the induced crosslinking formation of bio-adsorbents after irradiation. The surface topography and composition of samples were demonstrated by using SEM. In conclusion, natural bioproduct or waste bioproduct has been successfully prepared as a high-efficiency adsorbent with satisfactory performance in heavy metal removal from aquatic ecosystems. The natural bioproduct or waste bioproduct is a new promising adsorbent for the removal of heavy metals from industrial wastewater.

Poster: S3 Accelerators and Synchrotron Radiations - Board: P117 / **18**

Sensitivity of GEB function of MCNP pulse height spectra on CLYC7 scintillator detector

Authors: Sawarin Buakham[1]; Siriyaporn Sangaroon[1]

Co-authors: Kunihiro Ogawa [2]; Mitsutaka Isobe [2]

[1] *Mahasarakham university*

[2] *National Institute for Fusion Science*

Corresponding Author: 62010212024@msu.ac.th

The Cs_2LiYCl_6:Ce or CLYC crystal is an inorganic scintillator which has been developed for the γ-ray and neutron measurement with the high detection efficiency, high resolution, no need unfolding technique. To enhance the measurement of the fast neutron, the CLYC with ^{7}Li-enrichment (hereafter referred to as CLYC7) scintillator are developed. In this work, the response of the CLYC7 detector to γ-ray is obtained using ^{137}Cs γ-ray calibration source and calculated using Monte Carlo N-Particle transport code (MCNP). A comparison of measured and calculated γ-ray spectra is complicated by the fact that physical radiation detectors have finite energy resolution. In this study, we treated detector energy resolution effect by Gaussian energy broadening (GEB) in MCNP pulse height spectra simulation. We observe the parameters in the GEB function that provided a spectrum that matches the experimental spectrum, especially on the photopeak region. The detail sensitivity of GEB function on CLYC7 scintillator detector will be presented in this work.

Poster: S3 Accelerators and Synchrotron Radiations - Board: P118 / **7**

Optimization for Fuel Loading and Thermal Hydraulic Analysis for TRR-1/M1 Research Reactor

Author: KANOKRAT TIYAPUN[None]

Co-author: SAENSUK WETCHAGARUN

Corresponding Author: kanokrat@tint.or.th

TRR-1/M1 reserach reactor is loaded with 8.5% and 20% weight of uranium standard fuel elements. Fuel elements must periodically be shuffled to the reactor core in order to optimize the power, flux distribution and reactivity excess. The Reactivity Initiated Accident (RIA) analysis has been performed for rapidly removal sample from the reactor core and reactivity insertion rate of a sample is assumed to be $1.00/s. The objective of this study is to demonstrate that TRR-1/M1 could be operated safely for 1.3 MW power after shuffling with new core loading configurations containing these 20% weight fuel elements with high burn up in the B ring instead of 8.5% weight. The thermal–hydraulic parameters have been calculated to ensure that the safety margins are sufficient. Therefore, COOLOD-N2 and EUREKA-2/RR for TRR-1/M1 reactor was modelled for steady state and transient conditions coupled with MCNP transport code to calculate coolant and fuel temperature in the core and some parameters in the axial distribution of Departure from Nucleate Boiling Ratio (DNBR) for the hottest channel. The conclusion is that the high burnup 20% weight fuel elements located in B ring had no significant influence on the safety of the reactor. For RIA, the results shown that the negative temperature coefficient which is the negative feedback characteristics of TRIGA provided safety even at larger magnitudes of reactivity during reactor transients. The accident analysis shown that the fuel temperature increases only slightly since the transient is very short, therefore, insignificant energy produced during the accident to heat up the fuel. The maximum fuel temperature occurs for this study is below the safety limit for TRR-1/M1.

Keywords: reactor fuel, core loading, Reactivity Initiated Accident, transients

Poster: S4 High Energy and Particle Physics - Board: P120 / **342**

Study of imaging system in Proton computed tomography with data acquisition from ALPIDE sensor

Author: Nakarin Ratsuntia[1]

[1] *Suranaree university of technology*

Corresponding Author: patong29149@gmail.com

Cancer, the second leading cause of death worldwide, causes people death by growing normal cells larger than cells larger than its boundaries and invade adjoining organs of the body. Currently, proton therapy is one of the radiotherapy techniques for cancer treatment, which is more effective in many ways compared to conventional photon therapy. That's because of unique depth-dose characteristics of the proton. Proton computed tomography (pCT) is an imaging technique prior to the proton therapy. For proton therapy plan, it will be easier and uncomplicated for calculation in proton therapy if we used the same type of particle in imaging process and therapy process, because both processes will provide the same particle interaction with matter. Nowadays, imaging system for medical purposes has been being developed in many research groups. We're also working on it by this work. We went to KCMH Proton Center to do pCT experiment. Proton beam with Gaussian profile is exposed, pass through our sample, and then proton data will be tracked by ALPIDE sensor. We're still facing many errors that we can't control so far. The result from sensor shows the ratio of data from proton that interact on sensor is quite low significantly, so we perform pre-processing data by using mean filter on it instead of median filter or gaussian filter. The result looks a bit better but It's not enough for real using in clinical industry yet, so we're trying to find a technique for image quality improvement to acquire the best 3D reconstruction for pCT by using Inverse radon transformation in the final process.

Poster: S4 High Energy and Particle Physics - Board: P121 / **289**

Optical Transient Counterpart to GW Event with TAROT Telescopes

Authors: Kanthanakorn Noysena[1]; Alain Klotz[2]; Michel Boer[3]

[1] *NARIT*

[2] *IRAP*

[3] *ARTEMIS*

Corresponding Author: kanthanakorn@narit.or.th

The detection of gravitational waves (GWs) from LIGO and Virgo interferometers opened a new era for multi-messenger observations especially with the coincident detection between GW events and gamma-ray burst (GRB) detection. The first GW event detected by LIGO on the 14^{th} September 2015 (Abbott et al. 2016) was a binary black hole merger (BBH) until August 2017 nine other mergers of black holes were detected during runs O1 and O2. Exceedingly the most interesting object for multi-messenger astronomy was the merger of binary neutron star (BNS) detected on 17^{th} August 2017 (Andreoni et al. 2017). The merger was detected in various electromagnetic waves and allowed to confirm the kilonova model (Metzger et al. 2010). This research started with the analysis of images recorded by the TAROT telescopes during runs O1 and O2 to detect new optical sources associated to black hole mergers; GW150914, GW170104 and GW170814. The analysis pipeline was developed to detect new sources by matching the image data with the Gaia catalog data release 1, the angular distance between objects in the image and in the catalog were used to define new sources. We then process the candidates to validate them as possible new unknown objects. Though several possible candidates were detected in the three gravitational wave source error boxes studied, none of them were confirmed as a viable counterpart. Even though none of optical transient had been detected but the limiting magnitude of the particular BBH event of 14^{th} August 2017 gave new constraints about the hypothetical link with gamma ray bursts (Noysena et al. 2019). Three GW events were observed with TAROT allowing us to constrain $\alpha < 10^{-5}$, the fraction of energy emitted by gravitational waves converted into optical light. An approximately 100% coverage of localization of GW170814 was observed at 0.6 days after GW triggering with no evidence of optical transient and 65% of 147 optical light curves of GRBs known redshift were excluded. The optical follow up of GW sources by TAROT and a new method to increase the efficiency of the detection pipeline are pioneering experiences forward to the next GW counterpart in the next observing run O4 of GW observatory, we could find more optical evidence from the GW merger events.

Poster: S4 High Energy and Particle Physics - Board: P122 / **217**

A demonstration of absolute polarization angle calibration at 6 GHz using ATCA

Author: Kitiyanee Asanok[1]

Co-authors: Koichiro Sugiyama [1]; Montree Phetra [2]; Thanapol Chanapote [1]

[1] *National Astronomical Research Institute of Thailand*

[2] *Graduate School, Chiang Mai University, National Astronomical Research Institute of Thailand*

Corresponding Author: kitiyanee@narit.or.th

We will demonstrate the polarization calibration for obtaining the absolute polarization angle from the continuum polarization calibrators at 6 GHz. The data including calibrators and maser sources were observed by the Long Baseline Array (LBA) under the project V452E which aims to study the magnetic field structure in high-mass star-forming regions (HMSFRs). In order to obtain the correct magnetic field orientations in HMSFR, the absolute polarization angle has to be known. We used the calibrator data only from Australia Telescope Compact Array (ATCA), the LBA station which provides the highest sensitivity and sufficient resolution for this purpose. Summary processes are as follows; (a) PKS 1934-638 is the unpolarized primary calibrator and will be used as the flux scale for other calibrators (b) gain, bandpass, and antenna leakages will be determined for all sources, and (c) the image cubes of 1921-293 will be created and absolute polarization angle will be measured at the peak of total intensity. The calibration was performed using the Common Astronomy Software Applications (CASA) package. This angle will be used as the reference value for the polarization calibration of the LBA under the same project code.

Poster: S4 High Energy and Particle Physics - Board: P123 / **213**

Holographic RG flows from four-dimensional N=6 and N=2 gauged supergravities

Author: [redacted][None]

Corresponding Author: nutives@gmail.com

In quantum field theories, interactions between particles can be studied by using Feynman diagrams. Calculating Feynman diagrams in strong interaction between particles results in infinity values. This problem can be solved by using a process of renormalization that is the method of removing an infinity. Invariances under scaling form a group called renormalization group. Some renormalization group flows (RG flows) describe deformations of a conformal field theory (CFT) to another conformal or non-conformal theories, resulting in the deformations of a UV conformal fix point to another fixed point or a non-conformal phase in the IR. In this work, we study holographic RG flows from N=6 gauged supergravity with SO(6) gauge group. The solutions describe RG flows from the N=6 CFT to non-conformal field theory in three dimensions driven by mass deformations by the so-called AdS/CFT correspondence or AdS/CFT holography. We also discuss RG flows from N=2 gauged supergravity obtained from a truncation of N=8 supergravity.

Poster: S4 High Energy and Particle Physics - Board: P124 / **220**

Exploring the extinction in the line of sight of the Galactic bulge through the VVV data

Author: Ponlawat Yoifoi[None]

Co-author: Supachai Awiphan [1]

[1] *NARIT, Thailand*

Corresponding Author: ponlawat.yoi@gmail.com

The study of the bulge of the Milky Way galaxy is still one of the main puzzles for the Galactic studies. Exploring stars in this region is quite challenging due to not only myriad stars which are tightly packed together in the bulge but also the interstellar dust in the galactic plane which restrict the observation. In order to observe the bulge's stars through the dust, infrared observations are needed. In this study, we will focus on the Color-Magnitude Diagram (CMD) of the bulge's stars which represent both the number of stars, brightness and colour properties of stars in the area. The observation data from the Vista Variables in the Via Lactea (VVV) are compared with the simulations from the Besan\c{c}on Galactic model in order to the statistic and dynamics of the bulge. The convolution technique and 2D-cross correlation will be applied to the model to fit the data. From the result, the corrected extinction map of the bulge is presented.

Poster: S4 High Energy and Particle Physics - Board: P125 / **225**

Internal and external effects on Ganymede's footprint location

Author: Tatphicha Promfu[1]

Co-authors: Jonathan Nichols [2]; Suwicha Wannawichian [3]; John Clarke [4]; Marissa Vogt [4]; Bertrand Bonfond [5]

[1] *Department of Physics and Materials Science, Faculty of Science, Chiang Mai University*

[2] *Department of Physics and Astronomy*

[3] *Department of Physics and Materials Science, Chiang Mai University*

[4] *Center for Space Physics*

[5] *LPAP, STAR Institute*

Corresponding Author: ptatphicha@gmail.com

Ganymede is one of Galilean moon whose orbit is inside Jupiter's magnetosphere. The interaction between Ganymede's magnetosphere and magnetospheric plasma around the moon. This interaction results in currents carried along the magnetic flux tube to Jupiter's ionosphere, and a bright spot called Ganymede's footprint (GFP). This work presents the location shifts of GFP in two parts. In the first part, we compared overall data of GFP location which are taken in 2007 and 2016 by Hubble Space Telescope (HST) in comparison with the average path by Bonfond et al., 2017, and the predicted locations from the 4 internal field models: GAM, VIPAL, JRM09, and JRM33. The footprints from observations show the clear discrepancies at system III longitude about 140° - 150° (the kink region) for both our data and Bonfond et al.'s average path in comparison with the predicted locations from VIPAL, JRM09, and JRM33. Nevertheless, the locations of GFP tend to be consistent with the GAM model at system III longitudes about 145° - 150° for the data observed in 2007. In the second part, we present the variation of GFP location in comparison with the evidence of volcanic eruptions on Io (internal factor) and the solar wind compression (external factor). We selected 4 specific cases which have similar CML and system III longitude to assess the effects of internal and external factors. In addition, we compared GFP locations with the field line mapping from the magnetodisc model (Nichols et al.,2015). The model results show the effects of two parameters which are the hot plasma parameter (K_h) and mass outflow rate from Io ($\dot{M}$). This study also considers the different cases of solar wind compression resulting in different boundary of the magnetosphere, which is chosen to be 80 R_J and 50 R_J. The polar projection for the 4 cases reveals the shifts in the poleward or equatorward direction of GFP. Furthermore, the polar projection also shows that the main emission moves toward the poles under the solar wind compression.

Poster: S4 High Energy and Particle Physics - Board: P126 / **267**

The Engineering Design of the Ultra-High Vacuum Chamber for Astrochemistry Experimental Station

Author: Watchara jaikla[1]

Co-authors: Assoc.Prof. Piyarat Nimmanpipug [2]; Chutipong Suwannajak ; Monchai Jitvisate ; Nahathai Tanakul [3]; Sakhorn Rimjaem [2]; Ukrit Keyen [3]; pitch wongkummoon [2]

[1] *NARIT*

[2] *Chiang Mai University*

[3] *National Astronomical Research Institute of Thailand (Public Organization)*

Corresponding Author: watcharanat@gmail.com

In astrochemistry research, which studies the chemical processes under space-like conditions, experiments need to be done under those extreme conditions. This includes ultra-low pressure of about or less than 10^{-10} Torr and extremely low temperature of about 80K. Therefore, it is necessary to build a device capable of responding to such research condition. In this work, we present the engineering design of the experimental chamber to demonstrate the space-like conditions. The main chamber is cylindrical in shape of 32-cm diameter and 35-cm height is built with 1-cm thick stainless-steel grade 304 to withstand the extreme pressure difference. Nine stainless-steel tubes with different diameters are welded to the main chamber to represent ports for connecting with a high efficiency turbo pump, which can provide a vacuum of 10^{-10} Torr, a cooling sample stage, gas injection units, and IR optical ports. The cooling stage with a sample holder located in the center of the chamber is connected with a liquid nitrogen dewar via an aluminum base with high heat transfer to maintain the extremely low temperature condition at the sample. After the main chamber is pumped to the required level of pressure, the interested molecules can be injected onto the sample holder through a gas injection unit. The resulted chemical species formed on the sample holder surface can be probed through IR spectroscopy using an FTIR spectrometer and a MCT detector connected to the chamber. The IR resulted spectrum will reveal the finger-prints of the chemical substants formed on the sample holder surface.

Poster: S4 High Energy and Particle Physics - Board: P127 / **282**

Reveal chemical compositions in the exoplanetary atmospheres using the transmission spectroscopy technique

Author: Thammasorn Padjaroen[1]

Co-authors: Supachai Awiphan [2]; Siramas Komonjinda [1]

[1] *Chiang Mai University*

[2] *NARIT, Thailand*

Corresponding Author: veenus33@gmail.com

The Earth, without its atmosphere, would be a rocky planet with no oceans, clouds, or life. In order to discover the presence of extraterrestrial life, the chemical compositions of the exoplanetary atmosphere should be revealed. Until now, there have been thousands of exoplanets discovered, including more than 3,000 transiting exoplanets. Transmission spectroscopy technique, which studies exoplanetary atmospheres during their transits, is widely used to study the atmosphere of transiting exoplanets. Presently, this technique has been used to study the atmospheres of a number of exoplanets. Nevertheless, the tools and methods of exoplanetary analysis might differ in each work, which might provide different atmospheric parameters. Consequently, in this work, the 1,517 published transit light curves of 163 exoplanets are used to analyse their atmospheric composition using TransitFit and PLATON packages, python exoplanetary fitting packages based on nested sampling algorithms. The light curves were used to determine the physical properties and transit depth using TransitFit. Finally, there are 14 exoplanetary systems which can be analysed for their atmospheric compositions using the PLATON package.

Poster: S4 High Energy and Particle Physics - Board: P128 / **161**

Thermodynamics of AdS Black String from Renyi entropy in de Rham-Gabadaze-Tolley Massive Gravity Theory

Authors: [redacted][1]; Chun-Hung Chen[1]; [redacted][1]

[1] [redacted]

Corresponding Author: p.rawat08@hotmail.com

The de Rham-Gabadadze-Tolley (dRGT) black string solution is a cylindrically symmetric and static solution of the Einstein field equation with graviton mass. By investigating the thermodynamic properties of the dRGT black string, we found that the structure of graviton mass can provide the Hawking-Page phase transition. Since the dRGT black string entropy is a non-extensive quantity, we examine the non-extensive nature of the black string by using Renyi entropy. We found that the structure of the phase transition is significantly modified. In particular, there exists the swallow tail behavior of the Gibb free energy. This implies that there is the additional first order phase transition at which the temperature is higher than the usual one. As a result, the non-extensive nature of the black string provides a new phase of the black string which is both locally and globally stable.

Poster: S4 High Energy and Particle Physics - Board: P129 / **153**

The period variation of an eclipsing binary system BQ Ari.

Authors: Ladda Deesuan[1]; Pranita Sappankum[1]; Ronnakrit Rattanamala[2]; Siramas Komonjinda[3]; Supachai Awiphan[4]; Suwanit Wutsang[1]

[1] *National Astronomical Research Institute of Thailand (Public Organization), 260 Moo 4, Donkaew, Mae Rim, Chiang Mai, 50180, Thailand*

[2] *Faculty of Science and Technology, Nakhon Ratchasima Rajabhat University, Nakhon Ratchasima 30000, Thailand*

[3] *Chiang Mai University*

[4] *NARIT, Thailand*

Corresponding Author: ronnakrit.r@gmail.com

In this study, we focus on the period variation of the eclipsing binary star BQ Ari. The observation data was obtained from the Thai Robotic Telescope at Spring Brook Observatory (TRT-SBO) from 2019 to 2020 and the Regional Observatory for Public, Chachoengsao (ROP-CCO) in 2021. The data are combined with the data from the Transiting Exoplanet Survey Satellite (TESS) in Sector 42 and 43. In order to study the period variations of BQ Ari, the times of minima were extracted from the light curves. From the result, 5, 4, 3 and 299 new times of minima were obtained from the data of TRT-SBO (2019), TRT-SBO (2020), ROP-CCO and TESS, respectively. The O-C diagram of BQ Ari shows that the system has a periodic variation with the period of 6-8 years, which might be caused by the Applegate mechanism or the M dwarf orbit around system.

Poster: S4 High Energy and Particle Physics - Board: P130 / **119**

Development of Data Archive for the Spectroscopic Data from Thai National Observatory (TNO)

Authors: Onjira Krataithong[None]; Kunakorn Topurin[None]

Co-authors: Supachai Awiphan [1]; Pakakaew Rittipruk [1]

[1] *NARIT, Thailand*

Corresponding Authors: onjira_kra@cmu.ac.th, bright_kunakorn@hotmail.com

In astronomical researches, a large amount of astronomical data provides astronomers access to research material via an astronomical data archive. In Thailand, The Thai National Observatory (TNO) has been fully operational with both photometric and spectroscopic instruments for a decade and is currently developing next-generation spectroscopic instruments. Despite this, TNO's public data archive facility is still incomplete. The NARIT grant enables us to design and develop a spectroscopic data archive from TNO's next-generation spectroscopic instruments. We're working on a flexible data archiving platform based on MongoDB that can handle large amounts of data. MongoDB is a search engine that is fast and effective, versatile for both structured and unstructured data, and expandable for long-term data storage. Astronomers will have access to and be able to download public data to a local drive. The archive will allow astronomer to search for the Raw images with the preview option to verify the data before downloading. In the future, calibrated spectroscopic data from our spectroscopic pipeline, such as HiFLEx, can be added into the database.

Poster: S4 High Energy and Particle Physics - Board: P131 / **120**

Collective expansion of K-mesons in heavy-ion collisions on the effect of in-medium Kaon potential and the nuclear equation of state

Author: Phacharatouch Chaimongkon[1]

Co-authors: Nutkamol Suwannasri [1]; Oraorn Kaewchot [1]; Yaphakhakorn Chaimongkon [1]; Panadda Sittiketkorn [2]; Natthaphat Thongyoo [3]; Pornrad Srisawad [3]; Kristiya Tomuang [4]

[1] *University of Phayao*

[2] *Nakhon Sawan Rajabhat University*

[3] *Naresuan University*

[4] *Siam Technology College*

Corresponding Author: phacharatouch.ch@gmail.com

The production cross sections of K^+ as a function of the transverse kinetic energy (m_T–m) on a nuclear equation of state for K^+ production in heavy ion-collision by using the quantum molecular dynamics model (QMD) is focused for this work. Production of a cross-section of K^+ from ^{58}Ni+^{58}Ni collision at energy 1.93 A GeV and rapidity range (y_{cm}) from -0.69 to 0.06 are considered. The production cross sections of K^+ as a function of the transverse kinetic energy are computed and compared with the KaoS experiments. The theoretical calculations execute with and without Brown-Rho (K^+N) potential as well as a soft and hard equation of state (soft and hard EOS). The result displayed the theoretical calculations with the soft EoS are analogous to the hard EoS. The theoretical calculation with the soft and hard EOS while taking into account the Brown-Rho (K^+N) potential is consistent with the KaoS experiment, this indicates that the production cross-sections of K^+ as a function of the transverse kinetic energy have a great sensitive probe to examine the equation of state at high temperature and high density.

Poster: S4 High Energy and Particle Physics - Board: P132 / **142**

Maser polarization simulation in the circumstellar envelope of an evolving star

Authors: Montree Phetra[1]; Malcolm Gray[2]; Kitiyanee Asanok[3]

Co-authors: Busaba H Kramer [4]; Koichiro Sugiyama [2]; Thanapol Chanapote [2]; Waraporn Nuntiyakul [5]

[1] *Graduate School, Chiang Mai University, National Astronomical Research Institute of Thailand, Chiang Mai 50200, Thailand*

[2] *National Astronomical Research Institute of Thailand*

[3] *National Astronomical Research Institute of Thailand, 260 Moo 4, T. Donkaew, A. Maerim, Chiang Mai, 50180, Thailand*

[4] *Max Planck Institute for Radio Astronomy, Germany, National Astronomical Research Institute of Thailand*

[5] *Department of Physics and Materials Science, Faculty of Science, Chiang Mai University, Chiang Mai, 50200, Thailand*

Corresponding Author: mont21812@gmail.com

Introduction: An important phenomenon in a pulsing AGB (Asymptotic Giant Branch) star is the variability of its circumstellar envelope. The study of stimulated radiation called SiO maser (Microwave Amplification by Stimulated Emission of Radiation) in the inner edge of the envelope shows fluctuations in polarization during the stellar pulsation period which is caused by the unstable magnetic field around the AGB star and needs to be investigated in order to understand it.
Aim: Simulate the maser signal and polarization by using a computer code to describe the circumstellar envelope of the AGB star for comparison with the observations.
Methods: i) Generate the energy transition of the stimulation matrix ii) Simulate the first stimulation from an electric field background iii) Convert the radiation to the frequency by using Fourier transform iv) Simulate the observation by amplifying radiation along a line of sight within the medium toward an observation position.
Results: At this stage, we set the tubular maser cloud with a constant magnetic field strength toward the observer. The program can simulate the maser signal and polarization, brighter when stimulating with a longer medium; the simulated polarization agrees well with expectations for this magnetic field orientation. Further works need to be carried out by testing this program with the obtained data from real observations.

Poster: S4 High Energy and Particle Physics - Board: P134 / **68**

Transmission spectroscopy analysis of water vapor for the exoplanets atmospheres using HST database.

Author: Thansuda Chulikorn[None]

Corresponding Author: meanbexo09@gmail.com

At present, the study of extrasolar planets is one of the research topics that are of interest to study in astronomy, because such studies can answer questions about the existence of extraterrestrial life and the ability of human habitation on other planets which is one of the important factors of living ability of organisms similar to life on Earth is the presence of H2O on the ground, on the surface or in the atmosphere of the planet. Nowadays, astronomers have discovered water in the atmospheres of more than 10 exoplanets by the transmission spectroscopy technique. However, in the study of each exoplanet's atmosphere, we used different techniques and tools. Therefore, confirming the findings with techniques and other equipment is still essential. This project presents an analysis of the transmission spectroscopy of water vapour for the exoplanets' atmospheres using the Hubble Space Telescope database. We have brought images during the transit of the Neptune-mass exoplanet HAT-P-26b to create a light curve, then a light curve was obtained to analyse the planet's physical properties, including transmission spectrum of the exoplanet which can be used to analyse the composition of the water vapour for the exoplanets atmospheres. The results of this study provided that HAT-P-26 b's atmosphere has water vapour same with previous studies. This confirmed the presence of atmospheric H2O for HAT-P-26b.

Poster: S4 High Energy and Particle Physics - Board: P135 / **58**

Monte Carlo analysis for enhancing radiation safety of Thai neutron imaging system

Author: Weerawat Pornroongruengchok[1]

Co-authors: Sarinrat Wonglee [1]; Thawatchart Chulapakorn ; Sutasinee Kotayee [1]; Piyanud Thongjerm [1]; Thiansin Liamsuwan

[1] *Thailand Institute of Nuclear Technology (Public Organization)*

Corresponding Author: weerawat@tint.or.th

Thailand Institute of Nuclear Technology (Public Organization), TINT, has established the Thai Research Reactor TRR-1/M1 and continuously developed a neutron imaging (NI) system for better non-destructive inspection. Neutron tomography (NT) is currently conducted with a neutron flux of 1e5 n/cm2s. Due to the strength of the neutron source, image acquisition is made by increasing exposure time to improve image quality. However, it would cause a high radiation level around the neutron imaging room and the reactor hall. Adequate radiation shielding is thus needed to improve radiation protection and safety. In this study, we implemented the geometrical model of the NI room in a Monte Carlo simulation developed with Particle and Heavy Ion Transport System (PHITS version 3.07) to optimize the material, thickness, and position of the shielding. Lead and borated polyethylene (12% boron) were mainly used as a shielding material for the design to reduce gamma ray and neutron. The added shielding will be mainly installed around a neutron shutter, at the entrance of the imaging room and above the room. The simulation was performed at the power reactor of 1 MW. The total number of simulated particles was about 1e8 (7 repeats) to make the simulated results achieve good statistics. Detectors were set in the area of the imaging room to study radiation intensity. The radiation profile and intensity were determined at the condition that the shutter is open and closed, corresponding to neutron beam off and on, respectively. The simulated results show that the added shielding could enhance the radiation safety for the staff and the public and collimate the neutron beam and radiation in the NI station. In addition to improving radiation shielding, the neutron camera and the scintillation screen have been deteriorated due to long use. Therefore, changing a new neutron camera is further planned to improve the NI system.

Poster: S4 High Energy and Particle Physics - Board: P136 / **70**

Gamma Irradiation Induced the Conversion of 5-Hydroxymethylfurfuraldeh under Aqueous and Dimethyl Sulfoxide Solution

Authors: Nurulsafeelanaria Benwannamas[1]; Tanagorn Kwamman[2]; Threeraphat Chutimasakul[2]

Co-authors: Sataman Phongphak [2]; Sakchai Laksee [2]

[1] *Walailak University*

[2] *Thailand Institute of Nuclear Technology (Public Organization)*

Corresponding Authors: nurulsafeelanaria.be@mail.wu.ac.th, threeraphat.chu@gmail.com

5-Hydroxymethylfurfuraldehyde (HMF) is one of the furan derivatives that dehydrate from biomass-based reactants and can further oxidize into a bioplastic substitute. Generally, the oxidation reaction can be accomplished under high temperatures accompanied by the catalyst and oxidizing agent. Those traditional methods required expensive costs and enlarged chemical waste on big batch experiments. Herein, radiation technology has been inspired to apply in HMF conversion due to its ability to upscale for industrial applications. The study of HMF was conducted under gamma irradiation without catalyst in both organic solvent and aqueous solution. The gamma radiation is generated from Cobalt-60 source with a dose rate of 1.7 kGy/h and accumulates to the absorbed dose of 10, 20, and 30 kGy. Gamma-ray was found to partially conversed HMF, and the conversion increases respected to the gamma dose increase. HPLC analyzed the unirradiated and irradiated samples with a C18 column and 0.1% THA:MeOH (80:20) mobile phase. The obtained HPLC chromatogram showed that there is HMFCA intermediate formed after irradiation, and its formation can be enhanced in the presence of base. In addition, having strong base in the system can also drive the conversion forward to FFCA intermediate. Effect of solution solvent was noticed to be crucial key under irradiation while the atmospheric gases have almost no effect. The calculated percentage conversion of both HMF and FDCA under gamma irradiation implied its stability in DMSO and sensibility in DI, so biphasic solvent might be an attractive choice for converting the reactant to the tolerated products.

Poster: S4 High Energy and Particle Physics - Board: P137 / **5**

Metallicity Analysis of Proxima Centauri at 0.004 < Z < 0.01

Author: Bea Marie Cajandig[1]

Co-authors: Frank Kelvin Martinez [1]; Lhevy Geraldo [1]

[1] *Rizal Technological University*

Corresponding Author: bmcajandig@rtu.edu.ph

The metallicity of Proxima Centauri is a quantity of this red dwarf star that is particularly unknown due to heavy molecules that grow on the stellar atmosphere and photosphere for stellar temperatures below 5000 K. The stellar evolution code Modules for Experiments in Stellar Astrophysics (MESA) and the Vienna Atomic Line Database (VALD) are used to investigate observational and spectral data from Proxima Centauri. Metallicity of 0.004 < Z < 0.01 creates minute differences in their respective models' results. The model with the greatest luminosity value, Proxima Centauri at Z=0.004, has $6.1329x10^8$ years left in its simulated existence. Reduced metallicity resulted in greater brightness, according to the Proxima Centauri simulation. As a result, stellar life expectancy is shortened. The link between log L–log R and log Teff–log g is directly proportional, according to the linear regression performed on the data of model Z=0.004. On the other hand, log L–log g, log R–log g, and log Teff–log R are inversely proportional. In this study, a preliminary metallicity analysis of Proxima Centauri is presented. The spectral lines of Proxima Centauri's atmosphere were calculated using the VALD database and the MESA simulation model's parameters.

Poster S5: Quantum Technology - Board: P138 / **132**

Influence of temperature on laser diode inside external cavity diode laser

Authors: Nattawut Suksawat[1]; Sitti Buathong[1]; Sarayut Deachapunya[1]

[1] *Department of Physics, Faculty of Science, Burapha University*

Corresponding Author: 63910192@my.buu.ac.th

We study the influence of temperature on laser diode inside an external cavity diode laser (ECDL) with a cateye reflector mirror type. This type of ECDL uses a focused beam of laser directed to an external mirror and reflected back to the laser to adjust the laser frequency with the variation of the cavity length. The input current and temperature of the ECDL can also be adjusted to a proper frequency. However, the influence of the temperature has a strongly effect on the laser. Therefore, the study of the temperature variation has been conducted. The cavity length of the ECDL was fixed during the experiments. The laser wavelength was measured by a spectrometer. A rubidium saturated absorption spectroscopy was also employed to monitor the D2 hyperfine transitions for the optimization conditions.

Poster S5: Quantum Technology - Board: P139 / **124**

Simulation of Three-Nodes Quantum Network with Entangled Photon Pair Source (EPPS) Protocol via International Space Station (ISS)

Author: Poramat Chianvichai[1]

Co-author: Sujin Suwanna [1]

[1] *Mahidol University*

Corresponding Author: poramat.chianvichai@gmail.com

Quantum computers offer algorithms that can potentially solve impactful problems that classical algorithms are inefficient or incapable. As a classical network enhances classical computing performance, a quantum network can do so with quantum computers, and it has become one of the active research topics in quantum communication. It is how to connect two or more quantum objects (qubits) to improve computational power and implement the quantum algorithm. Currently, there are many models and protocols of a quantum network. Here we investigate a quantum network with the entangled photon pair source (EPPS) with a dynamic node, such as a low earth orbit (LEO) satellite, to distribute single photons. Entangled photons are sent from the middle node, swapped with matter qubits at the end nodes, and a Bell pair is created between the matter qubits at the end node. Modelling the International Space Station (ISS) as the middle node, we simulate a quantum network based on EPPS and study the parameters that affect the network performance. We use the quantum state fidelity as an indicator of this performance because it is widely used and desirable in quantum communication. Our proposed quantum network has three nodes of varying distance which act as the ground stations, which we suppose they are located in Chiang Mai, Bangkok and Songkhla provinces. The location of the ground stations and the ISS trajectory [1] will be located with respect to Earth's longitude-latitude coordinates and transformed into a relation of the distance between the ground stations and the ISS as a function of time. This quantum network is simulated with qwanta software [2] based on the Python programming language. We find that distance of the node and measurement errors affect the quantum state fidelity due to photon loss, where the measurement errors have stronger effects. With longer coherent time, the fidelity can meet the minimum requirement of 0.84 for quantum key distribution between Chiang Mai, Bangkok and Songkhla via the ISS node. Finally, we used the first-order approximation and sensitivity analysis to indicate which parameter greatest effect the model. Our research shines light on a possible creation of a quantum network for Thailand by implementing EPPS on a LEO satellite.

Poster S5: Quantum Technology - Board: P142 / **75**

Size Separation of FAPbBr3 Nanocrystals through Differential Centrifugation

Author: Kunlasatree Kunsaeng[None]

Co-author: Yingyot Infahsaeng [1]

[1] *Division of Physics, Faculty of Science and Technology, Thammasat University*

Corresponding Author: ying.11122@hotmail.com

Lead halide perovskite quantum dots (QDs) have attracted much attention for an optoelectronic application. Size dependence properties of QDs have been extensively studeied Herein, formamidinium lead halide (FAPbBr3) QDs have been successfully synthesized at room temperature under an open-air atmosphere. A different particle sizes of FAPbBr3 were rapid separated by using a differential separation method. The particle sizes of perovskite QDs were achieved in the diameter range of 20 – 200 nm. As a result, a small particle size was obtained from a high centrifugal speed. Some aggregation of QDs can be observed from the precipitation with low centrifugal speed. Photoluminescence and absorbance of size-selected perovskite QDs have been investigated. The results of photoluminescence spectra shown that a slightly blue shift and narrow full width at half-maximum of 24 nm has been observed. Thus, there are the possibility to use a convenient differential separation method for size selection of perovskite QDs applications.

Keyword: Perovskites, Quantum dots, Differential centrifugation

Poster S5: Quantum Technology - Board: P148 / **292**

High Speed Video Analysis of Magnetic Rollers

Authors: Kanokporn Intakaew[1]; Pornrat Wattanakasiwich[None]

[1] *Department of Physics and Materials Science, Chiang Mai University*

Corresponding Author: kanokporn.21993@gmail.com

This research consisted of three objectives (1) to study the basic principles of magnetic rollers (2) to construct a demonstration about magnetic force using the motion of magnetic rollers, and (3) to analyze the motion of the magnetic rollers using high speed video analysis techniques. Each magnetic roller is constructed from Neodymium permanent magnets, rechargeable batteries, and aluminum foil. The magnetic roller motion is based on magnetic force and torque. It can move when the same magnetic poles are facing each other. These basic physics principles are used to design the demonstration. The demonstration and activity sheet were used to teach 30 students enrolled in the Fundamental Physics 2 course. They were first-year students in geology and second-year students in mathematics at Faculty of Science, Chiang Mai University. As results, most students struggled with using the right-hand law to determine the direction of torque. Finally, the rolling motions of the magnetic rollers were analyzed using high-speed video analysis technique and Tracker program. Values of angular acceleration and terminal velocity of the magnetic rollers were determined from the tracking position versus time. As a result, angular acceleration and terminal velocity depend on current and magnetic field strength. To predict the center-of-mass velocity as a function of time, the induced electromotive force (emf) in the magnetic rollers was derived using Faraday disk. The velocity as a function of time can be described by the equation v(t)=v_t (1-e^((-t)⁄T)), which is consistent with the analysis results. However, the experimental results of terminal velocities were not in agreement with the predicted values. This might be the assumption that the magnetic field strength of the magnet is constant, which is not.

Poster S5: Quantum Technology - Board: P156 / **131**

Laboratory implementation of Fourier Transform Infrared (FTIR) spectrograph using a super-continuum laser

Authors: Nirawit Kunanta[1]; Pornapa Artsang[2]

Co-author: Panomsak Meemon [1]

[1] *Suranaree University of Technology*

[2] *National Astronomical Research Institute of Thailand*

Corresponding Author: nirawit.kunanta@gmail.com

Fourier Transform Infrared (FTIR) spectroscopy is a technique to indirectly measure spectrum of electromagnetic wave over a broad range. It is based on low-coherence interferometry. The short coherence of a broadband light is measured in the form of an interferogram and then Fourier transformed to obtain a spectral content of light. FTIR has been used to probe interaction between matters and electromagnetic wave, espetially in the wavelength region, where a dispersive spectrometer is not efficient if not impossible. FTIR is self-calibrated with only one part movement. In addition, FTIR collects all wavelengths simultaneously rather than individually as compared with that of dispersive spectrometer. It is widely used in many fields, such as material science, medical science, and also industrial applications. In this work, a custom design of laboratory prototype of FTIR system using a supercontinuum laser as a light source with the wavelength in range of 1,500 – 2,400 nm (6,667 - 4,167 cm^{-1}) will be presented. The system was designed to be a common path of monochromatic and broadband interferometer in a free space Michelson interferometer setup. An interferogram of a monochromatic laser at 532 nm (18,797 cm^{-1}) was used for correction of the phase distortion in the interferogram of the broadband light source. Both broadband and monochromatic lasers share optical components on the same interference system until before entering detectors. They are separated to two separated photodetectors by using a long-pass dichroic mirror. The movable mirror was computer-controlled by the piezoelectric actuator that was placed in the translation manual stage. The result spectrum was analyzed and then compared to the input broadband laser for further performance improvement.

Poster S5: Quantum Technology - Board: P157 / **285**

Design and build of time domain optical coherence tomography for high resolution by using broadband supercontinuum pulse laser

Author: Yutana Lenaphet[1]

Co-author: Panomsak Meemon [2]

[1] *Suranaree university of technology*

[2] *Suranaree university of technology*

Corresponding Author: phet.yutana@gmail.com

The objective of this work is to design and build an imaging system of time domain optical coherence tomography (TD-OCT) with a resolution about 3 micrometers in all directions. Our TD-OCT system was setup based on Michelson interferometer. The depth-resolution can be improved by applying a broadband supercontinuum pulse laser as light source. The lateral-resolution can be improved by using microscope objective with high numerical aperture. This imaging system focuses on material samples that need to be studied internal structure.

Poster S5: Quantum Technology - Board: P159 / **191**

Optimization of adiabatic optical coupling between Silicon nitride and Germanium-based nanostructures for energy-efficient photonic integrated circuits

Authors: Natdanai Khongpetch[1]; Papichaya Chaisakul[2]; Pichet Limsuwan[3]

[1] *Kasetsart University*

[2] *Kasetsart University and Université Paris-Sud*

[3] *King Mongkut's Institute of Technology Ladkrabang*

Corresponding Authors: natdanai.khon@ku.th, fscipac@ku.ac.th

Combining photonics with electronics is identified as one of the viable solutions to accommodate data traffic increase in an energy-efficient manner for various applications such as optical interconnect, quantum computing, sensing, and environment with favorable price-volume curve. Therefore, photonic-electronic integration on Silicon (Si) has shown strong potential to become the new technology platform for modern society with good economic and environmental sustainability [1-4]. The current Si photonics based on high refractive index contrast between Si and SiO2 can have adverse effects in terms of power durability, temperature stability, and technological robustness [4, 5]. In this regard, silicon nitride (Si3N4) has been viewed as a promising Si-compatible platform as it has a significantly-lower thermo-optics coefficient while remaining monolithically integrable with Si substrate. Nevertheless, efficient integration of Si3N4 with other Ge-based optical components, such as Germanium (Ge) or Ge/SiGe quantum wells, remains critically challenging due to large refractive index difference between Si3N4 (n ~ 2) and Ge (n~ 4.3).

This paper aims to propose an integration scheme between these materials that would allow efficient optical propagation based only on these Si-compatible materials, which would potentially allow both photonic and electronic components to be integrated on bulk Si for low-energy consumption. It will theoretically investigate the integration scheme between the Si3N4 optical circuitry and active Ge-based photonic components. On bulk Si, we envision to integrate Si3N4 platform side by side with Ge components. The integration between Ge-based optoelectronic devices and Si3N4 passive optical circuitry on bulk silicon wafer requires development of efficient couplers. Therefore, for optical coupling between the active Ge and Si3N4 materials, the paper will report a double tapered structure incorporating optical mode transformers in both sections. The objective is to match the optical mode from the active optoelectronic part to the passive circuit and vice versa. The project will focus on 3D FDTD simulation to obtain a good coupling design.

This research and innovation activity is funded by National Research Council of Thailand (NRCT).

[1] D. Thomson et al., Journal of Optics 18, 073003 (2016)
[2] X. Wang and J. Liu, Journal of Semiconductors 39, 061001 (2018).
[3] https://optics.org/news/12/4/13 (retrieved on 22 June 2020)
[4] G. Chang, Advanced Photonics, 3(3), 030501 (2021)
[5] Z. Zhang et al., Science and Technology of Advanced Materials 18(1), 283–293 (2017)

S1 Physics Innovation - Board: INV-S1-1 / **372**

Digitalization of smell: development of chemical sensors from lab to startup business

Author: Teerakiat Kerdcharoen[1]

[1] *Department of Physics, Faculty of Science, Mahidol University, Bangkok 10400, THAILAND*

Corresponding Author: teerakiat@yahoo.com

Chemo-sensory system is an essential part of the living organism ranging from the smallest bacterial cells up to the most complex neural systems as presented in human. In fact, the sense of smell especially in mammalian species (i.e., dogs and human) occurs at the nanoscale. By transduction of the chemical interactions between the odor molecules with the receptor proteins into electrical signals, smell perception including recognition and memory would be possible. At present, nanoscience of smell attracts a great interest from both academic and industry, particularly in terms of artificial olfaction. Technological applications of artificial noses (aka electronic nose) are vast: for examples, quality assurance of foods, beverage and agricultural products, health-care diagnostics, environmental monitoring, security systems etc. In this lecture, the development of electronic nose from the discovery of sensing materials to the fabrication of chemical sensor array up to the integration into various forms of electronic nose systems, such as portable, handheld and wearable devices, will be presented. We have explored numerous sensor materials based on different sensing mechanism, i.e., metal oxides, porphyrins/phthalocyanines, carbon nanotubes and conductive polymers, in order to span the applications in broad areas. In addition, techniques of hybridization between the sensor materials as well as transduction principles have been examined, leading to enhanced functionality and flexibility of the new electronic nose systems. Especially in this lecture, real-world applications of our electronic noses to assess the quality of foods, diagnose cancer, determine the health status of individuals and monitor the environmental conditions will be demonstrated. Development of a startup business based on this research will be provided in this lecture.

Keywords: chemical sensor, electronic nose, smell, artificial sense

S1 Physics Innovation - Board: INV-S1-2 / **375**

How to make important ideas in science learnable? A design case study of an educational robotics toolkit

Author: Arnan (Roger) Sipitakiat[None]

This work discusses a design framework based on “idea-power” established by the late MIT professor Seymour Papert. The GoGo Board is used as a case study of an educational robotics toolkit that follows this design principle by focusing on making important ideas in STEM learnable more than specific technical skills such as circuit assembly and low-level programming. A collection of fieldwork examples is shown based on the GoGo Board’s 20-year history and case-studies from schools in Thailand, Brazil, USA.

S1 Physics Innovation - Board: O-S1-1 / **263**

Colorimetric Sensor for Formaldehyde Detection Using Thiol-Functionalized Polydiacetylene and Zinc Oxide Nanocomposites

Authors: Papaorn Siribunbandal[None]; Rawat Jaisutti[None]; Sayan Pudwat[None]; Tanakorn Osotchan[None]

Corresponding Author: papaornsiribunbandal9@gmail.com

Formaldehyde detection is an important method to protect harmful effect on human health. This study aimed to develop a colorimetric sensor for detecting formaldehyde based on thiol-functionalized polydiacetylene (PDA) and zinc oxide (ZnO) nanocomposites. PDA/PDA-SH/ZnO liposomes exhibit a color change from blue to red in the presence of formaldehyde in the range of 100 to 1000 ppm. This color change was easily visualized by the naked-eye and optical absorption spectroscopy. With increasing concentration of formaldehyde, the absorption intensity at 640 nm dramatically decreased, and new absorption peak appeared at 540 nm. The colorimetric response value increase when the concentration of formaldehyde was increased. In addition, the quantitative color change of PDA/PDA-SH/ZnO sensor can be extracted using color RGB images captured by a smartphone. These results suggest a possibility to develop PDA/PDA-SH/ZnO sensor for detecting formaldehyde in real applications.

Keywords: Polydiacetylene, Conjugated Polymer, Nanocomposites, Formaldehyde Detection, Colorimetric Sensors, Digital Image

S1 Physics Innovation - Board: O-S1-7 / **85**

A baby mobile as a STEM activity for promoting students' learning and interest in a simple harmonic motion

Authors: Chalongchai Teevasuthornsakul[1]; Panupon Samaimongkol[1]

Co-author: Nareerath Niyomsin [2]

[1] *Burapha University*

[2] *Benjamanusorn School*

Corresponding Author: panupon.sa@go.buu.ac.th

This paper presents an alternative approach to enhance students' understanding of a simple harmonic motion (SHM) in that baby mobiles were used as a hands-on activity through a game-based STEM lesson. The subject comprised 28 eleventh grade (mattayom five) students of a public high school in Chanthaburi province, Thailand. The activity was conducted in two consecutive parts. The first part started with a brief review of SHM followed by a simple pendulum experiment so that students learned how length of the string, mass of the bob and other quantities affect the period of an oscillating motion. For the second part, a baby mobile competition was assigned to groups of four students for which necessary materials were provided. Students in each group needed to brainstorm, plan, and create their own baby mobile that meets the competition criteria. The winner of the game would share the successful strategy and receive a tiny reward for positive reinforcement. Results, after the completion of this activity, shows a remarkable improvement of students' understanding after post-activity test (mean = 8.57 out of 10.00, S.D. = 1.61) when compared to pretest (mean = 2.93 out of 10.00, S.D. = 1.52). In addition, the satisfaction survey reveals that students felt more enjoyable and were engaged in the activity with an average score of 4.05 out of 5.00. These findings suggest that integrating a hands-on STEM activity with specific course contents may be one of the potential approaches that promotes students' engagement and conceptual understanding in physics.

S1 Physics Innovation - Board: O-S1-2 / **186**

Analysis and prediction of vegetation, croplands, and urbanization change in the philippines using data satellite images between 2001-2018

Authors: Earon Cabasal[1]; Jayvee Miguel Pucio[1]; Ryan Manuel Guido[None]; Jason Kalaw[1]

[1] *Rizal Technological University*

Corresponding Author: eardcabasal@rtu.edu.ph

Urbanization in the Philippines is at a fast pace. As it grows, urban land expansion increases. It results in the conversion of the different land areas in the country. To determine its changes, this study used geographic information system images by using data products of MODIS Terra and Aqua from NASA EOSDIS, it provides satellite images of the Philippines' cover and land use. Eighteen (18) satellite images were gathered and used in this study. The findings showed that the National Capital Region and Cebu islands regions are the most urbanized areas in the country.
Analysis revealed that both urbanization and vegetation landcover increases while the cropland landcover gradually declines. Multiple linear regression analysis revealed that these variables are significant to each other. It also revealed a positive relationship between urbanization and vegetation, while both showed a negative relationship towards cropland landcover. For the next five (5) years, the Philippines' data revealed that urbanization will increase immensely and expand to 3,181.4523 km² in 2023 from the current 2,952.63 km². Thus, the continuous expansion of two variables revealed that there will be a loss in cropland landcover and will only be 40,215.3680 km² in 2023 from the current 63,139 km² total area, which will be very crucial for agriculture and food security in the country.

S1 Physics Innovation - Board: O-S1-8 / **231**

Using a pre-instruction math test to predict first-year physics exam results

Authors: Meta Popanao[None]; Michael Smith[1]; Puangratana Pairor[2]

[1] *Suranaree Institute of Technology*

[2] *School of Physics, Institute of Science, Suranaree University of Technology*

Corresponding Author: meta.ppn@gmail.com

We investigated the results of pre-instruction mathematics test and introductory physics exams of two groups of first-year engineering students at Suranaree University of Technology. We intend to examine the test results to identify factors that predict exam results in the first-year physics course. The first and the second groups took their physics classes in the first and second trimester of the academic year 2020 respectively. Here, we report our analysis of the pre-instruction math tests and claim that they meet reasonable standards for reliability and validity. As a by-product of this investigation, we found that there was no gender gap in the math test results.

S1 Physics Innovation - Board: O-S1-3 / **189**

UV germicidal rays working with timer and motion sensors

Authors: Chatpong Kobkam [None]; Kachain Dangudom[None]

Corresponding Author: d.kachain@gmail.com

As a result of the coronavirus (Covid-19) epidemic, the public has become actively involved in bodily sanitation. The 'New Normal' lifestyle now focuses on cleanliness and disinfection to prevent the spread of germs. This research designed and programmed a microcontroller for a UVC disinfection system using an Arduino board as an open-source electronics platform operated with a motion sensor (PIR) and a time control module (RTC). The optical properties of an 8 Watt (W) UVC source were measured. The four UVC sources investigated had wavelengths ranging from 251 to 577 nm. A UVC wavelength of 251 nm eradicates germs but also destroys tissues and is harmful to humans. Experimental results showed that UVC intensity decreased with distance from the source according to the exponential decay function. A control system, installed inside a building to kill germs when there are no humans or pets, can control UVC light source operation with a maximum power of 2 kW. Operational time can be adjusted by settings on the control box, while as an additional level of safety, the system can be turned off if a motion sensor detects movement. Movement detection distance at an angle of -90 to +90 degrees was recorded. Results gave 11 m detection distance at an angle of 0 degrees, with more than 3 m detection distance at -60 to +60 degrees, as suitable for installation above a door. This timer and motion sensor-operated UV germicidal ray system can be safely deployed to keep rooms germ free.

S1 Physics Innovation - Board: O-S1-9 / **167**

How Does Student Skill on Interpreting Circular Motion Situation Change in an Online Physics Classroom?

Authors: Arunee EAMBAIPREUK[1]; Narumon Emarat[2]

Co-author: Kwan Arayathanitkul [2]

[1] *Division of Science Education, Department of Education, Faculty of Education, Kasetsart University*

[2] *Department of Physics, Faculty of Science, Mahidol University*

Corresponding Author: arunee.ea@ku.th

"How to teach effectively" has become challenging to many teachers after their classrooms were moved to an online platform. For high-school physics, we found that students struggled to grasp the concept when learning in the online classroom. Circular motion is the topic that is difficult to focus on details. They could not understand the content well while concentrating on the screen. Some of them lost the attention during the class. The aim of this work is to investigate the achievement of using collaborative learning to teach the first three steps of circular motion problem solving. The three steps are (i) identifying the path of motion and its radius, (ii) drawing a free-body diagram, and (iii) finding the components of forces acting on the object. The method was applied to an online physics classroom with 12 high-school students of science and mathematics program. Finding of the research was interpreted by pre- and post-tests, and video recording during the teaching. The result showed that there were more students who could interpret the circular motion situation correctly than the beginning of the class. Their understanding has been improved. They could interpret the path of motion and the forces acting on the object and some of them could find the centripetal force correctly. Moreover, there was an interaction between the students that related to their understanding of the topic. Details on how collaborative learning was conducted for an online teaching will be given, along with the limitation and future improvement.

Keywords: High school physics, Circular motion, Collaborative learning, and Centripetal force

S1 Physics Innovation - Board: O-S1-10 / **185**

ATTITUDES AND MOTIVATION OF INTERNSHIP STUDENTS TOWARDS PHYSICS, ASTRONOMY, AND SPACE SCIENCE SATELLITE TECHNOLOGY VIRTUAL INTERNSHIP PROGRAM

Authors: Antriman Orleans[1]; Ryan Manuel Guido[None]

[1] *Philippine Normal University*

Corresponding Author: rmdguido@rtu.edu.ph

The impact of the pandemic on the education sector is severe. It paralyzed the operations and administration of teaching and learning in response to fulfilling the need of the students to do an internship while at home. The Rizal Technological University (RTU) Center for Astronomy Research and Development (CARD) was able to redesign its internship program for students. The Physics, Astronomy, and Space Science Satellite Technology Virtual Internship Program (PASSTVIP) was developed to accommodate students who wanted to pursue research engagements at the convenience of their homes. The program aims to introduce the nature of physics, astronomy, and space science satellite technology through satellite databases and explore its relevance to research and development relative to the Philippine setting. The students were able to do data gathering, explore the Philippines using the data from the satellite of the National Aeronautics and Space Administration (NASA), and process these data thru Python coding with the assistance of their assigned mentors. The students were able to produce a ready Scopus conference paper.

The correlation was determined in the apparent links between attitude and motivation toward the PASSTVIP internships responses the interns. Both scales were supported, as well as the internship evaluation form. The participants were 168 undergraduate students who had undergone PASSTVIP from September 2020 to June 2021 in a synchronous and asynchronous setup. It showed that the PASSTVIP was rated as outstanding due to the uniqueness of exposure and the inspiring tasks from a satellite point of view. Students may have varying measures of their attitudes and motivation. As part of the evaluation form, open-ended questions demonstrate that students value satellite data and have explored the world through earth observations. They have also extended their learnings through coding analysis of earth data, geophysics, and earth observation which they also have cherished the research tasks. The students regarded their internship as exemptional due to its peculiarity, which involved physics, astronomy, and space science satellite technology training. While the students' attitudes and motivations are minimal, their responses to the internship program are impressive.

It is then proved that online internships can be done, applying scientific concepts with the aid of technology and equipment. Also, it imparts to make the students and the community explore the benefits and solutions that can be provided by space science and satellite technology in the country.

S1 Physics Innovation - Board: O-S1-4 / **94**

Simulation Sensitivities Study to the Wind Characteristics over Uttaradit Rajabhat University at Lamrang Thungkalo campus with WRF model

Author: Chainarong Raktham[1]

Co-authors: Jitranud Jitprasert [2]; Thanakit Nanfun [2]; Warin Ta-on [2]

[1] *Uttaradit Rajabhat University*

[2] *Faculty of Education, Uttaradit Rajabhat University*

Corresponding Authors: glaraktham@gmail.com, jitranud6869@gmail.com, physics61.124@gmail.com

This research is the WRF model initial application for wind investigation over Uttaradit Rajabhat University at Lamrang Thungkalo campus under some physical limitations. Its objective is to study weather simulation sensitivities specifically of wind characteristics over the campus on each domain sizes and on each season from selected time periods. Major three case studies are hot season case, rainy season case and cold season case. This experiment was conducted under two-way nested dynamical downscaling techniques, which nested domain (D02, 12km grid size) are within coarse domain (D01, 36km grid size). The National Centers for Environmental Prediction (NCEP) Final (FNL) operational global analysis data were used for initial and boundary conditions brought into WRF Preprocessing System (WPS). The cumulus physics process was controlled by Betts-Miller-Janjic (BMJ) cumulus parameterization, while simple ice scheme (WSM3) was used for microphysics. The NCAR Command Language (NCL) was utilized for graphic visualization. The results found that, WRF is firstly sensitive to domain size which finer domain can improve regional phenomena for coarser domain. Secondly, WRF can well simulate major winds in each case (southern wind in hot season, cyclonic flow in rainy season and northeastern wind in cold season). Thirdly, wind speeds in nested domain are mostly (greater than 50%) under light breeze (less than 3 m/s) agreed with all cases in coarse domain. Wind speeds In both domain were in accordance with TMD observed temporal variation. Fourthly, the vertical updraft was between -0.10 and 0.35 m/s which the highest speed was in hot season, while d02 enhance higher updraft than d01. Finally, high atmospheric stability can be detected from skew-T log P diagram during cold season case. Hence, WRF model can be applied to Uttaradit Rajabhat University at Lamrang Thungkalo campus to analyze the wind characteristics for all atmospheric levels.

S1 Physics Innovation - Board: O-S1-11 / **103**

Compact and easy-to-use smartphone based experimental set for studying simple and damped harmonic motion patterns.

Author: Somporn Buaprathoom[1]

[1] *Mahidol Wittayanusorn School*

Corresponding Author: somporn.bpt@mwit.ac.th

An experimental set for studying harmonic motion patterns was developed in this research. It was designed to be compact and easy to use. It employs sensors in general smartphones to track trajectory patterns of the object moving in both simple and damped harmonic motions. This experimental set can be remotely controlled and collected trajectory data. The data and patterns of trajectory of the studied object can also be real-time displayed and collected by other devices (computers, tablets or smartphones) which students can use for more analysis. Testing the functionality of the presented experimental set, it was found that there was a good consistency between the trajectory patterns collected from the experimental set and simulated from the theory. To evaluate the usage of the experimental set, it was applied to Physics classes. It was found that the students had improved their understanding of harmonic motion pattern by 34.50 percent. These results show that the proposed experimental set can be used for studying harmonic motion patterns effectively.

S1 Physics Innovation - Board: O-S1-5 / **190**

Night-time Human Mobility during Pandemic in the Philippines as Observed by VIIRS Satellite

Author: Ryan Manuel Guido[None]

Corresponding Author: rmdguido@rtu.edu.ph

A recent study has investigated and studied the growing body of research endeavors on human mobility during quarantine periods, employing a variety of methodologies and procedures. There are also numerous approaches to assessing human mobility using light pollution data. This study focuses on analyzing data on light pollution and the COVID-19 cases in the Philippines. The Visible Infrared Imaging Radiometer Suite (VIIRS) satellite data can be used to quantify light pollution as human mobility in the Philippines while the country has employed different quarantine classifications in the different regions. For this investigation, NASA's EOSDIS Worldview website provided the light pollution data while the Philippines' Department of Health (DOH) for the COVID-19 cases. It revealed that between early April and late August 2020, the number of COVID cases and light pollution increased. From September to January 2021, COVID cases decrease, while human mobility is almost constant. From February to April 2021 the number of COVID cases has immensely increased. This could be explained as an effect of the increased human activity between December 2020 and January 2021 which is the Christmas season in the country. Since August 2020, human contact has been intense, resulting in a rise in COVID cases that peaked between March and April 2021 and then declined in May 2021. As a result of this study's findings, light pollution VIIRS satellite images can be utilized to identify suspected COVID-19 cases in an area. When creating a full paper, there are numerous additional factors and variables to consider. Once the flexible quarantine period is extended, dates may be further investigated.

S1 Physics Innovation - Board: O-S1-12 / **218**

Development of Circular Motion Experiment Set with the Reduction of Friction for High School Physics Students

Author: Anucha Pratumma[None]

Co-authors: Mongkol Sapankaew ; Kitisak boonkham [1]

[1] *Mahidol Wittayanusorn school*

Corresponding Authors: anucha.pra@mwit.ac.th, mongkol.sap@mwit.ac.th, kitisak.bnk@mwit.ac.th

The teaching of uniform circular motion in high school Physics consists of a combination between theoretical background and experimental method. In particular, the experimental study can emphasize the concept of centrifugal force for the object moving in a circular path. The experiment set has been developed to study the relationship between the centrifugal force and the moving period. However, the effect of friction in the conventional experiment set has been neglected leading to the deviation of the expected results. In this study, we have developed the circular motion experimental set with the reduction of friction between a hollow tube and a string. The plastic tube in the conventional experiment set was replaced by an aluminum rod to reduce friction at the surface connected to the string. By collecting the experimental data, the mass moving in the circular path was evaluated and showed high accuracy with a deviation of 0.58%. In contrast, a high discrepancy (up to 35%) was observed in the conventional setup due to the surface roughness of the plastic tube. Therefore, the results obtained from our studies can be used to enhance student learning on the uniform circular motion subject in high school.

S1 Physics Innovation - Board: O-S1-6 / **333**

Flow dependence of handheld breath analyzer for body fuel utilization monitoring

Authors: Chan Sricharoen[None]; Tanakorn Osotchana[1]; Tanant Waritanantaa[2]

[1] *Physics Department, Faculty of Science, Mahidol University*

[2] *School of Materials Science and Innovation, Mahidol University*

Corresponding Author: chanproactive@outlook.com

Home healthcare medical technologies have been gaining popularity and are more affordable in recent years. Exhaled breath analysis has potential in this field and the development of gas sensor technology has enabled us to build a small affable breath analysis device together with the electronic nose concept. In this work, a handheld breath analyzer was developed for monitoring body fuel utilization. A hybrid gas sensor array, including electrochemical, optoacoustic, and chemo-resistive gas sensors was used to provide accurate measurement of oxygen and carbon dioxide in exhaled breath. The bypass configuration volume flow measurement method was developed to fit in a small portable device. The result shows that both oxygen and carbon dioxide sensors are flow-dependent due to individual slow response time of each sensor type. The response of optoacoustic sensor is relatively slower than those of other sensor types. Thus, a mathematical model was developed to correct the individual sensor value to get more accurate value of body fuel utilization. The comparing protocol for known concentration of the oxygen and carbon gases with various flow rate was conducted and the model of transfer functions to reconstruct original gas concentration was proposed.

S1 Physics Innovation - Board: INV-S1-3 / **370**

Green energy applications under ANSEE project in Khao Yai National Park

Authors: Santi Maensiri [1]; Worawat Meevasana[1]; Unchista Wongpratat[None]; supansa musikajaroen[None]

[1] *School of Physics, Institute of Science, Suranaree University of Technology*

Corresponding Author: worawat@g.sut.ac.th

With the growing concern of climate change and the reduction of CO_2 emission, the Advanced Nanomaterials for enhancing Sustainable Energy and Environment in Dong Phayayen - Khaoyai World Hertage (or ANSEE project) was initiated. Prototypes of green energy applications, especially relating to customized batteries, have been installed and tested in the Khao Yai National Park and farms near the park. The applications include hybrid-off-grid solar system for tourists and office, EV motorcycles, EV charging stations and off-grid solar systems for farming. In this talk, we will describe about the customization processes relating to energy storage and the environmental/financial/social benefits.

Keywords: renewable energy, energy storage, battery application, CO2 emission, environmental sustainability

S1 Physics Innovation - Board: O-S1-30 / **265**

Competition of SARS-CoV-2 Delta and Omicron variants: A modeling study

Authors: Chatchapat Chaiaiad[1]; Nattawadee Arbsuwan [1]; Charin Modchang[2]; Sudarat Chadsuthi[3]

Co-author: Busara Pattanasiri [1]

[1] *Department of Physics, Faculty of Liberal Arts and Science, Kasetsart University Kamphaeng Saen Campus, Nakhon Pathom 73140, Thailand*

[2] *Biophysics Group, Department of Physics, Faculty of Science, Mahidol University, Bangkok 10400, Thailand*

[3] *Department of Physics, Faculty of Science, Naresuan University, Phitsanulok 65000, Thailand*

Corresponding Author: chatchapat.k@ku.th

Throughout the COVID-19 pandemic, SARS-CoV-2 has been mutated several times into new variants. Some of them are classified as variants of concern (VOCs) by the World Health Organization, such as Alpha (B.1.1.7), Beta (B.1.351), Gamma (P.1), Delta (B.1.617.2), and Omicron (B.1.1.529). In this work, we developed an extended Susceptible-Exposed-Infection-Recovered model with cross-immunity between two co-circulating strains to investigate the transmission and competition of two VOCs, Delta and Omicron, that recently emerged in Thailand during the mid and late 2021. Here, the basic reproduction number of the Omicron variant was estimated higher than that of the Delta variant. The results showed that the Omicron variant has a significantly faster transmission, leading to a higher number of infected cases than the Delta variant. Moreover, lowering cross-immunity induced by primary infection also increases the re-infection rates. These results suggested that the capacity of transmission illustrated by the basic reproduction number and cross-immunity play an important role in determining the competition and equilibrium of transmission.

S1 Physics Innovation - Board: O-S1-31 / **152**

Mathematical modeling of vaccination strategies for COVID-19 in Thailand

Authors: Nattawadee Arbsuwan[1]; Chatchapat Chaiaiad[1]; Kan Sornbundit[2]; Suparinthon Anupong[3]; Charin Modchang[3]; Sudarat Chadsuthi[4]

Co-author: Busara Pattanasiri [1]

[1] *Department of Physics, Faculty of Liberal Arts and Science, Kasetsart University Kamphaeng Saen Campus, Nakhon Pathom 73140, Thailand*

[2] *Ratchaburi Learning Park, King Mongkut's University of Technology Thonburi, Ratchaburi, Thailand*

[3] *Biophysics Group, Department of Physics, Faculty of Science, Mahidol University, Bangkok 10400, Thailand*

[4] *Department of Physics, Faculty of Science, Naresuan University, Phitsanulok 65000, Thailand*

Corresponding Author: nattawadee.a@ku.th

COVID-19 vaccination is an important role to reduce the chance of infection and lower the risk of hospitalization and death. However, the vaccination is far less effective with the recent emergence of the Omicron variant. In addition, vaccine protection after vaccination may wane over time, thus receiving additional booster doses is significant to maintain the protection. In this work, we applied an extended SEIR model with vaccinations to investigate the impact of the vaccination rate of primary and additional doses on the spread of the COVID-19 pandemic in Thailand. The results shown that the booster vaccination rate has a major impact on the reduction of infection. These results suggest that the high coverage of booster vaccination remains crucial for reducing the spread of COVID-19.

S1 Physics Innovation - Board: O-S1-13 / **235**

An estimation of net radiation from global solar radiation in the main regions of Thailand

Author: Korntip Tohsing[None]

Corresponding Author: korntip.tohsing@gmail.com

Net radiation can be used for different purposes especially for studying the energy or radiation balance, which can be further analyzed to investigate a global warming. In order to utilize these applications, it is necessary to know the amount of net radiation in that area. This can be done by installing a net radiometer for measuring the net radiation. However, there are few monitoring stations of net radiation compared to a global solar radiation in Thailand. Therefore, this research aims to analyze a statistical characteristic of the measured net radiation and to develop a model for estimating the net radiation from the global solar radiation at four solar monitoring stations in the main regions of Thailand, namely Chiang Mai, Ubon Ratchathani, Songkhla and Nakhon Pathom during the year of 2017 to 2021. The results showed that the average net radiation of these stations was between 8-12 MJ/m². The relationship between daily and monthly average daily net radiation and global solar radiation was found to be a linear. After that, the developed model was validated by comparing the estimated and measured net radiation. The discrepancy between the calculated net radiation and that obtained from the measurements was presented in terms of root mean square difference (RMSD) and mean bias difference (MBD) ranged from 6.98% to 16.03% and -1.82% to 6.77%, respectively.

S1 Physics Innovation - Board: O-S1-32 / **173**

Association of COVID-19 pandemic with meteorological and PM 10 in Thailand using LSTM models

Author: Chanidapa Winalai[1]

Co-authors: Charin Modchang [2]; Sudarat Chadsuthi [1]

[1] *Department of Physics, Faculty of Science, Naresuan University*

[2] *Department of Physics, Faculty of Science, Mahidol University*

Corresponding Author: pch.winalai@gmail.com

The first SARS-CoV-2 infections were discovered in Wuhan, China, and then the virus became the pandemic known as "COVID-19". In Thailand, the COVID-19 situation is still on going and is extremely serious in the central region of the country. To understand the pandemic in Thailand, we investigated the association of three variables, temperature, relative humidity, and the concentrations of PM 10, on the number of cases. We applied a long short-term memory model (LSTM) to predict the number of cases from these associated factors, in the central region of Thailand. This study observed the COVID-19 reported cases from Open Government Data. The meteorological variables data were obtained from the Global Surface Summary of the Day (GSOD), and the PM 10 data was obtained from the World Air Quality Index (WAQI). The results showed that the variables related to the number of COVID-19 cases and could be used to predict the number of cases. We also studied the effect of time lags to the number of cases.

S1 Physics Innovation - Board: O-S1-14 / **193**

Carbon electrode for perovskite solar cell

Author: Supavidh Burimart[None]

Corresponding Author: supavidhb@gmail.com

High-efficiency perovskite solar cell (PSC) normally utilizes metals such as gold or silver as the electrode to achieve the highest power conversion efficiency (PCE) as possible due to their high charge transfer properties. However, there are some disadvantages of the metal electrodes such as high price, high-temperature deposition requirement, and low hydrophobicity. Recent studies show that carbon has a great potential for being PSC's electrode due to its adequate conductivity, proper work function, flexible nature, hydrophobicity, low cost, and low energy input for fabrication. This work focuses on improving a commercially available carbon electrode material for perovskite solar cell by adding carbon black to increase its flexibility and conductivity, yielding reduction of resistivity by 50% measured with a 4 point probe. To further improve mixability between the carbon paste and the carbon black, different solvents were explored. Smaller pore size, smother morphology, better charge transfer, and homogeneous conductance distribution of the carbon film were achieved. The power conversion efficiency more than 15% with little hysteresis was demonstrated with the enhanced carbon electrode.

S1 Physics Innovation - Board: O-S1-33 / **242**

The determination of the effectiveness of mouth covering method while coughing using Background-oriented schlieren technique

Authors: Phongthep Chansamphan[None]; Watcharapath Khaiophueng[None]

Co-authors: Nirut Pussadee ; Pakorn srirathat

Corresponding Authors: pongtep_boy@hotmail.com, tendison@gmail.com

Many airborne infections can easily be transmitted from a patient through coughing, sneezing, or even talking. This encourages awareness of wearing a mask as a protection. This research demonstrates the dispersion characteristics of exhaled airflow through the different ways of protection using background-oriented schlieren (BOS) technique to visualize the air flow around facial area of a demonstrator. Circumstances such talking and coughing under the different modes of protection were video recorded and processed with a MATLAB PIVlab toolbox to visualize the characteristics of the airflow around facial area. It was found that there is always air leakage out from protected masks while coughing in which surgical mask performed poorly when compared with N95 masks. Nonetheless, wearing mask can significantly reduce the speed of airflow.

Nonetheless, there is a small amount of dispersion of the airflow from the protected circumstances. The characteristics of each dispersion relate to the shape of the mask. The high potential of the protection can be respectively classified as N95 mask without valve, N95 mask with valve, and surgical mask. On the other hand, all protection has a potential in reducing airflow dispersion comparing to unprotected circumstance.

S1 Physics Innovation - Board: O-S1-15 / **187**

The Relationship of Solar Activity to Western North Pacific Tropical Cyclone Frequency

Authors: Eliezer Caccam[1]; Ryan Manuel Guido[None]; John Christian Lequiron[2]

[1] *Rizal Technological University*

[2] *Kumunidad Philippines*

Corresponding Author: etcaccam@rtu.edu.ph

Western North Pacific is the most active TC Basin globally as the season runs whole year round and Sun is the main driver of Earth's Climate, although climate drivers are the ones that affect the typhoon season. As presented in the literature studies, there are few research studies have investigated the relationship between SSN and Tropical Cyclones, but it is done in a specific location or basin. This research will fill in the gap of finding the relationship between SSN and TC in the Western North Pacific as part of the recommendation of the said studies. Datasets that were used were from Japan Meteorological Agency, Solar Influences Data Analysis Center, and National Oceanic Atmospheric Administration. The researcher investigated the relationship between Solar Activity and Tropical Cyclone Frequency with the use of Pearson Correlation, Linear Regression Analysis, and T-Value. The researcher found out that the results of the analysis are mostly in negligible correlation and not significant in terms of overall season, Solar Minimum and Maximum basis, and ENSO phases which concludes that a). there is no overall significant correlation between SSN and WNP-TCF, b). there is no significant correlation between SSN and WNP-TCF during Solar Minimum and Solar Maximum, c). there is no significant relationship between SSN and WNP-TCF during El Nino and La Nina. Thus, this study found out that Sunspot Number doesn't have much effect to the Tropical Cyclone Frequency in the Western North Pacific Basin and likely that Anthropogenic Aerosols and Climate Oscillators plays the role in the Tropical Cyclone Activity.

S1 Physics Innovation - Board: O-S1-34 / **262**

Air convection demonstration via background-oriented schlieren technique

Authors: Phongthep Chansamphan[None]; Watcharapath Khaiophueng[None]

Co-authors: Nirut Pussadee ; Pakorn srirathat

Corresponding Authors: pongtep_boy@hotmail.com, tendison@gmail.com, pakornsrirathat01@gmail.com

Convection is one of the heat transfer mechanisms in which heated fluid expands and rises while the cooled fluid shrinks down. The air convection occurs naturally but difficult to be observed when there is a slight difference between temperature of heated object and the ambience. Schlieren imaging technique is mostly used to visualize the motion of the fluid itself. This method, however requires high accuracy and expensive optic devices. Background-oriented schlieren (BOS) is an optical measurement technique where the velocity field of the viewing region could be visualized. In this study, air flow field around ice cube, hand and candle flame were constructed and the converted air speed were measured using Particle Image Velocimetry (PIV) technique from MATLAB PIVlab toolbox. The results showed that the BOS technique can be similarly used to visualize the air convection around the testing objects when comparing to schlieren technique yet significantly costs less in expenditure.

S1 Physics Innovation - Board: O-S1-16 / **211**

A model for estimating solar ultraviolet radiation for vitamin D photosynthesis

Authors: Sumaman Buntoung[1]; Pradthana Laiwarin[1]

Co-authors: Serm Janjai [1]; Rungrat Wattan [2]

[1] *Department of Physics, Faculty of Science, Silpakorn University, Nakhon Pathom 73000, Thailand*

[2] *Department of Physics, Faculty of Science, Silpakorn University, Nakhon Pathom 73000, Thailand*

Corresponding Author: laiwarin_p@silpakorn.edu

Solar ultraviolet radiation has both beneficial and drawback impacts on human health. Excessive exposure to ultraviolet radiation is hazardous for human. For example, it can cause skin cancer, cataracts and suppression of the immune system. On the other hand, solar ultraviolet radiation is a part of the vitamin D photosynthesis in the human skin. It is needed in the process of synthesize previtamin D in the epidermis to 25-hydroxyvitamin D via the liver and kidneys. Although Thailand is located in the equator where solar radiation is relatively high, the number of patients with vitamin D deficient is increasing. Therefore, the instantaneous amount of solar ultraviolet is needed to be known. This can be measured by using a spectrophotometer together with the vitamin D action spectral response. However, in Thailand, such ground-based instrument is very scarce. To solve this problem, this work aims to develop an empirical model for estimating hourly solar ultraviolet radiation for vitamin D synthesis under all sky condition using atmospheric parameters.
A spectrophotometer (model DMc150, Bentham Instruments) is used together with a CIE action spectral response to obtain the measured solar ultraviolet radiation for vitamin D synthesis (UVvitD) at Nakhon Pathom province, Thailand. The input of the model consists of cloud index from Himawari satellite, total ozone column from OMI/AURA satellite, aerosol ptical depth from an AERONET sunphotometer and air mass from a well-known formula. The data used in this work are in the period of 2016-2018. The result shows that UVvitD obtained from the measurement and that calculated from the model are consistent with root mean square difference (RMSD) of 17.1% and mean bias difference (MBD) of −9.2%. In further work, this model will be generalized in order to apply for all regions in Thailand.

S1 Physics Innovation - Board: O-S1-35 / **55**

DEVELOPMENT OF NANOBUBBLES CARRIER IN DRUG DELIVERY SYSTEM OF MELATONIN ENCAPSULATED PARTICLE

Author: Prutchayawoot Thopan[1]

Co-authors: Vitsanusart Atyotha [1]; Likit Temprom [2]; Kiyoshi Yoshikawa [3]; Vishnu Thonglek [4]; Sriprajak Krongsuk [2]

[1] *Department of Applied Physics, Faculty of Engineering, Rajamangala University of Technology Isan Khon Kaen Campus*

[2] *Department of Physics, Faculty of Science, Khon Kaen University*

[3] *Institute of Atomic Energy, Kyoto University*

[4] *Faculty of Engineering, Rajamangala University of Technology Lanna Payap Campus*

Drug delivery system (DDS) has been extensively interested in scientific area such as medical science, environment, industry, agriculture and food processing. In this work, nanobubble (NB) was developed as carrier in the DDS and applied in the niosome particle. The DDS had been prepared by jointing of MNB technology, mechanical technique (ball milling) and niosome particle. Drug particle consists of NB (carrier), surfactant (span 60), additive (cholesterol) and drug (melatonin). Stability and viability of the drug particle system had been defined by size and zeta potential for a moth which measured every week (total 5 times in a month). The size and zeta potential had been measured by the dynamics light scattering (Malvern Zetasizer analyzer). Melatonin encapsulation was measured by the dialysis method. The particle sizes and zeta potential of the drug particle system are an average 300 nm and -30 mV, respectively. And melatonin encapsulations are about 60%. From results can be concluded that the conditions of surfactant at span60 : cholesterol molar ratio of 1.5 : 0.5 is a proper condition. And all conditions are stability for a month as the NB carrier in drug particle system.
Keyword: Drug delivery system, Nanobubble, Niosome, Melatonin

S1 Physics Innovation - Board: O-S1-17 / **44**

A mathematical study on the effects of fluid density on the impact cavity formation

Authors: Pattarapon Tanalikhit[1]; Sarith Chopara[2]; Siripon Sutthiwanna[3]

Co-author: Wittaya Kanchanapusakit [4]

[1] *Department of Physics, Korea Advanced Institute of Science and Technology*

[2] *Kamnoetvidya Science Academy (KVIS)*

[3] *Korea Advanced Institute of Science and Technology*

[4] *Department of Physics, King Mongkut's University of Technology Thonburi*

Corresponding Author: sarith_c@protonmail.com

A cavity formed from an impact of a ball on a fluid surface will begin to collapse into two volumes: one wrapping around the ball and another rising to the surface. The experiment measuring the volume of the rising cavity suggested that it is the same across different liquid densities. This research presents a mathematical model to explain the phenomenon and its correspondence with the experimental results under a certain condition. The method used in this research is a good practice for applying fluid mechanics to explain a real-life phenomenon.

S1 Physics Innovation - Board: O-S1-36 / **133**

Experimental and theoretical studies of spread factor of swine blood- and deionized water-drop on glass surface.

Author: Suparat Raweenroj[1]

Co-author: Paisarn Duangjak na ayudhya [1]

[1] *University of Phayao*

Corresponding Author: 61204430@up.ac.th

The spread factor of liquid-stains on glass surfaces, following both perpendicular and non-perpendicular impact velocity, had been studied with a view to understanding whether surface-specific properties affect the size and shape of the stain. According to the properties of swine blood, there is a ratio of the area of change when the blood strikes the surface to the area of the blood when it contracts to equilibrium. Therefore, this research aim to impact to 2 types of surfaces, namely clean glass surface and coated with commercial non-adhesive glass surface, resulting in significant size or shape of the blood droplets. When a drop of blood impacted on glass surface, it is found that the droplet radiates and adheres to the surface. As for the water proofed coating surface, it was found that at low heights, the droplets of blood radiated and retracted into equilibrium. As the height increased, Spatter stains were formed around the drop of blood. Therefore, the rate of rebound is 53-62% . This works has demonstrated some of fundamental systematic sources of the conventional formula for interpreting elliptical stains and established some of the basic theory on which to develop the interpretation casework stains on other surfaces, in the future.

S1 Physics Innovation - Board: O-S1-37 / **196**

The Python Programming Code on Cloud Computing Service for the Stellar Photometry Astrophysics Teaching

Author: Watcharawuth Krittinatham[1]

Co-authors: Kreetha Kaewkhong [2]; Narumon Emarat [3]

[1] *University of Phayao*

[2] *Faculty of Education, Chiang Mai University,*

[3] *Mahidol University*

Corresponding Author: watcharawuth.krittinatham@gmail.com

Nowadays, there is much software used for both education and astronomy research. For photometry, license software and high performance of computer's operating system are required, which are a fund limitation for some schools in Thailand. Thus, in this article, we develop and present the Demonstration Photometry Scripts for Astrophysics Teaching (DPSAT version 1.0). The program is designed to work on cloud computing services via internet browsers to avoid the hardware and operation requirement pain points. The DPSAT is programming on flexible, low-cost, on-trend language, Python, and Jupyter Notebook online editor. In advance, our new code supports the home-use image or video file format, i.e., jpg, png, or mp4. Thus it will be more accessible for teachers and students who do not have the standard astronomical instruments. The DPSAT measures the stellar light intensity from the time-series still-images or video files from a smartphone or another digital device. The code can extract video files into sequenced still images, then transform the RGB color space images into greyscale. The light intensity signal of selected pixels is counted with a simple aperture method in time series. It shows the results, for example, the mean signal, standard variation, measured signal as light intensity versus time, and image of light sources. This will be fruitful for low-cost and easily accessible for teaching astrophysics subjects.

S1 Physics Innovation - Board: O-S4-3 / **51**

A Modification of Newton's Cooling Law with Correlation to Fractional Derivative

Authors: Kumkup Keeratisiwakul[1]; Pat Vatiwutipong[1]; Supphanat Anantachaisophon[1]

[1] *Kamnoetvidya Science Academy*

Corresponding Author: supphanat_a@kvis.ac.th

Newton's cooling law provides a linear differential equation governing the rate of heat loss of a heated body using the temperature difference of the body with the environment. However, the prediction of Newton's cooling law still did not fit with the data under the laboratory framework. Previous works have modified Newton's cooling law by incorporating fractional derivatives as a basis of their models, and in particular cases of convective fluid, higher correlations with the experimental data can be observed. In this study, to model the empirical value obtained from the experiment, the conventional model is enhanced by appending a new parameter as the exponent of time in the differential equation. The comparison is shown between the conventional Newton's cooling law and the modified model, along with its adjusted R-Squared value from the regression of the experimental data, which results in a significant enhancement from the conventional model. In a numerical relationship between the two parameters, correlation of this newly proposed model is found with an established model of Newton's cooling law using Caputo type fractional derivative, thereby providing some support to the theoretical basis of the model. Moreover, the performance of this modified model is to a certain degree higher than the fractional derivative model.

S1 Physics Innovation - Board: O-S1-19 / **99**

Monte Carlo study of uncertainty propagation in Euler rotational kinematic equation

Author: Noparit Jinuntuya[1]

Co-authors: Chanasorn Nutsathaporn [1]; Sakchai Chomkokard [1]; Wiwat Wongkokua [1]; Somchoke Ruengittinun [1]

[1] *Kasetsart University*

Corresponding Author: chanasorn.nut@ku.th

We perform a Monte Carlo simulation to study the propagation of uncertainty in Euler rotational kinematic equation. The rate gyro data from an IMU sensor (mpu6050) are inserted into the Euler rotational kinematic differential equation to calculate the sensor orientation, which is specified by its Euler angles. The uncertainty of sensor orientation is determined by simulating the variation of rate gyro input due to its uncertainty obtained from the calibration process. We find that the uncertainties of the Euler angles grow with time. Their values are proportional to the square root of time elapse. We find also that the rate of change of uncertainties are linearly proportional to the sampling time and the square of uncertainties of rate gyro data. These results interestingly resemble the behavior of a Wiener process, with the step size of random walk depends on the time step. We can use these results as a criterion to choose a suitable IMU due to the characteristic of the integrated rate gyro sensor, especially in the application like the vehicle tracking or posture warning for elderly/disable people, where the precise sensor orientation is needed for a long period of operation.

S1 Physics Innovation - Board: O-S1-38 / **65**

The application of machine learning based on OpenCV for automatic digital dial gauge calibration

Author: Sirichanya Thamphet[1]

Co-authors: Noparit Jinuntuya [2]; Wiroj Sudatham [1]

[1] *National Institute of Metrology (Thailand)*

[2] *Kasetsart University*

Corresponding Author: sirichanyat@nimt.or.th

The traditional method of dial gauge calibration is time consuming and a measurement result is depending highly on human errors. To overcome this problem, an automatic measuring system based on machine vision has been proposed. This paper presents an application of machine learning based on Open CV for automatic digital dial gauge calibration. The k-Nearest Neighbors algorithm is applied for characters recognition of the dial gauge panel. The dial gauge tester developed in this study has a calibration and measurement capability (CMC) of approximately 0.0012mm. Even though the image of a dial gauge reading is slightly disturbed due to reflected light, the algorithm indicates efficient characters recognition of dial gauge reading. In this study, a calibration result from the developed method and traditional method were compared using a commercial digital dial gauge with a measuring range of 10 mm. The result shows good agreement with a comparable measurement uncertainty, approximately 0.008 mm. The automatic calibration system, however, has many great advantages over the traditional method as the algorithm can eliminate most human errors and also can reduce measurement time by 70%.

S1 Physics Innovation - Board: O-S1-20 / **101**

Coordinates transformation method for pointer gauge reading by machine vision

Author: Pitsamai Jinuntuya[1]

Co-authors: Noparit Jinuntuya [2]; Wiroj Sudatham [3]

[1] *Rangsit University*

[2] *Kasetsart University*

[3] *National Institute of Metrology Thailand*

Corresponding Author: fscinpr@ku.ac.th

In this report we present a machine vision algorithm for pointer gauge reading based on coordinates transformation. Since a pointer gauge is a polar representation of a linear scale, it is possible to transform its polar reading to the original linear counterpart. Once the picture of a pointer gauge is captured digitally, we can assign the polar positions to each pixel of the image. Those polar coordinates can be plotted on a rectangular frame to form a transformed image. The scale lines and the pointer are transformed to point vertically (or horizontally). Locations of the scale lines and pointer can be obtained from their pixel histograms maxima. An advantage of our algorithm is that we can avoid the complication of the conventional algorithm, e.g., Hough transformation, to find the orientation of pointer and scale lines. We have tested the algorithm with the ideal and real image of pointer gauges. In the latter case, even though there are some noises on the transformed image, the locations of pointer and scale lines can still be easily found from their histogram maxima. The other advantage of the algorithm is that, due to the polar structure of the gauge, the algorithm does not strongly depend on the orientation of the gauge with respect to the camera. We have tested the case where the camera is not pointed perfectly perpendicular to the gauge panel. Our algorithm still works quite well. Again, we can avoid the difficulty of the conventional algorithm that can strongly depend on the configuration of the camera and the pointer gauge.

S1 Physics Innovation - Board: O-S1-39 / **144**

An Approach to The Development of Raman Spectroscopy System for Field Usage

Author: Thiti Saeyee[None]

Co-authors: Surawut Wicharn ; Suwan Plaipichit ; Chokchai Puttharugsa ; Prathan Buranasiri

Corresponding Author: thiti.zeven@g.swu.ac.th

Raman spectroscopy is a spectroscopic technique that is used to analyze the chemical constituents or structure of molecules and can be applied to solid, liquid, and gas materials. This technique has been widely used in various fields such as analysis of medicine constituents in a pharmaceutical application, narcotic classification, examination of explosive substances for forensic medicine, and usage in quality control of semiconductor and microelectronics process industry. The Raman technique relies upon the inelastic scattering of photons, which is called Raman scattering. The Raman signal, which is either lower or higher energy than the incident photon due to inelastic scattering, is emitted when excited sample molecules at a virtual energy state transiting to the ground state in a short time.

Commercially, almost Raman spectrometers are constructed with many optical and electrical parts for fluorescence noise and background reduction and Raman signal enhancement. Consequently, almost commercial Raman spectrometer systems were neither compact nor carriable for field usage purposes. Therefore, in this study, we propose an approach to develop a compact Raman spectrometer that can be used in the field. Our system is only composed of necessary components such as a laser source, lens, and compact spectrometer. These components are designed to be set up in a compact area. Then, the raw Raman signal from a compact optical system with large noise and background signal is filtered by using a polynomial fitting-based Vancouver algorithm. The Vancouver algorithm is chosen because it is more accurate and faster than other methods in noise and background removal. According to the experiments, we found that our approach can give distinguish Raman peaks of the paracetamol sample, which is very close to the signal from the commercial system. Therefore, our designed system approach will be applied to make the Raman spectrometer for field usage in near future.

S1 Physics Innovation - Board: O-S1-21 / **146**

The moment of inertia of a Mahogany seed

Authors: Pattarapon Tanalikhit[1]; Bodin Worrasookwanich[2]; Nattanon Chaidet[3]; Kritsada Tadta[3]

Co-author: Wittaya Kanchanapusakit

[1] *Department of Physics, Korea Advanced Institute of Science and Technology*

[2] *126 Pracha Uthit Rd., Bang Mod, Thung Khru, Bangkok 10140, Thailand*

[3] *King Mongkut's University of Technology Thonburi*

Corresponding Authors: bodin.leng@gmail.com, nattanon0783@gmail.com, kritsadatadta@gmail.com

During the fall of a Mahogany seed, its wing-like structure is used to create rotational motion to propel itself further. The following research is concerned with the moment of inertia of the seed, which is the basis for analysing the rotational dynamics of the body. The formula used for calculating the moment of inertia was derived based on the approximated geometry of the seed. The inhomogeneity in mass distribution was also considered, and three experiment setups were performed to measure the moment of inertia. The results from these experiments are in an acceptable range of variations. However, the comparison between the formula and the results of the experiments suggests that the empirical factor of 2 must be introduced to the formula. The source of discrepancy is due to the resistance in the system. The obtained semi-empirical formula can be applied in the further study of the Mahogany seed's motion. Moreover, the techniques used in this research could be applied as good practice in high school and undergraduate physics laboratories.

S1 Physics Innovation - Board: O-S1-40 / **288**

DESIGN AND DEVELOPMENT OF THE TRIGGER SYSTEM FOR PROTON COMPUTED TOMOGRAPHY APPLICATIONS

Author: Passakorn Phumara[1]

Co-author: Chinorat Kobdaj [2]

[1] *Suranaree University of Technology (TH)*

[2] *Suranaree University of Technology*

Corresponding Authors: passakorn.phumara@cern.ch, kobdaj@g.sut.ac.th

Proton computed tomography (pCT) is a novel radiography technology that is used for treatment planning in proton therapy with better benefit of higher position accuracy than the conventional radiography. This work focused on the design and construction of a synchronizing system, the so-called the pCT trigger controller as a key communication part in the pCT prototype. This controller was designed using the MEGA2560 pro mini as a microcontroller unit (MCU). The MCU connected to the SAMKOON SK-070FE HMI touchscreen using Universal Asynchronous Receiver/Transmitter (UART) to create a graphical user interface (GUI) based on Modbus protocol via the C language program. The controller was tested at King Chulalongkorn Memorial Hospital (KCMH) on August 2021 and March 2022. It was found that the controller can send the programmed signals to control the rotational stage, ALPIDE sensors, and TSS interface box of the proton beam in a desired sequence. Where the ALPIDE sensor interfaced with EUDAQ2 software to record the hit map of protons on ALPIDE's active area.

S1 Physics Innovation - Board: O-S1-22 / **117**

Assessment of annual effective dose due to inhalation and ingestion of radon from groundwater at Kantharawichai District, Maha Sarakham Province

Author: Vitsanusat Atyotha[1]

Co-authors: Phachirarat Sola [2]; Apiwat Boonkhuang [1]; Junthara Somtua [3]

[1] *Rajamangala University of Technology Isan, Khon Kaen Campus*

[2] *Thailand Institute of Nuclear Technology (Public Organization)*

[3] *Regional Health Promotion Center 7, KhonKaen*

Corresponding Author: vitsanusat.at@rmuti.ac.th

Assessment of annual effective dose due to inhalation and ingestion of radon from 43 groundwater samples at Kantharawichai District, Maha Sarakham Province by using Radon Gas Monitor ATMOS 12 DPX. The results were as follows: 1. radon concentrations in groundwater were ranged from 1.04 – 21.87 Bq/L with the mean value of 8.27 Bq/L., 2. The annual effective dose due to inhalation from groundwater (Dinh) was ranged from 2.61 – 54.68 μSv/y with the mean value of 20.66 μSv/y. The annual effective dose due to ingestion from groundwater (Ding) was ranged from 0.19 – 3.94 μSv/y with the mean value of 1.49 μSv/y., 3. The annual effective dose on organs, namely the dose on lungs (Dinh-lung) was ranged from 6.26 – 131.24 μSv/y with the mean value of 49.59 μSv/y, and the dose on stomach (Ding-stomach) is 0.45 – 9.45 μSv. /y and has a mean of 3.57 μSv/y., and 4. The mean of excess lifetime cancer risk (ELCR x 10-4) in males was 0.88 and in females, it was 0.96. The results will be compared with the action levels of various organizations, including: The maximum allowable radon concentration in water is 11.1 Bq/L, according to United States Environmental Protection Agency, and The allowable annual effective dose due to inhalation and ingestion of radon from groundwater (D) is 100 μSv/y, according to the World Health Organization. The result of analysis by comparing the data of research with the action levels of various organizations can indicate the safety of inhalation and ingestion of groundwater radon in the research area.

S1 Physics Innovation - Board: O-S1-41 / **319**

An Application of Autocollimator for Surface Profile Measurement

Author: Surasak Kaewpho[1]

Co-authors: Chaturaporn Kerdkaew [1]; Korakot Samnasen [1]; Sakchai Chomkokard [1]; Theera Yaemglin ; Wiwat Wongkokua [1]; Noparit Jinuntuya [1]

[1] *Kasetsart University*

Corresponding Author: surasak.kaew@ku.th

The autocollimator is a non-contact angle measuring instrument using the geometric light reflection principle. The instrument can be used in scientific research and industrial applications with high resolution. In this work, we propose an application of the autocollimator for surface profile measurement. We use an autocollimator to directly measure the tangent profile of a surface. The results can be interpreted as the first partial derivative of the surface along 2 reference axes. The higher derivatives can then be calculated. For second-order bi-quadratic approximation, the second derivatives are used to estimate the bending and twisting of a local surface. We compare our results with that of the industrial, high-resolution interferogram. The results agree well with the RMSE ranging from 2 nm to 10 nm.

S1 Physics Innovation - Board: O-S1-23 / **251**

Experimental Study of Tap Water Activated by Commercial Fruit and Vegetable Purifier

Authors: Juthathip Suwanchatree[1]; Shaima Masae[2]; Somsak Dangtip[3]; Suebsak Suksaengpanomrung[3]; Wasin Nupangtha[4]

[1] *Faculty of Sciebce, Prince of Songkla, Hatyai, Songkla,*

[2] *Faculty of Science, Prince of Songkla University*

[3] *Thailand Institute of Nuclear Technology*

[4] *Thailand Institute of Nuclear Technology*

Corresponding Authors: somsakd@tint.or.th, wasinn@tint.or.th

Green and clean diets are on focus for consumers with healthy and safety concerns. Good source of safe and clean vegetables and fruits are vital. Vegetables and fruits are often found on market shelves in below standard of good agricultural practices. Pesticides and other chemical residues are found in those fruits and vegetables which may connect to many late complication issues in health. Various methods are utilized as common wisdom to fight the problem. Some methods are more practical and handier. This contribution has studied properties of tap water after activation by a commercial fruit and vegetable purifier. Chlorine, which is present in tap water, is bound with hydroxyl radical from electrohydrolysis by an apparatus to form hypochlorous acid. The activated water is found to peak at 291 nm in its absorbance with a UV-Vis spectrophotometer. Properties of water were studied under various experimental settings such as comparing with activation of de-ionized water, as a function of (i) operating time, (ii) storing time of input tap-water, (iii) storage time of activated water and (iv) water volume. Concentration of hypochlorous acid is calibrated against commercial ready-to-use acid.

S1 Physics Innovation - Board: O-S1-43 / **323**

A Design of Laser Triangulation System with Combined Diffuse and Specular Reflection Modes for Dull and Shiny Surface Measurements

Author: Chaturaporn Kerdkaew[1]

Co-authors: Surasak Kaewpho [1]; Areeya Srisakron [1]; Sakchai Chomkokard [1]; Theera Yaemglin ; Noparit Jinuntuya [1]; Wiwat Wongkokua [1]

[1] *Kasetsart University*

Corresponding Author: chaturaporn.ko@ku.th

Conventional laser triangulations are designed to measure the depth or height on a dull or rough surface. This can be done by projecting a light perpendicularly to the surface and capturing the spot of the diffuse reflection which is scattered from the surface. However, for a shiny or smooth surface, the specular reflection dominates, and it is difficult to detect diffuse reflection. We may modify the system setting to capture the specular reflection, with the cost of losing the diffuse reflection information. In this article, we proposed a design of dual diffuse and specular reflection mode of laser triangulation. The advantage is that there is no need to repeat alignment and calibration processes when we change the measuring mode, so we can easily select the measuring mode that is suitable for each surface. We have described the system setting, the calibration results, and the uncertainty evaluations for the laboratory-scale experimental demonstration, where we can achieve the resolution of micrometer for both measuring modes.

S1 Physics Innovation - Board: O-S1-24 / **257**

The study of ring surface water wave generated by impacting droplets of using Free surface synthetic schlieren (FS-SS) technique.

Authors: Pakorn srirathat[None]; Phongthep Chansamphan[None]; Nirut Pussadee[None]

Co-author: Watcharapath Khaiophueng

Corresponding Authors: pakornsrirathat01@gmail.com, pongtep_boy@hotmail.com, nrtpssd@gmail.com

The surface water wave can be easily seen in everyday life. Extracting crucial wave characteristics is however challenging since the wave propagation phenomena occurs so rapidly to measure its characters. Free surface synthetic schlieren (FS-SS) offers a great visualization technique of surface water disturbance using invert gradient algorithm of background patterns. In this study, a ring surface water wave generated by falling water droplet was investigated using MATLAB PIVlab and PIVmat toolboxes to reconstruct 3D surface of the ring wave. Wave properties including wave packet profile and phase speed were readily extracted from the technique. The wave pattern could salon be further used in determining surface tension and wave damping coefficient.

S1 Physics Innovation - Board: O-S1-43 / **347**

Online Monitoring and Control of 3D Printer with Open Source Software and Embedded Systems

Authors: PIYACHON KETSUWAN[1]; SIRIKAMON SAENGMEE-ANUPHARB[1]

[1] *University of Phayao*

Corresponding Author: piyachon.ke@up.ac.th

OctoPrint is a powerful open source 3D printer software what user can control and monitor printing jobs with its own online server that suitable for remote and isolated work. The Raspberry pi 3 B+ is hardware for installing Octopi that including Raspbian operating system and OctoPrint software. An USB webcam was connected for live viewing of printing processes and the ESP32 microcontroller with filament runout sensor was communicated to Raspberry pi 3 B+ for notify user when filament was runout or back to work resume through LINE mobile application. The Google Calendar and LINE mobile application were used for jobs booking of multiple users that will notify before and after finish printing for each user. The Power relay circuit was used for shut down the Raspberry pi 3 B+ when complete printing to save energy and electricity.

S1 Physics Innovation - Board: O-S1-25 / **148**

A study on optics: Invisibility properties of a lenticular lens

Authors: Bangon Prasutham[None]; Pattarapon Tanalikhit[1]; Tusmee Hayeebeelung[None]; Thanabodi Worakitthamrong[2]

Co-author: Wittaya Kanchanapusakit

[1] *Department of Physics, Korea Advanced Institute of Science and Technology*

[2] *King Mongkut's University of Technology Thonburi*

Corresponding Authors: bangon.prasutham@gmail.com, tusmee.mie@gmail.com, thanabodi.tan@gmail.com

An invisible cloak is an appliance that is frequently mentioned in many pieces of non-scientific literature as an attention-grabbing component. It can cause any desired object to disappear while the observer will still see its surroundings, i.e., the object under its effect becomes translucent. A similar effect can be demonstrated in laboratories by using optical instruments such as a lenticular lens. The mechanism in which the lenticular lens uses to hide the object was theoretically and experimentally investigated in this research through the knowledge of geometrical optics, especially the ray-tracing analysis. A discussion on the aspects of wave optics was also conducted to obtain a comprehensive understanding of the phenomenon. To verify the theory, a computational simulation was created based on the proposed theory. The simulation result was compared with results from the experiment under various conditions such as the distance from the object to the lenticular lens. The method used in this study can be applied in the classroom to enhance students' understanding of the geometrical optics and wave phenomenon.

S1 Physics Innovation - Board: O-S1-44 / **332**

Comparison of an Auto-Regressive with Exogenous Variable (ARX) Model to that of the Artificial Neural Network (ANN) in Simulating a Solar Vapour Compression Refrigeration System

Author: Sattra Sirikaew[1]

Co-authors: Serm Janjai [2]; Somjet Pattarapanitchai [2]

[1] *Department of physics, Faculty of Science, Silpakorn University*

[2] *Department of Physics, Faculty of Science, Silpakorn University*

Modelling is a power tool in a development of an engineering system. In this study, a solar vapour compression refrigeration system was modelled by two machine learning approaches, namely ARX and ANN and the performance of these two approaches were compared. The solar refrigeration system is composed mainly of a vapour compression unit, two 300W-solar modules, two 12V-batteries with the capacity of 200 Ah (each) and a charge controller. Ten experiments were carried out. Water contained in a bottle was used as cooling loads. The load of 10, 20, 30, 40, 50, 60, 70, 80, 90 and 100 liters were employed in the experiments. Data obtained from the experiments with the loads of 10, 30, 50, 70 and 100 liters of water were used to construct the model and experiments with the loads of 20, 40, 60, 80 and 90 liters of water were employed to test the performance of the model. The difference of the load temperature from the experiments and those predicted by the models, in terms of the percentage of root mean square difference relative to a mean measured values (RMSD) was used as an indicator of the performance of the models. It was found that the RMSD of ARX model and ANN model were 4.3% and 5.4%, respectively. We conclude that ARX approach performs batter than ANN approach for this system.

S1 Physics Innovation - Board: O-S1-27 / **62**

The effects of hair-cell polarity on the dynamics of two coupled hair-cell bundles of the inner ear

Author: Tanawat Ngampattrapan[1]

Co-author: Yuttana Roongthumskul [1]

[1] *Chulalongkorn University*

Corresponding Author: tanawatngampattrapan@gmail.com

Hair cells are the sensory receptors of the auditory and vestibular systems. A bundle of cilia situated atop each hair cell, termed the hair-cell bundle, is deflected upon an impinging of a mechanical force. This subsequently modulates the open probability of mechanically gated ion channels. Owing to the asymmetry in the geometry of the hair-cell bundle, individual hair cells are polarized and display the maximal response to a force applied in a certain direction. The auditory organs of most vertebrates comprise primarily hair cells with identical polarity, whereas hair cells of the vestibular system are organized in two opposite polarities. To understand the advantages of the bi-polarity arrangement of hair cells, we employ the theoretical framework of active nonlinear oscillators to investigate the dynamics of a system of two coupled hair-cell bundles with opposite polarity. Each hair-cell bundle is described by a nonlinear oscillator poised near a supercritical or subcritical Hopf bifurcation. Our results from numerical simulations reveal that a system of coupled hair-cell bundles with opposite polarity can undergo a limit-cycle oscillation, but with a significantly altered value of the critical control parameter. Predictions from the model further demonstrate that reversing the polarity of a hair-cell bundle can enhance the response of the system to a bi-directional constant force, as well as a periodic force, with respect to the displacement of a system of two identical hair-cell bundles.

S1 Physics Innovation - Board: O-S1-45 / **271**

Investigation of plasma activated water in the growth of green microalgae (Chlorella spp.)

Authors: Chokchai Yatongchai[1]; Prangnapat Silapasert[1]; Sureeporn Sarapirom[1]

[1] *Maejo university*

Corresponding Author: prangnapat.silapasert@gmail.com

The reactive oxygen nitrogen species (RONS) from plasma activation is intensively used in agriculture, particularly in the regulation of seeds germination and plants growth. It shows a promising effect on increasing the germination rate and promoting the growth of plants. This research employs plasma activated water (PAW) in cultivation of green algae (*Chlorella spp.*). The objective of this research was to introduce a comparison between the use of different fluids for cultivation of green microalgae. The used fluids were fertilized water, simulated-fertilized water, tap water, tap water treated with activated plasma for 2.5, 5.0 and 7.5 minutes. Samples of green microalgae were cultivated in these waters for 7 days. A comparative investigation was conducted and reported. It was found that concentration of the reactive oxygen nitrogen species increased with the treatment time. According to the growth of green algae, the plasma activated water provided a better result than any other until day 2. This indicates an effect of RONS on promoting the growth of green algae. Upon completion of the test, the fertilized water showed the highest growth. This finding could be distributed to a rapid reduction of the reactive oxygen nitrogen species. However, a well-controlled plasma activation would make PAW possible for industrial uses in the future.

Keywords: plasma activated water (PAW), green microalgae, *Chlorella spp.*, growth rate and plasma arc discharge.

S1 Physics Innovation - Board: O-S1-27 / **258**

Modeling the navigation of a weaver ant in a simple, unfamiliar environment

Authors: Lattawat Charoonratana[1]; Michael Smith[1]; Sukrit Suksombat[1]; Theerawee Thiwatwaranikul[1]; Panyaphong Paisanpan[1]

[1] *Suranaree University of Technology*

Corresponding Author: lat.poom@gmail.com

The ant species Oecophylla smaragdina, commonly known as the weaver ant, is native to tropical Asia and Africa. Ants are known for highly-organized, co-operative behavior and weaver ants are particularly adept at working together, in numbers, to accomplish large-scale tasks. Considered an example of a coherent many-body system, weaver ants have been studied by researchers in various fields. As a first step towards understanding weaver ant coordinated motion, we want to find the algorithm that a single ant employs for its own navigation. Having previously tracked the motion of individual ants within a small, bounded arena, we here present a simple theoretical model that can describe this motion. We show that their navigation can be adequately modeled as Brownian motion: the ant velocity changes by random impulses drawn independently from a robust probability distribution. Using establish Brownian motion theory, we show that the ant's tendency to remain near boundaries can be explained as a result of pure chance: having been stopped at the boundary, random motion is unlikely to bring the ant back to the arena interior. All qualitative aspects of ant motion are captured by a model with few parameters and without any assumption that an ant has preferences for position or velocity.

S1 Physics Innovation - Board: O-S1-46 / **272**

Utilization of DBD plasma in shelf-life extension for climacteric fruits

Authors: Chokchai Yatongchai[1]; Konkanok Udtachee[2]; Sureeporn Sarapirom[1]

[1] *Maejo University*

[2] *Maejo University*

Corresponding Author: konkanok.benzz@gmail.com

Tomato, mango, banana and durian are climacteric fruits characterized as having high respiration rate during the ripening. Generation of ethylene is actively involved in metabolic activities leading to the ripening. Inhibition of the ethylene generation is therefore able to delay the ripening. Typically, the ethylene generation is dependent on temperature, oxygen level and fruit injury which includes mechanical damage, diseases, and insect infestation. These factors stimulate the generation of ethylene. To overcome this issue, low CO2, low temperature and the use of ethylene absorbent are conventionally required. However, in the current work, a technique using dielectric barrier discharge (DBD) plasma was proposed. DBD plasma could not only eliminate ethylene but also moisture in the package in a short period. In this work, a comparative study was done on storing cultivated banana, papaya and mango in different ways of storage: non packed, packed in a paper box, packed in a paper box treated with 5-minute plasma, packed in a paper box sealed with plastic wrap, packed in a paper box sealed with plastic wrap and treated with 5-minute plasma and packed in a paper box sealed with plastic wrap and treated with 10-minute plasma. It was found that the cultivated banana samples ripened in sequence, when packed in (1) the paper box sealed with plastic wrap, (2) the paper box, (3) non-packed, (4) the 5-minute plasma box, (5) the paper box sealed with plastic wrap and treated with 5-minute plasma (6) the paper box sealed with plastic wrap and treated with 10-minute plasma. This suggests that C2H4 was successfully removed by a DBD plasma reactor.

S1 Physics Innovation - Board: O-S1-28 / **239**

Networks structure and entropy of stocks in the Stock Exchange of Thailand (SET)

Author: Nawee Jaroonchokanan[None]

Co-authors: Teerasit Termsaithong [1]; Sujin Suwanna [2]

[1] *Learning Institute, King Mongkut's University of Technology Thonburi, Bangkok, Thailandl*

[2] *Department of Physics, Faculty of Science, Mahidol University, 10400 Bangkok, Thailand*

Corresponding Author: nawee.jao@student.mahidol.ac.th

In this article, we investigate the network structure of stocks in the Thai stock market from 2008 to 2020, applying the correlation distance as weights and the average of correlations as a criterion for deciding whether two stocks are connected. We can access and filter strongly correlated and weakly correlated stocks in a financial network using different average correlation thresholds ($\mu-5\sigma$, $\mu-3\sigma$, μ, $\mu+3\sigma$, $\mu+5\sigma$). The results indicate that during high volatility situations, such as the global financial crisis in 2008 and the COVID pandemic in early 2020, the network's characteristic path length decreases, whereas the clustering coefficient increases. These findings suggest that the network structure has shrunk in size, and stocks are now tightly linked, resulting in a similar trend of price and return behaviors observed in many stocks during financial crises. Also, the minimal level of network entropy implies that the complexity decreases, and each node of the network has lost its ability to perform independently across stock sectors. Furthermore, we discover that the banking and utility sectors have the highest probability of being a hub of the network clusters. This research can contribute to the explanation of stock clustering in terms of entropy and network topology.

Keywords: stock network measurement, network entropy, financial market, econophysics

S1 Physics Innovation - Board: O-S1-47 / **371**

The study of spin effects on the bouncing trajectory of a ball

Authors: Ai Tungsatitchai [1]; Ratchaphon Noiaek[1]

[1] *Kamnoetvidya Science Academy, Wang Chan Valley, Rayong 21210, Thailand*

Corresponding Author: ai.tungsatitchai@gmail.com

In all sports involving a ball, spin is heavily utilized to alter the ball's course. A spinning ball has more kinetic energy of the same ball traveling with the same translational velocity. The additional energy comes from the rotation of the ball. This extra hidden energy can affect the trajectory of the ball as the ball interact with the floor or even with the air. Dimples are placed on the golf balls to increase the friction with the air making the spin effects on the trajectory more pronounced. Good pitchers can curve the trajectory of a baseball by throwing the ball with a lot of spin. In this work, we use simple tools to study of how spin affect the bouncing trajectory of a ball. The height of the ball when thrown with different spins, such as back spin, top spin, and no spin, will be investigated in this experiment. The heights of the bouncing balls were collected using a high-speed phone camera and evaluated with a video analysis software. The height ratio of basketball with spin-launching is higher than without. The height ratio of back spin launches is higher than that of top spin launches. The bouncing angle will affect back spin, whereas the angular velocity will affect top spin. By launching the basketball with spin, the height ratio of the bouncing ball can be enhanced. The changes in the bouncing angles and trajectories due to spin will also be discussed. We believe that a simple setup used in this experimental study can be applied to study the behaviors of many other movement of objects.

S1 Physics Innovation - Board: O-S1-47 / **53**

Fabrication of Radiative Cooling Matrix through Low-Cost Scalable Method and High Adaptability

Author: Pongporn Wintakorn[None]

Corresponding Author: pongporn.wit@student.mahidol.edu

Radiative cooling is a passive cooling process that requires no additional input of energy which can be used as a cooling process in various fields. Though many radiative cooling materials have been conducted to improve efficiency in temperature reduction during the past few years, the scalability and the applicability are equally important. With high efficiency and low scalability, applications of the radiative cooling film would be severely limited. In this research, doctor blade coating technique was explored as a high scalability process, and the resulting thickness of the obtained film remained within the desirable range of 11-13 um, which correspond to the atmospheric window. The field experiment performed on the rooftop confirmed that the doctor blade-film can reduce the temperature by 3-4 ℃ below the ambient, comparable to the performance of the commercial radiative cooling film and the lab-based spin coating film. Moreover, by forming the patterns with the sizes between 8-13 um on the film, additional resonance in the atmospheric window range could be induced, enhancing radiative cooling efficiency.

S1 Physics Innovation - Board: O-S1-48 / **291**

A model for estimating global spectral solar radiation under all-sky conditions for Nakhon Pathom station Thailand

Author: Sunisa Khakhu[1]

Co-authors: Itsara Masiri [1]; Rungrat Wattan [1]; Serm Janjai [1]

[1] *Department of Physics, Faculty of Science, Silpakorn University, Nakhon Pathom 73000, Thailand*

Corresponding Author: khakhu_s@silpakorn.edu

Global spectral solar irradiance is of importance for various solar energy applications such as photovoltaic systems and selective surfaces of flat plate solar collectors. In this study, a model for estimating global spectral solar irradiance under all-sky conditions for Nakhon Pathom station (13.82°N, 100.04°E) Thailand was developed. The model expresses the global spectral solar irradiance under all-sky conditions as a multiplication of two functions. The first function is a global spectral solar irradiance under clear sky condition and the second function is an expression of a cloud modification factor. This factor is a function of satellite-derived cloud index. To obtain the first and the second functions, global spectral solar irradiance was measured at Nakhon Pathom station in Thailand for the year 2017-2019 using a spectroradiometer (EKO, model MS-710). Ancillary data such as aerosol optical depth and precipitable water were obtained from an AERONET sunphotometer installed at the same station. The validation of the model was carried out using an independent data set from the same station for the year 2020. It was found that the global spectral solar irradiance from the measurement and that calculated from the model were in reasonable agreement, with the discrepancy in terms of root mean square difference (RMSD) and mean bias difference (MBD) of 12.39% and -0.64%, respectively.

S1 Physics Innovation - Board: O-S1-49 / **138**

Hydrogen sulfide (H2S) detection system in risky areas with real-time display via smartphone

Authors: Wiphu Kitsamret[None]; Thanyathon Tueanwiradet[None]; Titat Uttawat[None]

Corresponding Authors: wiphu.kit_g30@mwit.ac.th, thanyathon.tue_g30@mwit.ac.th, titat.utt_g30@mwit.ac.th

In the past few years, there were accidents that caused people to die from hydrogen sulfide gas. This is due to the lack of warning system and appropriate measuring equipment. General commercial hydrogen sulfide detectors are not suitable to use in the risk area as users have to take them into the area which could be dangerous if the gas concentration exceeds the limit. Therefore, the purpose of this research was to develop an innovation that can remotely detect hydrogen sulfide concentration, display detected results to the users via smartphones. It also alerts when the concentration is in hazards level. This innovation was designed to be compact and easy to use. It applies a microcontroller (Arduino) combine with a MQ-136 gas sensor to measure hydrogen sulfide concentration. Measured results are real-time analyzed to determine the hazards of the gas and user recommendations. All measured and analyzed results are displayed both onsite and online. An OLED display is used to show the results for onsite. A buzzer is also used to warn the users when the gas concentration is at a dangerous level. For online display, the users can remotely monitor all results via their mobile devices (smartphones or tablets). Thingspeak.com was used as platform to collect results. A mobile application was created using MIT App inverter to retrieve the results and display them on mobile devices. The innovation prototype was tested to measure hydrogen sulfide gas in the range of 0-200 ppm. The operation of the prototype is in accordance with all requirements. These results show that the prototype can be used for real-time remote hydrogen sulfide measurement.

Keywords: Hydrogen sulfide detection, microcontroller and sensor, remote measurement

S1 Physics Innovation / 379

Experiment and simulation of heat treatment for disinfection in the chicken farm using IR and UV irradiation

Authors: Jutarat Kaewthong[None]; Wuttipan Satienpaisan[None]; Kullapat Krabuansang[None]; Achira Sujarit[None]; Papichaya Chaisakul[None]; Nattaporn Chattham[1]; Surasak Chiangga[2]; Sompid Samipak[3]

[1] *Kasetsart University*

[2] *Department of Physics, Kasetsart University*

[3] *Department of Genetics, Faculty of Science, Kasetsart University*

Corresponding Author: wuttipan.s@ku.th

For chicken industry, hens are raised in large farmhouses which usually difficult to control for complete sanitation. It is very likely that contamination of chicken meat and eggs could occur. This research project aims to improve farmhouse floor disinfection and eggshell sanitization using UV and IR irradiation in aspects of time-saving, accuracy and environmental friendly.

Rice husks are widely used for flooring in chicken farm. Proper and reliable sanitization of the rice husk before their employment in the chicken farm is critical as one infection may cause result in a loss of an entire chicken batch in the farm. At present, most sanitization techniques are based on the use of sunlight or chemical product such as Formalin which may be subjected to human error or has detrimental effect toward to human health and environment. This project aims to develop and test a proof-of-concept prototype of rice husk disinfection apparatus by infrared irradiation for chicken farm flooring together with performing finite element analysis using Comsol Multiphysics to simulate heat transfer of IR radiation to rice husk. To identify the level of bacteria on rice husks experimentally after infrared irradiation, total aerobic plate count was investigated in order to identify the temperature and time duration required for efficient disinfection.

Another investigation to disinfect the chicken farm is replacing sanitization of eggshells by formaldehyde fumigation with UV disinfection instead. Treatment of UV light together with ozone and hydrogen peroxide is implemented for eggshell decontamination. A prototype UV irradiation system was built with special function that can rotate egg in all direction for complete sanitization of eggshell. The equipment was tested to treat eggshell coated with Salmonella sp. bacteria. Finite element analysis of UV penetration into eggshell was simulated using Comsol Multiphysics. The experimental result showed that egg sanitization using UV treatment together with ozone incubation give significant decrease of bacteria population. By adding hydrogen peroxide exposure to the process, the complete bacteria decontamination was achieved.

This work was supported by Kasetsart University Research and Development Institute (KURDI).

S2 Condensed Matter Physics - Board: INV-S2-1 / **357**

Alkali titanates as a bride for solid state chemistry and soft matter

Author: Tosapol Maluangnont[None]

Corresponding Author: tosapol.ma@kmitl.ac.th

Alkali titanates including the Andesson-Wadsley type $A_2O{\cdot}nTiO_2$ (A = alkali) and the lepidocrocite-type $A_xM_yTi_{2-y}O_4$ are diverse in crystal structure, composition, and microstructure including microcrystals or nanotubes. They are composed of tunnels or sheets of corrugated, double edge-shared $(Ti,M)O_6$ with varying lengths of such motifs, depending on the alkali-to-Ti ratio. The tunnel or the interlayer space allow many interesting physical properties such as ion/proton conduction, positive temperature coefficient of resistivity (PTCR) effect, etc. They also exhibit rich chemistry including intercalation, proton exchange, exfoliation, and reassembling, which are absent in denser alkaline titanate such as the $BaTiO_3$ perovskite. The nanosheets derived from layered alkali titanates display interesting dielectric properties with potential applications as pressure sensors and triboelectric nanogenerators (TENG). These materials therefore serve as a bridge for solid state chemistry and soft matter which is to be presented here.

S2 Condensed Matter Physics - Board: O-S2-1 / **308**

External pressure effects on superfluid density of isotropic s-wave superconductors

Author: Grittichon Chanilkul[None]

Co-authors: Arpapong Changjan [1]; Pongkaew Udomsamuthirun [2]; Tunyanop Nilkamjon [3]

[1] *Pathumwan Institute of Technology*

[2] *Srinakharinwirot University*

[3] *Prasarnmit Physics Research Unit, Department of Physics, Faculty of Science, Srinakharinwirot University*

Corresponding Author: gchanilkul@gmail.com

We investigated the effects of external pressure on the superfluid density of s-wave isotropic superconductors by the BCS theory and semi-classical approach. The analytic results obtained the equation of superfluid density with pressure variables involved were derived. After that, the derived equations were numerically calculated in used to predict the experimental results in the superfluid density of hydrogen sulfide(H3S) and Lanthanum decahydride(LaH10) superconductors. We found that when temperature rises, the superfluid density drops however, the superfluid density is highest near zero temperature.

S2 Condensed Matter Physics - Board: O-S2-2 / **198**

The temperature dependent surface critical magnetic field (Hc_3) of $K_{0.73}Fe_{1.68}Se_2$ superconductor by semi-anisotropic two band Ginzburg-Landau approach

Author: Suppanyou Meakniti[1]

Co-authors: Arpapong Changjan [2]; Pongkaew Udomsamuthirun [1]

[1] *Srinakharinwirot University*

[2] *Pathumwan Institute of Technology*

Corresponding Author: suppanyou.fern@gmail.com

In this study, we used a two-band Ginzburg-Landau technique to investigate the surface critical magnetic field (Hc3) of magnetic superconductors, with the first band being anisotropic superconductors and the second band being isotropic superconductors. Following the calculation of the 1st Ginzburg-Landau equation, a surface critical magnetic field and its temperature dependent surface critical magnetic field were solved analytically using the variation method. Based on Changjan and Udomsamuthirun's temperature dependency model, we discovered that fits best with experimental data of K0.73Fe1.68Se2 superconductors, vicinity of the critical temperature.

S2 Condensed Matter Physics - Board: O-S2-3 / **280**

Effect of annealing temperature on the structure and hardness of DC reactive magnetron sputtered CrAlN thin films

Authors: Nirun Witit-anun[1]; Adisorn Buranawong[1]

[1] *Burapha University*

Corresponding Authors: nirun.w65@buu.ac.th, adisornb@buu.ac.th

The chromium aluminium nitride (CrAlN) thin films were deposited on Si by using reactive DC unbalanced magnetron sputtering method from alloy target and then annealed in air at different temperatures for 1 hr. The effect of annealing temperature on the structure, chemical composition, morphology, and hardness of the films was characterized by XRD, EDS, FE-SEM, and Nanoindentation, respectively. The as-deposited thin films were solid solutions of (Cr,Al)N with (111), (200), and (220) planes. The film composes of chromium, aluminium, and nitrogen in different ratios, with slight oxygen. The lattice constant was in the range of 4.104 – 4.145 Å. The average crystal size was increased from 17.2 to 22.4 nm with an increase in annealing temperature. The result from the FE-SEM technique was revealed that the as-deposited films annealed at the low temperature showed the dense morphology, and turned to be the compact columnar structure at the high temperature of more than 700 OC. However, when the annealing temperature was increased up to 900 OC, a slight increase in oxygen content in the films. The film's hardness decreased from 67.3 GPa to 50.1 GPa with increasing the annealing temperature. In addition, the crystal structure or the oxides layer were not observed, showed that alloyed aluminium in the film can improve the oxidation resistance up to 900 OC.

S2 Condensed Matter Physics - Board: O-S2-4 / **41**

1-over-f noise characterization of random-network single-walled carbon nanotube photodetectors

Author: Yodchay Jompol[None]

Corresponding Author: yodchay.jom@mahidol.ac.th

The electronic properties of random networks of single-walled carbon nanotubes (SWCNTs) are probed by 1/f noise characteristics in a frequency range of up to 109 kHz as a function of bias voltages and the number of nanotubes deposited between asymmetrical-work function metal electrodes. The measured current-voltage characteristics of the devices exhibit rectifying and ohmic behaviour revealing Fermi-level depinning and pinning of the metal and one-dimensional contacts, respectively. The noise amplitude (A) characterizing the 1/f noise levels and the power-law exponents (β) of the devices are investigated in both reverse- and forward-bias voltages for different nanotube depositions at ambient temperature. In a few nanotube depositions, A is found relatively small (10^-5 to 10^-7) and the extracted β is exceeded 2 in the reverse bias, suggesting that charge-carrier trapping by the formation of the Schottky barrier is exhibited at the metal-nanotube contacts. Furthermore, as the number of nanotubes increases the device-channel resistance drops rapidly as the densely-packed inter-tube junctions are formed between the two electrodes. The observed A is found 1.5 times higher than that obtained in the devices with fewer nanotube depositions. This result shows that the 1/f noise of the SWCNT devices is dominated by the device resistance due to the inter-tube junctions under a finite bias. Our experimental observation agrees well with that of the previous works using carbon nanotube films for implementing hybrid-silicon Schottky barrier photodetectors.

S2 Condensed Matter Physics - Board: O-S2-5 / **35**

Investigation of the high-field transport, Joule-heating-driven conductivity improvement and low-field resistivity behaviour in lightly-reduced free-standing graphene oxide papers

Authors: Krongtham Thamkrongart[1]; Harihara Ramamoorthy[1]; Kanokwan Buapan[1]; Tinna Chiawchan[1]; Ratchanok Somphonsane[1]

[1] *King Mongkut's Institute of Technology Ladkrabang*

Corresponding Author: harihara.ra@kmitl.ac.th

Free-standing reduced graphene oxide (rGO) has been gaining popularity for its use in supercapacitors and battery applications due its facile synthesis, multi-layered structure, and high-current carrying capacity. Pertinent to the successful implementation of such applications, however, is the need to develop a thorough understanding of the electrical properties of such materials when subject to high applied electric fields. In this work, we undertake a detailed study of high-field electrical properties of mm-scale, lightly-reduced, rGO papers. Our results reveal that the I–V curves exhibit substantial nonlinearity with associated hysteresis that depends strongly on the applied electric field. The nonlinear behaviour which was interpreted using conventional transport models of Fowler–Nordheim tunneling and space charge limited conduction revealed that while these models provided good qualitative fits to our data, they were quantitatively lacking, thus leaving the issue of high-field transport mechanisms in rGO open for debate. Careful I–V cycling experiments with measurement time-delay introduced between cycles revealed that the observed hysteresis contained recoverable and non-recoverable parts that we identified as arising from charge trapping and Joule heating effects, respectively. Time-dependent measurements showed that these effects were characterized by two distinct time scales. Importantly, the Joule heating was found to cause a permanent conductivity improvement in the rGO via the 'current annealing' effect by effectively eliminating oxygenated groups from the rGO. The analysis of the electrical breakdown in our samples resembled a thermal runaway-like event that resulted in premature damage to the rGO. Finally, we investigated the low-field resistivity in the 80 K–300 K temperature range. The reduced activation energy analysis revealed a robust power law behaviour below 230 K, while deviating from this trend at higher temperatures. For samples that received current annealing treatment, a reduced value for the power law exponent was obtained, confirming the effective lowering of disordered regions.

S2 Condensed Matter Physics - Board: O-S2-6 / **34**

Remote Mesoscopic Signatures of Induced Magnetic Texture in Graphene

Authors: Nargees Arabchigavkani[1]; Ratchanok Somphonsane[2]; Harihara Ramamoorthy[3]; Guanchen He[4]; Jubin Nathawat[None]; S Yin[None]; B Barut[4]; K He[None]; M. D. Randle[4]; R Dixit[4]; K. Sakanashi[None]; N. Aoki[None]; K. Zhang[None]; L. Wang[None]; W.-N. Mei[None]; P. A. Dowben[None]; J. Fransson[None]; J. P. Bird[4]

[1] *University at Buffalo, State University of New York*

[2] *King Mongkut' s Institute of technology Ladkrabang*

[3] *King Mongkut's Institute of Technology Ladkrabang*

[4] *University at Buffalo, State University of New York at Buffalo*

Corresponding Author: ratchanok.so@kmitl.ac.th

Mesoscopic conductance fluctuations are a ubiquitous signature of phase-coherent transport in small conductors, exhibiting universal character independent of system details. In this work, however, we demonstrate a pronounced breakdown of this universality, due to the interplay of local and remote phenomena in transport. Our experiments are performed in a graphene-based interaction-detection geometry, in which an artificial magnetic texture is induced in the graphene layer by covering a portion of it with a micromagnet. When probing conduction at some distance from this region, the strong influence of remote factors is manifested through the appearance of giant conductance fluctuations, with amplitude much larger than (e^2)/h. This violation of one of the fundamental tenets of mesoscopic physics dramatically demonstrates how local considerations can be overwhelmed by remote signatures in phase-coherent conductors.

S2 Condensed Matter Physics - Board: O-S2-7 / **343**

Electrospun carbon nanofibers decorated by TiO2 hollow nanospheres for high-performance flexible supercapacitor electrode

Author: Suchunya Wongprasod[1]

Co-authors: Nantawat Tanapongpisit [2]; Nguyễn Huyền [3]; Hoàng Quý Văn [3]; Sangmo Kim [3]; Peerawat Laohana [2]; Santi Maensiri [2]; Worawat Meevasana [2]; Chung Wung Bark [4]; Wittawat Saenrang [2]

[1] *Suranaree University of Technology*

[2] *School of Physics, Institute of Science, Suranaree University of Technology*

[3] *Department of Intelligent Mechatronics Engineering and Convergence Engineering for Intelligent Drone, Sejong University*

[4] *Department of Electrical Engineering, Gachon University*

Corresponding Author: namtipnaya@gmail.com

Nowadays, clean and sustainable energy with flexible energy storage devices has gained more attention. Therefore, among various energy storage systems, flexible supercapacitors (SCs) are standing out due to their high capacity, high power density, high flexibility, and long cyclic lifetime. In this work, the electrochemical performances of carbon nanofibers decorated by TiO2 hollow nanospheres (hTiO2-CNFs) supercapacitor electrodes are studied. The hCNF-TiO2 were synthesized using an electrospinning method followed by heat treatment. The inner structure, morphology, crystal structures, distribution of elements, and specific surface areas of the samples were characterized by Transmission Electron Microscopy (TEM) and Field Emission Scanning Electron Microscope (FE-SEM), X-Ray Diffraction (XRD), Energy-dispersive X-ray spectroscope (EDS), and Nitrogen adsorption/desorption isotherms (BET), respectively. In addition, the electrochemical properties were studied by using Cyclic Voltammetry (CV), Galvanostatic Charge-Discharge (GCD), and Electrochemical Impedance Spectroscopy (EIS). It was found that the specific capacitance of the bare-CNF electrode (170.03 F g-1 at a current density of 0.5 A g-1) was improved after being embedded with 5 wt% TiO2 hollow nanospheres (185.70 F g-1). Furthermore, the hCNF-TiO2 exhibits high cycling stability, retaining 98% after 2000 cycles. This shows that TiO2 hollow nanospheres can help enhance the efficiency of the CNF electrode. As a result, this might pave a way for the development of high-performance flexible supercapacitors.

S2 Condensed Matter Physics - Board: O-S2-8 / **312**

Improving quality of graphene grown on copper foil by physical polishing, wet-chemical polishing and thermal annealing pretreatment processes

Author: Methawut Sirisom[1]

Co-authors: Noppadon Nuntawong [2]; Pattana Suwanyangyaun [1]; Sakuntam Sanorpim [1]; Sukkaneste Tungasmita [1]; Taworn Intaro [1]; Warakorn Yanwachirakul [1]

[1] *Department of Physics, Faculty of Science, Chulalongkorn University, Pathumwan, Bangkok, 10330, Thailand*

[2] *Nantional Electronics and Computer Technology Centre (NECTEC), Khlong Luang, Patumthani, 12120, Thailand*

Corresponding Author: methawut847005@gmail.com

Pretreatment processes including physical polishing (PP), wet-chemical polishing (WP), and thermal annealing for smoothing a surface of copper (Cu) foil were optimized for high-quality graphene growth. In this work, the cu foil with a small thickness of 25 μm has been used as a substrate. Preliminarily, a substrate surface was smoothed by the PP process using Brasso as a polishing substance. The substrate was next etched by the WP process using phosphoric acid (H_3PO_4) as an etchant in order to further reduce a surface roughness and remove surface contamination. For the condition of WP process, an etchant concentration was varied from 30 to 60%, and an etching period was adjusted to 60, 90, and 120 s. Finally, the substrate was thermally annealed with a nitrogen gas for 10 min before growing graphene. An annealing temperature was varied from 860 to 940 °C. After the pretreatment processes, graphene was grown on the prepared cu foil substrate by direct-liquid-injection chemical-vapor deposition (DLI-CVD) technique using cyclohexane (C_6H_{12}) as a carbon precursor and nitrogen as a carrier gas. A growth temperature was fixed constantly at 920 °C, and C_6H_{12} was injected into the reactor with a flow rate of 0.5 g/min and pulse frequency of 0.5 Hz for 6 min. The surface morphology of Cu foil observed by optical microscopy exhibits that the substrate treated by PP and WP with the conditions that H_3PO_4 concentration is 45% and etching period is 90 s provides the smoothest surface without being damaged by the etchant. When the annealing temperature is assigned to 880 °C, the room-temperature Raman spectra measured with a 473-nm excitation shows that an intensity ratio of 2D to G peak (I_{2D}/I_G) is enhanced above 2. This result indicated that a monolayer graphene could be successfully formed at this optimized temperature.

S2 Condensed Matter Physics - Board: O-S2-25 / **50**

Dielectric and non-ohmic properties of Ca2Cu2-xGexTi4O12 ceramic composites

Author: Jirata Prachamon[1]

Co-author: Prasit Thongbai [2]

[1] *Khon Kaen University*

[2] *khon kaen university*

Corresponding Author: jirata.pra@gmail.com

In this work, the dielectric and non-Ohmic properties of $Ca_2Cu_2{-}xGe_xTi_4O_12$ ($CaCu_3Ti_4O_12/CaTiO_3$ composite) ceramic with additions of GeO_2 (x = 0, 0.025, 0.050 and 0.100) were prepared using a solid‐state reaction method. X-ray diffraction technique was used to confirm the second phases of CaCu3Ti4O12 and CaTiO3 phases was detected in all the ceramics. The slight decrease in the grain sizes of $Ca_2Cu_2 - xGe_xTi_4O_12$ ceramics can be observed using a scanning electron microscopy. The results revealed that ceramics sintered at 1060 ℃ for 6 h exhibited slightly different dielectric permittivity (~ 1784 – 2645), and the dielectric loss tangent was still very low (~ 0.036 – 0.018) at 1 kHz. This should be associated to insulating grain boundaries with activation energies of 0.80 eV by substitution of $Ge^(4+)$ for x = 0.050. The electrical responses of grains boundaries and internal interfaces were investigated using impedance spectroscopy. Strongly enhanced dielectric responses and variation in nonlinear electrical properties can be well described based on the electrical responses at internal interfaces of the ceramic composites.

S2 Condensed Matter Physics - Board: O-S2-26 / **78**

Metal-Insulator Transition effect on Graphene/VO2 via temperature dependent Raman Spectroscopy

Author: Kittitat Lerttraikul[1]

Co-authors: Wirunchana Rattanasakuldilok ; Salinporn Kittiwatanakul [1]

[1] *Chulalongkorn University*

Corresponding Author: kittitat.l@outlook.com

Vanadium dioxide (VO2) is a material which has a special characteristic that can change its properties drastically called metal-Insulator transition (MIT). The MIT of VO2 occurs at temperature about 68C under atmospheric pressure which change its phase from monoclinic to rutile phase, result in their different properties and structure. This characteristic of VO2 can be used for application such as smart windows[1]. Moreover, some material can be used to improve VO2 film quality. In this work, bilayer-graphene were deposited on top of VO2/Al2O3 of 50 nm and 100 nm VO2 and were studied via temperature-dependent Raman spectroscopy technique. The results from Raman spectrum indicate that the lattice parameter mismatch between bilayer-graphene and VO2 induce compressive strain on graphene and in-plane tensile strain on VO2 according to the observed blue shift of VO2 Raman modes. From the temperature-dependent Raman results, the monoclinic VO2 Raman peaks diminished as temperature reach 60-65℃ while the TMIT measured by temperature dependent resistance of bare VO2 is equal to 70℃. Moreover, an unexpected behavior from graphene can be observed in graphene/VO2. For graphene/SiO2 G-peak position tends to red shift as temperature increase[3]. However, the G-peak position observed from graphene/VO2 structure begins with red shift and turn to blue shift at ~60℃ instead of only red shift.

References
[1] Y. Cui, Y. Ke, C. Liu, Z. Chen, et al. Thermochromic VO2 for Energy-Efficient Smart Windows. Joule, Volume 2, Issue 9-2018, 1707-1746. https://doi.org/10.1016/j.joule.2018.06.018
[2] Zhou, H., Li, J., Xin, Y., Cao, X., Baoa, S., and Jin, P. (2015). Enhanced optical response of hybridized VO2/graphene films. J. Mater. Chem. C, 3(19), 5089-5097. doi:10.1039/C5TC00448A
[3] Wang, W., Peng, Q., Dai, Y. et al. Temperature dependence of Raman spectra of graphene on copper foil substrate. J Mater Sci: Mater Electron 27, 3888–3893 (2016). https://doi.org/10.1007/s10854-015-4238-y

S2 Condensed Matter Physics - Board: INV-S2-2 / **356**

Magnetic Bacterial Cellulose and Carbon Fiber Nanocomposites

Author: Supree Pinitsoontorn[None]

Corresponding Author: psupree@kku.ac.th

In this talk, I will present my ongoing research on the theme of bacterial cellulose nanocomposites. Bacterial cellulose (BC) is a natural polymer with a three-dimensional network of nanofibers. It is produced by cultivation of certain types of bacteria strain. The structure and properties of BC are very unique. It exhibits remarkable mechanical properties, porosity, water absorbency, moldability, biodegradability, and excellent biological affinity. Moreover, it possesses highly porous nanostructure with very high surface area, which makes it an ideal substrate to host other nanomaterials. Several types of nanoparticles have been incorporated in BC to improve the characteristics and properties. In my group, we have focused on impregnation of various kinds of magnetic nanoparticles in BC to make flexible magnetic membranes, which can be utilized for several applications, such as actuators, sensors, electromagnetic shielding, information storage, and anti-counterfeit materials. Furthermore, by pyrolysis, BC transforms into carbon nano-sponge, which can be used for heavy metal adsorption or oil adsorption. I will summarize the work I have been doing in the past 4 years, and an outlook for the future work.

S2 Condensed Matter Physics - Board: O-S2-9 / **248**

Characterization of TiN thin film deposited by reactive DC unbalanced magnetron sputtering at different N2 flow rates

Authors: Nirun Witit-Anun[1]; Siriwat Alaksanasuwan[2]

[1] *Burapha University*

[2] *Phranakhon Si Ayutthaya Rajabhat University*

Corresponding Author: siriwat.aru@gmail.com

Titanium nitride (TiN) thin films were deposited on Si substrates by reactive DC unbalanced magnetron sputtering from metallic Ti targets. The effect of N2 flow rate, in the range of 1.0–4.0 sccm with 1 sccm increment, on the structure of the as-deposited TiN films was investigated. The crystal structures were identified by the GI-XRD technique. The thicknesses, microstructures, and surface morphologies were observed by the FE-SEM technique. The elemental compositions were evaluated by the EDS technique. The hardnesses were measured by the nano-indentation technique. The film's colors were measured by the UV-VIS spectrophotometer. The results showed that the as-deposited films had an fcc structure with (111), (200), (220), and (311) planes. The lattice constant and the crystallite size were ranging from 4.211–4.239 Å and 17.8–24.6 nm, respectively. The as-deposited films showed a nanostructure with a crystal size of less than 25 nm. The thickness of films decreases from 1254 nm to 790 nm with increasing in the N2 flow rate. The elemental composition of the films (Ti and N contents) depended on the N2 flow rates. The cross-sectional analysis of films by the FE-SEM technique showed a compact columnar structure. The hardness of films measured by the nano-indentation technique was increased from 4.5–19.4 GPa with increasing in the N2 flow rates. The color of the film was measured in the CIE L*a*b* system showing that the film deposited with optimal N2 flow rates was close to the color of 24K gold.

S2 Condensed Matter Physics - Board: O-S2-10 / **237**

Improvement in Reproducibility of Large-scale Perovskite Solar Cells Using Automatic Liquid Injection in Antisolvent Method

Author: Watcharakiart Insri[None]

Co-authors: Thanawat Kanlayapattamapong [1]; Saowalak Homnan [1]; Duangmanee Wongratanaphisan [1]; Atcharawon Gardchareon [1]; Pipat Ruankham [1]

[1] *Chiang Mai University*

Corresponding Author: w.insri28@gmail.com

Organic-inorganic hybrid perovskites are currently some of the most promising photovoltaic materials to produce highly efficient and cost-effective solar cells. Currently, many approaches have been proposed to prepare high-quality perovskite layers. The antisolvent technique is an effective and widely used method that can be done by dropping antisolvent into the rotating precursor surface during the spin-coating process. This technique is used to rapidly decrease the precursor's solubility, leading to a crystal-like uniform and dense perovskite layer. In the development of perovskite solar cells, three main areas are being developed: efficiency, stability, and reproducibility. This work concentrates on improving a reproducible and large scale (>1 cm^2) perovskite solar cells by using an automatic liquid injection machine in the antisolvent method. Moreover, the properties of the perovskite solar cells were compared with the devices prepared by manual liquid dropping. Liquid drops with the automatic liquid injection machine are more accurate and consistent. The characteristics can reduce tolerances from manual production. Our work increases the reproducibility and the precision for the development of large-scale perovskite solar cells. It also increases the production capacity and reduces waste generated during the production process.

S2 Condensed Matter Physics - Board: O-S2-11 / **260**

Synthesis of (Zn + Nb) co-doped TiO2 rutile nanoparticles and dielectric properties

Authors: Narong Chanlek[1]; Pairot Moontragoon[None]; Theeranuch Nachaithong[None]; prasit thongbai[None]

[1] *Suranaree University of Technology (TH)*

Corresponding Author: theerna@kku.ac.th

$Zn^2 + /Nb^5+$ co-doped TiO_2 (ZNTO) nanocrystalline powders were prepared by a combustion process. A pure rutile-TiO_2 phase of powders and sintered ceramics with a dense microstructure was achieved. Both co-dopants were homogeneously dispersed in the ceramic microstructure. The presence of oxygen vacancies was confirmed by Raman techniques. The thermally activated giant-dielectric relaxation of ZNTO ceramics was observed. Removing the outer-surface layer had a slight effect on the dielectric properties of ZNTO ceramics. The density functional theory (DFT) calculation showed that, in the energy preferable configuration, the 2Zn atoms are located near the oxygen vacancy, forming a triangle-shaped ZnVoTi defect complex. This defect cluster was close to the diamond-shape 2Nb2Ti defect complex. Thus, the electron-pinned defect-dipoles (EPDD) can be formed. The giant-dielectric relaxation process of the ZNTO ceramics might be attributed to the interfacial polarization associated with electron hopping between $Zn^2 + /Zn^3+$ and $Ti^3 + /Ti^4+$ ions inside the grains, rather than due to the surface barrier layer capacitor (SBLC) or EPDD effect.

S2 Condensed Matter Physics - Board: O-S2-12 / **38**

Giant Dielectric Response and Maxwell–Wagner Relaxation in Isovalent and Pentavalent Co–doped Rutile–TiO_2

Author: Yasumin Mingmuang[None]

Co-author: Prasit Thongbai [1]

[1] *Khon Kaen University*

Corresponding Author: y_mingmuang@kkumail.com

Due to their high potential for use in ceramic capacitors, high–performance giant dielectric properties (HP–GDPs), i.e., high dielectric constant (ε′), low loss tangent (tanδ), and the temperature stability of ε′ over a wide temperature range ($\Delta\varepsilon'/\varepsilon'_{25}$(%)) < $\pm$15, of acceptor/donor (***A***/***D***) codoped–TiO_2 ceramics have been widely studied since the discovery of a new In^{3+}/Nb^{5+} codoped rutile–TiO_2. In this presentation, HP–GDPs of the TiO_2–based oxides were achieved in Sn^{4+}/Nb^{5+} codoped rutile TiO_2 (SnNTO) ceramics. SnO_2 isovalent (I^{4+}) dopant was employed to replace the ***A*** dopants. The SnNTO samples with different Sn^{4+}/Nb^{5+} concentrations (x = 0.01–0.05) were prepared using a standard solid–state reaction (SSR) method . The X–ray diffraction patterns of all the SnNTO ceramics showed only a single–phase rutile–TiO_2 (JCPS 21–1276) without any impurity phases. A highly dense microstructure of all SnNTO samples consisted of grains and grain boundaries. The average grain size slightly enlarged from 1.6 to 2.6 μm, which was caused by the diffusion of oxygen vacancies ($V_o^{\bullet\bullet}$) due to the existence of multivalent Sn^{2+}/Sn^{4+} ions. The dielectric properties of the SnNTO ceramics showed a high ε′ (~10^4), very low tanδ (<~0.05), and a low $\Delta\varepsilon'/\varepsilon'_{25}$(%) < $\pm$15 values in a wide temperature range. The origin of HP–GDPs was investigated using impedance spectroscopy (IS). The dielectric response was described by Maxwell–Wagner relaxation.
Keywords: TiO_2; Giant dielectric constant; Codopant; Grain boundary; Maxwell–Wagner relaxation

S2 Condensed Matter Physics - Board: O-S2-13 / **17**

Versatile, Low-Cost, and Portable 2D Material Transfer Setup with a Facile and Highly Efficient DIY Inert-Atmosphere Glove Compartment Option

Authors: Harihara Ramamoorthy[1]; Kanokwan Buapan[1]; Rathchanok Somphonsane[1]; Tinna Chaiwchan[1]

[1] *King Mongkut's Institute of Technology Ladkrabang*

Corresponding Author: harihara.ra@kmitl.ac.th

Research in van der Waals heterostructures has been rapidly progressing in the past decade, thanks to the art of sequential and deterministic placement of one two-dimensional (2D) material over another. The successful creation of heterostructures however has relied largely on expensive transfer systems that are not easily accessible to researchers. Although a few reports on low-cost systems have recently surfaced, the full functionality, portability features, and overall effectiveness of such systems are still being explored. In this work, we present an "all-in-one" low-cost transfer setup that is compact, lightweight, and portable and which can be quickly installed with a facile and do it yourself (DIY)-style anaerobic glovebox option that performs at par with commercial anaerobic systems. The "installable" glovebox option means the user has the convenience of quickly converting the working environment into an inert one when air-sensitive 2D materials are used. The lowest RH values obtained in our glovebox is <3%, and the O2 levels rapidly drop from 21% to less than 0.1% in just a few minutes of purging the chamber with inert gas. The transfer system is also equipped with a light-weight PID-controlled substrate heating option that can be easily assembled within just a few hours. We test the versatility of our low-cost system by the successful creation of hexagonal boron nitride (hBN)-encapsulated graphene and hBN-encapsulated molybdenum disulphide (MoS2) heterostructures using the hot pickup technique and graphene-hBN, MoS2-hBN, twisted MoS2, and twisted MoS2 on hBN stacks using the wetting technique, and a MoS2-hBN-graphene vertical tunneling heterostructure was formed using a combination approach. The effectiveness of the DIY glovebox is proven with the demonstration of extended stability of freshly exfoliated black phosphorous (BP) flakes, their encapsulation between thin hBN layers, and the formation of electrically contacted BP devices with a protective hBN top layer. At an overall price point of approximately 1000 $, the versatile setup presented here is expected to further contribute to the growth of research in 2D materials, in particular, for researchers initially faced with overcoming a huge entry-level threshold to work in the field of 2D materials and van der Waals heterostructures.

S2 Condensed Matter Physics - Board: INV-S2-3 / **355**

Electron-pinned defect-dipole and internal/surface barrier layer capacitor effects for high-performance giant dielectric oxides

Authors: Prasit Thongbai[None]; Nateeporn Thongyong[None]

Co-authors: Wattana Tuichai ; Noppakorn Thanamoon ; Pornjuk Srepusharawoot ; Porntip Siriya ; Narong Chanlek ; Pornjuk Srepusharawoot ; Masaki Takesada ; David P Cann

Excellent giant dielectric properties (ExGDPs) of dielectric oxides have been widely investigated due to their significant potential for many applications, especially for ceramic capacitors. However, low loss tangent (tanδ) and temperature coefficient ($\Delta\varepsilon'(T)/\varepsilon'_{RT}$) are difficult to achieve. In this presentation, we show systematic strategies for moving beyond conventional material problems in order to obtain a material that meets the practical requirements. The electron-pinned defect-dipole (EPDD) and internal/surface barrier layer capacitor (IBLC/SBLC) effects in TiO_2-based materials are proposed for obtaining the ExGDPs with high ultra-low tanδ (<0.01) and very high dielectric permittivity (>104) with temperature coefficient less than $\pm$ 15% over the temperature range of -55 – 200 °C. The relevant electric polarization mechanisms in the $TiO_2$2-based materials are described.

S2 Condensed Matter Physics - Board: O-S2-14 / **290**

Improving Heterointerface Abruptness of InGaAs/InP Superlattice by Optimizing a Purging Period of Group-V Gas

Author: Warakorn Yanwachirakul[1]

Co-authors: Masakazu Sugiyama [2]; Yoshiaki Nakano [3]

[1] *Department of Physics, Faculty of Science, Chulalongkorn University*

[2] *Research Center for Advanced Science and Technology, The University of Tokyo*

[3] *Department of Electrical Engineering and Information System, The University of Tokyo*

Corresponding Author: warakorn.y@chula.ac.th

An abruptness of InGaAs/InP heterointerfaces in the superlattice (SL) structure grown by metal-organic vapor-phase epitaxy has been improved by optimizing a gas-purging period of tertiary-butyl phosphine (TBP) onto the InGaAs terminated surface, and tertiary-butyl arsenide (TBA) onto the InP terminated surface. The non-abrupt heterointerface is a result of intermixing layer formation caused by two main effects: (1) carry-over and (2) diffusion of group-V atoms. The sample composes of 20 periods of InGaAs (2 nm)/InP (10 nm) epitaxially grown on the InP substrate in [001] direction. The In composition in InGaAs was adjusted to be 53% which is a lattice match to InP. The layer structure was characterized by high-resolution X-ray diffraction. Crystal quality and relaxation were analyzed from the reciprocal space mapping result recorded around diffraction from the InP (-2-24) asymmetric plane. Lattice mismatch and layer thickness were examined by the 2θ-ω results around the InP (004) symmetric plane. In this work, we proposed a model in order to estimate the thickness of intermixing layers by using the Fourier transform of a periodic trapezoid-shape scattering function to fit an intensity of high-order satellite diffraction peaks. Since InGaAs has a lower energy gap than InP, the InGaAs layer could be considered as a quantum well (QW) inserted between the InP barriers. Hence, we also analyzed the QW shape of SL structures via the ground-state transition energy characterized by room-temperature photoluminescence. Our results show that purging the InGaAs terminated surface with TBP for 2-4 s could effectively remove residual As atoms and reduce As carry-over into the next-grown InP. By purging the InP terminated surface with TBA, even though an effect of P carry-over is reduced, the structure becomes more suffered from diffusion of As atoms into the beneath InP layer.

S2 Condensed Matter Physics - Board: O-S2-15 / **154**

EFFECT OF ANNEALING CONDITIONS ON VO2 THIN FILMS PREPARED BY SOL-GEL METHOD

Author: Pongsatorn Panburana[1]

[1] *Chulalongkorn University*

Corresponding Author: miloboy_th@hotmail.com

EFFECT OF ANNEALING CONDITIONS ON VO2 THIN FILMS PREPARED BY SOL-GEL METHOD
Sub.Lt.Pongsatorn Panburana, Salinporn Kittiwatanakul

Abstract
Vanadium Dioxide has attracted considerable attention because of the metal-semiconductor phase transition at 68oC. This reversible transition changes crystal structure from monoclinic to rutile resulting in tremendously change of transmittance and reflectance of Infrared wavelength and electrical resistance making VO2 thin film potential candidate for energy-saving smart windows (automatically block heat).
However, its preparation is very challenging due to the multivalence of Vanadium element. In this study, we explored different annealing conditions for thin films synthesized by sol-gel method which has advantage over other methods such as lower cost, simpler process and ability to make large scale thin film.
In the experiment, we used vanadium (V) triisopropoxy oxide (VO(OC3H7)3) as precursor. The annealing conditioned explored are annealing temperature and annealing time of thin films in low pressured Argon rich atmosphere. The spin-coated films were annealed at 350-530 °C for 30 minutes, while another set were annealed at 450 °C for 30, 60, 90, and 120 minutes. Then the films were characterized with Raman spectroscopy and temperature dependent resistance measurement. The results show that the longer the annealing time and the higher the temperature are better for film formation —closer to VO2 (higher V:O ratio).
In addition, the effect of various substrate types was also explored, another set of thin films were coated on c-plane sapphire (c-Al2O3) and Soda lime glass (SiO2) to compare the effect. Then the films were characterized with Raman spectroscopy and X-Ray Diffraction. The result showed that sapphire substrate yielded better film formation.
Keywords: VO2 thin film;; Argon atmosphere; electrical resistance property; annealing temperature ; XRD; Raman spectroscopy spectroscopy

S2 Condensed Matter Physics - Board: O-S2-16 / **29**

PREPARATION OF UiO-66-MOFs FROM PLASTIC BOTTLE WASTE FOR GAS ADSORPTION MATERIAL APPLICATION

Author: Chawisa Visanupornprasit[None]

Corresponding Author: chawisa_v@kkumail.com

Nowadays, the most anxious problem is global warming which caused by an emission of CO2. To solve this problem, this research proposes the use of high porosity, stability, and simple synthesized material, metal-organic framework (MOFs). The aim of this work are synthesis and chemical modification of MOFs, UiO-66(Zr) that prepared from plastic waste, polyethylene terephthalate (PET). Hydrothermal technique was carried out for depolymerization of PET to produce orgainic ligand, BDC, then modulated synthesis technique for UiO-66(Zr). FTIR showed O=C–O in carboxylate group in BDC at 1675 cm−1and a smaller band at 1508 cm−1 presented C=C vibration of a benzene ring. These are summarized that is the success of synthesizing BDC from PET. However, to confirm a chemical structure NMR will be reported. The further step are using hydrothermal and ultrasonication techniques to synthesize combination two of UIO-66 with NH2, NH2-GO, and NH2-GMA functional groups and their characterization. After that, investigation of their CO2 absorption efficiency will be examined.

S2 Condensed Matter Physics - Board: O-S2-17 / **37**

Ab-initio study and Atomistic spin model simulations of α-Cr2O3 thin films

Author: Boonthum Kunyangyuen[1]

Co-authors: Salinporn Kittiwatanakul [1]; Udomsilp Pinsook [1]

[1] *Chulalongkorn University*

Corresponding Author: boontamyang03@gmail.com

The bulk Cr_2O_3 (Chromia) is one of the candidates for voltage-controlled spintronics which is a key element for magnetoelectric random access memory (MERAM) due to its antiferromagnetic and magnetoelectric effects in high temperature. However, engineering applications MERAM require thin films to reduce the voltage required and the chromia films might have different physical and magnetic properties from bulk ones because of film surface effects. Therefore, Density Functional Theory (DFT) study and the Atomistic spin model were used to investigate the effects of bulk and film chromia in this work. The results from DFT calculations showed that the Density of states (DOS) and Band structures of chromia films might be induced by defects and surface interaction with substrates. In order to calculate the Neel temperature (T_N) and magnetic properties, we need to extract the exchange interaction constants from the classical Heisenberg model and DFT results, which we evaluated up to the fifth nearest neighbors (J1-J5). Finally, the exchange coupling constants were used as parameters in the atomistic spin model i.e., Monte Carlo simulation and the Landau–Lifshitz–Gilbert (LLG) equation to calculate its magnetic properties such as magnetization (M), magnetic susceptibility (χ_M), T_N, and hysteresis loop etc. Moreover, the LLG equation is also used to visualize and simulate spin dynamics of chromia films.

Keywords : Antiferromagnets, Exchange interaction constants, Neel temperature, Atomistic spin model

References

[1] Saha, C. N. (2020). Fabrication of Micron Scale Test Structures for Magneto-Electric Chromia (Cr_2O_3) Thin Films (Doctoral dissertation, State University of New York at Buffalo).
[2] Sun, C. (2018). Structure Study of Magnetic Thin Films for Voltage Controlled Spintronics by Scanning Transmission Electron Microscopy Experiment and Density Functional Theory Calculations. The University of Wisconsin-Madison.

S2 Condensed Matter Physics - Board: O-S2-18 / **32**

Classification of metal polyhydride critical temperature using support vector machine

Authors: Udomsilp Pinsook[None]; Vichayuth Imchitr[None]

Corresponding Author: 6470186723@student.chula.ac.th

The recent experimental and theoretical search for near-room temperature superconductors have shed light of interest on metal hydride as the critical temperature can vary from a few kelvins to over 200 kelvins. One problem occurring in the theoretical research of the material is that the traditional way of studying thermal superconductivity material is through calculation of electron-phonon spectral function which cost enormous amount of time and computational resource. Here we propose machine learning method (Support vector machine) to classify the critical temperature of the material without calculating electron-phonon spectral function. The features used in the model are based on electronic properties occur from hydrogen atom in the molecule and consideration effect of electron localization function which have strong correlation to the temperature, this set of features can be obtained faster and with less computational resources than directly find the critical temperature. Decision boundary from the model can categorize most material in the dataset and thus speed up the quest for future high-temperature hydrogen-based superconductors.

S2 Condensed Matter Physics - Board: O-S2-19 / **309**

On the origin of high performance V2O5 cathodes of aqueous Mg-ion batteries: A computational study

Author: Panupol Untarabut[None]

Co-authors: Ittipon Fongkaew [1]; Anchalee Junkaew [2]; Sirisak Singsen [3]; Suwit Suthirakun [4]

[1] *School of Physics, Institute of Science, Suranaree University of Technology, Nakhon Rachasima, Thailand 30000*

[2] *National Nanotechnology Center (NANOTEC), National Science and Technology Development Agency (NSTDA), Pathum Thani 12120, Thailand*

[3] *School of Physics, Institute of Science, Suranaree University of Technology, Nakhon Ratchasima, Thailand 30000*

[4] *School of Chemistry, Institute of Science, Suranaree University of Technology, Nakhon Rachasima, Thailand 30000*

Corresponding Author: untarabut.p@gmail.com

Vanadium pentoxide (V2O5) is one of the promising cathode materials for Mg-ion batteries owing to its high capacity, safety, and low toxicity. However, it still suffers from sluggish charge transport kinetics and low stability. To overcome these problems, experiments reported that using aqueous electrolytes dramatically improves ion diffusion and capacity of V2O5-based cathode. Proton from water in the electrolyte may alter battery performance but its role remains unclear. Herein, we used density functional calculations to examine the effect of proton on the improved charge transfer properties and stability of Mg-proton co-intercalation to reveal the role of aqueous electrolyte. We find that protons prefer to intercalate into V2O5 and reside at vanadyl oxygen atoms. Upon proton intercalation, the band gap of V2O5 decreased from 2.17 eV to 0.07 eV suggesting better electronic conductivity. In addition, it improves Mg-ion diffusion where the diffusion barrier is reduced from 0.89 to 0.49 eV in the vicinity of intercalated proton. This work unravels the role of water in electrolyte in the enhanced cathode performance which could be used to better design cathode materials or electrolyte for Mg-ion batteries.

S2 Condensed Matter Physics - Board: O-S2-20 / **157**

First principles study on thermal conductivity of nitrogen substituted diamane

Author: Sakarn Khamkaeo[1]

Co-authors: Teerachote Pakornchote [1]; Annop Ektarawong [2]; Thiti Bovornratanaraks [1]

[1] *Chulalonkorn University*

[2] *Chulalongkorn University*

Corresponding Author: sakarn.k23@gmail.com

Over the last decade since the discovery of graphene, two-dimensional materials have gained a great attention due to their outstanding properties suitable for fabrication of next generation nanodevices. A single-layered diamond or diamane, whose high stiffness and high thermal conductivity are inherited from its bulk counterpart, is a candidate for heat dissipating device applications. Unfortunately, pristine diamane is structurally unstable without passivation of dangling bonds on it surfaces by H, F, and OH. Recent theoretical studies have suggested that site-specific substitution of N for C can stabilize the diamane's structure without surface termination. Despite its superhard properties inherited from bulk carbon nitrides, thermal properties of N-substituted diamane have not been explored. In this work, we investigate thermal properties of N-substituted diamane using density functional theory and Boltzmann transport equation in the relaxation time approximation. Our results show that the flexural phonon branch, which is typically observed in two-dimensional materials, appears in the phonon dispersion relation of N-substituted diamane and it contributes large thermal conductivity to the material. Also, we estimate the thermal conductivity of N-substituted diamane as a function of temperature, and the results are discussed in comparison with that diamond.

S2 Condensed Matter Physics - Board: O-S2-21 / **49**

First-principles prediction of configurational order-disorder phase transition in $((Ti_{1-x}V_x)_{1/3}Mo_{2/3})_3C_2$ MXene alloys

Authors: Chayanon Atthapak[None]; Annop Ektarawong[1]; Teerachote Pakornchote[2]; Thiti Bovornratanaraks[None]

[1] *Department of Physics, Faculty of Science, Chulalongkorn University, Bangkok, Thailand.*

[2] *Department of Physics, Faculty of Science, Chulalongkorn University*

Corresponding Author: 6370198123@student.chula.ac.th

Transition-metal carbides/nitrides (MXenes) and their alloys, the largest family of two-dimensional materials, are gaining a lot of attention in the material research community due to their high potential in many applications, e.g., batteries, supercapacitors, electromagnetic and interference shielding. In this work, we investigated the thermodynamic stability of $((Ti_{1-x}V_x)_{1/3}Mo_{2/3})_3C_2$ MXenes (TVMCs), using the first-principles calculation based on density functional theory and cluster-expansion formalism. Our results suggest that Mo atoms prefer to substitute in the outer metal layers of TVMCs, and such occupying behavior is a crucial factor that determines the thermodynamic stability of TVMCs. On the other hand, Ti and V atoms residing in the inner metal layer of them are predicted to weakly interact with each other and their atomic configuration has a minimal impact on the stability of TVMCs. The transition temperatures between configurational order and disorder phase whose Ti, V, and Mo atoms reside in TVMCs have been predicted, and the possible existence of configurationally disordered TVMCs has also been discussed.

S2 Condensed Matter Physics - Board: O-S2-22 / **140**

Fabrication and characterization of the Si p-n junction prepared by thermal diffusion

Author: Nanthawat Toarun[1]

Co-authors: Pattanaphong Janphuang [2]; Tanachat Eknapakul [3]; Prayoon Songsiriritthigul [4]; Chanan Euaruksakul [5]

[1] *School of Physics, Suranaree University of Technology,*

[2] *Synchrotron Light Research Institute (Public Organization)*

[3] *Suranaree University of Technology*

[4] *Suranaree University of Technology*

[5] *Synchrotron Light Research Institute (Public Organization),*

Corresponding Author: armdes4291@gmail.com

This work presents fabrication and characterization of a p-n junction in Si. The p-n junction was fabricated simply by thermal diffusion of n-type Si wafer with boron deposited on the surface. The depth of the p-n junction was primarily predicted by the Fick's law of diffusion. Boron deposition was carried out in a vacuum system using an electron beam evaporator. The deposited samples were annealed in the same vacuum system to introduce boron diffusion into the Si substrate. V-I curve measurements were performed to characterize the electrical properties of the p-n junction. Appropriated depth and width of depletion region will be discussed for application of X-ray detectors.

Keywords: boron diffusion, p-n junction, thermal annealing, electron beam evaporation, silicon semiconductor

S2 Condensed Matter Physics - Board: O-S2-23 / **22**

Synthesis of antibacterial nanofibers composite from poly butylene succinate and copper nanoparticle as a filter layer in a surgical mask

Author: Jaggawut Suwannachot[None]

Corresponding Author: jaggawuts@kkumail.com

The outbreak of COVID-19 affects a daily life of human beings so protective equipment such as surgical masks is become essential. In this research, the development of filter layers for surgical masks from poly butylene saccinate (PBS) fiber nanocomposite which is a biodegrable polymer and copper nanoparticle (Cu NPs) that can inhibit microorganisms and can be synthesized from organic substances by electrospin technique, The spinning condition at a potential difference of 20 kV and a speed of 40 ml/hour was used in nanofiber fabrication. By using a co-solvent system between chloroform and dichloromethane, a composite solution was prepared. From scanning electron microscopy technique, it was found that the nanofiber size of polybutylene saccinate was 750 nm, However, when comparing with the size of PBS composite nanofibers were not significantly different. Further, the antimicrobial inhibition of nanocomposite was performed using 0.1% with CuNPs. Then, physical properties such as absorbance properties will be studied by UV-visible spectroscopy. Mechanical properties of nanofibers will be test by UTM. Additionally, the pressure of air passing through the filter layer will be test in order investigate its application in surgical mask.

S2 Condensed Matter Physics - Board: O-S2-24 / **111**

High–Performance Giant Dielectric Properties of (Tb+Nb) Co–Doped TiO2 Ceramics

Author: Noppakorn Thanamoon[1]

Co-author: Prasit Thongbai [1]

[1] *Khon Kaen University*

Corresponding Author: t_noppakorn@kkumail.com

Giant dielectric (GD) ceramics have been extensively reported in recent years due to their potential for use in high–performance capacitors. However, the strong temperature stability of high dielectric permittivity ($> 10^3$) and low dielectric loss tangent (tanδ < 0.05) have been difficult to accomplish. In this work, a novel GD oxide was discovered in (Tb+Nb) co–doped TiO_2 (TNTO) ceramics. Their colossal ε´ (~$4.7—5.3\times10^4$) and ultra–low tanδ (~0.006 – 0.007) were achieved at 30℃ and 1 kHz. Moreover, their temperature coefficient of ε´ (Δε´ /ε´) values at 1 kHz were less than |±15%| over the temperature range from –60℃ to 210℃, which encounter the primary desire in X9R–type capacitor. Interestingly, their low tanδ (~ 0.033–0.045) still appears at 200℃. These outstanding dielectric behaviors of TNTO ceramics were investigated via characterization of their phase structures, microstructures, and impedance spectroscopy (IS) analysis. The observation of electrical heterogeneity of semiconducting grains and high insulating layers indicates that interfacial polarization exists in the TNTO ceramics leading to the GD behaviors. Besides, the dispersed second phase particles in their microstructures could reduce their ε´ and tanδ values. Therefore, the appropriate second phase particles fraction could tune the TNTO's dielectric properties as required.

S3 Accelerators and Synchrotron Radiations - Board: INV-S3-1 / **197**

Can Fusion Energy Contribute in Achieving Carbon Neutrality in Thailand?

Authors: Nopporn Poolyarat[None]; Somsak Dangtip[1]; Thawatchai Onjun[None]

[1] *Thailand Institute of Nuclear Technology*

Corresponding Author: somsakd@tint.or.th

Fusion reactions fuse light nuclei to form a heavier nucleus and release a huge amount of energy. In tokamaks and stellarators, this starts by heating magnetically-confined plasma until the light nuclei could overcome a Coulomb barrier and reach fusion conditions. Neutrons, one of the two products of the fusion reactions, are then captured with its kinetic energy converted to electricity generation. This MeV-scale reaction energy produces essentially no greenhouse gases. International-wise, fusion reactors at 1000-MW scale are envisaged as an alternative and GHG-free energy source in 2040s to 2050s. With such a plan for commercialization of fusion energy technology in a global stage, is Thailand ready to incorporate this advanced energy source in its energy mix by the time? Thailand aims to reach carbon neutrality in 205x and net zero emissions by 206x. Can fusion energy then contribute to strengthen the electricity stability in this bold plan? Is our ecosystem in terms of infrastructure, frontier sciences, research and development and human resource development for fusion technology up and ready to meet this grand demand? This contribution aims to address this question, summarize the preparation and project the ways forward.

S3 Accelerators and Synchrotron Radiations - Board: O-S3-1 / **112**

Three-Dimensional Simulation of the Supersonic Molecular Beam Injection in Thailand Tokamak 1

Author: Kitti Rongpuit[1]

Co-authors: Apiwat Wisitsorasak [1]; Jiraporn Promping [2]

[1] *king mongkut's university of technology thonburi*

[2] *thailand institute of nuclear technology*

Corresponding Author: kitti.phy@mail.kmutt.ac.th

Fueling in tokamaks is important for plasma confinement and operation. It can be realized by three main methods: gas puff, pellet injection, and supersonic molecular beam injection (SMBI). The SMBI can deliver the fuel more effective than the gas puff, and Thailand Tokamak 1 which is under development may potentially employed this fueling technique. In this work, we develop a simulation for studying the plasma dynamics during the SMBI in TT1. The simulation is based on the fluid model which includes the continuity equation, energy balance equations, momentum equation, continuity of fuel equation, and momentum of fuel. BOUT++ code is used to numerically solve these equations by a finite difference method in three-dimensional space. The initial results show that when SMBI of the hydrogen gas is launched into the plasma with a speed of 600 m/s, the electron density in the edge immediately increases due to the dissociation and ionization processes. The ion and electron temperatures subsequently decrease. The full analysis of the simulations hopes to benefit for designing of the injector and experimental plan for TT1 in the future.

S3 Accelerators and Synchrotron Radiations - Board: O-S3-2 / **80**

On the analysis of the fast-ion motion in Thailand Tokamak-1 using NUBEAM and LORBIT codes

Authors: Worathat Paenthong[1]; Apiwat Wisitsorasak[1]

Co-authors: Siriyaporn Sangaroon [2]; Jiraporn Promping [3]

[1] *King Mongkut's University of Technology Thonburi (KMUTT)*

[2] *Mahasarakham University*

[3] *Thailand Institute of Nuclear Technology (TINT)*

Corresponding Author: worathatsome@gmail.com

Thailand Tokamak-1 (TT-1) will be the first tokamak setting up at Thailand Institute of Nuclear Technology (TINT) in Nakorn Nayok province, Thailand. In the initial operation phase, the hydrogen plasma will be performed with Ohmic heating. In the future, the neutral beam injection (NBI) will be used as the auxiliary heating to achieve the high-performance plasmas. The goal of this study is to investigate the beam ion birth profile generated by NBI using NUBEAM code, taking into consideration of the possible beamline geometry and beam ion energy in this machine. Furthermore, the full orbit motion of the model beam ions is analyzed by the collisionless Lorentz-Orbit (LORBIT) Code. The effects of the beam geometry including the tangency radius, shape, and power of the beam ion source will be conducted for assessing the beam ion confinement capability and engineering constraints. The detailed modeling of beam ion birth profile generated by NBI and the feasibility of NBI installation in TT-1 will be presented.

S3 Accelerators and Synchrotron Radiations - Board: O-S3-3 / **116**

3D Range-Modulators: Near field simulations with FLUKA and comparison with film measurements

Author: Warisara Charuchinda[1]

Co-authors: Felix Horst [2]; Yuri Simeonov [3]; Christoph Schuy [4]; Petar Penchev [3]; Per Poulsen [5]; Mateusz Sitarz [5]; Simon Busold [6]; Claire-Anne Reidel [2]; Michael Folkerts [7]; Miriam Krieger [6]; Narumon Suwonjandee [1]; Burin Asavapibhop [1]; Marco Durante [2]; Klemens Zink [3]; Uli Weber [2]

[1] *Chulalongkorn University, Bangkok*

[2] *GSI Helmholtzzentrum für Schwerionenforschung, Darmstadt, Germany*

[3] *Institut für Medizinische Physik und Strahlenschutz, Technische Hochschule Mittelhessen, Giessen, Germany*

[4] *GSI Helmholtzzentrum für Schwerionenforschung, Darmstadt, Germany*

[5] *Danish Center for Particle Therapy (DCPT), Aarhus, Denmark*

[6] *Varian Medical Systems Particle Therapy, Troisdorf, Germany*

[7] *Varian Medical Systems, Inc., Palo Alto, California, US*

Corresponding Author: c.warisara@hotmail.com

The 3D range-modulator is an innovation used in particle delivery systems that can create a highly conformal and homogeneous dose distribution in the target volume with mono-energetic beam, providing an option for high dose rate FLASH therapy (exploiting the Bragg peak) [1,2].
In the normal case, the modulators are positioned far away from the target in order to avoid the fluence ripples resulting from the periodic structure of the modulators [1]. To understand the fluence structure of protons induced by the 3D range-modulators and determine the minimum distance at which the fluence is homogeneous enough for the treatment, FLUKA Monte Carlo simulation package was used to observe the fluence distributions in the air or water after protons undergoing the modulators. The highest fluence ripple was spotted at a few centimeters from the modulators and then faded away as the distance increased, which can be described by the edge scattering effect and later by the blur-out of the overlapping contributions from the pins. Moreover, the dose distribution in water was investigated, particularly for small distances between the modulators and the water phantom.
Furthermore, the Monte Carlo results were compared with *Gafchromic EBT-3* film measurements irradiated with a 3D-printed range modulator prototype and show a good qualitative agreement.
Prospectively, the strong dose inhomogeneity's which appears in the proximal part of the target, could introduce a kind of 'mini beam' normal-tissue sparing by the 3D range-modulators.

Keywords: Proton therapy, 3D range-modulators, FLUKA Monte Carlo simulation, Edge scattering, Fluence and dose ripple
Ref.: [1] Yuri Simeonov et al 2017 Phys. Med. Biol. 62 7075, [2] Yuri Simeonov et al 2022 Biomed. Phys. Eng. Express 8 035006

S3 Accelerators and Synchrotron Radiations - Board: O-S3-4 / **91**

The Effect of Magnetic Topology of Polywell Fusion Devices on The Electron Confinement Time

Author: Rattacha Boonchoo[None]

Co-author: Boonyarit Chatthong [1]

[1] *Division of Physical Science, Faculty of Science, Prince of Songkla University*

Corresponding Author: r.boonchoo.394@gmail.com

This work study the effects of magnetic field topology of polywell fusion device on electron confinement time. Several polywell designs are used including a cube configuration (6 coils), dodecahedron configuration (12 coils), double-layer configuration (14 coils) and disco configuration (26 coils). The results of magnetic field structure are investigated by using numerical simulations based on finite element method. In addition,the effect of electrical current in each coil on the observe magnetic field is also investigated. Electron beams are injected into each configuration in order to determine the decay behavior of electron numbers. The probability of loss is defined with loss cone, which can be used to predict what configuration yield the most electron loss. It is found that the increase of coils current does not affect the probability of loss. However, it demonstrates that the dodecahedron configuration yield highest probability of loss. The confinement time study shows that the dodecahedron configuration yields better confinement than cube and double-layer configuration. The disco configuration yields the best results, confining electrons for the longest time of about 20 μs.

S3 Accelerators and Synchrotron Radiations - Board: O-S3-5 / **92**

Investigation of an edge transport barrier formation in fusion tokamak using the BOUT++ framework

Author: Thiti Aungcharoen[None]

Co-author: Boonyarit Chatthong [1]

[1] *Division of Physical Science, Faculty of Science, Prince of Songkla University*

Corresponding Author: 6110210181@psu.ac.th

The heat and particle transport equations are used to study the formation of an edge transport barrier (ETB) in a tokamak plasma based on the two-field bifurcation concept. These equations are simultaneously solved by a numerical method using the BOUT++ physics framework resulting in plasma pressure and density profiles as a function of time and plasma radius. The transport effects include both neoclassical and anomalous effects, where the latter can be suppressed by the flow shear mechanism. The flow shear is proportional to the multiplication of the pressure and density gradients. The main heat and particle sources are localized at the center and edge of the plasma, respectively. The result shows that when the heat or particle source surpasses its threshold value, there will be the formation of the ETB at the plasma edge. As a result, pressure and density at the center are enhanced. Moreover, the effect of varying neoclassical and anomalous transport coefficients on the pressure and density profiles is also investigated. It is found that as the transport values are increased, the plasma performance drops, and at some point, the plasma can no longer form an ETB. The results are compared with those solved by MATLAB from previous research work for benchmarking purposes. This research is supported by TSRI Fundamental Fund project number 91526.

S3 Accelerators and Synchrotron Radiations - Board: O-S3-6 / **104**

The study of fusion neutrons captured in Tritium breeding blanket of Tokamak wall using GEANT4

Author: Paphatchaya Kheawyoi[None]

Co-author: Boonyarit Chatthong

Corresponding Author: 6110210241@psu.ac.th

This work studies the phenomenon of neutron transport simulation and the ratio between incident neutrons and produced tritium breeding of fusion blanket on various materials. The aim is to investigate the local Tritium Breeding Ratio (TBR) after neutrons pass through 5 meters thickness of the 30 degrees angle of cylindrical-shape breeding blanket of different materials using GEANT4 simulation framework. For all simulations, G4HadronPhysicsQGSP_BIC_HP Physics list, materials i.e., 6Li+7Li, 6Li, Li2O, Li17Pb83, Li4SiO4, Li2ZrO3, and Li2TiO3 are used. The results show that the local TBR of Li2O and Li17Pb83, two of the most popular materials, are 0.9595 and 0.96091, respectively, for 0.025 eV neutron energy at room temperature. For 50 eV neutron energy, the local TBR of Li2O and Li17Pb83 are 0.35613, and 0.36256 respectively. Their local TBR decreases when faster neutrons pass through the blanket. Still, they stand out from other components, i.e., Li4SiO4, Li2ZrO3, and Li2TiO3. In addition, temperature effects on the local TBR is also investigated. It is found that higher temperature only slightly decreases the local TBR on all materials. This research is supported by TSRI Fundamental Fund project number 91525.

S3 Accelerators and Synchrotron Radiations - Board: INV-S3-2 / **334**

Intense Helicon Plasma in the Thailand Linear Device

Author: Mudtorlep Nisoa[None]

Corresponding Author: nmudtorl@mail.wu.ac.th

High-density linear plasma devices can produce plasmas similar to that of the Tokamaks[1,2]. But, they are simple and compact than the tokamaks. The linear devices are much more cost-effective than the tokamaks for research on plasma material interactions.
In this research, a linear helicon plasma device with permanent magnets was fabricated. A half-turn helical antenna and 13.56 MHz RF were used to excite helicon wave of m = +1. The 800 G magnetic field is uniform in the vicinity of the antenna. Ar gas was used for the plasma discharges. The electron temperatures and plasma densities were obtained by using optical emission spectroscopy(OES) and Langmuir probe. When the helicon waves were excited by RF power more than 400 W, high-density plasmas of more than 10^13 cm^(-3) were obtained. The electron temperatures were in the ranges of 1 – 5 eV. The linear helicon plasma device developed in work is excellence for the studies of plasma material interaction (PMI) for development of fusion related materials. The ion fluence, similar to that of the plasma-facing wall in tokamaks, can be investigated.

Reference
1. Caughman et al., Plasma source development for fusion-relevant material testing, Journal of Vacuum Science & Technology A: Vacuum, Surfaces, and Films 35, 03E114 (2017)
2. R. H Goulding et al., Progress in the Development of a High Power Helicon Plasma Source for the Materials Plasma Exposure Experiment, Fusion Science and Technology, (2017)

S3 Accelerators and Synchrotron Radiations - Board: O-S3-7 / **302**

Design of Dipole Magnets for Siam Photon Source II

Author: Prapaiwan Sunwong[1]

Co-authors: Pariwat Singthong [2]; Prayoon Songsiriritthigul [3]; Supachai Prawanta [2]; Supat Klinkhieo [4]; Thongchai Leetha [2]

[1] *Synchrotron Light Research Institute (Public Organization)*

[2] *Synchrotron Light Research Institute*

[3] *Suranaree University of Technology*

[4] *Synchrotron Light Research Institute, SLRI*

Corresponding Author: prapaiwan@slri.or.th

Two types of dipole magnets are designed for the storage ring of Siam Photon Source II, the second synchrotron light source in Thailand. Magnetic field at the magnet center is 0.87 T, which bends a 3.0 GeV electron beam with the bending radius of 11.532 m and consequently the synchrotron radiation is generated. The first type of dipole magnet is a standard dipole with the magnet gap of 36 mm. The other type is designed for Infrared (IR) beamline with the larger magnet gap of 59 mm to accommodate a wide opening angle of IR radiation. The magnets are designed such that the applied operating current is the same while the turn number of magnet coils and the magnet gap are allowed to be different. Therefore, a single power supply can be used to excite all dipole magnets in the storage ring which will be connected in series. Magnet modelling and magnetic field calculation of dipole magnets are performed in Opera-3D. The magnet poles are shimmed near the edges to improve magnetic field homogeneity to be within the requirement of 2×10^(-4) within the good field region. Mechanical analysis of magnet structure is performed in SOLIDWORKS and ANSYS where the maximum deformation of 18 - 23 micrometers is found at the magnet pole and the first-mode natural frequency is higher than 200 Hz.

S3 Accelerators and Synchrotron Radiations - Board: O-S3-8 / **54**

DESIGNING AND SIMULATION OF A LOW-ENERGY SINGLE ION IRRADIATION SYSTEM FOR BIOLOGICAL SAMPLE BOMBARDMENT

Author: Prutchayawoot Thopan[1]

Co-authors: Kittikhun Prakrajang [2]; Vitsanusart Atyotha [1]; Liang Deng Yu [3]; Udomrat Tippawan [4]

[1] *Department of Applied Physics, Faculty of Engineering, Rajamangala University of Technology Isan, Khon Kaen Campus*

[2] *bDepartment of Applied Physics, Faculty of Science, Maejo University*

[3] *Thailand Center of Excellence in Physics, Commission on Higher Education*

[4] *Plasma and Beam Physics Research Facility, Department of Physics and Materials Science, Faculty of Science, Chiang Mai University*

Corresponding Author: prutchayawoot.th@rmuti.ac.th

In our previous experiments, biological samples of naked DNA were bombarded by decelerated low energy ion beams (< 100 eV). The results found that the DNA could be damaged to induce single strand breaks (SSBs) and double strand breaks (DSBs). However, mechanisms of the low energy ion beam interaction with biological samples are unclear yet, particularly on the hot spot issue, namely what and where the most vulnerable spots of DNA are. As relevant mechanisms need deep understanding, we have planned and prepared to develop a low-energy single ion irradiation system for highly localized and does-controlled ion bombardment of DNA.

In the system, the ion beam energy is decreased by the existing deceleration lens, then the low-energy ion beam passes through μm slits and finally, low energy single ions are obtained by beam scanning from scanner plates and detected by a single ion detection device, as shown in Fig 1. Conceptual designing, calculation and simulation of the low-energy single ion system are presented in this report. The significance of developing such a system is not only in studying fundamentals of the ion-DNA interaction but also in investigation of ion irradiation fabrication and effects on microelectronics.

Keywords: Designing and simulation; Low-energy single ion; Deceleration lens; Beam scanning.

S3 Accelerators and Synchrotron Radiations - Board: O-S3-9 / **354**

Specific activities of natural and anthropogenic radionuclides in organic Sungyod rice samples collected from Don Pradu sub-district in Pak Phayun district in Phatthalung province, Thailand

Author: Prasong Kessaratikoon[1]

Co-authors: Patcharapa Charoenmak [2]; Nopparit Changkit [3]; Ruthairat Boonkrongcheep [4]

[1] *Department of Physics Faculty of Science Thaksin University Songkhla Campus*

[2] *Undergraduate Student, B.Ed. (Science-Physics) Program, Faculty of Education, Thaksin University, Songkhla, 90000, Thailand*

[3] *Thailand Institute of Nuclear Technology (Public Organization), Nakhon Nayok, 26120, Thailand*

[4] *Research Assistance, Nuclear and Material Physics Research Unit, Department of Basic Science and Mathematics, Faculty of Science, Thaksin University, Songkhla, 90000, Thailand*

Corresponding Author: prasong_mi@hotmail.com

The small amounts of natural and anthropogenic radionuclides that accumulate in some human staple diets can cause harm to the health of consumers. In order to examine the level of radioactive background in staple food of Thai people, specific activity of natural (40K, 226Ra and 232Th) and anthropogenic (137Cs) radionuclides were studied and evaluated in 28 samples of organic Sungyod rice collected from Don Pradu sub-district, Pak Phayun district in Phatthalung province. The hyperpure germanium (HPGe) detector and gamma-ray spectrometry analysis system which were set-up in advanced laboratory in Thailand Institute of Nuclear Technology (public Organization) or TINT were employed to perform some measurements and analysis for this study. It was found that the average values of specific activities of 40K, 226Ra, 232Th and 137Cs were 24.11 ± 2.01, 0.28 ± 0.07, 0.17 ± 0.06 and < 0.10 Bq/kg respectively. In addition, the average values of 40K, 226Ra and 232Th were also used to evaluate some related radiological hazard indices which are gamma-absorbed dose rate (D), radium equivalent activity (Raeq), external hazard index (Hex) and annual external effective dose rate (AEDout). Furthermore, by using the AEDout value, the excess lifetime cancer risk (ELCR(outdoor)) in this area would be also evaluated and presented. Moreover, Office of Atoms for Peace (OAP) annual report data, Thailand and global radioactivity measurement and calculations were used to compare and discussed with the present results. According to all results from this study, the organic Sungyod rice in the studied area were not only the low level of background radiation diet but also safe to consume.

S3 Accelerators and Synchrotron Radiations - Board: O-S3-10 / **301**

G4beamline simulation for rotating telescope at SLRI BTF

Author: Jetnipit Kaewjai[1]

Co-authors: Chinorat Kobdaj [2]; Kritsada Kittimanapun [3]; Natthawut Laojamnongwong [2]

[1] *Suranaree University of Technology (TH)*

[2] *Suranaree University of Technology*

[3] *Synchrotron Light Research Institute*

Corresponding Author: jetnipit.kaewjai@cern.ch

ALICE (A Large Ion Collider Experiment) is one of the CERN experiments along LHC that studies quark-gluon plasma, a state of matter thought to have formed shortly after the big bang. By 2021, a plan to upgrade the ALICE Inner Tracking System has been proposed and the Monolithic Active Pixel Sensor, a novel silicon sensor technology, will be employed. The ALICE PIxel DEtector is the name of the new sensor (ALPIDE). The ALPIDE sensor is planned to be investigated with a rotating telescope at the Synchrotron Light Research Institute Beam Test Facility using a 1.2 GeV electron beam. A part of this work is to study the pixel sensor telescope when the angle of the Device Under Test (DUT) plane changes. Simulation has been performed with the G4beamline software. Once the G4beamline simulation is completed, a ROOT file is produced. The beam profile and correlation plot are then analyzed. These data were used to calculate the scattering angle, which was found to be between 0.0098 and 0.0102 rad when a DUT was not rotated. Furthermore, the simulation result was compared to the theoretical calculation.

S3 Accelerators and Synchrotron Radiations - Board: O-S3-11 / **327**

Fabrication and development of neutron shielding materials based on natural rubber and boron carbide

Author: Jittinun Saenpoowa[1]

[1] *surana*

Corresponding Author: m6300425@g.sut.ac.th

Neutron shielding materials were fabricated based on natural rubber (NR) and boron carbide (B4C) as their main components. Natural rubber, which contains a lot of hydrogen, can lower the energy of a neutron. Boron carbide, which contains a lot of boron, may absorb neutrons. The shielding materials were created with boron carbide concentrations of 0, 20, 40, and 60 parts per hundred rubber (phr) and thicknesses of 2, 5, 10, and 15 mm. The manufactured materials will be examined for neutron absorption efficiency using an Am/Be neutron source at the Radiation Measurement Laboratory at the Nuclear Engineering Department, Faculty of Engineering, Chulalongkorn University. In this example, the findings will be compared to those of a Monte Carlo N-Particle (MCNP) transport code and silicone rubber sold in Japan by Atom Shield Co., Ltd.

S3 Accelerators and Synchrotron Radiations - Board: INV-S3-3 / **366**

SPS-II: A 4th Generation Synchrotron Light Source in Southeast Asia

Author: Prapong Klysubun[1]

[1] *Synchrotron Light Research Institute (TH)*

Corresponding Author: prapong.klysubun@cern.ch

Siam Photon Source II (SPS-II) will be the first and only 4th generation synchrotron light source in South-East Asia region upon its completion. The accelerator complex consists of a 150 MeV linac and 3 GeV booster synchrotron combination acting as an injector, and a 3 GeV electron storage ring based on a modified 6 Bend Achromat (6BA) lattice. The modified 6BA, or Double Triple Bend Achromat (DTBA) lattice, is adopted because the emphasis is put on maximum utilization of the medium-size storage ring. It is planned that several components will be manufactured domestically. A half-cell prototype of the SPS-II storage ring was successfully developed, demonstrating the domestic fabrication capability. In this talk, the details of the machine design along with prototype development will be described.

S3 Accelerators and Synchrotron Radiations - Board: INV-S3-4 / **364**

Radioisotope Application for Plant and Process Inspection in Petroleum and Petrochemical

Author: Dhanaj Saengchantr[None]

Co-authors: Akara Akaranate ; Tosaporn Passadu ; Umpai Sookbumperng ; Thitirat Rattanawongwiboon

Corresponding Author: dhanaj.s@gmail.com

Since discovering of radioisotope materials, scientists and engineers tried to apply them into many ways to take the advantage from its penetration characteristic. This paper aims to introduce its usefulness as an important tool for process investigation in petroleum and petrochemical plants. Mostly, petroleum and petrochemical plants are continuously operating for more than three years per cycle before a turn-around maintenance. During the operation, the malfunction could be possible and may cause the process upset, consequently, the products are out of specification. The applications can be one or more than one of three techniques, i.e. transmission technique, emission technique and back-scattering technique. Mostly, transmission and emission techniques are using gamma rays sources (^{60}Co and ^{137}Cs) while back-scattering technique used to neutron source (^{241}Am-Be) and thermal neutron detector. The examples of gamma ray applications for transmission technique are pipe-scan, on-steam distillation column scan, scanning of heat exchanger, radiographic testing, and industrial computed tomography. Whereas the emission techniques are using radiotracer for leak detection in heat exchanger, residence time distribution, etc. The examples of neutron backscattering applications are the sludge level in vessel determination, water accumulation in concrete foundation, and water accumulation in thermal insulation materials. The petroleum and petrochemical industries in Thailand have understood the benefits of utilizing these techniques. The result from investigation can be used for preventive and corrective maintenance, process optimization, problem shooting as the result of techniques can identify the location of problem precisely. The usefulness of stated techniques has proven to have significant roles in certain applications which could not be replaced by other inspection techniques.

S3 Accelerators and Synchrotron Radiations - Board: O-S3-12 / **121**

Experimental study of radiolytic oxygen removal in irradiated water

Author: Pharewa Karoon[1]

Co-authors: Martina Fuss [2]; Chinorat Kobdaj [1]; Chutima Talabnin [1]

[1] *Suranaree University of Technology*

[2] *GSI Helmholtzzentrum für Schwerionenforschung GmbH*

Corresponding Author: pharephkr@gmail.com

The mechanism behind the biological sparing effect with ultra-high dose rate (FLASH) still remains unknown. One possibility is that the FLASH effect is caused by oxygen removal or the reaction of radiation-induced radicals with oxygen during irradiation. In this work, before studying the oxygen removal with FLASH irradiation, we decide to irradiate the samples with conventional dose rate (CONV) to investigate experimental oxygen removal in different liquids and study the radical production and reactions that arise in this dose rate range, for reference. Water samples were exposed to 50 Gy X-ray radiation dose at the dose rate of ~4.7 Gy/min. Each sample was irradiated for 2-3 irradiations. Dosimetry for the X-rays source was carried out using a Semiflex ionization chamber. The oxygen measurement was performed using a chemical optical sensor and observed online. The oxygen depletion was the highest in the first irradiation and then decreased in steps afterwards with the average values of 0.28, 0.25 and 0.23 μM/Gy in the first three irradiations, respectively. From the experimental results, we conclude that the decreasing behavior of oxygen removal is produced by the radical production and their reactions which compete with oxygen removal. The radicals created in previous steps might react with each other and reduce the reaction that should occur with the oxygen in the next irradiation. In addition, an increased oxygen removal was found in solutions containing organic molecules.

S3 Accelerators and Synchrotron Radiations - Board: O-S3-13 / **105**

ELMs Dynamics Simulations Based on Bifurcation Approach

Author: Danis Klanurak[None]

Co-authors: Boonyarit Chatthong [1]; APISIT DANG-IAD [2]

[1] *Division of Physical Science, Faculty of Science, Prince of Songkla University*

[2] *Prince of Songkla University*

Corresponding Author: 6410220035@psu.ac.th

The ELM phenomenon in fusion plasma is studied based on bifurcation concept. Three field transport equations including thermal, particle and toroidal momentum transports are solved simultaneously, resulting in the spatio-temporal prediction of plasma pressure, density, and toroidal momentum profiles. The transports include both neoclassical and anomalous effects with the velocity shear dependent suppression effect acting on only the anomalous channel. The results show plasma pressure, density and toroidal momentum profiles versus time and radius. It is found that the plasma can transit to H-mode once the threshold power is reached, resulting in the formation of an edge transport barrier. A peeling-ballooning model of edge localized mode, ELM, is included in form of thermal loss once the critical pressure gradient and current density has been reached. Frequency and amplitude of ELMs are investigated. The results exhibit ELMs phenomenon in which a periodically drop of pressure, hence a loss of energy can be observed. It is also found that changing of other model variables affect frequency and type of ELMs. This research is supported by TSRI Fundamental Fund project number 91526.

S3 Accelerators and Synchrotron Radiations - Board: O-S3-14 / **344**

A feasibility study of using BNCT to treat Cholangiocarcinoma (CCA)

Author: Yuwadee Malad[None]

Co-authors: Chinorat Kobdaj [1]; Chutima Talabnin [2]

[1] *School of Physics, Suranaree University of Technology*

[2] *Suranaree University of Technology*

Corresponding Author: tiw.physicsroom@gmail.com

Boron neutron capture therapy (BNCT) is a type of radiation therapy that utilizes the interaction of a stable boron (^{10}B) isotope and a thermal neutron to generate high-LET alpha and ^{7}Li particles that disrupt tumor cell DNA. Due to the low penetrating properties of alpha, the interaction is confined within cancer cells, and normal tissues are spared. BNCT has been demonstrated to be effective against specific types of cancer, including glioblastoma (GBM). The aim of this study is to apply BNCT to *cholangiocarcinoma* (CCA), which is a malignant tumor most prevalent in the northeastern part of Thailand. First, we measured L-p-Boronophenylalanine (L-BPA) accumulation in CCA cells using ICP-MS. Then, the survival curves of CCA cells exposed to neutron irradiation were investigated. The results show a relationship between neutron flux and the survival rates of CCA cells in our in vitro experiments. This gives us some insight on how to apply BNCT in CCA treatment.

S3 Accelerators and Synchrotron Radiations - Board: P110 / **128**

Conceptual design of a compact THz radiation source

Author: Siriwan Jummunt[1]

Co-authors: Supat Klinkhieo [2]; Thakonwat Chanwattana [1]; Thapakron Pulampong [1]

[1] *Synchrotron Light Research Institute (SLRI)*

[2] *Synchrotron Light Research Institute, SLRI*

Corresponding Author: siriwan@slri.or.th

The Siam Photon Source (SPS) in Thailand has been in operation for synchrotron radiation users since 2003. Since the light obtained from the synchrotron light source is the high-intensity radiation in the range from the infrared to high-energy X-rays, it has great attention in many areas of scientific research and industrial development. However, a wide variety of applications covering terahertz (THz) region needs to be fulfilled. The THz region covering the frequency range from 0.1 to 10 THz is a rich zone for various fields of research and industrial applications. Therefore, a compact accelerator based free-electron laser (FEL) with providing an intense THz radiation is particularly interesting. A high-power THz radiation source needs to be studied and developed to achieve the intense THz radiation at tunable frequencies between 0.5 THz and 5.0 THz, with a peak power of several megawatts (MWs) and narrow bandwidth. Design for high-power THz radiation source will be described and detailed in this paper.

S3 Accelerators and Synchrotron Radiations - Board: P111 / **129**

A study design of faraday cup for a 50 MeV electron beam current

Author: Siriwan Jummunt[1]

Co-authors: Sirilak Phetcharat [1]; Nawin Junthong [1]; Supat Klinkhieo [2]

[1] *Synchrotron Light Research Institute (SLRI)*

[2] *Synchrotron Light Research Institute, SLRI*

Corresponding Author: phleng309@gmail.com

The beam diagnostics to monitor the source performance constitutes an important part of particle accelerator. One of the key beam diagnostics is the charged particle beam current, the Faraday cup. This paper focuses on the design of Faraday cup for an electron beam energy between 5-50 MeV. For a good performance, the well-proved Monte Carlo codes of the PHITS has been performed to select the appropriate material types. The design achieved electron capture of around 99% by taking into account the penetration loss, the backscatter losses and the current leakage. The prototype Faraday cup is in the process of fabrication. The simulated results and detailed design will be presented.

S3 Accelerators and Synchrotron Radiations - Board: P115 / **74**

Development of a 6 MeV Electron Beam Energy Linac for Fruit Sterilization

Author: Somjai Chunjarean[1]

Co-authors: Nattawat Yachum [1]; Wiwek Phacheerak [2]; Surapong Kokkrathoke [1]; Surachai Pongampai [1]; Preecha Kulthanasomboon [1]; Siriwan Jummunt [3]; Supat Klinkhieo [1]; Keerati Manasatitpong [4]

[1] *Synchrotron Light Research Institute, SLRI*

[2] *Synchrotron Light Research Institute , SLRI*

[3] *Synchrotron Light Research Institute, SLRI*

[4] *Synchrotron Light Research Institute*

Corresponding Author: chunjarean@gmail.com

Treatment on fresh fruits, meet and food with ionizing radiation has been frequently chosen to destroy harmful pathogenic microorganism and oriental fruit flies. Electron beam linear accelerator (Linac) is commonly used as the source of irradiation to produce photon and electron in megavolt energy. A 6 MeV Linac designed for medical therapy has been developed for fresh fruit sterilization at Synchrotron Light Research Institute (SLRI). Physical design, fabrication, testing, and installation of the 6 MeV Linac with major auxiliary systems will be described in this paper. It is the first system designed, fabricates, and tested in-house for the fruit sterilization application at SLRI. This paper will also present results of beam dynamics in the standing wave Linac structure. Measurement results of electron beam after subassemblies are presented.

S4 High Energy and Particle Physics - Board: INV-S4-1 / **358**

Implications of the Interacting Quark EoS in the Quark Stars with 4D Einstein-Gauss-Bonnet gravity

Authors: Ayan Banerjee[None]; Daris Samart[None]; Phongpichit Channuie[None]; Takol Tangphati[None]

The detection of gravitational waves (GWs) from the binary neutron star (BNS) has opened a new window on the gravitational wave astronomy. With current sensitivities, detectable signals coming from compact objects like neutron stars turn out to be a crucial ingredient for probing their structure, composition, and evolution. Moreover, the astronomical observations on the pulsars and their mass-radius relations put important constraints on the dense matter equation of state (EoS). In this talk, we will consider a homogeneous and unpaired charge-neutral 3-flavor interacting quark matter with (m^4_s) corrections that account for the moderately heavy strange quark instead of the naive MIT bag model. In addition, we study a strange quark star in the context of recently proposed 4D Einstein-Gauss-Bonnet (EGB) theory of gravity. However, this theory is not well defined in four-dimensional spacetime. Thus, we thoroughly show that the equivalence of the actions in the regularized 4D EGB theory and in the original one is satisfied for a spherically symmetric spacetime. We pay particular attention to the possible existence of massive neutron stars of mass compatible with $M \sim 2M_{\odot}$. Our findings suggest that the fourth-order corrections parameter (a_4) of the QCD perturbation and coupling constant α of the GB term play an important role in the mass-radius relation as well as the stability of the quark star. Finally, we compare the results with the well-measured limits of the pulsars and their mass and radius extracted from the spectra of several X-ray compact sources.

S4 High Energy and Particle Physics - Board: O-S4-43 / **83**

Phased-resolved energy distribution of pulsar PSRJ1825-0935

Author: Nawamin Intrarat[1]

Co-author: Phrudth Jaroenjittichai

[1] *Chiang Mai University*

Corresponding Author: nminintrarat@hotmail.com

Pulsars are rapidly rotating and highly magnetized neutron stars that radiate non-thermal radio beams from their poles. The radio emission of pulsars usually remains stable in the averaged intensity of ~1,000 pulses or more, but some pulsars exhibit interesting features in emission variations on short and long timescales. In this research, we report the phase-resolved pulse-to-pulse energy distribution of pulsar PSRJ1825-0935 and found that the pulse profile's main component energy distribution is well described by a log-normal distribution. This pulsar has two different emission modes, B and Q modes, and we analyze the energy distribution of each mode energy separately.

Keywords: Pulsar, energy distribution

S4 High Energy and Particle Physics - Board: O-S4-44 / **89**

The Origin of Maser Flares

Authors: Anita Richards[1]; Malcolm Gray[None]; Bannawit Pimpanuwat[1]; Fraser Cowie[1]; Sandra Etoks[1]

[1] *University of Manchester*

Corresponding Author: malcolm.gray@manchester.ac.uk

Maser flares are spectacular increases in brightness of astrophysical masers over a typical timescale of weeks to months. I consider a number of plausible mechanisms for generating these flares and determine the most likely mechanisms on the basis of timescale, variability index and ability to support periodic flares. The flare mechanisms considered are overlap of clouds in the line of sight, shock compression, rotation of non-spherical clouds and variations in the flux of pumping and background radiation. I briefly introduce the analysis of the flares observed towards a small number of star-forming regions, and discuss the correlation and anti-correlation of flares in different transitions and molecular species. I set out possible roles for the new 40-m TNRT in detecting and monitoring maser flares.

S4 High Energy and Particle Physics - Board: O-S4-1 / **6**

SUSY Breaking and R-symmetry Breaking in Gauged Wess-Zumino Model

Author: Sirapat Lookrak[1]

Co-author: Udom Robkob [1]

[1] *Mahidol University*

Corresponding Author: nutdot@hotmail.com

In this work R-symmetry defined in Wess-Zumino model is determined to be broken spontaneously within broken supersymmetric vacuum according to O'Raifeartaigh potential containing scalar fields of R-charges of 0 or 2. The analysis is done on Coleman-Weinberg effective potential at one-loop level. We find that there can be gauge symmetry breaking and R-symmetry breaking if $m_X^2 < 0$ and scalar field with R-charge other than 0 or 2 exists. The gaugino mass at one loop is in the order of $\Lambda \ln \Lambda$ scale but the renormailization is required.

S4 High Energy and Particle Physics - Board: O-S4-45 / **96**

Machine learning application for dark matter - background classification in JUNO experiment

Authors: Jaruchit Siripak[1]; Nuanwan Sangungsuk[2]; Utane Sawangwit[3]; Yan Yu-peng[1]

[1] *Suranaree University of Technology*

[2] *Institute for the Promotion of Teaching Science and Technology*

[3] *National Astronomical Research Institute of Thailand*

Corresponding Author: jaruchit1112@gmail.com

Jiangmen Underground Neutrino Observatory (JUNO) has a potential to indirectly detect dark matter (DM), observing neutrino events from annihilations of DM trapped by the gravitational force in the solar core. Weakly interacting massive particle (WIMP) DM candidate with mass $>$ 3-4 GeV has significant solar capture rate. In this work, we simulate JUNO neutrino events from the most dominated WIMP annihilation channel, $\tau\tau^-$. Given the high-energy neutrinos from massive WIMPs, we extend the neutrino-nucleon interactions in the detector to include Quasi-Elastic (QE) and Deep Inelastic scatterings (DIS).

The most challenging background events in the energy range above 100 MeV is the atmospheric neutrinos. The pulse shape discrimination (PSD) method is usually applied to distinguish between DM and atmospheric neutrinos. In this work, we apply Machine Learning (ML) techniques to classify the background events and rare dark matter signals. We found that the Support-Vector Machine (SVM) algorithm gives the best results. Using ML, the accuracy of DM- atmospheric neutrino events classification up to 99.2% with similar f1-score is achievable. On the other hand, only 92-93% maximum accuracy is obtained using linear classification criteria in 3 parameters space. The preliminary JUNO WIMP indirect detection sensitivity will also be presented.

S4 High Energy and Particle Physics - Board: O-S4-2 / **27**

Memorization and Prediction Capability of Interacting Phase Oscillators

Author: Chanin Kumpeerakij[None]

Corresponding Author: k.chanin.ku@gmail.com

Nonlinear dynamical systems, such as well-tuned recurrent neural networks, have proved a powerful tool for modeling temporal data. However, tuning such models to achieve the best performance remains an outstanding challenge, not least because of the complex behaviors that emerge from interacting microscopic constituents. Here, we consider a minimal model of two interacting phase oscillators coupled to a thermal bath and driven by a common signal. We quantify the memory and predictive capability of the system with the mutual information between the phases of oscillators and the signals at different times. We show that the interaction between oscillators can increase the information between the system and the signal. We attribute this behavior to an increase in the effective signal-to-noise ratio, resulting from a stronger correlation between the oscillators. Our work offers a first step toward a systematic approach to optimize interacting nonlinear dynamical systems for memorizing and predicting temporal patterns.

S4 High Energy and Particle Physics - Board: O-S4-46 / **98**

Orion's Magnetic Gems

Authors: Evgenii Semenko[None]; Iosif Romanyuk[1]; Ilya Yakunin[1]; Dmitry Kudryavtsev[1]; Anastasia Moiseeva[1]

[1] *SAO RAS*

Corresponding Author: eugene@narit.or.th

We present the results of the most complete up-to-date spectropolarimetric survey of early-type peculiar (CP) stars in the association Orion OB1. The final sample contains 31 magnetic stars or 55% of the whole CP population in Orion OB1. For 14 CP stars, the longitudinal magnetic field exceeding approximately 500 G was detected for the first time. We show that the percentage of the magnetic CP stars and the field strength drop sharply with age. The mean longitudinal magnetic field in the young subgroup OB1b (log t=6.23) is confidently three times stronger than in the older subgroups OB1a (log t=7.05) and OB1c (log t=6.66). We conclude that the observed trends come from the different initial conditions in star formation regions. Meantime, in the Orion Nebula, a place with the youngest stellar population (log t < 6.0), the magnetic field appeared only in 20% of CP stars. Such occurrence drastically differs from 83% of magnetic CP stars in the nearby subgroup OB1c. We consider this effect an observational bias caused by the significant portion of the very young population with the signatures of Herbig Ae/Be stars.

S4 High Energy and Particle Physics - Board: O-S4-23 / **145**

Solar gamma-ray analysis during the latest solar cycle using FERMI-LAT data

Authors: Daiki Hazama[None]; Jitpanu Arunotai[None]

Co-authors: Thanyanan Somnam ; Suttiwat Madlee ; Anucha Pratumma

Corresponding Authors: daiki.haz_g30@mwit.ac.th, jitpanu.aru_g30@mwit.ac.th

The Sun is a well-known source of gamma rays emitted from cosmic rays during solar activity. It exhibits the variations over an approximately 11-year cycle due to the changes in the Sun's magnetic field. In this work, we studied photons of energy of 0.1 – 10 GeV from the Sun disk detected by the Large Area Telescope (LAT) onboard of the *Fermi* Gamma-ray Space Telescope (*Fermi*), moving in the low-earth orbit at an altitude of about 550 km. We present the solar gamma-ray variations during the latest solar cycle between 2009 and 2021 of the latest versions of the LAT event selection (Pass 8). The results show the relationship between the solar gamma rays and the number of sunspots. This study provides a better understanding of the solar gamma rays, solar magnetic activity, and cosmic rays.

S4 High Energy and Particle Physics - Board: O-S4-41 / **165**

Auroral Initial Brightening and Maximum Poleward Expansion Locations based on POLAR/VIS and POLAR/UVI Observations

Author: Suwicha Wannawichian[1]

Co-author: Yukinaga Miyashita [2]

[1] *Department of Physics and Materials Science, Chiang Mai University*

[2] *Space Science Division, Korea Astronomy and Space Science Institute, Daejeon, Republic of Korea, Department of Astronomy and Space Science, Korea University of Science and Technology, Daejeon, Republic of Korea*

Corresponding Author: suwichawan@gmail.com

The locations of Earth's auroral initial brightening and maximum poleward expansion are indicated as the magnetic latitudes, when the auroral breakup is expected to occur at magnetic local time between 22:00-1:00. Auroral images taken by the Visible Imaging System (VIS) and the Ultraviolet Imager (UVI) instruments onboard POLAR spacecraft reveal the variation of the locations that different auroral phases, initial brightening and maximum poleward expansion, took place. From different substorm events, the locations of the auroral phases appear to be highly variable. Quantitative analysis of the times and locations of both phases are presented via the time-series plots, keograms, and intensity profiles, for VIS; 557.7, 130.4, 391.4, 630.0 nm and for UVI; lbhl, lbhs, 130.4, and 135.6 nm emissions. For aurora associating with low-energy, "soft", precipitating electrons, the responsive auroral emissions were shown in Polar/VIS 3914 Å, Polar/VIS 5577 Å, and Polar/VIS 6300 Å. On the other hand, the FUV auroras are presented in Polar/UVI images, representing the results of higher energy precipitating auroral particles (mostly electrons). Those visible auroras appear to be mostly expansive to higher latitude in comparison to the FUV auroras. The different locations of the auroral initial brightening and the less extensive FUV aurora are due to the different origins and distributions of high energy electrons in the magnetotail. Moreover, the location variation for different substorm events, in corresponding to the solar wind conditions, will be discussed.

S4 High Energy and Particle Physics - Board: O-S4-4 / **57**

Charmed baryon pair production in effective Lagrangian and Regge approaches

Author: Thanat Sangkhakrit[1]

Co-authors: Sang-In Shim [2]; Yupeng Yan [3]; Atsushi Hosaka [4]

[1] *School of Physics and Center of Excellence in High Energy Physics and Astrophysics, Suranaree University of Technology and Research Center for Nuclear Physics, Osaka University*

[2] *Research Center for Nuclear Physics, Osaka University*

[3] *School of Physics and Center of Excellence in High Energy Physics and Astrophysics, Suranaree University of Technology*

[4] *Research Center for Nuclear Physics, Osaka University and Advanced Science Research Center, Japan Atomic Energy Agency*

Corresponding Author: tanattosan@outlook.jp

Strange and charmed baryon pair productions in proton-antiproton collisions are studied in effective Lagrangian and Regge approaches. Unknown parameters from both models are determined from the comparison with the existing data for strangeness productions. Then, we predict charm production cross sections by extrapolating the amplitudes for strangeness productions to those for charm. From our study, charm production cross sections are about 10^{-4} to 10^{-5} times smaller than those of strangeness productions. Our results can be tested in the future experiments at $\bar{\text{P}}$ANDA.

S4 High Energy and Particle Physics - Board: O-S4-5 / **66**

Parameters of a potential model for tetraquarks from S- and P-wave charmonium mesons

Author: Nattapat Tagsinsit[None]

Co-authors: Zheng Zhao ; Christoph Herold [1]; Yupeng Yan [1]; Kai Xu

[1] *Suranaree University of Technology*

Corresponding Author: nattapattagsinsit@gmail.com

The masses of low-lying S-wave and P-wave charmonium mesons are evaluated in a constituent quark model (CQM) where the Cornell-like potential and Breit-Fermi interaction are employed. All model parameters are imported from the previous work of S-wave meson mass calculation. Two sets of complete bases are constructed by using the harmonic oscillator wave function, and the Sturmian wave function, respectively. In the calculations, the bases size is $N = 38$, and the length parameters of the complete bases are adjusted to determine the eigenvalues. The thus established model with one set of parameters may be applied to study higher excited meson states as well as tetraquark systems.

S4 High Energy and Particle Physics - Board: O-S4-6 / **81**

Review of Fluid-Gravity Correspondence

Author: Thepprasith Svetatula[None]

Corresponding Author: lnwphysics96@gmail.com

Fluid-Gravity correspondence is an effective theory of AdS-CFT correspondence in a long-wavelength regime. The correspondence represents the map between Einstein equations in AdS bulk and hydrodynamics on the boundary. In particular, we demonstrate the construction of the energy-momentum tensor of the fluid on the boundary from various types of black holes in the bulk of AdS spacetime up to the first order in derivative expansion.

S4 High Energy and Particle Physics - Board: O-S4-7 / **107**

Search for BSM Higgs bosons using Machine Learning techniques

Authors: Jinna Waiwattana[1]; Natha Pitakkultorn[1]; Pakorn Saksirimontri[1]

Co-authors: Chayanit Asawatangtrakuldee [2]; Vichayanun Wachirapusitanand [2]

[1] *Mahidol Wittayanusorn School*

[2] *Chulalongkorn University (TH)*

Corresponding Authors: jinnawaiwattana@gmail.com, pimpicha.pit_g30@mwit.ac.th, pakorn.sak_g30@mwit.ac.th

Although the discovery of the 125 GeV Higgs boson has confirmed the Higgs mechanism of the Standard Model (SM), many theories beyond the Standard Model (BSM) has been introduced to solve several phenomena not explained by the SM. One example is the Two Higgs Doublet Models (2HDM), the simplest extension of the SM Higgs sector, that predicted the existence of additional Higgs bosons. In this study, we investigate the use of supervised learning of machine learning method which is hypothesized to be more effective than traditional cut-based method, to search for BSM Higgs bosons decaying into bottom-antibottom quark pairs ($H \rightarrow bb$), the dominant Higgs boson decay channel. We train machine learning models to classify whether events detected by the detector belongs to $H \rightarrow bb$ process (signal) or multijet process (background) based on simulated proton-proton collisions within the Compact Muon Solenoid (CMS) detector. The evaluation matrix is calculated to compare the classification efficiency of models using Neural Networks (NN) and Tree based models. The results show that machine learning models can classify signal and background processes with significant improvement and can be used as signal-background discriminator for further statistical analyses searching for BSM Higgs bosons.

S4 High Energy and Particle Physics - Board: O-S4-8 / **113**

Proton Track reconstruction in a Telescope for Proton Computed Tomography

Author: Arnon Songmoolnak[1]

Co-authors: Chinorat Kobdaj [2]; Christoph Herold [1]; Dieter Roehrich [3]; Ralf Keidel [4]; Helge Egil Seime Pettersen [5]; Denis Petrov [6]

[1] *Suranaree University of Technology*

[2] *Suranaree University of Technology (TH)*

[3] *University of Bergen (NO)*

[4] *Fachhochschule Worms (DE)*

[5] *Haukeland University Hospital*

[6] *University of Applied Sciences Worms*

Corresponding Author: d5910212@g.sut.ac.th

Proton computed tomography (pCT) is a medical scanning technology suitable for treatment planning of proton therapy. Suranaree University of Technology, together with the Bergen pCT collaboration, is currently constructing a pCT prototype for clinical trials. This study aims to reconstruct proton tracks generated from a Monte Carlo simulation which can be applied to 3-dimensional image reconstruction. Our simulation is built on Geant4 via Gate toolkits. We analyze a simultaneous irradiation of the telescope with the KCMH proton beam implementing a track following algorithm written in python. Hereby, each node or hit point will identify its subsequent node within the next detector layer as the one within minimum distance. We fix the ratio of the number of reconstructed track hits to Monte Carlo hits at 75%. The pencil beam at 220MeV has 3.3 mm of spot sigma. With 200 primary protons in simulation, the reconstruction efficiency can achieve 84%.

S4 High Energy and Particle Physics - Board: INV-S4-2 / **360**

Highlights of LHC Run-2 and Preparation for Run-3 and High Luminosity LHC

Author: Norraphat SRIMANOBHAS[None]

Corresponding Author: phat.s@cern.ch

Starting from June 2022, LHC will start Run-3 with proton collisions at 13.6 TeV. In this talk, highlight results from LHC Run-2 will be presented. The physics plan for Run-3 for both LHC and non-LHC experiments to be discussed. In addition, we will also discuss on the plan for high luminosity LHC which is expected to start in 2029.

S4 High Energy and Particle Physics - Board: O-S4-24 / **179**

\emph{Gaia} Early Data Release 3 peculiar velocity distribution of Galactic high-mass x-ray binaries

Author: Pornisara Nuchvanichakul[1]

Co-authors: Poshak Gandhi [2]; Christian Knigge [2]; Puji Irawati [3]; Suwicha Wannawichian [4]; Zhao Yue [2]

[1] *Chiang Mai university*

[2] *University of Southampton*

[3] *National Astronomical Research Institute of Thailand*

[4] *Chiang Mai University*

Corresponding Author: pornisara_nuc@cmu.ac.th

High-mass X-ray binaries (HMXBs) are systems in which a neutron star or black hole accretes material from a massive companion. They can be roughly divided into three main classes: (i) wind-fed compact objects with supergiant donors; (ii) compact objects accreting from the decretion disc of a Be star; (iii) compact objects accreting via a disc from a Roche-lobe filling companion. All HMXBs must have experienced a core-collapse supernova event during their evolution. The kick associated with this event should affect the space velocity of the system in a way that depends on the state of the binary at the time of the explosion. Here, we test whether the different evolutionary histories of HMXBs have left a detectable imprint on their peculiar velocities. Using data from Gaia Early Data Release 3 (Gaia EDR3), we first calculate the peculiar velocities (V_p) and associated uncertainties for 55 well-known HMXBs. The peculiar velocity distribution shows some evidence for bimodality, suggesting the existence of two distinct populations: one characterised by low velocities ($< 50\,\mathrm{km\,s^{-1}}$), the other characterised by high velocities ($> 50\,\mathrm{km\,s^{-1}}$). The existence of a high-velocity population is surprising for such massive systems. We use Monte Carlo simulations to set firm lower limits on V_p for all of our targets, finding that at least 5 systems in our sample have $V_p > 75\,\mathrm{km\,s^{-1}}$ at probability (p) $< 2e^{-5}$.

S4 High Energy and Particle Physics - Board: O-S4-25 / **181**

Analysis of the gamma-ray halo candidate 3HWC J1928+178 with Fermi-LAT data.

Authors: Supphakit Wiweko[None]; Armelle Jardin-Blicq[1]; Maneenate Wechakama[2]

[1] *NARIT*

[2] *Kasetsart University*

Corresponding Author: supphakit.w@ku.th

The detection of a very extended gamma-ray emission around the Geminga and Monogem pulsars at TeV energies has set a new class of gamma-ray sources called gamma-ray halo. These objects are characterised by the presence of a rather old pulsar (~100 kyr), emitting electrons and positron that are escaping and diffusing away into the interstellar medium, producing a large scale gamma-ray emission by inverse Compton scattering. A gamma-ray halo has also been detected at GeV energy around Geminga by the Fermi-LAT. Appart from Geminga and Monogem, a few other gamma-ray halo candidates have been proposed, amongst them the TeV source 3HWC J1928+178 detected by HAWC.
In this contribution, I present the analysis of the region of 3HWC J1928+178 with 13 years of fermi-LAT data, in order to assess the presence of a gamma-ray halo around 3HWC J1928+178 at GeV energies.

S4 High Energy and Particle Physics - Board: O-S4-26 / **183**

Investigation of Open Cluster NGC 7789 Using GAIA EDR3 Data

Authors: Jason Kalaw[1]; Princess Tucio[1]; Ryan Manuel Guido[None]

[1] *Rizal Technological University*

Corresponding Author: pbtucio@rtu.edu.ph

We present the initial study on the membership determination of the open clusters in Cassiopeia. Proper motion and parallax of stars collected in the Gaia Early Data Release 3 are used to derive the cluster members by employing the Hierarchical Density-Based Spatial Clustering of Applications with Noise (HDBSCAN) algorithm which is further improved upon using a Gaussian Mixture Model. We showed that HDBSCAN is great for determining values while GMM is great for determining the frequency and degree of a star's membership in a cluster. We calculate the parallax and distance of the NGC 7789 cluster center to be 0.1994 ± 0.11 mas and 18637 ± 333110 pc respectively. The position of the cluster center is calculated to be α = 359 ′16 ,″56.44 δ = 56 ′42 ″38.46 and proper motion to be μα = -1.386 ± 0.68 mas/yr and μδ = -1.052 ± 0.37 mas/yr. Our results are consistent as well with the known values from the previous studies. The stars in NGC 7789 show very little movement on proper motion and might be caused by fainter observations. The cluster is peppered with younger stars in the main phase sequence with several blue stragglers and redder stars in the turnoff region.

S4 High Energy and Particle Physics - Board: O-S4-9 / **115**

Modification of hadron multiplicity ratios at the chiral phase transition

Authors: Christoph Herold[1]; Thiranat Bumnedpan[None]; Jan Steinheimer[None]

[1] *Suranaree University of Technology*

Corresponding Author: thiranat.b6119577@gmail.com

We investigate the impact of a first-order chiral phase transition and critical point on hadron multiplicity ratios. We model the dynamical expansion of the hot and dense matter created in a heavy ion collision with a Bjorken hydrodynamics expansion coupled to the explicit evolution of the chiral order parameter at center-of-mass energies from 2 to 10 GeV. Hereby, the chiral dynamics is implemented using a Langevin equation including dissipation and noise. We find a strong enhancement of the entropy-per-baryon S/A at lowest energies which is created at the non-equilibrium first-order phase transition. By mapping the initial and final S/A to a hadron resonance gas, we are able to quantify the shift of hadron multiplicity ratios.

S4 High Energy and Particle Physics - Board: O-S4-10 / **134**

Non-minimal scalar field coupling to gravity with holographic effect in non flat universe

Author: Amornthep Tita[None]

Corresponding Author: amornthepti61@nu.ac.th

We investigate scalar field minimally coupled to gravity in the framework of holographic dark energy with apparent horizon cutoff in non flat universe. Dynamics of the model are studied by rewriting the Friedmann equation which modified by holographic effect in the form of autonomous differential equations system. In the model, we consider in pure kinetic ($V(\phi) = 0$), power law potential ($V(\phi) = V_0\phi^2$), and exponential one ($V(\phi) = V_0e^{-\alpha\phi}$). We obtain fixed points and also analyze the nature and their stability of each fixed points. We found that de Sitter attractor solutions which corresponds to the dark energy era are obtained in the case of non minimal coupling scalar field with powerlaw and exponential potentials in flat universe.

S4 High Energy and Particle Physics - Board: O-S4-27 / **195**

Unveiling Circumstellar Structure of High-mass Protostars via Multiple Species of MASERs in KaVA-LP with EAVN

Authors: Koichiro SUGIYAMA[1]; Tomoya HIROTA[2]; Kee-Tae KIM[3]; Kitiyanee ASANOK[4]

Co-authors: Jungha KIM [5]; Ross A. BURNS [6]; Busaba H. KRAMER [7]; Thanapol CHANAPOTE [4]; Andrey M. SOBOLEV [8]; Montree PHETRA [9]; Taufiq HIDAYAT [10]; Zulfazli ROSLI [11]; Mohammad HAFIEDUDDIN [12]; KaVA Science Working Group members SFR

[1] *NARIT: National Astronomical Research Institute of Thailand (Public Organization), Thailand*

[2] *NAOJ: National Astronomical Observatory of Japan, Japan*

[3] *KASI: Korea Astronomy and Space Science Institute, Republic of Korea*

[4] *NARIT, Thailand*

[5] *KASI, Republic of Korea*

[6] *NAOJ, Japan; KASI, Republic of Korea*

[7] *Max Planck Institute for Radio Astronomy, Germany; NARIT, Thailand*

[8] *Ural Federal University, Russia*

[9] *Chiang Mai University, Thailand*

[10] *ITB: Institut Teknologi Bandung, Indonesia*

[11] *Universiti Malaya, Malaysia*

[12] *ITB, Indonesia*

Corresponding Author: koichiro@narit.or.th

Circumstellar structures, such as inclination and opening angles of outflow/jet cavities, thickness and flaring angle of disk surrounding an central object, and so on, is crucial to understand formation processes of high-mass stars and their evolution more quantitatively by determining a spectral energy distribution (SED) accurately that provides us information of the spectral types and to investigate evolutionary phases of high-mass stars. The science working group for star formation researches in KaVA (KVN and VERA Array) has thus initiated a large program (LP) of multi-epoch very-long-baseline-interferometry (VLBI) monitoring studies toward high-mass protostars with multiple species of MASERs (microwave amplification by stimulation emission of radiation) using KaVA, in which each different species maser possibly traces each different significant phenomenon in jet/outflow/disk (T. Hirota, K.-T. Kim, et al.: https://radio.kasi.re.kr/kava/large_programs.php\#sh3). This VLBI monitoring has enabled us to measure proper motions of the maser emissions on the sky plane and understand 3-dimensional (3-D) spatial/velocity structures and dynamics on the circumstellar structures. In this presentation, we would like to show the outline of this large program and the progress for one of follow-up observations: imaging survey and monitoring observations of the 6.7 GHz methanol masers with the East-Asian VLBI Network (EAVN). These EAVN follow-up observations have been conducted in the 2021A open-use semester for 11 target sources that were selected from KaVA-LP source list, and we succeeded imaging their spatial/velocity distributions in 4 sources, in which a source presented a structure evoking an association with a disk and accurate absolute coordinates for some sources were obtained with phase-referencing technique as well. We will also touch the on-going EAVN open-use monitoring in the 2022A semester to measure 3-D structures for the detected high-mass protostars.

S4 High Energy and Particle Physics - Board: O-S4-11 / **143**

The production of charged particles and the kaonic nuclei K-p, K+anti-p in pp collisions at √(s) = 7 TeV and K-pp, K+anti-pp in Au + Au collisions at beam energy 130 GeV

Author: Natthaphat Thongyoo[1]

Co-authors: Pornrad Srisawad [2]; Kristiya Tomuang [3]; Panadda Sittiketkorn [4]; Phacharatouch Chaimongkon [5]; Yu-Liang Yan [6]; Ayut Limphirat [7]; Chinorat Kobdaj [7]; Yupeng Yan [7]

[1] *Physics Naresuan University*

[2] *Naresuan university*

[3] *General Education, Siam Technology College*

[4] *Faculty of Science and Technology, Nakhon Sawan Rajabhat University*

[5] *Department of Physics, School of Science, University of Phayao*

[6] *China Institute of Atomic Energy*

[7] *School of Physics, Suranaree University of Technology*

Corresponding Author: arm_smart_pp@hotmail.com

Abstract. We study the production of charged particles and the kaonic nuclei K^-p, $K^+\overline{p}$ in pp collisions at $\sqrt{s_{NN}}$ = 7 TeV and K^-pp, $K^+\overline{pp}$ in Au + Au collisions at beam energy 130 GeV. The PACIAE model is used to calculate the charged particles, and the DCPC model is used to calculate the kaonic nuclei. Results showed that the yield of charged particles was consistent with ALICE and STAR experimental data. The yield per even of K^-p and $K^+\overline{p}$ are calculated to be the order of 10^{-3} . The yield per even of K^-pp was greater than the yield of $K^+\overline{pp}$. The kaonic nuclei K^-pp and $K^+\overline{pp}$ are probably formed by K^+(or K^-) directly trapping two protons (or antiprotons). Since there are no experimental data available on this observable at present, our work may provide a guide for future experiments.

S4 High Energy and Particle Physics - Board: O-S4-28 / **147**

Searching for dark matter with the Cherenkov Telescope Array.

Authors: Armelle Jardin-Blicq[1]; Chaimongkol Duangchan[2]; Chakrit Pongkitivanichkul[3]; Patipan Uttayarat[4]; Maneenate Wechakama[2]; Tanech Klangburam[3]; Wararat Treesukrat[4]; Daris Samart[3]; Utane Sawangwit[1]; Alejandra Aguirre-Santaella[5]; Miguel Sánchez-Conde[5]

[1] *NARIT*

[2] *Kasetsart University*

[3] *Khon Kaen University*

[4] *Srinakharinwirot University*

[5] *Autonomous University of Madrid*

Corresponding Author: armelle@narit.or.th

Thailand is involved in the next generation of Cherenkov Telescopes, the Cherenkov Telescope Array (CTA). Amongst the main CTA key science cases is the search for dark matter (DM). With a sensitivity one order of magnitude better than current instruments, CTA will be in a unique position to discover a DM signal in the GeV and TeV energy domain, or, in the absence of it, to significantly improve the current DM limits.
In this contribution, I will introduce the principle of gamma-ray detection from the ground using Cherenkov Telescopes and in particular CTA. I will illustrate the search for a signal from dark matter annihilation using simulated data from two dwarf spheroidal galaxies, Draco and Sculptor.

S4 High Energy and Particle Physics - Board: O-S4-12 / **159**

Anisotropic flow in Au + Au collision at 1 A GeV by using Quantum Molecular Dynamics Model

Author: Phacharatouch Chaimongkon[1]

Co-authors: Jiraphat Phusamlee [1]; Natha Onintr [1]; Nuttawut Kantham [1]; Natthaphat Thongyoo [2]; Pornrad Srisawad [2]

[1] *Department of Physics, School of Science, University of Phayao, Amphoe Muang, Phayao 56000, Thailand*

[2] *Naresuan University*

Corresponding Author: dewyphone37@gmail.com

Anisotropic flow in Au + Au collision at 1 A GeV using a quantum molecular dynamics model was concentrated. The direct flow of proton (v_1) as a function of rapidity (y_0) at intermediate energy around 1 A GeV and impact parameter from 0.25 to 0.45 fm with the nuclear equation of state (soft and hard equation of state) were computed and compared with FOPI experiment. The results showed that the direct flow of proton as a function of the rapidity with a soft equation of state was consistent with the FOPI data. The behavior of the nuclear equation of state at high temperature and high density could be explained by the calculation result of the proton flow from Au + Au collision at intermediate energy.

S4 High Energy and Particle Physics - Board: O-S4-29 / **151**

Selection efficiency of galactic-scale outflow at z ~0.1: Imaging vs Spectroscopy

Author: Kantapon Jensangjun[None]

Co-author: Suraphong Yuma [1]

[1] *Mahidol University*

Corresponding Author: kantapon.jen@student.mahidol.ac.th

Galactic-scale outflows driven by active galactic nuclei (AGNs) have been invoked to explain the quenching of star formation in massive galaxies. Large statistical outflow samples are required to study to fully understand their impact on galaxy evolution. The most traditional technique to distinguish the outflowing gas from non-outflowing gas is to detect the blueshifted-wings in the absorption and/or emission-line profiles as they represent the outflowing motion of the gas. However, this technique requires spectra with high signal-to-noise (S/N) ratio to decompose outflowing components. Over past decades, many researchers have developed a new technique to obtain a significant number of galaxies with large-scale outflow by reconstructing images of [O III]$\lambda\lambda 4949, 5007$ emission using narrowband and/or broadband images. Nevertheless, the gas kinematics of the outflows selected from this technique are less studied. To answer this question, we compare the selection efficiency of the galactic-scale outflows from broadband images and spectroscopy. We apply both of the outflow selection techniques to 165 local galaxies ($z \sim 0.1$) observed by the Mapping Nearby Galaxies at APO (MaNGA) survey, the latest integral-field spectroscopic survey of the Sloan Digital Sky Survey (SDSS). Fourty-seven ($\sim 28\%$) galaxies are classified as AGNs based on line diagnostic diagrams and multi-wavelength observations. We construct [O III] images using the SDSS broadband images together with a continuum subtraction of the galactic continuum. We find that the area of [O III] emission-line regions are positively correlated with the outflow velocities, as traced by the 98\% extent of Na ID $\lambda\lambda$5890,5896 absorption lines with a power-law slope of 0.64$\pm$0.16. We discuss the selection efficiency and applications of the broadband images to study the AGN feedback with large statistical samples.

S4 High Energy and Particle Physics - Board: O-S4-13 / **162**

Soliton Solution to Schamel-Korteweg-de Vries Equation with Shooting Method

Author: Chainarong Taepanich[1]

Co-authors: Boonlit Krunavakarn [1]; Sarun Phibanchon [2]

[1] *Department of Physics, Burapha University*

[2] *Faculty of Education, Burapha University*

The Schamel-Korteweg-de Vries (SKdV) equation is the equation which described weakly ion-acoustic wave in cold plasmas. The soliton solution to the Schamel-Korteweg-de Vries equation can be determined by the shooting method. The spectral method is applied to study the time evolution of this solution. This can experimentally confirm that the solution is stable.

S4 High Energy and Particle Physics - Board: O-S4-30 / **238**

Simulating AGN feedback and its evolution in galaxy mergers: case study for NGC 5252

Author: Manus Boonmalai[1]

Co-authors: Utane Sawangwit [2]; Suwicha Wannawichian [1]

[1] *Department of Physics and Materials Science, Chiang Mai University*

[2] *NARIT*

Corresponding Author: manusboonmalai@gmail.com

We use numerical simulations to study the evolution of merging galaxies. This study focuses on the AGN-driven feedback mechanism which could be responsible for outflow gas on kpc scales observed in Seyfert galaxies. The galaxy's initial conditions were created to mimic observational properties of a galaxy NGC 5252. The object is one of the interesting seyfert galaxies, showing an extended [OIII] emission out to ~10 kpc scales and appears to contain an off-nucleus ultraluminous X-ray (ULX) source, CXO J133815.6+043255, with optical spectral properties similar to Low-Luminosity AGNs (LLAGNs). The high angular resolution very long-baseline interferometry (VLBI) observations have also showed that it is a promising candidate of dual radio-emitting AGN system. Furthermore, the off-nucleus ULX component in the NGC 5252 is believed to be a stripped remnant of a merging dwarf. To study the formation and evolution of such a system, the supermassive black hole (SMBH) accretion physics module is employed in the smoothed-particle hydrodynamics (SPH) simulations of merging galaxies, using GIZMO code. We will report on the progress of our on-going study which will be focusing on possible configurations and properties of the merging galaxies, the evolutions of the merging pair and AGN feedback that results in the observed properties of the system.

S4 High Energy and Particle Physics - Board: INV-S4-3 / **359**

High Energy Astroparticles from Antarctica

Authors: Achara Seripienlert[None]; Waraporn Nuntiyakul[None]

Corresponding Author: waraporn.n@cmu.ac.th

Cosmic rays are high-energy particles from space, i.e., the sun, the supernova explosion of stars, and other currently unknown sources by processes that are not fully understood. Magnetic fields influence the propagation of these particles in the solar wind and the magnetosphere of the Earth. We can investigate changes in these magnetic fields by recording variations and fluctuations in the cosmic ray intensity. Ground-or-sea-based neutron monitors are a standard tool for detecting atmospheric showers from 20 GeV-range primary cosmic rays of either solar or galactic origin. Configurations of neutron detectors may not be completely identical, and these differences lead to different energy-dependent effective areas (yield functions). Near Polar regions, the earth's magnetic field is less effective in keeping cosmic rays from reaching the atmosphere than near the equator; so lower-energy particles from the sun are admitted. We, in Thailand, have developed portable neutron monitors to investigate the energy spectrum of cosmic rays during ocean voyages to/from Antarctica and its solar modulation, i.e., variations over the typically 11-year sunspot cycle. The interesting new findings from these voyages and future approaches will be discussed.

S4 High Energy and Particle Physics - Board: O-S4-31 / **245**

Earth microlensing zone: how safe is the Earth from long-range detection by other civilisations?

Authors: Supachai Awiphan[1]; Suphakorn Suphapolthaworn[2]; Tanawan Chatchadanoraset[3]; Eamonn Kerins[4]; David Specht[4]; Nawapon Nakharutai[5]; Siramas Komonjinda[5]; Annie Robin[6]

[1] *NARIT, Thailand*

[2] *Hokkaido University*

[3] *Chiang Mai University Demonstration School*

[4] *University of Manchester*

[5] *Chiang Mai University*

[6] *Institut Utinam*

Corresponding Author: supachai@narit.or.th

To detect distant, low-mass exoplanets, the microlensing technique has been proven to be one of the most successful techniques. On the other hand, to detect the Earth as a rocky planet in the Solar system, the other technological civilisations could also use the microlensing technique. Assuming that technological civilisations have equal chance to be located around any star anywhere in the Galaxy, we can define the "Earth microlensing zone" (EMZ) as the region of the sky from which observers may most likely see Earth's microlensing signal. The EMZ can be thought of as the microlensing analogue of the Earth Transit Zone (ETZ) from where observers see Earth transit the Sun. Just as for the ETZ, the EMZ could represent a game-theoretic Schelling point for targeted searches for extra-terrestrial intelligence (SETI). To compute the EMZ, the Gaia DR2 catalogue with magnitude G<20 is used to generate Earth microlensing probability and detection rate maps to other observers. We then show that Earth could be observable on average of thousands per year.

S4 High Energy and Particle Physics - Board: O-S4-32 / **246**

The Development of the Astrophysical Laboratory for the Study of Interstellar Surface Chemistry

Authors: Chutipong Suwannajak[None]; Sakhorn Rimjaem[1]; Monchai Jitvisate[None]; Watchara Jaikla[2]; Ukrit Keyen[3]; Apichat Leckngam[3]; Piyarat Nimmanpipug[1]; Thanapong Phimsen[4]; Nahathai Tanakul[3]; Pitch Wongkummoon[1]

[1] *Chiang Mai University*

[2] *NARIT*

[3] *National Astronomical Research Institute of Thailand (Public Organization)*

[4] *Synchrotron Light Research Institute (Public Organization)*

Corresponding Author: chutipong@narit.or.th

Interstellar complex molecules can be formed in interstellar molecular clouds during the process of star formation. Those complex molecules can be later delivered to planets to serve the role of the building blocks of life. Therefore, understanding the interaction and formation processes of those complex molecules in interstellar conditions is crucial to the understanding of the origin of life. Interstellar complex molecules are thought to be formed in a solid phase, on a surface of icy dust grains in molecular clouds. The regions where the formation of the complex molecules occurs are generally cold with temperatures below 100 K and pressure of 10^{-10} mbar. Here we present the development of the astrophysical laboratory to study interstellar surface chemistry. The laboratory includes an experimental station to mimic the extreme conditions of interstellar molecular clouds and computational modeling of the chemical processes that occur in the interested physical conditions. The experimental station will be located at the PBP-CMU Electron Linac Laboratory, with the collaboration between NARIT, CMU, SUT, and SLRI. The setup includes an ultra-high vacuum chamber pumped to 10^{-10} mbar as the main chamber for the experiments. Connected to the sample holder in the main chamber is a liquid nitrogen dewar to maintain the temperature of around 80 K. The water and the interested molecules are injected through the gas injection unit onto the cold surface of the substrate to form an interstellar ice analog. The chemical products will be probed with mid-IR and far-IR from the FTIR spectrometer by the MCT detector connected to the chamber. Finally, we present examples of the experiments that can be done with this experimental setup. The experiments will allow us to understand the structures, intermolecular interactions, and formation processes of the complex molecules in interstellar cloud environments.

S4 High Energy and Particle Physics - Board: O-S4-14 / **170**

On the effectiveness of relativistic electron Acceleration at geosynchronous orbit during high-intensity, long-duration, continuous AE activity (HILDCAA) during 2015 - 2017

Author: Thana Yeeram[1]

[1] *Department of Physics, Department of Physics, Geoinformatics and Space Technology, Mahasarakham University*

Corresponding Author: thana.y@msu.ac.th

This study investigates the enhancements of relativistic electron flux (MeV) in the outer radiation belt that can cause anomalies of geosynchronous satellite systems. The enhancements occurred during High Intensity, Long Duration, Continuous AE Activity (HILDCAA) of 12 events during 2015 - 2017. The relativistic electron (0.8 - 2.0 MeV) flux measured by GOES-13 satellite and low-energy electron (40-130 keV) flux measured by POES satellite are examined. Results reveal that, in the long recovery phase, the relativistic electron flux increases, while the low-energy electron flux decreases. Typically, the enhancements of E > 0.8 and > 2.0 MeV electrons occurred promptly and ~1.0 day after the HILDCAA onset, respectively. Case studies show that the peak flux of > 2.0 MeV occurred about 2 days after the onset of short-period HILDCAA, while it occurred 4 days after the onset of long-period HILDCAA. The HILDCAA events with high amplitude and long-lasting Alfven waves with low solar wind dynamic pressure are associated with the long-lasting of sporadic injection of low energy electrons into the nighttime magnetosphere during the period of prolonged substorm (AE) activity.

S4 High Energy and Particle Physics - Board: O-S4-33 / **259**

A Computational Study of the Gas-Phase Formose-Like Reactions under the Interstellar-medium-like conditions

Author: pitch wongkummoon[1]

Co-authors: Chutipong Suwannajak [2]; Ukrit Keyen [3]; Sakhorn Rimjaem [1]; Assoc.Prof. Piyarat Nimmanpipug [1]

[1] *Chiang Mai University*

[2] *National Astronomical Research Institute of Thailand (Public Organization)*

[3] *CSML, NARIT*

Corresponding Author: wongkummoonpitch@gmail.com

Understanding the extraterrestrial origin of ribose, as one of the subunits of ribonucleic acid (RNA), is crucial to anticipating the formation of the building blocks of life under interstellar medium conditions. Under ordinary atmospheric conditions, the formation of sugar is suggested to occur through the formose reaction, where formaldehyde is solely used as the precursor in each of the iterative steps of the processes. On the other hand, sugar synthesis under interstellar medium conditions has evidently been shown to be significantly different from the terrestrial formose reactions due to the extremely low density of molecules and the very low temperature. In this study, we theoretically investigate the formose-like reactions for ribose formation catalyzed by a single proton through the mean of computer simulation based on first-principles density functional theory (DFT). The ribose formation reactions are modelled in the absence of solvation effects at absolute zero temperature to mimic the extremely low pressure and temperature found in interstellar molecular clouds. We observe that the presence of a proton gives rise to a more thermodynamically stable complex of the two reactive carbonyl compounds by bridging their oxygen atoms as required for the iterative formose reaction to proceed. In order to form a new carbon-carbon bond through an iterative process, only the region where the additional formaldehyde attaches to the existed protonated carbonyl compound is of great importance. Similar energy barriers for all the iterative steps during the ribose formation have been observed to be approximately 67 kcal/mol. Our findings show that a single proton can act as an efficient catalyst for the gas-phase ribose formation reactions. The results suggest that ribose formation can preferentially occur via the formose pathway in the presence of protons, which are presented in interstellar clouds.

S4 High Energy and Particle Physics - Board: O-S4-15 / **240**

sine-Gordon expansion method for the kink solion to Oskolkov equation

Authors: Nupan Kheaomaingam[1]; Sarun Phibanchon[2]; Songvudhi Chimchinda[1]

[1] *Department of Physics, Faculty of Science*

[2] *Faculty of Education, Burapha University*

Corresponding Author: songvudhi@buu.ac.th

The solutions of sine-Gordon equation will be used as the series solution for determining the kink solution of Oskolkov equation. The matching coefficients and choosing the some parameters of the series can provide the suitable solution. The numerical calculation with the kink soliton as the initial condition shows the stable solution can be found by this expansion method.

S4 High Energy and Particle Physics - Board: O-S4-34 / **299**

Thai National Telescope pointing and tracking: An analysis using secondary data product from science observation

Author: Puji Irawati[1]

Co-authors: Supachai Awiphan [2]; Vasu Kengkriangkai ; Somsawat Rattanasoon ; Eugene Semenko ; Apichat Leckngam ; Wiphu Rujopakarn ; Saran Poshyachinda ; Boonrucksar Soonthornthum

[1] *National Astronomical Research Institute of Thailand*

[2] *NARIT, Thailand*

Corresponding Authors: puji.irawati@narit.or.th, supachai@narit.or.th

The National Astronomical Research Institute of Thailand (NARIT) is currently developing new low resolution and high-resolution spectrographs for the Thai National Telescope. These instruments will be used for follow-up observations for spectral type characterisation and exoplanet detections. Such observation typically will need long exposure (> 1 hour) where the target has to stay inside the slit of the spectrograph during the observation. Therefore, information on the pointing accuracy and the tracking performance of the telescope is essential as part of the preparation works for these two instrumentations.

To gather these information, we look into past science data collected with the 2.4-m telescope between 2014 to 2022. These photometric data are then re-analysed to obtain the pointing coordinates and the x-y position of the target on the CCD. We choose only science data where the observations cover at least 4 hours or longer for the tracking analysis.

Our results show that the Thai National Telescope has a satisfactory pointing accuracy where in most cases, the targets are positioned within 5-40 arcseconds from given coordinates. While such accuracy is acceptable for photometric observation, it will pose a problem for the spectrographs because the width of the slit is usually only a few arcseconds. As for the tracking, we found that the telescope has a good tracking (drift <5 arcsec/hour for ULTRASPEC) with an exception for targets near the zenith with declination close to 18^{\circ}. However, we also found that the tracking after 2019 is worse compared to previous years. Further investigations are needed to find the cause of this issue.

S4 High Energy and Particle Physics - Board: O-S4-16 / **278**

Bianchi Cosmological Model with Quadratic Equation of State

Authors: Bjorn Jasper Raquel[1]; Willie Anthony Sapalaran[1]; Ludek Jirkovsky[2]

[1] *Rizal Technological University*

[2] *Institute of Business and Technology*

Corresponding Author: bjornjasper1@gmail.com

Recent discoveries regarding the existence of the large–scale structures in the universe, especially on the scales where the Cosmological Principle is expected to be accurate, pose a challenge to the Standard Model of Cosmology (ΛCDM model). These structures extend beyond 200 – 300 Mpc (Haines, Clowes, and Campusano, 2000; Gott III et al., 2005; Clowes et al., 2013; Horváth, Hakkila, and Bagoly, 2014, Lopez et al., 2021) provide strong evidence of anisotropy against the ΛCDM model as there should not be clumping of objects within that scale. The work of Migkas et al. (2020, 2021) also observed a similar anisotropic behavior of galaxy clusters towards a particular direction in the night sky. However, there is still no clear explanation for how to explain these observations. From this, the researcher aims to describe these anisotropies and their nature by viewing them through a theoretical lens.

S4 High Energy and Particle Physics - Board: O-S4-35 / **303**

Discovery of tsunami-like pulsation waves in the very fast rotating A-type stars

Author: David Mkrtichian[1]

[1] *NARIT*

Corresponding Author: davidmkrt@gmail.com

I will present the first result of our project on the search for high-degree nonradial pulsations in the very fast rotating bright A-f stars.
These pulsations look like the tsunami waves running over the stellar equator to the direction of rotation (prograde waves).
To search for the pulsating candidates, we used the photometric data from the NASA space telescope TESS and the high- and medium-resolution spectroscopy obtained with 2m class telescopes located in Europe and with the Thai National Telescope.
For all candidate stars, we discovered prograde waves having very large amplitude on the surface. We discussed the identification of the spatial structure of these oscillations.

S4 High Energy and Particle Physics - Board: O-S4-17 / **293**

Generalised Uncertainty Relations and the Problem of Dark Energy

Author: Matthew J. Lake[1]

[1] *National Astronomical Research Institute of Thailand (NARIT)*

Corresponding Author: matthewjlake@narit.or.th

We outline a new model in which generalised uncertainty relations, that govern the behaviour of microscopic world, and dark energy, that determines the large-scale evolution of the Universe, are intrinsically linked via the quantum properties of space-time. In this approach the background is treated as a genuinely quantum object, with an associated state vector, and additional fluctuations of the geometry naturally give rise to the extended generalised uncertainty principle (EGUP). An effective dark energy density then emerges from the field that minimises the modified uncertainty relations. These results are obtained via modifications of the canonical quantum operators, but without modifications of the canonical Heisenberg algebra, allowing many well known problems associated with existing GUP models to be circumvented.

S4 High Energy and Particle Physics - Board: O-S4-36 / **349**

Mock HI-galaxy catalogs and HI Mass Functions for future large-scale surveys

Authors: Narenrit Thananusak[None]; U Sawangwit[1]

[1] *National Astronomical Research Institute of Thailand (NARIT)*

Corresponding Author: n.thananusak@gmail.com

The 21-cm neutral hydrogen (HI) survey is an important probe for cold gas and galaxy evolutions in the local and low-redshift universe. One of the key measurements used to study evolution and properties of local star-forming galaxies is the HI mass function (HIMF). Among the interested topics in modern astrophysics, the study could potentially shed more light and offer explanations for the discrepancy between the ΛCDM standard model prediction and observed HI-galaxy number density (e.g. ALFALFA, HIPASS). The simulation also over-predicted the abundance of small satellite and low-mass galaxies. Both problems still requires sensitive instruments for more larger and deeper HI surveys to detect the populations of low-mass HI-galaxy. Currently, the HI-galaxy surveys could only reach down to $\sim 10^7$ Solar mass ($M_\odot$). Since, the next-generation radio surveys such as FAST or Australian Square Kilometer Array Pathfinder (ASKAP) will provide deeper any more sensitive data for reaching lower HI-mass and high-redshift HI-galaxies. The HI source catalogs from cosmological simulation (mock catalogs) are used to determine the expected HIMF from the upcoming HI surveys. We aim to compare the variability in the HIMF obtained from various mock catalogs, which were simulated with different parameters and purposes. This work also demonstrates the dissimilarities between the HIMF from recent semi-analytic model and the observed HIMF. Moreover, we aim to create an accurate mock catalog for the upcoming large HI-galaxy survey with the focus on calibrating the calculation of HIMF using both $1/V_{\rm max}$ and 2DSWML determination methods. We therefore determined the HIMF from various mock catalogs (e.g. Multidark, Boishoi and Millennium), which the HI mass was evaluated by using the cold gas mass for each object. We found that the HIMF are relatively diverse on $\leq 10^7 M_\odot$ HI mass compare to the observed HIMF, which could be the effect of the mass resolution of the mock catalogs.

S4 High Energy and Particle Physics - Board: O-S4-18 / **363**

Geometrical representation of the multi-dimensional consistency : 1-form case

Author: Thanadon Kongkoom[1]

Co-author: Sikarin Yoo-Kong [1]

[1] *The Institute for Fundamental Study (IF) Naresuan University, Phitsanulok, Thailand, 65000.*

A new notion of integrability called the multi-dimensional consistency for the integrable systems with the 1-form structure is captured in the geometrical language both in classical and especially quantum realms. A zero-curvature condition, which implies the multi-dimensional consistency, will be a key relation in context of Hamiltonian operator. Therefore, the existence of the zero-curvature condition directly leads to the path-independent feature in a mapping (which will be expressed in terms of the Wilson line), namely unitary multi-time evolution operators in the Schrödinger picture, introduced to alternatively capture integrability of the systems. Another important result is the formulation of the continuous multi-time propagator. This new type of the propagator exhibits the path-independent feature on the space of time variables. Consequently, a new perspective on summing all possible paths unavoidably arises as not only all possible paths on the space of dependent variables but also on the space of independent variables must be taken into account.

S4 High Energy and Particle Physics - Board: O-S4-37 / **36**

The Hubble tension problem with variation of the speed of light from Pantheon supernova dataset

Author: Teeraparb Chantavat[1]

[1] *Naresuan University*

Corresponding Author: teeraparbc@nu.ac.th

We investigate how the local and temporal variation in the speed of light may help alleviating the Hubble tension problem. The idea is motivated from the observed variation in the fine structure constant from spectra of quasar absorption systems which could potentially be caused by the change in the speed of light. To test the hypothesis, we use the data from Pantheon Supernova which contains 1,048 spectroscopically confirmed type Ia supernova within redshift range $0.01 < z < 2.3$. From our model, we find that the variation in the local speed of light $\Delta c/c = (-1.63 \pm 2.65) \times 10^{-5}$ and the temporal variation in the speed of light is $(1/c)(\mathrm{d}c/\mathrm{d}t) = (5.45 \pm 4.37) \times 10^{-20}$ year^{-1} which gives a slightly better constraint from any measurements to date. It is still inconclusive whether the data prefers larger or lower value of the speed of light in the past due to a large uncertainty. However, in all our models of variation in the speed of light, the Hubble tension problem is alleviated by having a lower value of H_0 at 69.84 ± 3.94 km s^{-1} Mpc^{-1} and $\sim 1\sigma - 2\sigma$ difference to the early-time value. Such a simple model has a potential leading to our better understanding of how the Hubble tension arises and our presumption to the laws of physics which may not hold true across the cosmic time.

S4 High Energy and Particle Physics - Board: O-S4-19 / **12**

Tension in rope coiling on a rotating plane

Author: Sitichoke Amnuanpol[None]

Corresponding Author: sitichok@tu.ac.th

Coiling of rope, fed from a height onto a rotating plane, progresses through a sequence of shapes, a hypotrochoid to an epitrochoid to a circle as frequency of plane increases. Feeding velocity controls the rate of length deposition on a plane and frequency of plane controls the rate of length transfer from a contact point, where rope first touches a plane. Formation of secondary loops of a hypotrochoid or an epitrochoid results from the faster deposition rate than the transfer rate. When these two rates are comparable, secondary loops disappear so the shape returns to a circle like in rope coiling on a static plane. In a reference frame corotating with rope, the Coriolis and centrifugal forces act only at the contact point, not extending to the portion of rope far above a rotating plane. For small deflection of rope, tension is inferred from the equations of motion with using the radius and frequency of a primary loop measured in experiments. Tension changes continuously at both the hypotrochoid-epitrochoid transition and the epitrochoid-circle transition, reminiscent of the features of a second order phase transition.

S4 High Energy and Particle Physics - Board: O-S4-38 / **79**

Improving Constraint on Evolution of Galaxies with Large-scale Outflow at z<1.5 with Subaru/Hyper Suprime-Cam Survey

Author: Suraphong Yuma[1]

[1] *Mahidol University*

Corresponding Author: suraphong.yum@mahidol.edu

It is widely believed that star-forming spiral galaxies stop their star formation activity and eventually evolve into the passively evolved elliptical galaxy. One of the key factors is the gas outflowing process that depletes the star-forming ingredient in the galaxy. In 2017, we reported the systematic search for large-scale outflowing galaxies at $z = 0.1 - 1.5$ covering the past 9 billion years of the universe. However, due to the small comoving volume at low redshifts, we could not detect any candidates at $z < 0.40$. In this study, we redo the search with newly available imaging data from Subaru/Hyper Suprime-Cam legacy survey. We found 819 candidates with large-scale outflow at $z = 0.1 - 1.5$. The number of samples increases more than 10 times as compared with the previous study. With this new result, we can make a meaningful constraint on the evolution of galaxies with gas outflow on a scale large enough to go beyond their stellar component. We also found that extended emission indicating the gas outflow is rather concentrated in the galaxy cluster than in the individual galaxy. Further study with follow-up spectroscopic observations shows that the gas outflow found in most samples originates from the intense star formation in a density-bounded ionization state without any evidence of fast radiative shock.

S4 High Energy and Particle Physics - Board: O-S4-20 / **14**

Investigation of perturbation effects on the periastron shifts of stellar orbits around super-massive black hole

Author: Bhattaradon Sukon[1]

Co-authors: Tirawut Worrakitpoonpon [2]; Poemwai Chainakun [2]

[1] *Suranaree University of Technolgy*

[2] *Suranaree University of Technology*

Corresponding Author: sut.t2n@gmail.com

Understanding of the dynamics of stars around the black hole is still incomplete. The Hubble Telescope discovered an evidence of the orbits of stars in the galactic centre that do not follow the Kepler's laws. In this work, we study the classical effects on the periastron shift. We select the Hernquist potential function for the galactic bulge to examine the rate of change of periastron angular position. We propose a computational approach based on the principle of classical mechanics to study that shift. As a result, we find that the initial speed of the star affects the orbit shape. For a selected initial speed, we get a precession rate of approximately 0.69, in arbitrary units. We expect that our numerical method is able to apply to other models of galaxies.

S4 High Energy and Particle Physics - Board: O-S4-43 / **256**

Study on halo structure of Helium-6 nuclei

Author: Chanatip Yensoung[1]

Co-author: Ruchipas Bavontaweepanya [1]

[1] *Department of Physics, Faculty of Science and Technology, Thammasat University*

Corresponding Author: chanatip.yen@gmail.com

The cosmos consists of various elements, which have many different isotopes. Some of those isotopes are stable nuclei, but some of those are radioactive nuclei. However, some radioactive isotopes have exotic properties, and these nuclei cannot be explained by the shell model. In this work, we studied the light neutron-rich nuclei, He-6, by using the halo structure model. We applied the Wood-Saxon potential and the hyperbolic cosine potential to calculate the nuclear density. We also compared our calculation results to the experimental results of He-6.

S4 High Energy and Particle Physics - Board: O-S4-21 / **23**

The effect of AGN feedback on shape of dark matter haloes

Author: Netipon Naree[1]

Co-author: Orrarujee Muanwong [1]

[1] *Department of Physics, Khon Kaen University*

Corresponding Author: netipon_naree_toei@kkumail.com

Galaxy haloes evolve through complex structure formation processes. Feedback from active galactic nuclei (AGN) plays an important role on the formation and matter distribution in haloes. We investigate the effect of AGN feedback on the shape of dark haloes formed in the EAGLE simulations and trace the evolution. Haloes from the 50 Mpc box simulation with and without AGN feedback are extracted at redshifts 0, 0.25 and 0.87, with high ($10^{13} - 10^{14.5} M$), intermediate ($10^{12} - 10^{12.5} M$), and low ($10^{11} - 10^{11.5} M$) mass ranges, containing approximately 20, 100 and 800 haloes at redshift 0, respectively. We average the triaxiality profile of haloes in each mass range at different redshifts. The triaxiality at r_{200} for the highest mass range for both simulations is simililar at all redshifts, but differ near the centre ($r < 0.1 r_{200}$). The effect of AGN on the shape is more pronounced at low and intermediate mass ranges, with haloes in the AGN simulation progressively become more prolate internally as they evolve to the present. However, shape of individual dark haloes may also be affected by other processes. We follow the evolution of triaxiality of 3 most massive haloes and find that outside $0.1 r_{200}$ the haloes exhibit change of shape erratically which could be due to merging. We conclude that AGN can affect the internal shape of haloes particularly in low and intermediate mass ranges, and that haloes are triaxial objects as a result of undergoing structural change through time.

S4 High Energy and Particle Physics - Board: O-S4-44 / **172**

Multi-frequency variabilities: blazar classification and statistical properties

Author: Rattanapong Yoyponsan[1]

Co-authors: Utane Sawangwit [2]; Siramas Komonjinda [1]

[1] *Chiang Mai University*

[2] *NARIT*

Corresponding Author: toey.yoyponsan@gmail.com

Blazars are a class of active galactic nuclei whose jets are aligned with the observer's line of sight. They are powerful multi-frequency emitters that exhibit rapid and violent variation. Based on optical emission lines, blazars are classified into two subclasses which are BL Lacertae objects (BL Lacs), and flat spectrum radio quasars (FSRQs). Various studies have shown that besides using emission lines, it is possible to use blazar variability to classify blazars into the aforementioned subclasses. We are investigating the use of blazar variability for blazar classification by using it as inputs in machine learning algorithms. In this work, we use the 5th edition of the Roma-BZCAT catalog as a reference. Optical and radio light curves are taken from 3 facilities, namely, Zwicky Transient Facility (ZTF), Gravitational-wave Optical Transient Observer (GOTO), and Owen Valley Radio Observatory (OVRO), observed during 2019-2020. From the data, we study the statistics of blazars variability which in turn are used to inform features extraction for machine learning. We will report on the results of the study, challenges, future opportunities, and discuss the classification performance. There are 766 BL Lacs and 1288 FSRQs in the analysis, each of which has at least 10 data points in both g and r band of the ZTF data. The light curves from the entire observation period are used to find the relation between g-r color evolution and the fractional variability in the r band. The pearson correlation of the relation is 0.73, while the spearman correlation is 0.76. The correlation values suggest that when blazars are more active in the g band, the variabilities in the r band tend to be less.

S4 High Energy and Particle Physics - Board: O-S4-22 / **108**

The potential scientific capabilities of the Evanescent Wave Coronagraph EvWaCo

Author: Matthew Ridsdill-Smith[1]

Co-authors: Anthony Berdeu [1]; Christophe Buisset ; Mary Angelie Alagao [1]; Supachai Awiphan [2]

[1] *NARIT*

[2] *NARIT, Thailand*

Corresponding Author: matthew@narit.or.th

The Evanescent Wave Coronagraph, EvWaCo, is an in-development prototype coronagraph, designed for use on the 2.4m Thai National Telescope (TNT), in the R and I-band filters. This work examines the astronomical capabilities of EvWaCo using the results from Fourier-analysis simulations. The coronagraph mask comprises a spherical lens placed in contact with a prism, utilising the principle of frustrated total internal reflection. On-axis light is transmitted through prism and the lens, whereas off-axis light is totally internally reflected within the prism, producing the mask's coronagraphic properties. Fourier optics simulations were applied to the EvWaCo prototype to analyse its performance, combining different sources of contrast degradation that will be present in the system. The simulations used for the main analysis assume a good night at the Thai National Observatory (TNO) and include the fitting error, aliasing and wave-front noise, providing a radially averaged contrast curve. From the contrast curve, the detection limit, as defined by a minimum signal to noise ratio of 5 for a typical observation time, can be calculated for different primary star magnitudes. The relative fluxes of various binary stars, with a range on spectral classes and separations, were modelled allowing comparison to the EvWaCo detection curves. The photon-noise limited detection curves provide a theoretical baseline for the performance that will be achieved with EvWaCo; they therefore give an indication of the types of objects EvWaCo can observe. Along with a broader discussion of observable objects, some potential known candidates for observations on the TNT using EvWaCo are suggested.

S4 High Energy and Particle Physics - Board: O-S4-42 / **169**

Photometric Variability of High Amplitude Delta Scuti Stars from AAVSO International Database

Author: Nareemas Chehlaeh[1]

Co-author: Nusreen Masae [2]

[1] *Prince of Songkla University*

[2] *Independent researcher*

Corresponding Author: nareemas.c@psu.ac.th

This research aims to study photometric variability and Fourier analysis of High Amplitude Delta Scuti stars (HADS), which are interesting short period variable stars with spectral types between A2 and F0. They are located in the area of the classical cepheid instability strip, which crosses the main-sequence (MS) on the Hertzsprung-Russell (H-R) diagram. The CCD photometric V-magnitude data of the selected HADS stars were acquired based on the AAVSO international database (American Association of Variable Stars Observers), which is the largest and most comprehensive digital variable star database. Time-series light curve data was accomplished using discrete Fourier transformation. The pulsating properties of the selected HADS stars were analyzed using the Period04 astronomical program. We obtained the times of maxima, magnitude changes and pulsation frequencies for each star. The study of the pulsation frequencies, *O-C* diagram, and period change of HADS stars can estimate their pulsation modes and their evolution. HADS stars are very important as standard candles that can be used to measure galactic distances.

S4 High Energy and Particle Physics - Board: P119 / **374**

Electromagnetic form factors of Δ-N transition

Author: Moh Moh Aung[1]

[1] *School of Physics, Institute of Science, Suranaree University of Technology, Nakhon Ratchasima 30000, Thailand*

Corresponding Author: mohmohaung231992@gmail.com

The three Jones-Scadron form factors G_M, G_E and G_C^* for the ΔN transition are derived in the dispersion theory and chiral perturbation theory at low Q^2 regions. The Q^2 dependence of magnetic dipole form factors are compared to the experimental data of the resonant multipoles $ImM_{1+}^{3/2}$. The decay rate of the Dalitz decay Δ-> Ne^-e^+ is also derived in one-photon production process.

S4 High Energy and Particle Physics - Board: P133 / **84**

The Transit Timing Variation and Atmosphere of WASP-43 b

Authors: Rattiyakorn Rattanasai[None]; Supachai Awiphan[1]; Siramas Komonjinda[2]; Eamonn Kerins[3]; Ronnakrit Rattanamala[2]

[1] *National Astronomical Research Institute of Thailand*

[2] *Chiang Mai University*

[3] *University of Manchester*

Corresponding Author: fourthastro@gmail.com

We perform transit timing variation (TTV) and transmission spectroscopy analyses of the planet WASP-43 b, which is a hot Jupiter exoplanet with an ultrashort orbital period 0.81347753±0.0000007 day. Ninety-three transit light curves are obtained from the VizieR database and the observation from National Astronomical Research Institute of Thailand (NARIT)'s telescopes. We combine the mid transit time from our data with 53 published mid transit time of WASP-43 b. The result shows that WASP-43 b has an orbital period change with the rate dP/dE = +10.0±2.1 milliseconds per year. The TTV analysis shows a possibility that the system has an additional planet that induced the TTVs amplitude signal of 0.000638±0.000081 days. If the body is located near the 1:2 mean-motion resonance orbit, the sinusoidal TTV signal could be caused by the gravitational interaction of 0.0478 ME. For the transmission spectroscopy analysis of WASP-43 b, the transit depths of twenty-seven filters are modelled by the PLATON fitting model. The model shows that the planet has a radius of 1.10 RJ with temperature 1724 K, Scatter factor of 8.92. The metallicity of the planet's atmosphere is 16.59 times that of the Sun. The C/O ratio in the WASP-43b atmosphere is 0.96.

S5 Quantum Technology - Board: INV-S5-1 / **368**

Quantum-inspired Computation for Optimization and Supervised Machine Learning

Author: Thiparat Chotibut[1]

[1] *Chulalongkorn University*

Corresponding Author: thiparat.c@chula.ac.th

Although fault-tolerant quantum computation theoretically promises revolutionary benefits for computational science, the hardware development of a scalable fault-tolerant quantum computer is still in its infancy. In this talk, we will demonstrate near-term benefits of quantum or quantum-inspired computation from our two recent works [1-2]. First, using Quantum Alternating Operator Ansatz (QAOA), an algorithm that can be implemented on a near-term quantum device or simulated on a digital computer, we solve a realistic large-scale financial optimization problem experienced by a Thai bank. We show that the presence of the QAOA can improve the expected net profit returned to the bank (in a loan collection problem) by approximately 70%, compared to when the QAOA is absent from the algorithm [1]. Secondly, we discuss the benefits of quantum-inspired approaches in supervised machine learning. In particular, we recast a sentiment analysis problem with a recurrent neural network (RNN), which is difficult to analyze due to intrinsic nonlinearities, as an equivalent problem using a quantum tensor network, which can be efficiently and more easily analyzed on a digital computer. Using an entanglement entropy as a proxy for information propagation, we show that, contrary to a common belief that long-range information propagation is the main source of RNNs' successes in sentiment analysis, single-layer RNNs harness high expressiveness from the subtle interplay between the information propagation and the word vector embeddings [2]. Our work sheds light on the phenomenology of learning in RNNs, using tools from many-body quantum physics.

References:
[1] https://arxiv.org/abs/2110.15870
[2] https://arxiv.org/abs/2112.08628 (New Journal of Physics, 2022)

S5 Quantum Technology - Board: O-S5-1 / **64**

Random-telegraph noise mitigation and qubit decoherence in solid-state experiments

Authors: Nattawut Kamjam[None]; Poramet Pathumsoot[None]; Areeya Chantasri[None]

Corresponding Author: nattawut.kam@student.mahidol.edu

Motivated by the current technology of solid-state qubits, which is one of the promising platforms for quantum computing, we are interested in the effects of random charge noises and how they can result in qubit decoherence. In this work, we model the charge noise as a random telegraph process (RTP), or a noise described by a two-state fluctuator, and analyze theoretical formulas for the RTP. We then construct a setup of a logical qubit with a qubit probe to measure the charge noise. Given the theoretical model, we investigate possible experimental parameters from the current experiments in the literature and numerically simulate the logical-qubit phase and its decoherence. Moreover, we analyze the recent phase-correction technique using Bayesian maps and show how the decoherence can be vastly improved.

NK acknowledges the support from the Development and Promotion of Science and Technology Talents Project (DPST). This work was supported by National Research Council of Thailand (NRCT) grant and N41A640120 and Australia-US-MURI grant AUS-MURI000002.

S5 Quantum Technology - Board: O-S5-2 / **76**

Estimating unknown qubit phase under telegraph noises using Recurrent Neural Network

Authors: Suttavee Rojanasirivanit[1]; Poramet Pathumsoot[1]; Areeya Chantasri[1]

[1] *Mahidol University*

Corresponding Author: suttaveeroj@gmail.com

Machine learning techniques have been widely used for many complex systems including quantum systems with noisy environments. In this work, we are interested in a system of qubits affected by the random-telegraph noise that could destroy the qubit coherence. We construct a theoretical model including one logical qubit and one probing qubit, the latter of which can be measured at various times and with various measurement bases to collect information of the unknown fluctuating noise. We then use the recurrent neural network (RNN), in particular the Long short-term memory (LSTM) model, to process the measurement readouts obtained from the probe qubit and train the machine to learn how to estimate the correct phase of the logical qubit. We show numerical results of the random qubit phase affected by the random noise and the estimation accuracy from the LSTM. The accuracy does depend on different parameters of the machine as well as the qubit sensitivity to noise.

This work was supported by National Research Council of Thailand (NRCT) grant, N41A640120 and Australia-US-MURI grant AUS-MURI000002. SR also acknowledges the Faculty of Science for a Sri Trang Thong scholarship.

S5 Quantum Technology - Board: O-S5-3 / **77**

Qubit decoherence and phase correction in Gaussian white-noise environment

Authors: Atirat Meunson[None]; Poramet Pathumsoot[1]; Nitipat Pholchai[2]; Areeya Chantasri[1]

[1] *Mahidol University*

[2] *King Mongkut's University of Technology North Bangkok*

Corresponding Author: tiwatirut@gmail.com

One of the main obstacles for implementing qubits in real experiments is the detrimental effects of environmental noises. Qubits in noisy environments can decohere quickly, i.e., losing their capability in processing quantum information. In this work, we are interested in analyzing the decoherence and possible ways to correct the phase errors due to the Gaussian white-noise. We consider a single logical qubit and investigate the qubit decoherence depending on different parameters of the white noise. We show analytical results of the qubit decoherence and verify them with numerical simulations. Moreover, we present a possible noise measurement and phase correction protocol that can be applied to estimate the effect of noise on the logical qubit. The quality of phase estimation does vary depending on the sensitivity to noise and the number of qubit probes used in measuring the unknown noise.

This work was supported by National Research Council of Thailand (NRCT) grant, N41A640120 and Australia-US-MURI grant AUS-MURI000002. TA also acknowledges Laser and Optic Research Group, Science and Technology Research Institute, KMUTNB for financial support.

S5 Quantum Technology - Board: O-S5-4 / **10**

Time-domain measurements with superconducting flux qubits for diabatic quantum annealing experiments

Author: Nuttamas Tubsrinuan[1]

Co-authors: Louis Fry-Bouriaux [2]; Gioele Consani [2]; Paul Warburton [3]

[1] *University College London*

[2] *London Centre for Nanotechnology,*

[3] *London Centre for Nanotechnology*

Corresponding Author: nuttamas.tubsrinuan.20@ucl.ac.uk

Quantum annealing is an optimization method conventionally performed in an adiabatic fashion. Adiabatic quantum annealing (AQA) gradually changes the Hamiltonian so that the system stays in an instantaneous ground state of the Hamiltonian at all times. However, this slow process could hamper computational speedup. In contrast, diabatic quantum annealing (DQA) allows transitions between the ground state and excited states during the anneal. Hence the annealing process can take less time, enabling quantum speedup. In theory, DQA could be achieved by exploiting the interference effect from the Landau-Zener-Stückelberg (LZS) transition as a shortcut to adiabaticity. Our goal is to execute the LZS experiment on high-Q superconducting flux qubits. Typically, the LZS experiment is performed in the steady state, using a continuous-wave drive. The result of averaging many drive cycles makes the definition of the environmental effect challenging. Instead of using a continuous-wave drive, we aim to use a single pulse sequence to drive the system through the avoided crossing just one time. This technique creates a sensitive probe for decoherence and gives better visibility of the environmental impact on the qubit. Here, we characterize and calibrate a superconducting device consisting of a flux qubit, a quantum flux parametron, and a tuneable resonator in a dilution refrigerator, which cools the device down to 10 mK. Device calibration is performed to account for the crosstalk among the qubit, the quantum flux parametron, and the tuneable resonator. Qubit two-tone energy spectroscopy is subsequently derived using continuous- wave measurements. Then, we establish a pulse readout measurement configuration for the LZS experiment towards DQA. Moreover, we investigate the impact of the readout pulse length when measuring a dispersive readout resonator. The results could suggest a suitable pulse length for the subsequent Rabi oscillation experiment.

S5 Quantum Technology - Board: O-S5-5 / **261**

Simulation of diatomic ground state energy in IBM quantum

Author: Nuttha Utsaha[1]

Co-author: Ruchipas Bavontaweepanya

[1] *Department of Physics,Faculty of Science and technology*

Corresponding Author: n.nuttha2543@gmail.com

Quantum computing is an interesting research and can be applied to many research areas, such as machine learning, optimization, and especially quantum simulation. In this work, we simulated the ground state energy of diatomic molecules: O2 and CO. We designed the ansatz for symmetric diatomic molecule, which is the O2 and asymmetric diatomic molecule, which is the CO. The designed quantum circuit was implemented in IBM quantum, and the results of the ground state enegy simulation can be compared with the experimental results.

S5 Quantum Technology - Board: O-S5-6 / **222**

The Dirac impenetrable barrier in the limit point of the Klein energy zone

Author: Salvatore De Vincenzo[None]

Corresponding Author: salvatored@nu.ac.th

We reanalyze the problem of a 1D Dirac single-particle colliding with the electrostatic potential step of height V_0 with an incoming energy that tends to the limit point of the so-called Klein energy zone, i.e., $E \to V_0 - \mathrm{m}c^2$, for a given V_0. In this situation, the particle is actually colliding with an impenetrable barrier. In fact, $V_0 \to E + \mathrm{m}c^2$, for a given high relativistic energy $E\,(< V_0)$, is the maximum value that the height of the step can reach and that ensures the perfect impenetrability of the barrier. Nevertheless, we notice that, unlike the non-relativistic case, the entire eigensolution never completely vanishes, neither at the barrier nor in the region under the step, but its upper component does satisfy the Dirichlet boundary condition at the barrier. More importantly, by calculating the mean value of the force exerted by the wall on the particle in this eigenstate and taking its non-relativistic limit, we recover the expected result.

S5 Quantum Technology - Board: O-S5-7 / **232**

Identifying Electronic Transition for 2 eV Hexagonal Boron Nitride Quantum Emitters

Author: Cheewawut Na Talang[None]

Co-authors: Sujin Suwanna [1]; Chanaprom Cholsuk [2]

[1] *Mahidol University*

[2] *Friedrich-Schiller University Jena*

Corresponding Author: cheewawut.nat@student.mahidol.ac.th

Quantum emitters (QEs) play crucial roles in quantum technology applications, especially for quantum key distribution. Recently, color-center defects in a two-dimensional hexagonal boron nitride (hBN) have revealed many promising properties, such as high brightness, operation under room temperature, and broad emission wavelengths, demonstrating that they are attractive candidates for QEs. Thus far, most experiments found the emitter at 2 eV range influenced by C-based defects; however, the nature of defects for such QEs remains unknown and uncovered. In this work, we investigate 2 eV emitters using density functional theory (DFT) with Perdew-Burke-Ernzerhof (PBE) functional. We aim to theoretically characterize the origin of the electronic transition and to further identify the possible 2 eV defects. Four different types of defects, namely C_BV_N, C_BC_N, N_BV_N, and $O_BO_BV_N$ have been unraveled. Our results suggest that all of studied defects except for C_BC_N are likely 2 eV emitters whereas C_BC_N is more likely to be a 4 eV emitter. This paves the way that not only C-based defects, but also non C-based defects emit at 2 eV. Furthermore, our defect formation energy calculation predicts that C_BC_N is the most thermodynamically favorable for synthesis, followed by N_BV_N, $O_BO_BV_N$ and C_BV_N.

S5 Quantum Technology - Board: O-S5-8 / **177**

Determination of the concentration of glucose-ethanol-water mixtures using spectroscopic surface plasmon resonance on smartphone

Author: Prasert Chimplikanon[1]

Co-author: Pakorn Preechaburana [1]

[1] *Thammasat*

Corresponding Author: prasert.chmp@gmail.com

The determination of the refractive index (RI) and concentration of ternary mixture of glucose, ethanol and water is demonstrated by smartphone platform based on the detection of the refractive index by using surface plasmon resonance (SPR) principle. The optical coupler has been specially designed for coupling the light from smartphone screen to excite SPR on the thin gold layer in contact with solutions and to guide the reflected light to the smartphone camera used as the detector. For this work, the RIs of glucose and ethanol solution was determined by using image processing technique; the captured images of each individual solution were processed to the SPR spectra which indicates the significantly different SPR shift corresponding to the RI changes. In order to estimate the individual concentration of ternary mixture, at least two independent calibration equations are needed. Hence, two color light sources with different color intensity denoted as color1 (R=255, G=0, B=0) and color2 (R=255, G=100, B=0) were used to construct the calibration equations of two binary solutions. Calibrations ware carried out using four ethanol-water and glucose-water solutions which were providing a linear response in the refractive index range of 1.341– 1.361 RIU (R2 = 0.977-0.992) with the resolution of 0.14 mL/dL, and 0.04 g/dL for ethanol-water and glucose-water solutions, respectively. As a result, the estimated concentration errors for each element of the prepared ternary solution were found to be less than 5%. Accordingly, our work demonstrates the successful experiment for the determination of concentration of ternary mixture on unmodified smartphone which provides a simple and reliable portable device.

S5 Quantum Technology - Board: INV-S5-2 / **361**

Quantum Simulation via Quantum Gas Microscope

Author: Pimonpan Sompet[1]

[1] *Department of Physics and Materials science, Faculty of Science, Chiang Mai University, Chiang Mai, 50200, Thailand*

Corresponding Author: pimonpan.sompet@cmu.ac.th

Quantum gas microscope is a powerful tool for studying complex atomic many-body quantum systems in optical lattices with a high-resolution imaging. This tool is used to investigate the interplay between charges and spins, which involves many exotic phenomena. In this talk, we will discuss about the utilization of quantum gas microscope of ultracold fermions (^{6}Li) in optical lattices for quantum simulation. Experimentally, we have a complete control over the onsite atomic interaction and the tunneling energy. Harnessing the full spin and charge detection, we directly measure spin-spin and spin-density correlations of the systems. This measurement allows us to observe the evolution of a doped Mott insulator from polaronic metal to Fermi liquid, and allows us to realize the symmetry-protected Haldane phase.

S5 Quantum Technology - Board: O-S5-9 / **254**

Active vibration isolator using piezoelectric actuator

Author: Nuttanan Tanasanchai[1]

[1] *Department of Physics and Materials Science, Faculty of Science, Chiang Mai University*

Corresponding Author: ohmnuttanan@gmail.com

Passive vibration isolation has been extensively used to mitigate a sensitive object from unwanted motions. It is a simple configuration consisting of an isolated object, a damper, and a spring in which excess vibration is suppressed by using its harmonic oscillator. However, resonance amplification at low-frequency range is a major weakness of this system. In this work, we add an active vibration isolation on the passive system to cancel unabsorbed vibrations. Our active system consists of an acceleration sensor, a PID control system, and a piezoelectric (PZT) actuator. The PZT is used as the vibration source to generate the counteracted vibration. The PZT effect can response in a wide-frequency range up to kHz and can provide a rigid system assembly. The PZT displacement can be precisely controlled down to sub-micron range. In this work, we investigate the behaviors of the actuator and the performance of our active vibration isolator. One prospect use of our active vibration isolator will be to protect the inertial mirror in the quantum gravimeter from the surrounding vibrations.

S5 Quantum Technology - Board: O-S5-10 / **307**

Atomic Vapor Glass Cell Fabrication for Quantum Experiment

Author: Apiwit Kaewko[1]

Co-authors: Narupon Chattrapiban [2]; Poompong Chaiwongkhot [2]; Pimonpan Sompet [2]; Nithiwadee Thaicharoen [2]

[1] *Chiang Mai University*

[2] *Quantum Simulation Research Laboratory, Department of Physics and Materials Science, Faculty of Science, Chiang Mai University*

Corresponding Author: apiwitkaewko@gmail.com

A vapor glass cell containing neutral atoms is an important tool for developing portable quantum devices. It can be used in quantum sensors, atom chips and cryptography devices quantum-related experiments involving quantum metrology, computation and communication. In this work, we find that the absorption coefficient of rubidium atoms in our home-made vapor cell decreases as the input power of light increases. We prepare the cell by filling it with rubidium atoms in a closed system at ambient pressure. We focus on the changes of the absorption profile based on the D2-transition while we change the power of the input laser. These changes are important in determining the absorption coefficient of vapor in the glass cell, which reflects restriction of ambient pressure on the working condition of our quantum devices. The absorption profile is compared with that obtained from the commercial cell.

S5 Quantum Technology - Board: O-S5-11 / **283**

OBSERVATION OF ZEEMAN SPLITTING IN RUBIDIUM ATOMS USING DOPPLER-FREE SATURATED ABSORPTION SPECTROSCOPY

Author: Prin Insang[1]

[1] *Department of Physics and Materials Science, Faculty of Science, Chiang Mai University.*

Corresponding Author: prininsang@hotmail.com

One of the most sensitive methods for magnetic field measurement employs quantum phenomena at atomic level. We use the Doppler-free saturated absorption spectroscopy to reveal the hyperfine levels of the rubidium atoms which obscured by the thermal broadening, we able to observe the splitting of energy levels due to an external magnetic field. Furthermore, effect of polarization of the light beam is changing the rubidium spectrum as a consequence to the optical pumping process. The measured of the energy separated subsistence an external magnetic field use toward to atomic magnetometry or analysis various theories.

S5 Quantum Technology - Board: O-S5-12 / **106**

Design and implementation of a laboratory prototype of a fiber-fed Fourier transform spectrograph for the Thai National Telescope

Author: Pornapa Artsang[None]

Co-authors: Panomsak Meemon ; christophe BUISSET [1]

[1] *National Astronomical Research Institute of Thailand*

Corresponding Author: pornapa.artsang@gmail.com

The Fourier transform spectrograph (FTS) is an important tool that has been applied in many fields of research. In astronomical observation, the FTS has been used for analyzing stellar objects. Most of FTS that hav been designed and used with large telescope are based-on free space design to maximize flux throughput at the detector. However, the limited space at a focal plane of a large telescope may lead to complex design of the FTS if not impossible. To overcome the space limitation, a fiber-fed design of FTS has gained more interest. The used of fiber to feed the star incoming flux from the telescope to the spectrograph makes comfortable for an optical alignment of the system. Nevertheless, the main challenge of the fiber-fed FTS is a low flux throughput due to a single point field of view and a transmission loss in the optical fiber. In this work, we report the development of the laboratory prototype of a fiber-fed FTS specifically designed for the Thai National Telescope (TNT). Off-the-shelf optical components have been mainly used in the implementation. To improve the signal-to-noise ratio of a low flux signal, a balanced detection scheme has been investigated. The simultaneous detection of scientific and metrology interferograms for correction of the phase distortion of the interferogram has been implemented. The phase distortion in the measured interferogram was corrected by using peak-valley positions of the metrology interferogram. The instrument line shape, corresponding with the spectral resolving power of the system was measured to be higher than 19,000. Furthermore, the scan range of the FTS was maximized to obtain the maximum spectral resolution of the implemented system. The achieved maximum optical path difference is currently about 30 mm.

S5 Quantum Technology - Board: O-S5-13 / **264**

Design and analysis of Hollow-core fiber with anti-resonant structure for Ethylene Detection

Authors: Kwanjira Joonmasa[1]; Panomsak Meemon[None]; Wanvisa Talataisong[None]

[1] *Student*

Corresponding Author: kwanjirajoonmasa@gmail.com

For fruit and flower transportation, ethylene gas is necessary to be detected. Various techniques are innovated, and the hollow core optical fiber is one of them. Its structure is suitable for flowing gas. So, it is used as a gas cell. This work proposed the nested hollow-core anti-resonant fiber made of Polyethylene Terephthalate (PET). Our structure is optimized to get the lowest loss at a wavelength of 3.2 um, which is related to the ethylene absorption band in the Mid-IR. The confinement loss is predicted from the numerical simulation in COMSOL. After trying to vary parameters such as core diameter and cladding tube thickness, we obtain a loss lower than 2 dB/m at the core diameter and cladding tube thickness of 108 um, and 2 um, respectively.

S5 Quantum Technology - Board: O-S4-39 / **160**

A Study of Unidirectional Gradient of Galactic Cosmic Ray Intensity at Different Cut-off Rigidities and Solar Magnetic Polarities

Author: Cherdchai Wuttiya[None]

Co-author: Thana Yeeram

Corresponding Author: leonid21ster@gmail.com

Galactic cosmic rays (GCRs) are energetic charged particles, mainly protons originated in supernova remnants. Near Earth, GCR intensity (n) is subjected by modulation mechanisms in the solar wind, which are changed along the solar cycles (SCs) indicated by heliospheric magnetic field (HMF). We have used GCR count rates as observed by neutron monitors at low-to-high cut-off rigidities (P_c) and polarity states (A) of the HMF to determine the North-South (NS) asymmetry of the n. The study times span the SCs 22/23, 23, and 24 during periods 1996–1998 ($A > 0$), 2004–2008 ($A < 0$), and 2015–2019 ($A > 0$), respectively. By using a new simple correction method for secular changes for n, we calculated the NS asymmetry of n denoted as $\delta n_{\mathrm{S-N}}/n$ with respect to the heliospheric current sheet (HCS) which is a thin region with large-scale wavy structure separating the north and south HMFs. The NS differences of corrected HCS tilt angle [α] for Earth's excursions in helio-latitude denoted as $\Delta\alpha^{\mathrm{E}}_{\mathrm{N-S}}$ show a comparably consistence and anti-correlation with the corrected $\delta n_{\mathrm{S-N}}/n$ particularly during $A < 0$ epoch (2004-2008) and $A > 0$ epoch (2015-2019 not 1996-1998). The aspect suggests the importance of heliospheric drift on asymmetric modulation and latitudinal gradient of GCRs in both periods. The unidirectional latitude gradient [$G_{\perp}$] derived from the relation of the consistencies between corrected $\delta n_{S-N}/n$ and $\Delta\alpha^{\mathrm{E}}_{\mathrm{N-S}}$. We found a strong positive correlation between $\delta n_{\mathrm{S-N}}/n$ and $G_{\perp}$ for all epochs and P_c .

S5 Quantum Technology - Board: O-S4-40 / **164**

Spectrum of H-atom in Gravitational Waves from Black Hole Binary

Author: Nontapat Wanwieng[None]

Co-authors: apimook watcharangkool [1]; Narupon Chattrapiban

[1] *Researcher*

Corresponding Authors: prof.nontapat@gmail.com, a.watcharangkool@gmail.com, narupon.ch@cmu.ac.th

We investigate the characteristic spectrum of Hydrogen atoms subjected to the gravitational wave (GW) produced by a compact binary inspiral, particularly the supermassive black hole binary (SMBHB). These atoms are assumed to be distributed in the source's local wave zone. The gravitational wave is mathematically described by the quadrupole formula of the linearized theory of General Relativity. The energy shifts and the spectrum of Hydrogen atoms are computed by the first-order perturbation theory in non-relativistic approximation. The effect of GW perturbation is analyzed in a strong-field, a weak-field, and an intermediate-field regime. The extraction of source parameters from the spectrum is also discussed.

S5 Quantum Technology - Board: INV-S5-3 / **367**

Towards the Optical Second: The next generation of Thailand Standard Time

Author: Piyaphat Phoonthong[1]

[1] *National Institute of Metrology (Thailand)*

Corresponding Author: piyaphat@nimt.or.th

Standard time and frequency are widely implemented in many systems: global navigation satellite system, high speed communication, and financial technology. Each application requires different accuracy and stability. Atomic clock has been used as the precise oscillator. In 1967, the energy level between two hyperfine ground states of Cesium 133 at 0 K has been defined as the standard unit of time. However, the next generation of the atomic clock, called "Optical Clock" has illustrated the uncertainty below 10^{-17}. The optical transition of various atoms and ions are selected as the second representative of second. NIMT has developed the next generation of atomic clock using an Ytterbium ion. The core technology i.e., electronics control, helical resonator and linear quadrupole trap has been designed and built in Thailand. The system has been successfully trapped single ion of Yb174.

S5 Quantum Technology - Board: O-S5-14 / **63**

Quantum Diamond Spectrometer for Magnetic Field Sensing

Author: Napoom Thooppanom[1]

Co-author: Sorawis Sangtawesin [1]

[1] *Suranaree University of Technology*

Corresponding Author: npkids2012@gmail.com

We build a quantum diamond spectrometer (QDS), outlined by Bucher et. al [1], to study the fluorescence of the nitrogen-vacancy (NV) center in diamond, a quantum defect that can be used as a qubit or quantum sensor. The QDS has several advantages to a traditional confocal microscopy, particularly in terms of measurement speed. The setup consists of a green laser excitation onto the diamond that is placed on an optical light guide for fluorescence detection. A microwave loop is then placed onto the diamond to deliver oscillating magnetic field to probe the NV center transition. Finally, permanent magnets are attached to a kinematic stage for tuning the transition energy of the NV center. With this setup, we can adjust the magnet distance, azimuthal angle, and polar angle with reference to the NV center axis for optimizing NV center fluorescence. We demonstrate measurements of NV center fluorescence as a function of microwave frequency and show the intensity drop at 2.87 GHz, showing the interaction at zero-field splitting, and measurements of the Zeeman splitting of NV center electronic spin from an external magnetic field in different orientations. The results can be used to perform vector magnetometry, which has potential applications in quantum sensing.

[1]. Bucher, D.B., Aude Craik, D.P.L., Backlund, M.P. et al. Quantum diamond spectrometer for nanoscale NMR and ESR spectroscopy. Nat Protoc 14, 2707–2747 (2019).

S5 Quantum Technology - Board: O-S5-15 / **21**

Optically Detected Electron Spin Resonance in Diamond for Vector Magnetometry

Author: Rapeephat Yodsungnoen[1]

Co-author: Sorawis Sangtawesin

[1] *Suranaree University of Technology*

Corresponding Author: r.yodsungnoen@gmail.com

Nitrogen Vacancy (NV) center is a defect in a diamond with unique optical transitions in the visible wavelength that is spin-dependent, allowing it to be utilized as an optical qubit or as a magnetometer. Our work primarily focus on magnetic field sensing with NV center, as they offer high sensitivity and high spatial resolution at the nanoscale level, along with ability to simultaneously measure magnetic field magnitude and direction. To exploit the NV center as a vector magnetometer, we use a confocal microscope retrieve photoluminescence (PL) emitted by the NV center, in combination with Optically Detected Electron Spin Resonance (OD-ESR) technique that probes the microwave frequencies corresponding to the NV electronic transition. In the OD-ESR, we vary applied microwave frequencies to change the spin population in the ground state triplet. If the applied microwave frequency is on resonance with the transition frequency between m_s=0 and m_s=±1, the measured PL will decrease. A magnetic field can be applied to split the m_s=±1 states, and the splitting depends on the magnitude and direction of magnetic field. As a result, two resonant transition frequencies can be used to determine the vector magnetic field experienced by the NV center, and four different orientations of the NV center in the diamond lattice can provide a complete 3-dimensional components of the magnetic field. In this work, we demonstrate simulated OD-ESR spectra of the NV center as a function of the magnitude and direction of the magnetic field. The results can be used to understand the experimental ODESR data in order to determine the magnetic field vector in nanoscale magnetometry, which can be used as quantum sensors.

S5 Quantum Technology - Board: O-S5-16 / **43**

Performance comparison of Amplitude-decorrelation and Speckle Variance algorithms for OCT Angiography

Author: Wuttikorn Kampong[None]

Co-authors: Jadsada Saetiew ; Yutana Lenaphet ; Kunakorn Palawong ; Panomsak Meemon

Corresponding Author: m6110086@g.sut.ac.th

Optical Coherence Tomography Angiography (OCTA) is a non-invasive imaging technique for microvasculature visualization. OCTA does not require injection of exogenous contrast agents, or fluorescent dye into blood circulation, which may cause allergic reactions as in fluorescein angiography (FA) and indocyanine green angiography (ICGA). OCTA differentiate blood vessel from static tissues by analyzing the variation of OCT speckle caused by moving particle in blood vessel. In this study, OCTA was implemented on a spectrometer-based spectral domain OCT that was built on Michelson interferometer. The OCT imaging systems was operated at 835 nm central wavelength with acquisition speed of 10,000 depth scans/s. Three methods of speckle analysis were implemented, i.e. Amplitude Decorrelation (AD), Speckle Variance (SV), and Intensity-to-Average Variance (IAV). Their performance for segmentation of blood vessels underneath skin were studied. In addition, the auxiliary methods of pixel averaging and split-spectrum were added to improve the signal-to-noise ratio of images. To compare the performance of the implemented algorithms, a flow phantom was constructed by embedding a capillary tube inside a petrolatum-based gel (tissue mimic material, or TMM). To mimic a blood flow beneath skin, dilute milk was pumped through the capillary with average flow speed of 2.0 mm/s by using a syringe pump system. The performances of each OCTA algorithm, in terms of signal-to-noise (SNR) ratio and contrast-to-noise (CNR) ratio, were measured and compared. The OCTA imaging system will be optimized for nailfold vasculature imaging. The ability to detect and visualize change in nailfold microvasculature pattern can help in diagnosis of many diseases, such as connective tissue disease, autoimmune rheumatic disease, ophthalmic disease, and coronary disease. Furthermore, OCTA technique is capable of in vivo volumetric imaging of capillary in real-time and hence can potentially be a powerful tool for skin diagnostics.

S5 Quantum Technology - Board: O-S5-17 / **294**

Quantum diffusion map for nonlinear dimensionality reduction

Authors: Apimuk Sornsaeng[1]; Ninnat Dangniam[None]; Pantita Palittapongarnpim[None]; thiparat chotibut[1]

[1] *Chulalongkorn University*

Corresponding Author: apimuk25@hotmail.com

Inspired by random walks on graphs, the diffusion map (DM) is a class of unsupervised machine learning that offers automatic identification of low-dimensional data structure hidden in a high-dimensional data set. In recent years, among its many applications, the DM has been successfully applied to discover relevant order parameters in many-body systems, enabling automatic classification of quantum phases of matter. However, a classical DM algorithm is computationally prohibitive for a large data set, and any reduction of the time complexity would be desirable. With a quantum computational speedup in mind, we propose a quantum algorithm for the DM, termed the *quantum diffusion map* (qDM). Our qDM takes as an input N classical data vectors, performs an eigendecomposition of the Markov transition matrix in time $O(\log^3 N)$, and classically constructs the diffusion map via the readout (tomography) of the eigenvectors, giving a total expected runtime proportional to $N^2 \text{polylog}\, N$. Finally, quantum subroutines in the qDM for constructing a Markov transition matrix and for analyzing its spectral properties can also be useful for other random-walk-based algorithms.

S5 Quantum Technology - Board: O-S5-18 / **137**

Determination of phase change correction on gauge block measurement in two different interferometric measurement system

Author: Angkoonna Pringkasemchai[None]

Co-authors: Kittisun Mongkolsuttirat ; Jedsada Wongsaroj

Corresponding Author: angkoonnap@nimt.or.th

Phase change correction is an important correction value of the end effect in an optical interferometry system. Normally, this value is used to compensate for gauge block measurement by an optical interferometry system based on ISO 3650:1998. Quartz plates and three different types of gauge block: steel, ceramic, and tungsten carbide were used in this study. Two different interferometric measurement systems in terms of fringe fraction (a phase shift method and an average slits method) were determined for the phase change correction by a five-stacking method. These results are used to determine the length measurement of gauge blocks in an optical interferometer technique and consequently, to evaluate the uncertainty of gauge blocks measurement. The preliminary results are shown that the value of phase change correction in a phase shift gauge block interferometer (PSGBI) system and a standard uncertainty are 35.3 nm and 6.2 nm, respectively. In contrast, the values from an average slits gauge block interferometer (ASGBI) system and a standard uncertainty are 66.0 nm and 6.4 nm, respectively. We found that the phase correction from the PSGBI system is lower than ASGBI about 20.6 nm because the PSGBI's wave-front correction is more complete than the systematic error of ASGBI leading to the low value of phase correction in the end effect. However, the lengths of gauge blocks of all three materials measured by the two different systems were consistent as assessed by En number. According to the study, we can conclude that phase change correction is based on the characteristics of each GBI system, material types of gauge block and optical plates such as the fringe fraction technique, and wavefront error compensation. Consequently, measurements that require a high accuracy should determine the phase change correction before each measurement due to this value is not interchangeable.

353

Characteristic of PSF membrane composites incorporated with TiO2 nannoparticles

Author: Chalad Yuenyao[1]

[1] *Phetchabun Rajaphat University*

Corresponding Author: chalay_2012@hotmail.com

Abstract: Characteristics of PSF composite membranes incorporated with titanium dioxide (TiO2) porous nanoparticles are studied in this research work. To investigate the physical and chemical properties, PSF membrane incorporated with TiO2 in quantities of 1% by weight were prepared. Preparation of membrane samples were initiated from the dissolving of pellet of PSF materials in NMP solvent and addition TiO2 nanoparticles. The membrane is formed by casting of the dope polymer solution on a glass plate and then immersed in DI water. Characteristics of prepared membrane samples were analyzed by different analytical techniques. Hydrophilicity of membrane surfaces was analyzed through measurement of water contact angle (WCA) while the morphology, pore size and physical structure were evaluated through the SEM micrographs. The crystallinity of TiO2 and PSF composite membranes was analyzed by x-ray diffractometer (XRD) while the mechanical properties and functional group transitions were analyzed by DMTA and FTIR, respectively. Porous property of TiO2 was also studied by TEM in this work. Research results showed that the addition of TiO2 porous nanoparticles affect the pore structure of the composite membranes. This makes the pore structure resembles a finger and nano-size pore appeared on the surface of PSF composite membranes. Additionally, TiO2 nanoparticle clearly affects the hydrophilicity of prepared membranes.

351

Effect of ZnO porous nanoparticles and plasma on the physicochemical properties of PSF membranes

Author: Chalad Yuenyao[1]

[1] *Phetchabun Rajaphat University*

Corresponding Author: charlady_2012@hotmail.com

Effect of ZnO porous nanoparticles and plasma on the physicochemical properties of PSF membranes
Oranut Yosma, Chalad Yuenyao
Department of Physics, Faculty of Science and Technology, Phetchabun Rajaphat University,
83 M. 11 Saraburi-Lom Sak Road, Sadiang Sub-district, Muang,
*Corresponding auther: charlady_2012@hotmail.com

Abstract
The purpose of this research was to study the effect of addition of ZnO porous nanoparticles in the matrix of polysulfone (PSF) membrane polymer and low-temperature plasma at atmospheric pressure. Phase inversion process was employed to prepare all of membrane samples in this work. To modify the surface properties, prepared membrane samples were treated by low temperature plasma at atmospheric pressure. Structure and wettability properties as well as compatibility between ZnO nanoparticles and the metrix of the PSF were investigated in details by using of various analytical techniques. Measurement of contact angle of pure water and fourier transform infrared (FTIR) spectroscopy were utilized to evaluate the wettability and change of functional group on the top skin surface of membrane samples. While morphological structure and mechanical properties were analyzed with scanning electron microscopy (SEM) and dynamic mechanical thermal analysis (DMTA), respectively. Moreover, the porosity and crystallinity of the ZnO particles was studied by transmission electron microscopy (TEM) and x-ray diffractometer (XRD), respectively. In this work, the membrane preparation is initiated by dissolving of PSF material and dispersion of ZnO particles in a solvent. The resulting dope solution was then casted on a clear, dry and smooth glass. Thickness of casted membrane was control at about 150 μm by a plastic tape. The first results showed that the addition of ZnO porous nanoparticles resulted in a significantly increase of hydrophilic properties of membrane surface. Morphological structure of membrane samples influenced by addition of ZnO particles. In addition, membrane samples treated by plasma further increase of hydrophilic properties, however, the hydrophilic properties decrease with time.
Keywords: Wettability, morphological structure , ZnO nanoparticles , polysulfone, atmospheric pressure plasma.

328

Experiment-timing controller based on a high-speed analog and digital output device

Author: Tanasin Sriwichai[None]

Co-authors: Narupon Chattrapiban [1]; Nithiwadee Thaicharoen [1]; Pimonpan Sompet [1]

[1] *chiang mai university*

Corresponding Author: slayerjoker.2543@gmail.com

Modern atomics physics experiments rely greatly on a precise control of physical quantities. This requires controlling multiple electronic devices to observe the behavior of quantum many-body systems. In this work, we develope an experiment-timing controller based on a high-speed analog and digital output device (HSADO: model USB-1208HS-4AO). This allow us to program our system with the best time resolution of 3us. We benchmark the HSADO with Helmholtz-coil and laser systems. These systems will be employed in a Magneto-Optical Trap experiment.

322

Construction and Characterization of an External Cavity Diode Laser Based on SiP and Modular-Controller Assembly

Author: Pongpol Parkprom[1]

Co-authors: Narupon Chattrapiban [2]; Pimonpan Sompet [1]; Nithiwadee Thaicharoen [1]

[1] *Chiang Mai University*

[2] *Chiang Mai University*

Corresponding Author: parkprom2000p@gmail.com

Narrow-linewidth tunable diode lasers are keys to various advanced quantum technologies. External cavity diode laser (ECDL) is a tunable laser with a linewidth narrow enough for defining a control of a two-level quantum system. To reach the highly precise frequency, the controller modules require excellent current and temperature stability. The controller for ECDL employs three main systems: a frequency, temperature and current control systems. We combine a piezo-stack driver module, a system-in-a-package (SiP) temperature controller, and a monolithic current driver module to stabilize laser diode. In this work, the design of an ECDL is based on the Littrow configuration. Our home-made tunable laser has a linewidth narrower than 1 MHz. The main benefits are inexpensive and narrow linewidth that makes it versatile in applications i.e. modelocking, laser cooling. All the above mentioned make ECDL a more necessary device in the laboratory and imperative to a person that implements ECDL to gets knowledge from it.

321

Emulating turbulence of atmospheric turbulence on wavefront distortion

Author: [redacted][1]

Co-authors: Poompong Chaiwongkhot [2]; Narupon Chattrapiban [1]; Nithiwadee Thaicharoen [1]; Pimonpan Sompet [1]

[1] *Chiang Mai University*

[2] *Mahidol University*

Corresponding Author: piyawatbeam007@gmail.com

Turbulence emulation is one of the most significant steps in wavefront distortion and aberration correction. In this study, we generate phase holograms with Zernike polynomials and project those holograms on a spatial light modulator (SLM) to emulate effects of turbulence on an intensity distribution from the distorted wavefront. We compare the emulated turbulence in a lab environment with a theoretical calculation. Furthermore, the next aim of this work is to decompose Zernike components from a distorted wavefront and use them for the correction of real atmospheric turbulence.\\

95

Discovery of tsunami-like pulsation waves in the very fast rotating A-type stars

Author: Mkrtichian David[None]

Corresponding Author: davidmkrt@gmail.com

We present the first results of the spectroscopic survey focused on the search for and the analysis of the high-degree non-radial pulsations in the fast rotating A-type stars. High-and medium-resolution observations of the sample of the bright fast-rotating stars were carried out with 2m-class telescopes located in Europe and with the Thai National Telescope. We report on the discovery of tsunami-like prograde non-radial pulsations in the majority of the target stars.

340

Characteristics of MSNs synthesized by structure directing method

Author: Artit Hutem[1]

Co-author: Chalad Yuenyao [2]

[1] *Department of Physics, Faculty of Science and Technology, Phetchabun Rajabhat University, 83 Moo 11 Saraburi-Lomsak Street, Sadiang sub-district, Muang district, Phetchabun 67000, Thailand*

[2] *Department of Physics, Faculty of Science and Technology*

Corresponding Author: chalady_2012@hotmail.com

The research project aims to synthesize and characterize of the high surface area monodisperse mesoporous silica nanoparticles (MSNs). The structure directing technique combined with the co-condensation and bi-phasic processes are employed to synthesize the MSNs in this work. The main structure directing agent used in the synthesis of MSNs in this work is myristyltrimethylammonium bromide (MTAB) while triethanolamine (TEA) and X-100 are utilized as co-structure directing agents. To create a bi-phasic environment, cyclohexane (CHX) is utilized. L-Arginine (LAG) is used as a catalyst to increase the rate of reaction. Ultrasonic wave of 40 kHz is used to swell of the directing agents. To investigate the characteristic properties of MSNs, as synthesized MSN samples are subjected to analyze by various analytical techniques. SEM and TEM are utilized to study the morphological structures and pore formed on each particles. Specific surface area (SSA), mean pore diameter and total pore volume at relative pressure of 0.99 are evaluated by the N2 adsorption-desorption isotherm testing combined with the calculation using BET and BJH techniques. Experimental results show that SSA of particles synthesized by using MTAB as a structure directing agent, is about 672 m2/g while SSA of particles synthesized by using a hybrid of MTAB+TEA and MTAB+X-100 is about 692 and 652 m2/g, respectively. Mean pore diameter and total pore volume of synthesized particles are about 4.9, 7.5, 3.9 nm and 0.83, 1.30, 0.63 cm3/g when MTAB, MTAB+TEA and MTAB+X-100 used as structure directing agents, respectively. The graph plots of N2 adsorption-desorption isotherm confirm the micro and meso-porous sizes on the synthesized particles. SEM and TEM images show the uniform dispersion of particle size and confirm the pore on each particles, respectively.

102

DARK MATTER PHENOMENOLOGY THROUGH OBSERVATION OF SOLAR NEUTRINO

Author: Suchakree Chiu[None]

Corresponding Author: suchakree_chiu@hotmail.com

The interactions between dark matter and standard model particles are still a mystery in particle physics. We have studied dark matter that is captured by the Sun through the solar neutrino which is produced from dark matter annihilation. This project analyzes neutrino data from IceCube in the context of the Higgs Portal model. Our work presents a constraint on the Dark matter-Proton spin-independent scattering cross-section and constraint on the Dark matter-Higgs coupling constant in the Higgs Portal model in the range of Dark matter mass between 100-3000 GeV.

313

Preparation of MOT for quantum simulation from Rydberg atom array

Author: Nuttida Kaewart[None]

Co-authors: Narupon Chattrapiban ; Nithiwadee Thaicharoen [1]; Pimonpan Sompet [1]

[1] *Quantum Simulation Research Laboratory, Department of Physics and Materials Science, Faculty of Science, Chiang Mai University*

Corresponding Author: nuttidakaewart@gmail.com

Quantum simulators based on an array of Rydberg atoms require low-entropy system, of which the temperature of the rubidium atoms are reduced toward an allowed temperature for atom trapping in an optical lattice. In this work, a standard magneto-optical trap (MOT) are employed to laser-cooled atoms, in which a trapping and repumping lasers are required for the trap stability. To cut down the number of lasers, both trapping and repumping frequencies are generated from a single laser source. The laser is initially locked to a crossover absorption peak between $5S_{1/2}F = 3 \rightarrow 5P_{3/2}F' = \{3, 4\}$ transitions from which sub-gigahertz acousto-optics modulators (AOMs) shifts its frequency toward resonance. The trapping laser is further modulated with another AOM at 1.5 GHz toward the repumping frequency in a double-passed configuration. Both frequencies bring down the MOT temperature near 300 μK at which an optical lattice of 1 mK deep can hold the cold atoms.

305

Metal-Insulator Transition effect on Graphene/VO2 via temperature dependent Raman Spectroscopy

Author: Kittitat Lerttraikul[1]

Co-authors: Wirunchana Rattanasakuldilok [1]; Autpittayakul Aketasaeng [1]; Salinporn Kittiwatanakul [1]

[1] *Chulalongkorn University*

Corresponding Author: aketasaeng@gmail.com

Vanadium dioxide (VO2) is a material which has a special characteristic that can change its properties drastically called metal-Insulator transition (MIT). The MIT of VO2 occurs at temperature about 68℃ under atmospheric pressure which change its phase from monoclinic to rutile phase, result in their different properties and structure. This characteristic of VO2 can be used for application such as smart windows, low power phase change switch, quantum simulator, etc. Moreover, some materials can be used to improve VO2 film quality. In this other work, bilayer-graphene were deposited on top of 50 nm and 100 nm VO2/Al2O3 and were studied via temperature-dependent Raman spectroscopy technique. The results indicate that the lattice parameter mismatch between bilayer-graphene and VO2 induce compressive strain on graphene and in-plane tensile strain on VO2 according to the observed blue shift of VO2 Raman modes. From the temperature-dependent Raman results, the monoclinic VO2 Raman peaks diminished as temperature reach 60-65℃ while the TMIT measured by temperature dependent resistance of bare VO2 is ~ 70℃. Moreover, an unexpected behavior from graphene can be observed in graphene/VO2. For graphene/SiO2 (without VO2 layer) G-peak position tends to red shift as temperature increase. However, the G-peak position observed from graphene/VO2 structure begins with red shift and turn to blue shift at ~60℃ (just around the transition) instead of only red shift, confirming the effect of VO2 proximity.

References
[1] Y. Cui, Y. Ke, C. Liu, Z. Chen, et al. Thermochromic VO2 for Energy-Efficient Smart Windows. Joule, Volume 2, Issue 9-2018, 1707-1746. https://doi.org/10.1016/j.joule.2018.06.018
[2] Zhou, H., Li, J., Xin, Y., Cao, X., Baoa, S., and Jin, P. (2015). Enhanced optical response of hybridized
VO2/graphene films. J. Mater. Chem. C, 3(19), 5089-5097. doi:10.1039/C5TC00448A
[3] Wang, W., Peng, Q., Dai, Y. et al. Temperature dependence of Raman spectra of graphene on copper foil substrate. J Mater Sci: Mater Electron 27, 3888–3893 (2016). https://doi.org/10.1007/s10854-015-4238-y

287

Investigating the large angle of a physical pendulum using a smartphone's sensors

Author: Chokchai Puttharugsa[None]

Co-authors: Theerawat Chatchawaltheerat ; Supitch Khemmani

Corresponding Author: chokchai@g.swu.ac.th

This work demonstrates the use of smartphone's sensors in recording experimental data for investigating the large angle of a physical pendulum. The smartphone (iPhone 5s) was attached to a beam to record simultaneously both the angular position and the angular speed of the beam oscillating about the pivot. The period and phase space of the oscillation were theoritically calculated and were compared with the experimental data. It was found that the experimental results agreed well with the theoretical calculations. We expect that this experiment based on a smartphone's sensors could be useful for physics teachers and encourage the interest of students.

221

The Dynamics of Pill Millipedes' Flipping

Authors: Nutchaya Preechanukul[1]; Rawinop Sodadee[1]; Parinya Sirimachan[1]; Pimsiri Danphisanuparn[1]; Tattep Lakmuang[1]

[1] *Kamnoetvidya Science Academy*

Corresponding Authors: nutchaya_p@kvis.ac.th, rawinop_s@kvis.ac.th, tattep_l@kvis.ac.th

Our research aims to find an equation of motion that can describe the flipping motion of the pill millipede (*Zephronia siamensis* Hirst). From observation, the flipping motion can be characterized into four types. Moreover, The pill millipede's shell curve that contacts the flat surface while flipping can be described as a form of the hyperbolic cosine function. So, the equation of motion of flipping can be derived. From the geometry of the cross-section of the pill millipede, we set a an angle between the vertical axis and the symmetry axis or critical angle that allows it to flip. We also set the maximum angle to be the angle between its symmetry axis to the last point that hyperbolic cosine has fitted the shell's curve. We have found that the critical angle must be smaller than the maximum angle to provide a successful flipping with minimal initial velocity. The equation of motion of flipping has been solved and tested by plotting the flipping angle as a function of time compared to the flipping angle from observation.

71

Coseismic changes in Chiang Mai Basin associated with the 5 May 2014 Mw 6.1 Mae Lao Earthquake detected using ambient seismic noise interferometry.

Authors: Chaninthon Rattanavetchasit[1]; Niti Mankhemthong[1]; Siriporn Chaisri[2]

[1] *Department of Geological Sciences, Faculty of Science, Chiang Mai University*

[2] *Department of Physics and Materials Science, Faculty of Science, Chiang Mai University*

Corresponding Author: chninthon_r@cmu.ac.th

Ambient seismic noise interferometry is a passive method that utilizes cross-correlation calculation between any two ambient noise traces for retrieving the subsurface seismic response. In this study, we investigate the temporal seismic wave velocity changes associated with the 2014 Mae Lao Earthquake in the Chiang Mai Basin located approximately 130 km away from the epicenter. The 5 years (2012-2016) continuous ambient seismic noise data used in this study are from 13 seismometer stations, 12 stations maintained by the Comprehensive Nuclear-Test-Ban Treaty Organization (CTBTO) (5 stations of three-component seismometers and 7 stations of vertical component seismometers), and one three-component station maintained by Incorporated Research Institutions for Seismology (IRIS). The 7 stations of vertical component seismometers are used for calculating daily cross-correlation functions between possible station pairs in the group array. While, at 6 stations with three-component seismometers, we perform daily single-station cross-component and autocorrelation of self-component. All possible correlation functions are processed with bandpass filters to enhance the 1–6 Hz frequency band and 0.33-1 Hz band, with earthquake (mainshock and aftershock) removal technique to create daily NCFs. The small timeshifts between all daily NCFs and the reference NCFs which are related to seismic velocity variation are estimated by the stretching method. We detect seismic velocity reductions after the mainshock in both filtered bands at several single stations and station pairs. Additionally, we observe seasonal variation due to rainfall and groundwater levels in the Chiang Mai Basin.

252

The study of pigment color mixing by microfluidic systems and smartphone technology

Authors: Hataiwat Palasak[1]; Puenisara Limnonthakul[1]

Co-author: Chaninan Pruekpramool [1]

[1] *Srinakharinwirot University*

Corresponding Author: mellamo_piik@hotmail.co.th

The students studied the color mixing concepts from elementary to high school classes. We found that they were still confused between light color mixing and pigment color mixing. Therefore, this research focuses on them and shows that we can apply the microfluidic systems and smartphone technology to prove and explain the pigment color mixing in clearly. The designing of microfluidic system is based on low cost, easy to fabricated and friendly to use. Then, the microfluidic systems were fabricated and applied the color measure application on smartphones to read the result of the pigment color mixing in real-time. The results show that the concentration of pigment color effect on the mixing of color shading. The students could study the pigment color mixing and microfluidic system at the onset of this experiment. The relation between the primary additive colors of light and additive colors of mixing colors was explained.

48

Application of Penman-Monteith method for estimating potential evapotranspiration over northern Thailand

Author: Sujittra Ratjiranukool[None]

Co-authors: Pakpoom Ratjiranukool [1]; Piyatida Jaichoom [2]

[1] *Chiang Mai Rajabhat University*

[2] *Chiang Mai University*

Corresponding Author: sujittra.r@cmu.ac.th

The estimation of evapotranspiration by Penman-Monteith method was studied over northern Thailand during the current period (1981–1999) and the future period (2080–2089). The calculation required daily meteorological datasets, for example, wind speed, temperature, relative humidity, and solar radiation intensity. The dataset in this research was simulated by a high-resolution regional climate model developed by Meteorological Research Institute (Japan) called Non Hydrostatic regional climate model (NHRCM) under RCP 8.5. The calculated potential evapotranspiration was analyzed by averaged annual cycle and probability density function at 14 meteorological stations over northern Thailand.

244

versatile setup to detect spontaneous parametric down conversion in BBO from a low cost laser-diode module

Authors: Ekkarat Phongopas[1]; Similan Pankaew[None]; Thanapat Phetvongsakul [None]

[1] *Division of Physics, Faculty of Science and Technology*

Corresponding Author: e_pong@tu.ac.th

A heralded single-photon source from spontaneous parametric down-conversion (SPDC) is the essential component of quantum optics laboratories. A new arrangement to produce a SPDC in BBO crystal is proposed. Two He-Ne lasers are used as guide beams through three diaphragms that are laid as vertexes of a triangle with angles of ±3 degrees to the crystal. With this configuration, the position of the detectors can be tuned precisely and easily. The heralded single- photon signal can be measured with a high signal-to-noise ratio. Even with a low-cost 405 nm diode laser module (1500 THB), the coincidental count rate is 408 count/s with the noise level at 22 count/s.

61

Quantum Diamond Spectrometer for Magnetic Field Sensing

Author: Napoom Thooppanom[None]

Co-author: Sorawis Sangtawesin [1]

[1] *Advisor*

Corresponding Author: npkids2012@gmail.com

We build a quantum diamond spectrometer (QDS), outlined by Bucher et. al [1], to study the fluorescence of the nitrogen-vacancy (NV) center in diamond, a quantum defect that can be used as a qubit or quantum sensor. The QDS has several advantages to a traditional confocal microscopy, particularly in terms of measurement speed. The setup consists of a green laser excitation onto the diamond that is placed on an optical light guide for fluorescence detection. A microwave loop is then placed onto the diamond to deliver oscillating magnetic field to probe the NV center transition. Finally, permanent magnets are attached to a kinematic stage for tuning the transition energy of the NV center. With this setup, we can adjust the magnet distance, azimuthal angle, and polar angle with reference to the NV center axis for optimizing NV center fluorescence. We demonstrate measurements of NV center fluorescence as a function of microwave frequency and show the intensity drop at 2.87 GHz, showing the interaction at zero-field splitting, and measurements of the Zeeman splitting of NV center electronic spin from an external magnetic field in different orientations. The results can be used to perform vector magnetometry, which has potential applications in quantum sensing.

[1]. Bucher, D.B., Aude Craik, D.P.L., Backlund, M.P. et al. Quantum diamond spectrometer for nanoscale NMR and ESR spectroscopy. Nat Protoc 14, 2707–2747 (2019).

212

BETAXANTHIN AND ANTHOCYANIN DYE-SENSITIZED SOLAR CELLS

Author: Pitchaporn kansit[1]

[1] *Lampang Rajabhat University*

Corresponding Author: pim_pizza@hotmail.com

Betaxanthin (BT) and anthocyanin (AT) pigments were extracted from coffee bean (C. arabica and C. robusta) and mulberry fruit (Morus alba L.), and 1:1 and 1:2 mixtures act as sensitizers were evaluated on the efficiency of dye-sensitized solar cells (DSSCs) with the area of 1x1 cm2 tested under 100 mW/cm2 of a simulated solar source. 8 nm diameter of anatase titanium dioxide (TiO2) sensitized with pure and mixed dye-sensitizers were painted on fluorine-doped tin oxide (FTO) conductive glass as the working electrode. Another electrode, graphite from soot candles was selected and I−/I3− ions as the electrolyte solution. The results showed the energy conversion efficiency of BT pigment is highest (ηBT = 5.37x10-4) due to its containing of three functions of hydroxyl, carbonyl, and amino groups assisted well to bind and transfer electrons ability to the TiO2 surface unlike AT pigment exclude amino group (ηAT = 3.74x10-4). In addition, the energy conversion efficiency decreased with increased amounts of anthocyanin dye in sensitized mixtures (ηBT:AT = 1.43x10-4 and ηBT:2AT = 3.08x10-5) may be due to the geometry of both pigment molecules and their functional groups are blocked by them-self, therefore, those are hardly transferred electrons ability to the TiO2 surface.

202

Observation of the photocurrent enhancement in reduced graphene oxide and silver nanoparticles composite films

Author: Chanatpol Tangkijtari[None]

Co-author: Yodchay Jompol

Corresponding Author: chanatpol.tan@student.mahidol.edu

We have observed an increase in the photocurrent of reduced graphene oxide (rGO) thin films by incorporating silver nanoparticles (AgNPs) on top of the films, making hybrid nanocomposite structures. With photoexcitation of a broad-wavelength spectrum of light (200 nm – 2500 nm), the increases have been found in all samples having AgNPs of different sizes and geometries deposited on top of the rGO that bridges between two source and drain electrodes on a cover-glass slide. In this study, AgNPs of diameters 30 nm and 200 nm and Ag nanoplates were implemented by drop-casting technique of 1 mg/ml on the diameter area of the rGO film ~ 1 – 2 mm^2. The current-voltage characteristics of these hybrid materials were carried out at an ambient temperature for different light powers. At a fixed 3 V bias, the measured current was changed from 0.4 μA to 4.29 μA, which is more than 1 order of magnitude without light illumination ("dark" condition), by adding AgNPs of 200 nm size. The increase of the current was found to 10.2 μA by illumination of light at 100 W output power ("light" condition), which gives rise to a photocurrent of 0.591 μA and hence photoresponsivity of up to ~ 25 mA/W on the absorption area of 1 mm^2 by only using the AgNPs to confine light. This finding is ascribed to electron transfers due to the plasmonic enhancement of the AgNPs to the rGO via conduction electrons participated in the film. Further work needs to be verified the time response to the photoexcitation of the samples to provide information on charge-carrier transports in such hybrid nanomaterials. We believe that our experimental results present the photodetection of the hybrid nanomaterials on thin-film transparent substrates that can extend to a large-scale manipulation on flexible and low-light weight polymer substrates.

199

Modeling and Simulation of Gd0.7Sr0.3MnO3 Prepared Material Electrodes for Asymmetric Supercapacitor

Author: pornchai chinnasa[1]

[1] *Program in Physics Rajabhat Mahasarakham University*

Corresponding Author: pornchai.ch@rmu.ac.th

This work uses modeling and simulation to investigate the impact of Gd0.7Sr0.3MnO3 on the preparation of material electrodes for asymmetric supercapacitors. Anode electrodes, cathode electrodes, and an electrolyte layer compose the supercapacitor structure. In this study, the COMSOL Multiphysics tool was used to investigate the electrochemical characteristics of a supercapacitor with a width of 3 mm and a length of 7 cm. Therefore, the COMSOL Multiphysics tool was used to build an asymmetric supercapacitor using a Na2SO4 and KOH solution as the electrolyte. The specific capacitance was 1051.44 and 928.36 F/g, and the equivalent serial resistance (ESR) was 4.82 and 7.26, respectively. The asymmetric super capacitor model was employed to raise the electrode thickness to 0.5, 1.0, 2.0, and 3.0 mm, respectively. An asymmetric supercapacitor filled with Na2SO4 solution was discovered to be an electrolyte and it was discovered that the resultant specific capacitance value showed a declining trend.

188

Preparation of NiWO4/TiO2 heterostructure for enhanced photo-electrochemical water-splitting performance

Authors: Chayanit Keeprawat Keeprawat[1]; Thiwakorn Chuebang[1]; Thanawat Ninsu[1]; Asanee Somdee[1]; Surangkana Wannapop[2]

[1] *King Mongkut's University of Technology North Bangkok*

[2] *kmutnb*

Corresponding Author: s6413021810018@email.kmutnb.ac.th

Hetero-junction on TiO2 is an effective the fast charge recombination and slow charge transfer kinetics, its significance to design the junction in photo-electrochemical (PEC) water splitting. The purpose of using NiWO4 is to extend the visible light absorption capacity and improve the charge transport and charge carrier lifetime of the TiO2 based photoanode. In this study, the hetero-junction of NiWO4/TiO2, NiWO4, and TiO2 by Hydrothermal process at a temperature of 160℃ for 12 hours. The samples were analyzed by X-ray Diffractometer (XRD), X-ray photoelectron spectroscopy (XPS), scanning electron microscope (SEM), Energy Dispersive X-Ray Spectroscopy (EDS), Transmission electron microscopy (TEM), High-resolution transmission electron microscopy (HRTEM). The optical absorbance of the TiO2, NiWO4, and NiWO4/TiO2 films were recorded using a UV-Vis spectrophotometer and by using the Kubelka-Munk function. The absorption spectra showed the energy bandgap of pristine TiO2 decreased after the NiWO4 enhancement. The samples were applied as photoanode for PEC water splitting cells. As a result, the NiWO4/TiO2 sample showed the best performance of the PEC water splitting process than the pristine TiO2 and pristine NiWO4 under solar simulation. Electrochemical impedance spectroscopy (EIS) revealed that the charge carrier and charge transport of the NiWO4/TiO2 material was improved. The photocurrent density generated by the NiWO4/TiO2 photoanodes was higher than the pristine TiO2 photoanode and pristine NiWO4 photoanode when they were applied as the photoanode in the photoelectrochemical cell.

182

Fabrication of Activated Carbon Synthesized from a Water Hyacinth as Electrode in Supercapacitor

Author: Dr. Tanachai Ponken[None]

Co-authors: Narinda Chenpeng [1]; wichaid ponhan ; Sathaphorn Aungchan [1]

[1] *Rajabhat Maha Sarakham University*

Corresponding Author: tanachai.po@rmu.ac.th

Activated carbon (AC) electrode was synthesized from a water hyacinth for application in a supercapacitor. AC was prepared from a water hyacinth sinter at 800 ˚C for 2 hours under argon (Ar) gas atmosphere. A water hyacinth activated carbon (WHAC) and AC samples were doped with potassium hydroxide (KOH) powder in the ratio as following WHAC (non-doping), WHAC-1:1, WHAC-2:1, WHAC-3:1 and WHAC-4:1, respectively. All samples physical characteristic exhibits the dark black color and uniform distribution which these indicated the complete burning. Structural properties were analyzed from XRD technique, conditions all shown the 002 plane and amorphous-like pattern. Surface area corrosion increased when the KOH amount increased from FE-SEM. The element compound of WHAC-1:1, WHAC-2:1, WHAC-3:1 and WHAC-4:1 obtained the carbon substance approximately of 91.00, 90.27, 90.27 and 91.20%, respectively which the carbon purity higher than WHAC (non-doping) (58.99% by atomic). Finally, the electrode electrochemical testing found that, the highest specific capacitance value obtained as high as 89.84 F.g-1 for the AC at the ratio of 2:1, the scan rate of 5 mV.s-1. Charge-discharge results found that, the electric discharge time of WHAC-1:1, WHAC-2:1 and WHAC-3:1 obtained time values longer than WHAC (non-doping) and WHAC-4:1. Properties of ratio of 2:1 (WHAC-2:1) indicates activated carbon purity, high surface area and the highest specific capacitance value, for that reason WHAC-2:1 suitable for application as the electrode for supercapacitors.

178

The Effects of Cellulose Particle Sizes on Biofilm from Longkong Peel

Author: Saryrung Khumtrong[None]

Co-author: Panupong Jaiban

Corresponding Author: saryrungkhumtrong@gmail.com

The effects of longkong cellulose particle sizes on its biofilm were investigated. The particle sizes were divided into 355, 125, and 75 um. The X-ray diffraction patterns confirmed the cellulose phase with the secondary phase in some sample. The second phase did not affect biofilm preparation. The FTIR analysis suggested a strong presence of carboxyl and hydroxyl groups in carboxymethylcellulose (CMC) powder, which synthesized from the cellulose particle size 75 um. The SEM and EDS observations revealed that the cellulose particle size of 75 um produced a smooth surface and homogeneity of biofilm. The decrease in particle size induced significantly the high water solubility of CMC and high reaction surface area, leading to high quality of biofilm. The light absorption of all biofilms was not different significantly. Herein, the result suggested that a high quality of biofilm from longkong peel could be produced using the cellulose particle size 75 um, which may be alternative bioproduct in near future.

216

The Effects of Microstructure on Dielectric and Piezoelectric Properties of Bilayer Ceramic Between Ba0.85Ca0.15Zr0.1Ti0.9O3 and BaTiO3

Author: Thanakrit Theethuan[None]

Co-author: Panupong Jaiban

Corresponding Author: thanakrit.theethuan08@gmail.com

Ba0.85Ca0.15Zr0.1Ti0.9O3 (BCZT), BaTiO3 (BT) ceramics, and BCZT/BT bilayer ceramic were fabricated by a solid-state reaction method. The used sintering condition for all ceramics was at 1,400 ℃ for 4 h. The BCZT/BT bilayer ceramic had a tetragonal structure with a second phase of starting oxides. The scanning electron microscopy (SEM) and energy-dispersive X-ray spectroscopy (EDS) confirmed the bilayer structure between BCZT and BT systems. The BCZT/BT bilayer ceramic promoted two-phase transition temperatures around 100 ℃ and 160 ℃, which belonged to BCZT and BT systems, respectively. The dielectric and piezoelectric properties of BCZT/BT bilayer ceramic were between BT and BCZT pure ceramics. The interface between BCZT and BT layer decreased the maximum dielectric constant of the bilayer ceramic. The result revealed that the bilayer ceramic had each system's characteristics and electrical properties, which might be applied in bilayer dielectric devices.

155

The Effects of Cellulose Particle Sizes on Biofilms from Lime Peel

Author: Sirintra Lokakaew[None]

Co-author: Panupong Jaiban

Corresponding Author: dear.sirintra@gmail.com

The effects of cellulose particle sizes of lime peel on biofilm were studied in this work. The cellulose particle sizes, i.e., 355, 250, 125, and 75 um, were examined for biofilm preparation. The XRD patterns revealed a main phase of cellulose in all samples. The presence of secondary phase did not affect biofilm preparation. The FTIR spectra indicated that the decrease in cellulose particle size enhanced carboxyl and hydroxyl groups of carboxymethyl cellulose (CMC) powder. The cellulose particle size 75 um had a strong presence of hydroxyl and carboxyl groups. This contribution significantly promoted high water solubility of CMC powder from 75 um and high-quality biofilm with smooth surface and homogeneity. The optical band gap of biofilms was about 4.75 – 4.88 eV. With these results, the investigation here revealed that the lime cellulose particle size 75 um produced high quality biofilm, which may be alternative bioproduct in the future.

15

ASSESSMENT OF NATURAL RADIOACTIVITY IN INDUSTRIAL LINE PRODUCTION WATERS

Author: Anan Omanee[1]

Co-authors: Archara Phattanasub [1]; Suwisa Sudchawa [1]; Panuwat Srimork [1]; Rachai Tunaumpai [1]; Sasikarn Nuchdang [1]; Wilasinee Kingkam [1]; Dussadee Rattanaphra

[1] *Thailand Institute of Nuclear Technology*

Corresponding Author: anan@tint.or.th

Five hundred water samples used in industrial line production from various sorts including food production and processing, portable water, and others (non-food) industries in the year 2021 were analyzed for gross alpha (GA), gross beta (GB) and tritium. The studied water samples included a set of tap water, surface water, consumption water, drinking water, deep well reclaimed water, waste water, soft water and other. GA activity concentrations in 5 of 500 analyzed samples could be detected and their mean concentrations were 0.285 to 0.275 Bq L-1, respectively. Almost all values were lower than the reference dose of 0.5 Bq L-1 which recommended by WHO for radioactivity in drinking water. GB activity concentrations in all samples cloud be detected and 3 samples exceeded the reference value (1.0 Bq L-1). The highest values for both GA and GB were found in surface water and waste water, respectively. The measured concentration of tritium showed to be lower than the minimum detectable activity (MDA). The results reveals that the water are safe for drinking and other used in industrial activities.

4

Extrinsic and intrinsic factors influencing the dielectric property and relaxation of $Li_{1/2}\ Y_{1/2}\ Cu_3\ Ti_4\ O_{12}$ ceramic

Authors: Jakkree Boonlakhorn[1]; Pornjuk Srepusharawoot[1]; Prasit Thongbai[1]

[1] *Khon Kaen University*

Corresponding Author: jboonlakhorn@gmail.com

In this study, a solid-state reaction technique was used to produce $Li_{1/2}\ Y_{1/2}\ Cu_3\ Ti_4\ O_{12}$ ceramic. The crystal structure, dielectric property, and electrical response were all thoroughly studied. Sintered ceramic crystal structure complies with the standard pattern of a body-centered cubic system with an Im3 space group (JCPDS no. 75-2188). Sintered $Li_{1/2}\ Y_{1/2}\ Cu_3\ Ti_4\ O_{12}$ ceramic had a high dielectric permittivity yield of 4702 and a low loss tangent of about 0.091. Impedance, admittance, and modulus spectroscopies were used to characterize the electrical factors of the sample. In addition, a computational approach based on density functional theory (DFT) was employed to determine structural data such as induced oxygen vacancies and charge densities in the structure. The experimental and theoretical findings suggest that the heterogeneous microstructure matching to the internal barrier layer capacitor model might be the primary origin of the colossal dielectric property of $Li_{1/2}\ Y_{1/2}\ Cu_3\ Ti_4\ O_{12}$ ceramic.

The 17th SIAM PHYSICS CONGRESS 2022

Suranaree University of Technology

“Carbon Neutrality”

22 - 24 JUNE 2022 AT KHAO YAI CONVENTION CENTER (KYCC), NAKHON RATCHASIMA, THAILAND

SCAN ME
FOR MORE INFORMATION